TRANSPORTATION RESEARCH RECORD 705

Subdrainage and Soil Moisture

TRANSPORTATION RESEARCH BOARD

COMMISSION ON SOCIOTECHNICAL SYSTEMS
NATIONAL RESEARCH COUNCIL

NATIONAL ACADEMY OF SCIENCES
WASHINGTON, D.C. 1979

Transportation Research Record 705
Price $4.00
Edited for TRB by Anne Ricker

mode
1 highway transportation

subject areas
62 soil foundations
63 soil and rock mechanics
64 soil science

Transportation Research Board publications are available by ordering directly from TRB. They may also be obtained on a regular basis through organizational or individual affiliation with TRB; affiliates or library subscribers are eligible for substantial discounts. For further information, write to the Transportation Research Board, National Academy of Sciences, 2101 Constitution Avenue, N.W., Washington, DC 20418.

Library of Congress Cataloging in Publication Data
National Research Council. Transportation Research Board.
Subdrainage and soil moisture.

(Transportation research record; 705)
Reports prepared for the 58th annual meeting of the Transportation Research Board.
Includes bibliographical references.
1. Road drainage–Addresses, essays, lectures. 2. Roads–Subgrades–Addresses, essays, lectures. 3. Soil moisture–Addresses, essays, lectures. I. Title. II. Series.
TE7.H5 no. 705 [TE215] 380.5'08s [625.7'34]
ISBN 0-309-02951-1 ISSN 0361 1981 79-20994

Sponsorship of the Papers in This Transportation Research Record

GROUP 2–DESIGN AND CONSTRUCTION OF TRANSPORTATION FACILITIES
Eldon J. Yoder, Purdue University, chairman

Compaction and Stabilization Section
Eugene B. McDonald, South Dakota Department of Transportation, chairman

Committee on Compaction
Charles M. Higgins, Louisiana State Department of Transportation and Development, chairman
Mehmet C. Anday, Marvin L. Byington, Robert C. Deen, J. M. Hoover, Eugene Y. Huang, Ernest Jonas, James E. Kelly, Charles Dabney Lamb, William B. O'Sullivan, John R. Sallberg, J. Chris Schwarzhoff, Charles H. Shepard, Donald Ray Snethen, Robert J. Weaver

Soil Mechanics Section
Lyndon H. Moore, New York State Department of Transportation, chairman

Committee on Subsurface Drainage
George W. Ring III, Federal Highway Administration, chairman
Charles C. Calhoun, Jr., Robert G. Carroll, Jr., Harry R. Cedergren, Charles J. Churilla, Allen L. Cox, Barry J. Dempsey, Edward N. Eiland, Gary L. Klinedinst, Arthur O. Kruse, Alfred W. Maner, Glen L. Martin, Edward M. Masterson, Lyndon H. Moore, Lyle K. Moulton, Russell B. Preuit, Jr., Hallas H. Ridgeway, Travis W. Smith, William D. Trolinger, Walter C. Waidelich, Clayton E. Warner, David C. Wyant, Thomas F. Zimmie

Geology and Properties of Earth Materials Section
David L. Royster, Tennessee Department of Transportation, chairman

Committee on Frost Action
Wilbur M. Haas, Michigan Technological University, chairman
Bruce G. Anderson, Barry J. Dempsey, Paul J. Diethelm, Albert F. Dimillio, Wilbur J. Dunphy, Jr., Gary L. Hoffman, Glenn E. Johns, Thaddeus C. Johnson, Miles S. Kersten, Clyde N. Laughter, R. Torrence Martin, George W. McAlpin, Richard W. McGaw, Stephen F. Obermeier, Robert G. Packard, Edward Penner, Alex Rutka, Henry W. Wallace

Committee on Environmental Factors Except Frost
Barry J. Dempsey, University of Illinois at Urbana-Champaign, chairman
Bud A. Brakey, Samuel H. Carpenter, T. Y. Chu, A. Alexander Fungaroli, K. P. George, Wilbur M. Haas, T. Allan Haliburton, John William Hewett, Robert D. Krebs, Robert P. Lottman, Robert L. Lytton, David E. Melick, Gene R. Morris, Franklin Newhall, James M. Ritchie, David F. Slusher, Donald Ray Snethen, Malcolm L. Steinberg, T. C. Paul Teng, Edgar Pierron Ulbricht, William G. Weber, Jr., Larry M. Younkin

John W. Guinnee, Transportation Research Board staff

Sponsorship is indicated by a footnote at the end of each report. The organizational units and officers and members are as of December 31, 1978.

Contents

Part 1
Subdrainage and Environmental Influences on Pavement Performance

Analysis of Parallel Drains for Highway Cut-Slope Stabilization

Rodney W. Prellwitz, Forest Service, U.S. Department of Agriculture, Missoula, Montana

Methods of analyzing parallel drains for highway cut-slope stabilization are introduced. The analysis procedure is based on the prediction of the phreatic surface location within a soil mass under steady-state seepage. Relative effectiveness of alternate drain spacings is determined by estimating the steady-state phreatic surface at a profile located midway between drains and by using analysis procedures for the design of parallel drains in agricultural field drainage. Applications are made to seepage from an infinite-slope source. Mathematical analyses for estimating steady-state phreatic surfaces at a blanket drain and cut-slope intercept with an infinite-slope seepage source are also introduced. An illustrative design problem is worked out in detail.

Since their introduction by the California Highway Department in 1939, drilled-in parallel drains have proved to be an effective means of achieving highway cut-slope stabilization (1). Unfortunately, little has been written on the analysis of the use of parallel-drain spacing for this purpose. In practice, drain spacings ranging from 3 to 15 m (10 to 50 ft) are often selected on the basis either of experience (1) or of the carrying capacity of the drainpipe (2). A design criterion is needed by which a designer can evaluate, before installation, the effectiveness of alternate parallel-drain spacings in lowering the groundwater, or phreatic, surface at a profile located midway between the drains. A relative stability analysis can then be made to evaluate drainage alternatives.

A recent article by Kenney, Pazin, and Choi (3) introduced a design criterion for evaluating the relative effectiveness of horizontal parallel drains based on predicting the increase in stability (factor of safety) without analyzing phreatic surface drawdown directly. Their solution was compared with that introduced in this paper in an earlier uncondensed draft (4).

BASIS FOR PARALLEL-DRAIN ANALYSIS

Drainage analysis in this paper is based on the following:

1. A predetermined maximum infinite-slope phreatic surface developed under seepage parallel to a drainage barrier in an unconfined aquifer (phreatic surface I in Figures 1 and 2)—seepage is assumed to be steady state at this critical condition;
2. An undrained steady-state phreatic surface extending from phreatic surface I to the intercept with the cut slope (phreatic surface U in Figures 1 and 2);
3. An estimated steady-state phreatic surface for a blanket drain installed at the same attitude as the parallel drains (phreatic surface D in Figures 1 and 2), extending from phreatic surface I to the drain; and
4. A steady-state phreatic surface estimated to exist at a profile midway between and parallel to two adjacent parallel drains (phreatic surface M in Figures 3 and 4). The rationale used is that, if drains are spaced infinitely far apart, phreatic surface M equals phreatic surface U; if spaced infinitely close together, phreatic surface M equals phreatic surface D.

FLOW-NET ANALYSES: PHREATIC SURFACES I, U, AND D

Flow-net solutions are possible for estimating phreatic surfaces U and D by using equipotential drops (Δh) from the infinite-slope phreatic surface I:

$$\Delta h = h \sin\theta \cos\theta \quad (1)$$

where h equals depth from phreatic surface to the drainage barrier and θ equals slope of the drainage barrier. Figure 1 shows the results of the flow-net analyses for phreatic surfaces U and D. Flow-net analyses are time consuming, and mathematical solutions that can be used to approximate these phreatic surfaces would be faster and readily adaptable to computer analyses.

MATHEMATICAL ANALYSES: PHREATIC SURFACES U AND D

Mathematical solutions for phreatic surfaces U and D are not readily found in the literature for infinite-slope seepage conditions. I have modified solutions by Casagrande and Kozeny (5, 6) developed for a reservoir seepage source to approximate phreatic surfaces U and D from an infinite-slope source. One can expect good correlation for phreatic surface U with the results of flow-net analyses for cut slopes with horizontal-to-vertical ratios of 1:1 (45°) or flatter. For cut slopes steeper than 45°, one may use a graphical approximation based on Casagrande's modified basic parabola (5, 6) procedure in conjunction with the following Equation 10 plotted with the origin at the toe of the cut slope.

Applications of mathematical solutions for phreatic surfaces U and D for seepage emanating from a reservoir source, as they apply to the procedure presented in this paper, were made in an earlier draft (4).

Phreatic Surface U

The vertical distance from the toe to the phreatic surface intercept of the cut slope from flow-net analysis (Figure 1) is

$$\Delta h_W = h_W \sin\theta \cos\theta \quad (2)$$

where h_W is the vertical distance from the toe to the projection of phreatic surface I. If the cut slope intercepts the drainage barrier, $h_W = h$. Corrected for approximate mathematical analysis,

$$\text{Set } X_U = 0 \text{ at } Y_{UO} = h_W \sin\theta \cos\theta (1 + \tan^2\theta)(1 + \tan^2\beta) \quad (3)$$

where β is the cut slope. For positive values of X_U (toward the toe)

$$Y_U = X_U \tan\beta \quad (4)$$

At the toe, $Y_U = 0$ and $X_{UO} = Y_{UO}/\tan\beta$. For negative values of X_U (toward phreatic surface I)

$$Y_U = (aX_U^2 - 2Y_{UO}X_U + Y_{UO}^2)^{1/2} \quad (5)$$

where a equals $\tan^2\theta$. At the intercept with phreatic surface I

$$Y_{UI} = h_i - X_{UI}\tan\theta \quad (6)$$

and

$$X_{U1} = (h_i^2 - Y_{UO}^2)/(2h_i \tan\theta - 2Y_{UO}) \quad (7)$$

where $h_i = h_w + X_{UO} \tan\theta$.

Phreatic Surface D

At the intercept of the drain with the barrier set $X_o = 0$ and

$$Y_{DO} = h \sin\theta \cos\theta \ (1 + \tan^2\theta) \quad (8)$$

Phreatic surface enters the drain vertically at (positive value for X_o)

$$X_{DO} = \tfrac{1}{2} h \sin\theta \cos\theta \quad (9)$$

For negative values of X_o (toward phreatic surface I)

$$Y_D = (aX_D^2 - bY_{DO} X_D + Y_{DO}^2)^{1/2} \quad (10)$$

where $a = \tan^2\theta$ and $b = Y_{DO}/X_{DO} + aX_{DO}/Y_{DO}$. At the intercept with phreatic surface I

$$Y_{DI} = h - X_{DI} \tan\theta \quad (11)$$

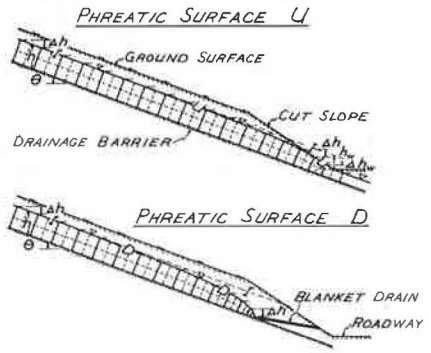

Figure 1. Flow-net analyses for phreatic surfaces U and D.

and

$$X_{DI} = (h^2 - Y_{DO}^2)/(2h \tan\theta - bY_{DO}) \quad (12)$$

If the drain does not intercept the barrier, a solution is possible by setting $X_o = 0$ at the end of the drain and using $h = h_w$ as previously defined.

PARALLEL DRAINS FOR AGRICULTURAL DRAINAGE

Parallel drains have been used successfully in agricultural drainage to lower the phreatic surface to predetermined levels (7, 8). Design criteria exist for both steady-state and transient-state infiltration of rainfall or irrigation water concentrated by a drainage barrier (see Figure 5). The analysis is two-dimensional, and vertical recharge is assumed.

Steady-State Analysis

Where rainfall is frequent, a steady-state analysis is made for the drain spacing (S) required to maintain the phreatic surface at the appropriate level. Figure 5 shows an idealized cross section across two parallel drains under steady-state drainage. The Dutch have pioneered the analysis for the steady-state case, and several solutions are possible (8). The most useful for adaptation to cut-slope stabilization is the Hooghoudt equation:

$$V = (8K_b dh_m + 4K_a h_m^2)/S^2 \quad (13)$$

where

- K_a = hydraulic conductivity (permeability) of the soil above the drainpipe,
- K_b = hydraulic conductivity (permeability) of the soil below the drainpipe,
- V = drain discharge velocity (or rainfall recharge rate),
- h_m = maximum phreatic surface height above the drain

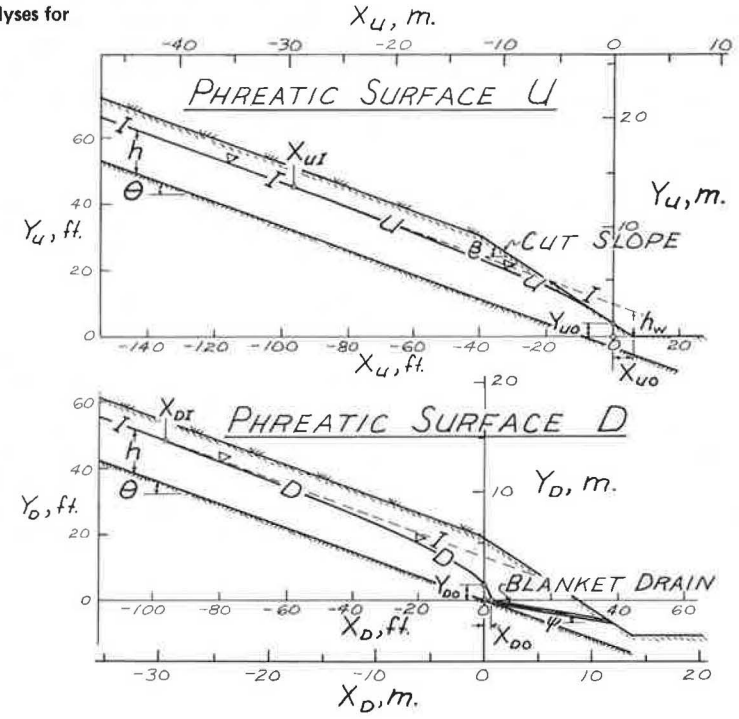

Figure 2. Mathematical analyses for phreatic surfaces U and D.

Figure 3. Results of analyses for phreatic surfaces M using three drain spacings.

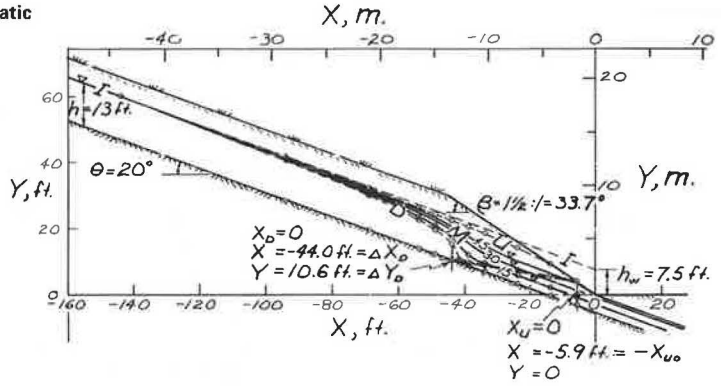

at a profile midway between the drains,
S = drain spacing,
D = depth from the drain to the drainage barrier, and
d = reduced equivalent depth corresponding to D (reduced to account for extra resistance at the drainpipe caused by radial flow).

For the case where $D < 1/4S$, the relationship between d and D has been developed based on work by Ernst and Hooghoudt (8).

$$d = D/[1 + (8D/\pi S)\ \ln(D/\pi r_o)] \quad (14)$$

where r_o is the radius of the drainpipe.

The typical drilled-in drainpipe used in cut-slope stabilization is slotted PVC plastic with an inside diameter of 3.8 cm (1.5 in). Figure 6 shows the relationship, by Equation 14, between d and D for this drainpipe at various drain spacings.

If the soil is assumed to be homogeneous, then $K_a = K_b = K$, and Equation 13 can be rewritten as an equation for drain spacing:

$$S = \{[4\ K\ h_m\ (2d + h_m)]/V\}^{1/2} \quad (15)$$

Transient-State Analysis

In the case of intermittent recharge, such as with irrigations or high-intensity rainfall, transient- or nonsteady-state analysis is used. Figure 5 shows an idealized cross section across two parallel drains under transient-state drainage. The solution for drain spacing (S) is based on lowering the phreatic surface developed by one irrigation (h_o) to a required level (h_t) within the time span (drain-out time) (t) between irrigations so that the following irrigation will not increase the phreatic surface beyond h_o. Several methods of solution are available; the most useful for adaptation to cut-slope drainage is the modified Glover-Dumm equation (8) for the drawdown ratio in the form

$$h_t/h_o = 1.16e^{-\alpha t} \quad (16)$$

where $\alpha t = [\pi^2 K(d + \frac{1}{2}\sqrt{h_o h_t})\ t]/N_e S^2 > 0.2$, N_e is effective porosity (specific yield) of the soil, and K and d are as defined for Equations 13 and 15.

PARALLEL DRAINS FOR HIGHWAY CUT-SLOPE DRAINAGE

The conditions are somewhat different for highway cut-slope drainage than they are for agricultural drainage. Long-term highway cut-slope drainage by parallel drains must be based on (a) steady-state seepage analysis of the maximum groundwater conditions expected during the design life of the highway, (b) recharge at the drains primarily from seepage flow along the drainage barrier, and (c) a three-dimensional analysis.

Figure 7 illustrates the three-dimensional nature of a typical parallel-drain installation for highway cut-slope stabilization. For cross section $B\text{-}B_1$ or $C\text{-}C_1$, as long as seepage is steady, the midpoint phreatic surface heights h_t and h_o, respectively, will not vary with time the way agricultural parallel drains do in the transient state. However, the midpoint phreatic surface height does decrease with successive down-slope cross sections ($h_t < h_o$). This suggests that the two-dimensional transient-state analysis (Equation 16) may be altered to a three-dimensional steady-state analysis (see Figures 5 and 7) by assuming that drains are installed parallel to the gradient of the drainage barrier and defining drain-out time (t) as the time required for seepage to travel between successive down-slope cross sections ($C\text{-}C_1$ to $B\text{-}B_1$).

In addition, the steady-state analysis (Equation 15) may be applicable to the conditions at the end of the drain (cross section $C\text{-}C_1$) if the discharge velocity (V) is defined as a comparable recharge velocity moving along the drainage barrier.

Alteration of the modified Glover-Dumm equation for the three-dimensional steady state can be done as follows. A replacement for drain-out time (t) to represent the time required for seepage to travel between successive down-slope cross sections can be derived by using Darcy's law (1). A variety of solutions is possible depending on the following:

1. How the hydraulic gradient i, equal to ratio between slope distance and slope height, is defined;
2. Whether this hydraulic gradient is assumed constant for a specific vertical cross section; and
3. How the flow distance (Z) between successive cross sections is determined.

Figure 4 illustrates a typical flow situation that might exist on a profile that is midway between drains (M). The most representative hydraulic gradient (i) between successive cross sections is somewhere between the phreatic surface gradient ($\Delta h_p/P$) and the barrier gradient ($\Delta h_B/B$). Also, the most representative flow distance (Z) is somewhere between P and B. The mean values of flow distance and hydraulic gradient are defined, respectively, as

$$Z = (P + B)/2 \quad (17)$$

and

$$i = (\Delta h_P + \Delta h_B)/(P + B) \quad (18)$$

From Darcy's law (1) we can derive an expression for drain-out time (t)

$$Q = K\,i\,A \quad (19)$$

where Q is seepage quantity, A is cross-sectional area normal to the flow, and K and i are as previously defined. Also discharge velocity is

$$V = Q/A = Ki \quad (20)$$

and seepage velocity is

$$V_s = V/N_e = Ki/N_e = Z/t \quad (21)$$

where N_e, Z, and t are as previously defined.

In terms of drain-out time (t),

$$t = Z/V_s = N_e\,Z/Ki \quad (22)$$

Substituting Equation 22 into Equation 16 yields the drawdown ratio

$$h_t/h_o = 1.16e^{-\alpha t} \quad (23)$$

where

$$\alpha t = [\pi^2 (d + \tfrac{1}{2}\sqrt{h_o h_t})\,Z]/S^2\,i > 0.2 \quad (24)$$

Alteration of the Hooghoudt equation for the three-dimensional case by substituting V = ki into Equation 15 yields

$$S = \{[4\,h_m\,(2d + h_m)]/i\}^{1/2} \quad (25)$$

When the drain contacts the drainage barrier, d = 0, and

$$S = (4\,h_m^{\,2}/i)^{1/2} \quad (26)$$

Equations 25 and 26 can be used in conjunction with phreatic surfaces U and D to estimate the practical range of drain spacings to be considered in the analysis. The hydraulic gradient is defined in the same manner as in the derivation of Equation 18. For the case where the drain contacts the barrier, the minimum practical drain spacing is

$$S_{min} \cong \{4\,Y_{DO}^{\,2}/\sin[(45° + \theta)/2]\}^{1/2} \quad (27)$$

where Y_{DO} is from Equation 8, and the maximum practical drain spacing is

$$S_{max} \cong \{4\,h_u^{\,2}/\sin[(\theta_u + \theta)/2]\}^{1/2} \quad (28)$$

where h_u and θ_u are height above the drain at the barrier and slope at that point, respectively, of phreatic surface U.

ILLUSTRATIVE PROBLEM

To illustrate how the above analysis might be used in an actual design problem, consider the highway cut illustrated in Figures 1 and 2.

Recommended Procedure

A more complete procedure that incorporates this method directly into a slope-stability analysis was given in an earlier draft (4). The following procedure pertains to drainage analysis only.

1. Construct phreatic surface U using either flow-net analysis or mathematical analysis or both (Equations 1-7).
2. Construct phreatic surface D using either flow-net analysis or mathematical analysis or both (Equations 1 and 8-12).
3. Estimate S_{min} and S_{max} using Equations 25-28 and select trial drain spacings.
4. Construct the phreatic surface M for the trial drain spacings. All should fall between phreatic surfaces U and D.
5. Begin the analysis at the intercept of phreatic surfaces D and I from flow-net analysis or Equations 11 and 12.

Figure 4. Definition of hydraulic gradient, drainage distance, and drawdown ratio between successive cross sections.

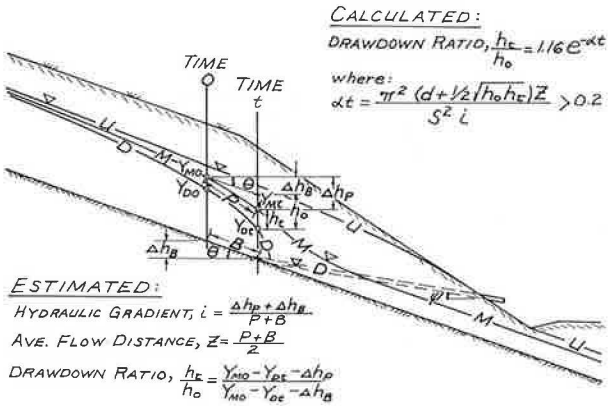

Figure 5. Two-dimensional agricultural drainage with vertical recharge.

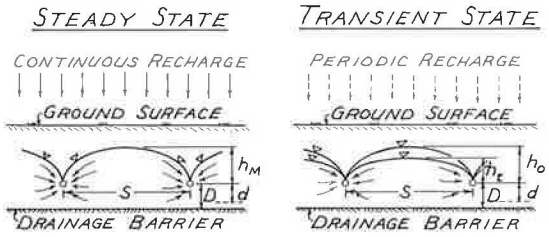

Figure 6. D versus d for a drainpipe of 3.8-cm (1.5-in) inside diameter.

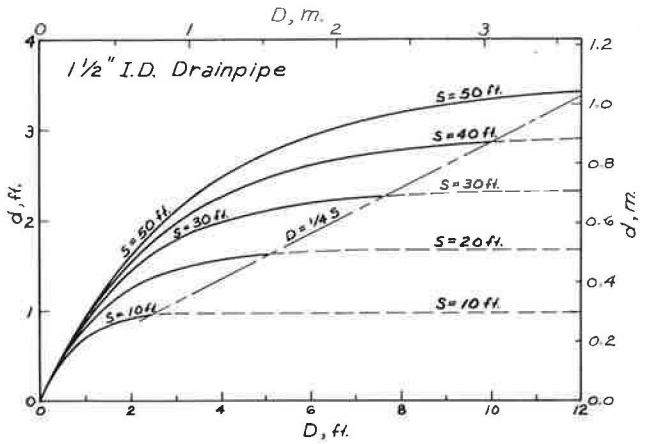

6. Divide into cross sections from intercept D-I(X_{DI}) to the intercept of phreatic surface U with the cut slope (X_{UO}). Cross sections should be spaced far enough apart so that $\alpha t > 0.2$ in Equation 24. Usually spacing larger than S/10 will satisfy this requirement.

7. For negative values of X_D, analyze as if the drain and drainage barrier were both located on phreatic surface D.

8. Between successive cross sections, determine drawdown ratio, h_t/h_o, through trial-and-error relaxation between estimation (see Figure 4) and calculation (Equation 23). Two or three trials are usually sufficient.

Solution

Infinite-slope conditions are h equals 4.0 m (13 ft) and $\theta = 20°$. Refer to Figures 7 and 8 and construct all phreatic surfaces from the same X-Y axis located at the toe of the cut.

Step 1. Phreatic Surface U

From columns 5 and 6 of Figure 8, calculate Equation 3 at $X_U = 0$:

$Y_{UO} = h_W \sin\theta \cos\theta (1 + \tan^2\theta)(1 + \tan^2\beta) = 1.2$ m (3.9 ft)
Then, with Equation 4 at the toe, $Y_U = 0$ and $X_{UO} = Y_{UO} / \tan\beta = 1.8$ m (5.9 ft)
From Equation 5 for negative values of X_U, we get
$Y_U = (\tan^2\theta X_U^2 - 2 Y_{UO} X_U + Y_{UO}^2)^{1/2}$ and
$Y_U = (0.132X_U^2 - 2.40 X_U + 1.44)^{1/2}$
Plot at
$X = X_U - X_{UO} = X_U - 1.8$
Intercept with phreatic surface I by Equation 7 for
$h_1 = h_W + X_{UO} \tan\theta = 2.9$ m (9.7 ft)
so that
$X_{UI} = (h_1^2 - Y_{UO}^2)/(2h_1\tan\theta - 2Y_{UO}) = -27.5$ m (-90.3 ft)
at
$X = X_{UI} - X_{UO} = -29.4$ m (-96.2 ft)

Step 2. Phreatic Surface D

From columns 9 and 10 of Figure 8, one can use Equation 8 at the contact of the drain with the barrier; $X_D = 0$ and
$Y_{DO} = h \sin\theta \cos\theta (1 + \tan^2\theta) = 1.4$ m (4.7 ft)
Equation 9 for phreatic surface intercept with drain is
$X_{DO} = \frac{1}{2} h \sin\theta \cos\theta = 0.6$ m (2.1 ft)
Equation 10 for negative values of X_D, where
$a = \tan^2\theta = 0.132$, gives
$b = Y_{DO}/X_{DO} + aX_{DO}/Y_{DO} = 2.32$
where
ΔY_D = conversion to common axis (see Figure 7) = 3.2 m (10.6 ft),
$Y_D = (aX_D^2 - bY_{DO}X_D + Y_{DO}^2)^{1/2} + \Delta Y_D$, and
$Y_D = (0.132X_D^2 - 3.35X_D + 2.08)^{1/2} + 3.2$.
Then plot at $X = X_D + \Delta X_D$, where ΔX_D is the conversion to common axis (see Figure 7)or -13.4 m (-44.0 ft)
$X = X_D - 13.4$
Equation 12 for intercept with phreatic surface I gives
$X_{DI} = (h^2 - Y_{DO}^2)/(2h \tan\theta - bY_{DO}) = -29.2$ m (-95.8 ft)
Begin drain-spacing analysis at $X_D = -30.5$ m (-100 ft) and at $X = X_D - 13.4 = -43.9$ m (-144 ft).

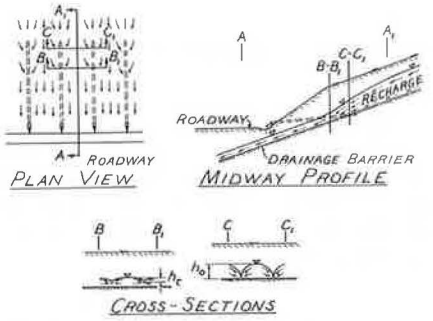

Figure 7. Three-dimensional highway cut-slope drainage with recharge along a drainage barrier.

Figure 8. Analysis for phreatic surface M in the problem in Figure 3 with a 4.6-m (15-ft) drain spacing.

PARALLEL DRAIN ANALYSIS - PHREATIC SURFACE CALCULATIONS Assumed Spacing, S = (1) 15 ft. Barrier Slope, θ = (2) 20.0 degrees

(3) X ft	(4) ΔX ft	U (5) X_U ft	U (6) Y_U ft	U (7) ΔY_U ft	U (8) θ_U degrees	D (9) X_D ft	D (10) Y_D ft	M (11) Y_{MO} ft	M (12) Y_{Mt} ft	ASSUMED (13) Δh_P ft	(14) Δh_B ft	(15) $\Delta h_P + \Delta h_B$ ft	(16) θ_M degrees	(17) P ft	(18) B ft	h_t/h_o (19) $P+B$ ft	(20) Z ft	(21) i ft	(22) $Y_{MO} - Y_{Dt}$ ft	(23) h_o ft	CALCULATED (24) h_t ft	(25) h_t/h_o	+ X_D Only: (26) Y_D ft	(27) D ft	(28) d ft	(29) $\frac{h_t h_o}{2}$ ft	(30) αt	(31) h_t/h_o
-144		-138.1	60.0			-100	60.0	60.0																				
	50	-90.3	42.5						41.1	18.9		37.1	20.7	53.5			106.7	53.3	0.348		0.5	0.42				0.387	2.60	0.09
-94		-88.1	41.7			-50	40.6	40.8	40.8	19.2	18.2	37.4	21.0	53.6	53.2		106.8	53.4	0.350	19.4	0.2	0.17				0.265	1.64	0.23
	25								40.9	19.1		37.3	20.9	53.5			106.7	53.4	0.350		0.3	0.25	28.8			0.300	2.01	0.16
									30.4	10.4		19.5	22.6	27.1			53.7	26.8	0.363		0.3	0.19				0.346	1.12	0.38
									30.6	10.2	9.1	19.3	22.2	27.0	26.6		53.6	26.8	0.360	10.7	0.5	0.31				0.447	1.46	0.27
-69		-63.1	33.2			-25	30.1	30.6	30.5	10.3		19.4	22.4	27.0			53.6	26.8	0.362		0.4	0.25	19.7			0.400	1.30	0.32
	15								23.3	7.3		12.8	26.0	16.7			32.7	16.3	0.391		0.6	0.25				0.600	1.10	0.39
									23.5	7.1	5.5	12.6	25.3	16.6	16.0		32.6	16.3	0.387	7.9	0.8	0.33				0.693	1.28	0.32
-54		-48.1	26.4			-10	22.7	23.5																				
	5								21.0	2.5		4.3	26.6	5.6			10.9	5.5	0.394		1.4	0.67				0.857	0.52	0.69
											1.8				5.3					3.9	2.1							
-49		-43.1	24.5			-5	19.6	21.0																				
	5								17.0	4.0		5.8	38.7	6.4			11.7	5.9	0.496		1.7	0.44				1.287	0.67	0.59
				2.0	21.8				17.4	3.6	1.8	5.4	35.8	6.2	5.3		11.5	5.7	0.482	5.7	2.1	0.54				1.431	0.76	0.54
-44 (=ΔX)		-38.1	22.5			0	15.3 (10.6 + 4.7)	17.4																				
	5			2.0	21.8				12.1	5.3		7.1	46.7	7.3			12.6	6.3	0.563		2.3	0.40	10.6 (=ΔY_D)			1.826	1.12	0.38
									12.0	5.4	1.8	7.2	47.2	7.4	5.3		12.7	6.3	0.567	7.6	2.2	0.38		0.50	0.45	1.786	1.09	0.39
-39		-33.1	20.5			+5	9.8	12.0																				
	5								9.6	2.4		4.2	25.6	5.5			10.8	5.4	0.387		0.7	0.54				0.477	0.87	0.49
									9.5	2.5	1.8	4.3	26.6	5.6	5.3		10.9	5.5	0.394	3.1	0.6	0.46	8.8	1.45	0.95	0.442	0.85	0.50
-34		-28.1	18.5			+10	8.9	9.5																				
	10								5.9	3.6			20.0															
											3.6		(=θ)															
-24		-18.1	14.2			+20	7.3	5.9																				
	10								2.3	3.6			20.0															
											3.6																	
-14		-8.1	9.4			+30	5.6	2.3																				
	8.1								-0.7	3.0			20.0															
											3.0																	
-5.9		-0.0	3.9			+38.1	4.2	-0.7															-3.3					

Step 3

Equation 27 gives
$S_{min} \cong (4\ Y_{Do}^2/\{\sin[(45° + \theta)/2]\})^{1/2} \cong 3$ m (10 ft)
From Figure 8, at $X_0 = 0$, $h_u = Y_U - Y_{0U} = 3.6$ m (11.9 ft), and $\theta_u = 21.8°$, Equation 28 gives
$S_{max} \cong (4\ h_u^2/\{\sin[(\theta_u + \theta)/2]\})^{1/2} \cong 12$ m (40 ft)
Use trial drain spacings S = 4.6 m (15 ft), 9.2 m (30 ft), and 13.7 m (45 ft).

Step 4. Phreatic Surface M

See columns 11 and 12 of Figure 8 for the solution for S = 4.6 m (15 ft). Similar analyses were made for S = 9.2 m (30 ft) and S = 13.7 m (45 ft). The resulting phreatic surfaces are plotted in Figure 3.

CONCLUSIONS

1. A method of estimating phreatic surfaces at the midway profile between parallel drains is introduced. Because of the large number of assumptions made in the derivation of practical mathematical analyses, the results must be considered approximate only.
2. The analysis procedure can be based on flow-net analysis or on a completely mathematical analysis. Using the mathematical analysis has the advantage in that it can be computerized by using the procedure from Figure 8 for an infinite-slope seepage source.
3. For a typical problem, the analysis procedure resulted in a range of drain spacings from 4.6 to 13.7 m (15-45 ft), which coincides well with the range commonly used in practice.
4. Further study is needed to define the optimum cross-sectional spacing to use in the analysis of a given drain spacing S. The analysis is sensitive to the cross-sectional spacing used. Using a wider spacing (ΔX in Figure 8) between cross sections results in a greater predicted drawdown. An optimum cross-sectional spacing (ΔX) as a function of drain spacing (S) is expected and needs to be verified by model study and experience.

REFERENCES

1. H. R. Cedergren. Seepage, Drainage, and Flow Nets. Wiley, New York, 1967, pp. 94-98 and 334-344.
2. W. V. Jones and R. Larsen. Investigation and Correction of a Highway Landslide. Proc., 8th Annual Idaho Engineering Geology and Soils Engineering Symposium, Pocatello, 1970, pp. 123-144.
3. T. C. Kenney, M. Pazin, and W. S. Choi. Design of Horizontal Drains for Soil Slopes. Journal of Geotechnical Engineering Division, Proc., ASCE, Vol. 103, No. GT11, Nov. 1977, pp. 1311-1323.
4. R. W. Prellwitz. Analysis of Parallel Drains for Highway Cut-Slope Stabilization. Proc., 16th Annual Idaho Engineering Geology and Soils Engineering Symposium, Boise, 1978, pp. 153-180.
5. A. Casagrande. Seepage Through Dams. In Contributions to Soil Mechanics, 1925-1940, Boston Society of Civil Engineers, 1963, pp. 295-336.
6. M. E. Harr. Groundwater and Seepage. McGraw-Hill, New York, 1962, pp. 52-54 and 64-69.
7. J. N. Luthin. Drainage Engineering. Krieger, Huntington, NY, 1973, pp. 149-169.
8. J. Wesseling. Subsurface Flow into Drains: Vol. 2—Drainage Principles and Applications. International Institute for Land Reclamation and Improvement, Wageninen, Netherlands, 1973, pp. 1-56.

Publication of this paper sponsored by Committee on Subsurface Drainage and Committee on Environmental Factors Except Frost.

Evaluation of Pavement Systems for Moisture-Accelerated Distress

S. H. Carpenter, M. I. Darter, and B. J. Dempsey, Department of Civil Engineering, University of Illinois, Urbana

The occurrence of moisture-accelerated distress (MAD) caused by poor internal drainage in a pavement is predictable after examining components of the pavement and its environment. MAD is defined as any distress primarily caused or accelerated by moisture. A fast, inexpensive method for identifying existing and potential MAD has been developed and provides a valuable tool to the maintenance engineer managing a system of pavements and the design engineer evaluating a single pavement for possible rehabilitation. In the procedure for evaluating MAD the following are done: Extrinsic and intrinsic factors are predicted, the condition of the pavement surface is surveyed, and the pavement is tested. Each of these is considered a level of refinement in determining the occurrence of MAD in the pavement system and represents increased cost. The extrinsic factors in level one are concerned with climatic influences on the moisture state of the pavement. The intrinsic factors are examined for likelihood of internal drainage problems caused by the materials and cross section being used. This provides an index of potential MAD problems. In the condition survey any existing distress on the pavement surface is directly measured. The final step is to conduct physical tests of the pavement, if it is felt that inadequate information has so far been obtained. This testing may be either destructive or nondestructive. By the final evaluation stage, one has sufficient working knowledge to make an accurate judgment as to the existence of or the potential for occurrence of MAD. One or more alternative maintenance and rehabilitation strategies can be selected, based on the evaluation results, to reduce or prevent MAD. The final selection of the alternative is based on the present condition of the pavement, traffic level, economics, and future requirements.

The data presented in this paper are part of an evaluation manual developed for field use by pavement engineers. The manual provides complete descriptions of how to identify pavements with poor internal drainage that potentially could deteriorate prematurely. Four distinct components have been examined that show a relationship to moisture-accelerated distress (MAD): extrinsic factors, intrinsic factors, condition survey, and testing.

Figure 1. Summer thermal gradations as calculated by Thornthwaite.

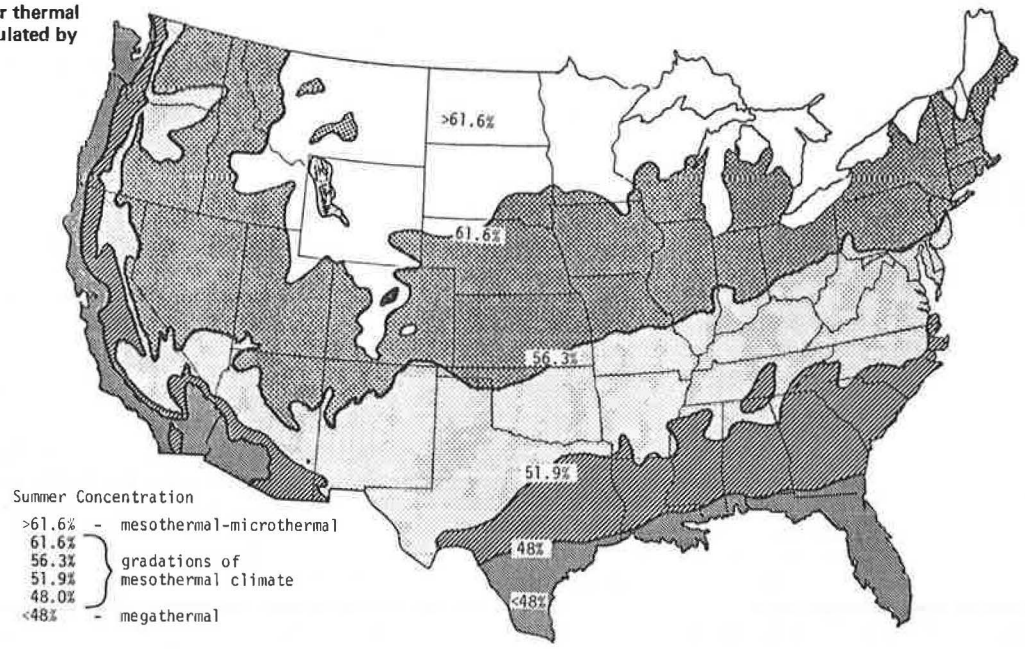

Figure 2. Distribution of Thornthwaite moisture index.

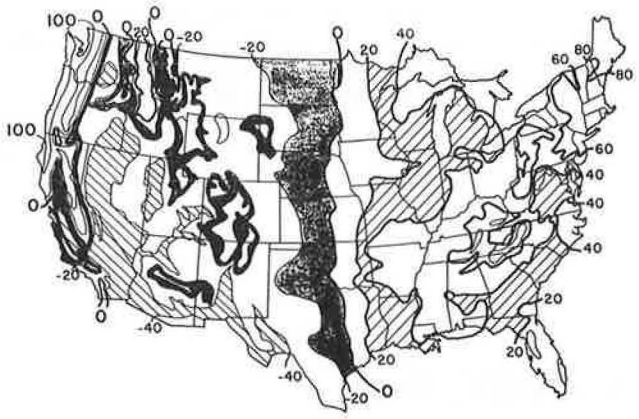

Extrinsic factors, those that influence the moisture condition in the pavement, primarily are climatic factors. The intrinsic factors represent the internal properties of the pavement that influence the moisture condition, including pavement type and material. The condition survey directly measures any existing distress on the pavement surface, which allows the condition and existing MAD to be determined. The testing may be either destructive or nondestructive and is used when the results from the first three are inconclusive concerning moisture presence.

These factors follow a logical sequence in determining, with a minimum of work, the potential that MAD has of occurring in a pavement or the possibility that MAD is responsible for the damage existing in the pavement. They represent a means of estimating the degree of MAD and can indicate what maintenance should or should not be done.

DEVELOPMENT

Extrinsic Factors

Extrinsic factors are the external factors that influence the moisture and its behavior. Climate is the major extrinsic factor that alters the moisture in a pavement system and causes the moisture to behave poorly. Temperature of and moisture in the soil are the two major climatic variables. The Federal Highway Administration currently recognizes four climatic zones (1). The north-south dividing line represents the mean freezing index value of 100, the east-west dividing line the point where yearly annual rainfall equals the yearly annual evaporation. As far as they go, these delineations do differentiate areas of different pavement performance. But they do not provide a means of differentiating within each zone on a rational basis.

To accurately identify the influence of climate on a pavement, it is necessary to have an accurate, if only relative, description of that climate. The major climatic classification schemes include the Koeppens (2) and the Thornthwaite classification schemes (3).

The Thornthwaite procedure is the only one that allows calculation of gradations in the numerical values. The same values that indicate relative moisture transport can also be used to indicate the relative severity of the winter. The Thornthwaite classification scheme uses the concept of potential evapotranspiration, or the amount of moisture that would leave the soil through evaporation and transpiration if there were an unlimited supply of water to the soil system. Obviously the more energy (heat) that reaches the earth's surface, the more water that will be removed. This is the indicator of winter severity: a comparison of the amount of potential evapotranspiration that accumulates in the three summer months with that of the total for the year. The greater the percentage the more severe the winter. Potential evapotranspiration does not occur when the temperature drops below 32°F (0°C).

Although there are doubts about the accuracy of the proposed calculation procedure used to estimate potential evapotranspiration (2), the scheme, which uses these numbers to delineate climate, is sound and has been found easier to apply than the more complicated energy-balance techniques. By comparing monthly rainfall with the monthly values of potential evapotranspiration, one may obtain indications of surplus or deficit moisture in the soil. The yearly balance is the

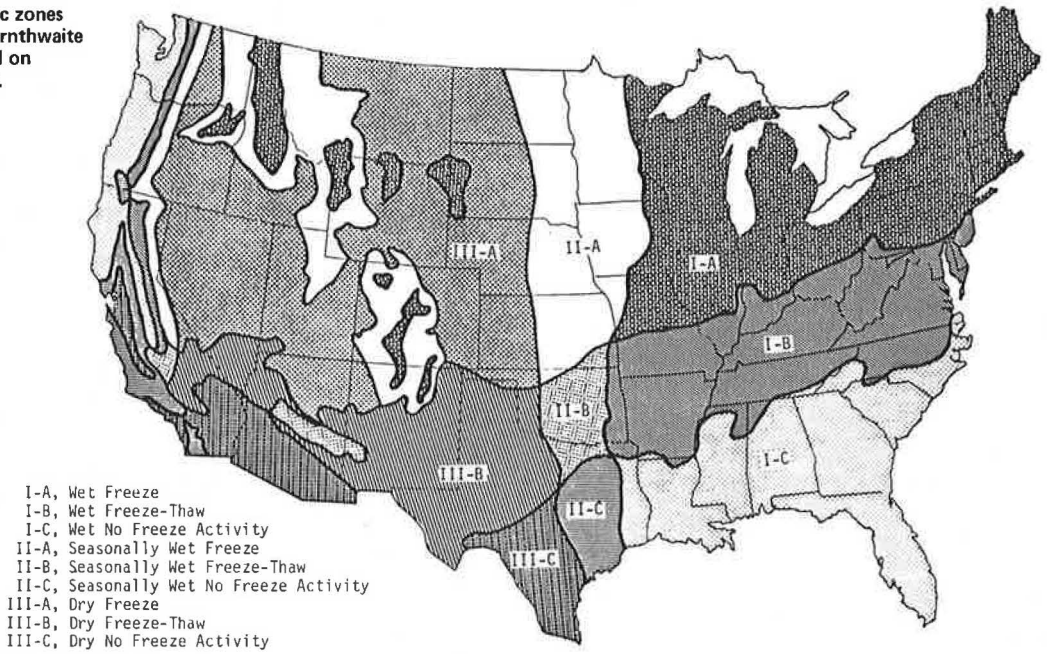

Figure 3. Climatic zones derived from Thornthwaite calculations based on material behavior.

moisture index of wetness and dryness in the soil.

The distribution of the summer thermal concentrations is shown in Figure 1 (3). The Thornthwaite moisture index is shown in Figure 2. These quantities allow for a continuous gradation between different climatic zones, which is far preferable to setting upper and lower bounds with no allowance for variation between them.

The climatic zones shown in Figure 3 were obtained from correlations with moisture and deformation studies and temperature influences. Each zone indicates an area where similar pavements will generally receive similar climatic inputs and thus perform similarly in terms of pavement structure (intrinsic factors). The following Roman numerals indicate the moisture regions and corresponding connotations: I—subgrade saturated all year and all soils generally illustrating poor performance characteristics unless stabilized; II—definite seasonal wet and dry periods shown in subgrade and performance varying greatly with the season and locale; III—subgrade generally very dry with little or no moist period and good performance exhibited by nearly all soils commonly used. The capital letters refer to the temperature regimes and corresponding connotations: A—severe winters, extremely low temperatures with high potential for frost damage in the subgrade; B—moderate winters with high potential for freeze-thaw activity throughout the winter extending deep into the base course; C—mild winters with some freeze-thaw cycling in surface course in north to high temperature stability problems in summer over entire region.

The map in Figure 3 illustrates areas of equal potential for moisture in the pavement system, regardless of the intrinsic factors. Obviously, if there is a high water table, performance will worsen. This is one of the items considered in the intrinsic analysis in the next section. The first step for the engineer is to determine which climatic zone he or she is in. The map given in Figure 3 should suffice for most locations, but the manuals provide procedures for numerical calculations when the engineer feels something other than a long-term average is needed to indicate the existing climatic conditions.

Intrinsic Factors

Intrinsic factors are those existing in the pavement or those built into it. With a given set of extrinsic factors, as previously discussed, the intrinsic factors will determine how water will behave and what the potential for MAD will be. The important intrinsic factors are

1. Pavement type,
2. Base and subbase drainability,
3. Subgrade drainability, and
4. Existing drainage.

Pavement type determines whether the base course will be exposed to a large or a small amount of water infiltrating through joints and cracks. The degree of infiltration, however, is dictated by the condition of the pavement and even more by the drainage capability of the base or subbase material. These will cause initial rapid removal of water entering by surface infiltration. If these materials build up high saturation values over a long period, permanent deformations may become excessive and pumping will develop at an accelerated rate.

The ability of a granular material to absorb or release water is a function of grain size, permeability, density, and other properties. The complexity of moisture flow, particularly unsaturated flow, has been demonstrated by Dempsey and Elzeftawy (4) in their mathematical model for moisture flow in pavements. This model is far too complicated to use for the initial study of potential moisture problems but is ideally suited for drainage analysis on a more refined level.

The ability of a pavement to absorb or drain water is the limiting factor for moisture entering through surface cracking. The ability of a crack to pass moisture is far greater than that of all but the most open-graded bases with little or no fines content (5).

The U.S. Army Corps of Engineers has used a procedure to estimate the time it takes to drain a saturated base-course drainage layer to a given percentage of the total amount that can possibly drain by gravity (6). This procedure requires that 50 percent

Figure 4. Drainability curves for granular base material.

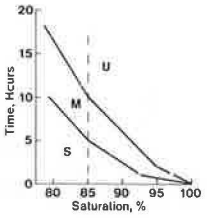

of the amount of water that can be removed must be removed within 10 days (7). This criterion was developed for airfield pavements where loading is not as frequent as it is for highways. For proper drainage in a highway application the time limit should be reduced appreciably. Another factor that must be considered is that draining half the water in a specified time does not take into account the actual moisture state of the material. A concrete sand may lose only 3 percent (by volume) of its water under gravity drainage, while a pea gravel may lose 40 percent. At the end of the specified time the sand will have a much higher saturation level and will exhibit decreased performance compared to the pea gravel. The reader is referred to the manuals for the actual calculation process (8, 9).

The critical saturation level has been established as 85 percent. This is a point where repeated loading damage increases drastically for granular materials (10). The desired time to reach this saturation has been determined as between 5 and 10 h. Figure 4 illustrates the criteria developed for granular material (8). These curves can be developed from

1. Roadway geometry,
2. Permeability estimate,
3. Effective porosity estimate, and
4. Gradation and percent fines.

A material classified as unacceptable will not flow water readily and in a wet climate will not have enough time to drain before another rainfall. This material would tend to remain above the critical saturation level. A marginal material will have slightly less fines and tend to remain nearer the critical saturation level.

The subgrade material also will experience moisture problems. The degree of severity will vary depending on texture, topography, and water-table depth. These factors are important in the agricultural classification of soils because they directly influence the drainage characteristics of the soil. Hole (11) used this classification for soils and applied a numerical value for each classification, which he termed the natural drainage index (NDI). It varies from -10 for an "excessively drained" i (good) soil to +10 for a "very poorly drained" k (poor) soil. The drainage terminology is readily available on most soil maps, and, although different from engineering terminology, it does describe the drainability of the subgrade material. This description can be used to indicate the relative ability of a subgrade to hold water.

Frequent changes in soil make the application of this indicator a very approximate procedure. In studies on concrete roads, Haas (12) showed very good relationships among the NDI, deterioration, and maintenance required. This indicator can, then, indicate where moisture is most likely to cause problems in a pavement, although the extent of the problems caused by the soil variation cannot be determined. NDI can be used to indicate areas where drains may be effective, according to soil conditions.

A subgrade was assumed to be impermeable when the drainability time for the granular layers was developed. If the subgrade is good it will aid the granular layer by providing vertical drainage to the water table, and marginal drainability will be altered to an acceptable level. If the subgrade is poor it cannot assist in draining the granular layer, and its performance will be low as indicated by Haas (12) and will produce accelerated distress. An intermediate subgrade will not aid the granular layer, nor will it have excessively poor performance.

Surface Condition

The extrinsic and intrinsic analysis will indicate the extent to which moisture problems may develop, but the surface condition points to the extent to which moisture has actually damaged the pavement. The type, amount, and severity of distress present are necessary to accurately describe the overall condition of the pavement. The presence of particular distress types, or their absence, can indicate the presence or absence of MAD.

The distress that is present can be examined with the classification indicated from the extrinsic and intrinsic analyses. The following situations could arise for a given pavement.

1. If only minor distress exists, the rate of deterioration will depend on the level of moisture predicted by the extrinsic and intrinsic evaluation. The higher the rating, the faster the deterioration and the sooner maintenance or rehabilitation needed.
2. If significant distress exists, this may or may not indicate moisture damage, depending on what distress is present. Moisture-related distress indicates maintenance or rehabilitation is needed (a) immediately if in a wet area, (b) soon if in a seasonally wet area, or (c) in the future if in a dry area.

Distress must be defined by type, severity, and quantity. Extensive research work has been recently accomplished in the development of distress-identification manuals for streets, airfields, and highways (9, 14, 16). This development required extensive field surveys in many parts of the United States and discussions with many engineers working in pavement evaluation, maintenance, and rehabilitation. Numerous training sessions have been held with field maintenance personnel to ensure that the definitions are practical and easy to use.

A composite pavement distress index, developed by Shahin and others (13, 16), combines the types, severities, and quantities of distress into a single value for any given pavement section. This was accomplished by defining a pavement condition index (PCI) as follows:

$$PCI = 100 - \sum_{i=1}^{p} \sum_{j=1}^{m_i} a(T_i, S_j, D_{ij})\, F(t, q) \quad (1)$$

where

- $a(\ )$ = deduct value depending on distress type T_i, level of severity S_j, and density (or quantity) of distress D_{ij};
- i = counter for distress types;
- j = counter for severity levels;
- p = total number of distress types for pavement type under consideration;
- m_i = number of severity levels for the ith type of distress; and

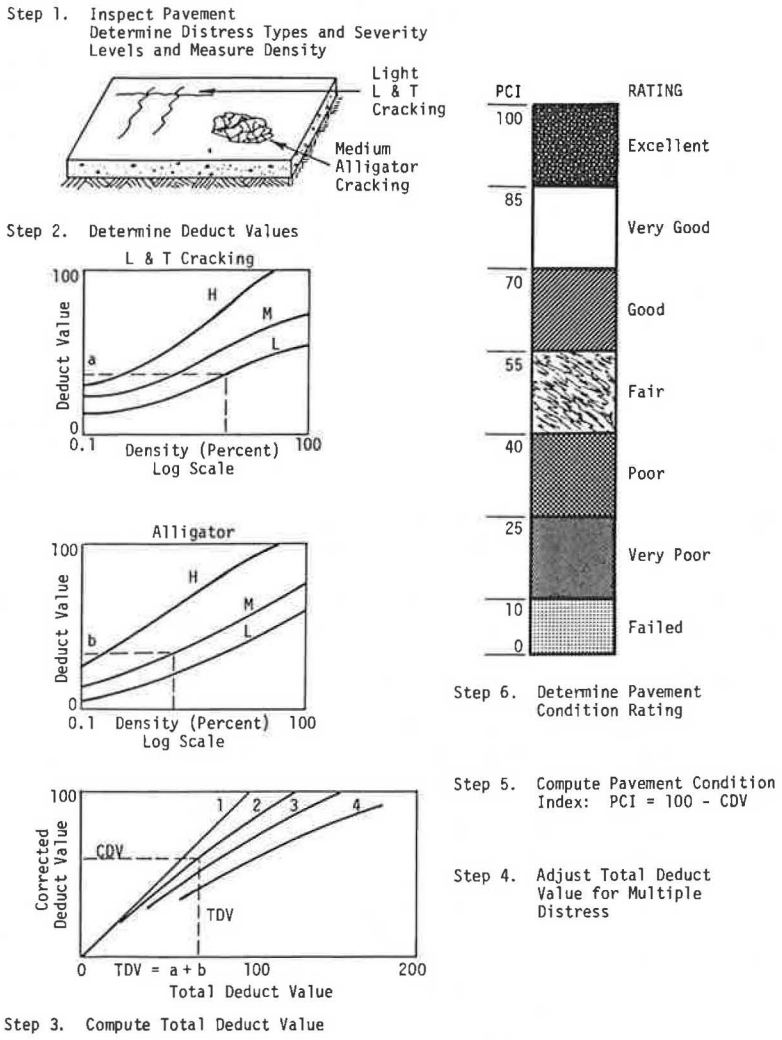

Figure 5. Steps to calculate the pavement condition index for a street.

$F(t,q)$ = an adjustment function for multiple distresses that vary with total summed deduct value (t) and number of deducts (q).

Deduct-value curves for each distress type and severity level were determined based upon the composite judgment of a large group of experienced pavement engineers. Thus, the calculated PCI of a given pavement section represents the overall engineering judgment of a large group of experienced engineers as to the pavement's structural integrity (protection of the investment, maintenance needs) and surface operational condition (user-related consideration). The steps necessary to determine the PCI for a given street are summarized in Figure 5. The procedure is very simple and straightforward, has been officially adopted by the U.S. Air Force, and is under trial implementation by other agencies.

The PCI rating deduct values can be used to indicate the distress condition that is related to moisture damage. A MAD index can be defined as the percentage of deduct values caused or accelerated primarily by moisture. The severity of this index will indicate how far developed moisture damage is and the rate at which further deterioration may be expected to develop. Combined with the extrinsic and intrinsic analysis, both the PCI and the MAD index can indicate the efficacy of installing drainage, performing maintenance, or reconstructing at the present time or in the immediate future (8).

Testing

A testing program is the final step in the analysis procedure and should be considered only when the previous three factors produce anomalous results. When moisture damage is predicted from extrinsic and intrinsic analyses but the condition index does not show any moisture damage, the properties of the pavement system must be investigated. The same must be done if there is extensive moisture damage, but the intrinsic and extrinsic factors indicate that no moisture problems should exist. Samples may have to be taken to the laboratory for testing, or the testing may be done in situ.

The major variables influencing the intrinsic analysis will be the moisture-related properties of the base, subbase, or subgrade. As such, the properties that might need to be determined will include

1. Gradation,
2. Clay content (type of fines),
3. Permeability,
4. Moisture content, and
5. Deformation characteristics.

These properties can be determined from laboratory tests of disturbed and undisturbed samples. The

permeability and deformation characteristics require undisturbed samples for laboratory testing. This can be quite expensive and impractical for the level of analysis conducted in this study. The more suitable approach would be to conduct an in situ permeability test (15) and appropriate deflection measurements of the pavement and shoulder. These tests, with gradation, mineral data, and moisture content, would indicate whether the intrinsic analysis based on original properties was in error and by what amount.

Given the additional data provided by the testing, a new intrinsic analysis will provide a new classification that is a better indicator of the moisture-related condition of the pavement.

APPLICATION

The four areas of analyses briefly presented here have been more fully explained in a series of manuals prepared for the Federal Highway Administration as a part of the subdrainage and shoulder rehabilitation project. These manuals detail the data used in constructing each procedure to obtain a true indication of the moisture influence on the pavement. The first two manuals present the research background for moisture and distress, respectively, and the third, which contains the procedures, is the manual to be used by the field and maintenance engineers to evaluate their pavements.

The evaluation manual contains step-by-step procedures that allow field personnel with a minimum of training to complete a MAD analysis. The person performing the extrinsic analysis may locate the pavement on a series of climatic maps. If he or she chooses he or she can use available climatic data from monthly weather bulletins and can calculate the variables for the desired number of years. The calculations for years the pavement has been in service will provide an indication of the actual moisture the pavement has been exposed to. For longer time in service, the moisture values will be closer to the long-term average values used to construct the maps. This analysis provides a climatic indicator that relates the severity of moisture available to the pavement itself.

The intrinsic analysis requires knowledge of the type of base or subbase material and the subgrade material. The base course is analyzed to determine its potential for retaining moisture. The subgrade is classified as to its drainability, from soil maps where possible. The combination of these two material classifications provides an indicator of the potential a pavement has to hold water and thus to increase the potential for moisture damage. When the extrinsic and intrinsic factors are combined, an indicator or potential MAD is formed where potentially available moisture is combined with moisture-sensitive materials. Using general descriptions of the expected behavior of the materials, the evaluator will have a physical description of the material in the pavement. This provides a clearer understanding of the expected behavior.

The distress-condition survey produces two numerical indices that are related to the overall condition (PCI) and the extent of moisture-related damage that has occurred in the pavement (MAD). The evaluator follows a step-by-step procedure to examine the pavement section under question and to determine the condition indices. The evaluator then enters a table in which the condition indices allow statements to be made concerning the present and future condition of the pavement.

Using these tables, the evaluator can obtain physical descriptions of his or her pavement section along with explanations relating the current state of the pavement to expected moisture damage in the future. Recommendations can be made concerning maintenance, rehabilitation, and use of subdrainage to alter the growth of moisture-related distress. The maintenance recommendations are coordinated with the results of a part of the overall project that determines what warrants subdrainage. That portion of the study requires more in-depth material property determination than is necessary for development of the manual presented in this paper. The general implications that are described in this surficial analysis are backed up quite well by the more detailed analysis.

SUMMARY

A manual has been prepared that allows an evaluator who has minimum experience or training to analyze a pavement section and determine whether the distress present is moisture related and if so to what extent. This field manual examines the potential for moisture-accelerated damage from the following viewpoints:

1. Extrinsic, or external, climatic influences;
2. Intrinsic, or internal, material properties;
3. Condition index, or the extent of moisture-related distress; and
4. Testing, or the use of tests to examine conflicting results.

By following a step-by-step procedure the evaluator will determine a number of moisture-related facts about the particular pavement section under investigation. Among these facts are

1. Origin of moisture problems caused by (a) climate or (b) a particular material in the base or subgrade;
2. Extent of moisture problems;
3. Usefulness of subdrainage in retarding deterioration; and
4. Recommendations for maintenance and rehabilitation.

ACKNOWLEDGMENT

Support for the project was provided by the Federal Highway Administration, Office of Research and Development. We are grateful for the technical coordination provided by George W. Ring III, contract manager.

The opinions, findings, and conclusions expressed are ours and not necessarily those of the Federal Highway Administration or the U.S. Department of Transportation.

REFERENCES

1. M. I. Darter. Design of Zero-Maintenance Plain Jointed Concrete Pavement: Vol. I—Development of Design Procedures. Federal Highway Administration, Rept. FHWA-RD-111-77, 1977.
2. H. J. Critchfield. General Climatology, 3rd Ed. Prentice-Hall, Englewood Cliffs, NJ, 1974.
3. C. W. Thornthwaite. An Approach Toward a Rational Classification of Climate. Geographical Review, Vol. 38, No. 1, 1948, pp. 55-94.
4. B. J. Dempsey and A. E. Elzeftawy. Moisture Movement and Moisture Equilibria in Pavement Systems. Univ. of Illinois, Urbana, Interim Rept. IHR-604, 1976.
5. B. F. McCullough, A. Abou-Ayyash, R. W. Hudson, and J. D. Randall. Design of Continuously Reinforced Concrete Pavements for Highways. NCHRP Project 1-15, Final Rept., 1975.
6. W. E. Strohm, Jr., E. H. Nettles, and C. C.

Calhoun, Jr. Study of Drainage Characteristics of Base Course Materials. HRB, Highway Research Record 203, 1967, pp. 8-28.
7. E. S. Barber and C. L. Sawyer. Highway Subdrainage. HRB, Proc., Vol. 31, 1952, pp. 643-666.
8. S. H. Carpenter, M. I. Darter, and S. Herrin. A Pavement Moisture Accelerated Distress (MAD) Identification System. Vol. I. Federal Highway Administration (in preparation).
9. M. I. Darter and S. Herrin. Pavement Distress Identification Manual. Vol. II. Federal Highway Administration (in preparation).
10. A. J. Haynes and E. J. Yoder. Effects of Repeated Loading on Gravel and Crushed Stone Base Course Materials Used in the AASHO Road Test. HRB, Highway Research Record 39, 1963, pp. 82-96.
11. F. D. Hole. Suggested Terminology for Describing Soils as Three-Dimensional Bodies. Soil Science Proc., Vol. 17, No. 2, 1953, pp. 131-135.
12. W. M. Haas. Drainage Index in Correlation of Agricultural Soils With Frost Action and Soil Performance. HRB, Bull. 111, 1955, pp. 85-98.
13. M. Y. Shahin, M. I. Darter, and S. D. Kohn. Development of a Pavement Maintenance Management System: Vol. I—Airfield Pavement Condition Rating. U.S. Air Force Civil Engineering Center, Tindall Air Force Base, FL, Technical Rept. AFCEC-TR-76-27, Dec. 1976.
14. M. Y. Shahin, M. I. Darter, and S. D. Kohn. Development of a Pavement Maintenance System: Vol. II—Airfield Pavement Distress Identification Manual. U.S. Air Force Civil Engineering Center, Tindall Air Force Base, FL, Technical Rept. AFCEC-TR-76-27, Dec. 1976.
15. U. L. Maytin. A New Field Test for Highway Shoulder Permeability. HRB, Proc., Vol. 41, 1962, pp. 109-124.
16. M. Y. Shahin, M. I. Darter, and S. D. Kohn. Development of a Pavement Condition Index for Roads and Streets. U.S. Army Construction Engineering Research Laboratory, Champaign, IL, Interim Rept. M-232, May 1978.

Publication of this paper sponsored by Committee on Subsurface Drainage and Committee on Environmental Factors Except Frost.

Influence of Precipitation, Joints, and Sealing on Pavement Drainage

Barry J. Dempsey, Department of Civil Engineering, University of Illinois, Urbana
Quentin L. Robnett, School of Civil Engineering, Georgia Institute of Technology, Atlanta

A study was conducted to determine the influence of precipitation, joints, and sealing on drainage of concrete pavements. Detailed drainage studies were conducted on four pavement test sections. Two jointed concrete pavement test sections were located on I-85 near Atlanta, and one continuously reinforced concrete pavement test section and one reinforced jointed concrete pavement test section were located on I-57 near Champaign, Illinois. Subsurface drainage was installed on the Georgia test pavements as part of the test preparation. Subsurface drainage on the Illinois test pavements had been installed previously as part of a shoulder rehabilitation program. All drainage outflows were measured by specially designed flowmeters capable of continuously monitoring volumes. All precipitation data were obtained on an hourly basis from weather stations near the pavement test sites. Analysis of data indicated that pavement drainage outflow was significantly related to precipitation. It was also found that the edge joint was a major factor contributing to water infiltration into pavement systems. Edge-joint sealing was found to reduce water infiltration in the jointed concrete pavement test sections in both Georgia and Illinois. Edge-joint sealing on the continuously reinforced section in Illinois did not significantly reduce surface infiltration. No measurable drainage outflow was observed on the completely sealed pavement test section in Georgia.

Water is a fundamental variable in most problems associated with pavement construction, design, behavior, and performance. Moisture usually has very significant effects on pavement systems because the structural section and subgrade are often susceptible to large variations in moisture content and are strongly influenced by surrounding climatic conditions.

The problem of water in pavements has long been of concern to engineers. Cedergren and O'Brien (1) have listed over 225 abstracts of pertinent literature on the subject of subdrainage. Recently Dempsey and others (2) completed a state-of-the-art review of the existing literature on and current practices for subdrainage, shoulder structures, and maintenance of pavement systems for the Federal Highway Administration.

Methods for controlling moisture in pavement systems can generally be classified in terms of protection through the use of waterproofing membranes and anticapillary courses, the use of materials insensitive to moisture changes, and water evacuation by means of subdrainage. Ridgeway (3), Ring (4), Woodstrom (5), and Barksdale and Hicks (6) have all reported on the problem of water infiltration through cracks and joints of concrete pavements and have indicated that the performance life of many concrete pavements could be extended by improved protection and drainage of the structural section. Darter and Barenberg (7) have indicated that protection of the structural pavement section and subgrade by adequate sealing of joints and cracks can help prolong pavement life.

Although water-related distress is obvious in pavement systems, few studies have been conducted to determine the pavement conditions that contribute to water problems and the procedures that will best mitigate these problems. Ridgeway (3) and Barksdale and Hicks (6) have conducted controlled field tests to determine the percentage of surface water infiltrating into pavement systems. Ridgeway (3) measured infiltration rates for both portland cement concrete and asphalt concrete pavements in Connecticut. Barksdale and Hicks (6) conducted tests at two Georgia Interstate locations that have plain jointed portland cement concrete traffic lanes and asphalt concrete shoulders. These studies have indicated that

Table 1. Detailed description of drainage test sites.

Item	Test Site G1	G2	I1	I2
Location	Georgia I-85N, Fulton County, 16 km southwest of Atlanta	Georgia I-85N, Fulton County, 16 km southwest of Atlanta	Illinois I-57S, Champaign County, 8 km south of Champaign	Illinois I-57N, Champaign County, 8 km south of Champaign
Surface course				
Type	Plain jointed portland cement concrete without dowel bars	Plain jointed portland cement concrete without dowel bars	Continuously reinforced portland cement concrete	Reinforced jointed portland cement concrete with dowel bars
Width	7.3 m	7.3 m	7.3 m	7.3 m
Thickness	25.4 cm	25.4 cm	20.3 cm	25.4 cm
Joint spacing	9.1 m	9.1 m	-	30.5 m
Transverse slope	0.83% sloped to outside shoulder	0.83% sloped to outside shoulder	1.56% crowned at centerline	1.56% crowned at centerline
Longitudinal slope	1.00%	1.00%	0.25%	0.25%
Length of test section	30.5 m	30.5 m	153.3 m	151.8 m
Width of test section	7.3 m	7.3 m	3.7 m	3.7 m
Date constructed	1964	1964	1965	1965
Base course				
Type	Crushed granite, dense graded	Crushed granite, dense graded	Crushed limestone, Illinois CA 8	Crushed limestone, Illinois CA 8
Thickness	40.6-60.9 cm	40.6-60.9 cm	10.2 cm	15.2 cm
Saturated hydraulic conductivity	4.7 μm/s	4.7 μm/s	3.5 μm/s	3.5 μm/s
Subgrade				
Type	A-4	A-4	A-6	A-6
Saturated hydraulic conductivity	10 μm/s	10 μm/s	1 μm/s	1 μm/s
Shoulders				
Type	Asphalt concrete on cement-treated aggregate	Asphalt concrete on cement-treated aggregate	Bituminous aggregate mixture, reconstructed 1976	Bituminous aggregate mixture, reconstructed 1976
Width	0.6 m inside, 3.1 m outside	0.6 m inside, 3.1 m outside	1.2 m inside, 3.1 m outside	1.2 m inside, 3.1 m outside
Thickness	5.1 cm asphalt concrete 15.2 cm cement-treated aggregate	5.1 cm asphalt concrete 15.2 cm cement-treated aggregate	20.3 cm	20.3 cm
Subsurface drainage				
Type	Corrugated plastic pipe, constructed Oct. 1977	Corrugated plastic pipe, constructed Oct. 1977	Concrete pipe, constructed 1976	Concrete pipe, constructed 1976
Diameter	10.2 cm I.D.	10.2 cm I.D.	15.2 cm I.D.	15.2 cm I.D.
Location	Adjacent to pavement edge	Adjacent to pavement edge	Adjacent to pavement edge	Adjacent to pavement edge
Depth	86.4 cm	86.4 cm	55.9 cm	60.9 cm
Drainage envelope	Crushed granite, open graded	Crushed granite, open graded	Concrete sand	Concrete sand
Saturated hydraulic conductivity	400 μm/s	400 μm/s	46 μm/s	46 μm/s
Test site drainage area	248.1 m^2	233.6 m^2	560.8 m^2	555.2 m^2

Note: 1 km = 0.62 mile; 1 m = 3.3 ft; 1 cm = 0.39 in; 1 μm/s = 0.284 ft/day; 1 m^2 = 1.2 yd^2.

Figure 1. Plan view of test sections G1 and G2.

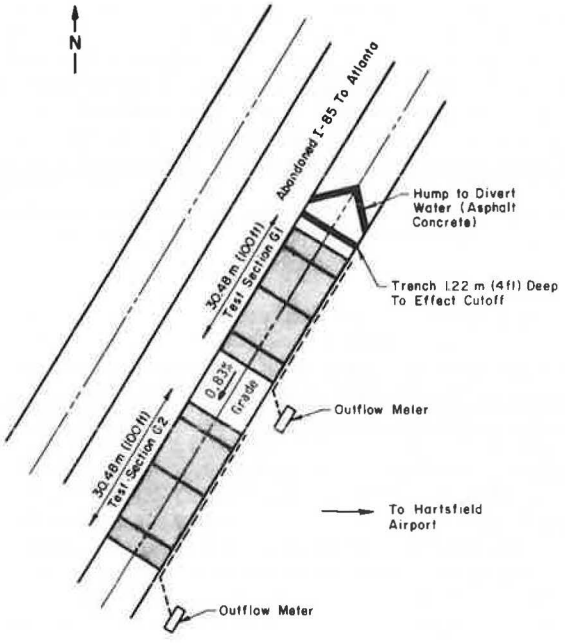

Figure 2. Subdrainage system constructed at test sections G1 and G2.

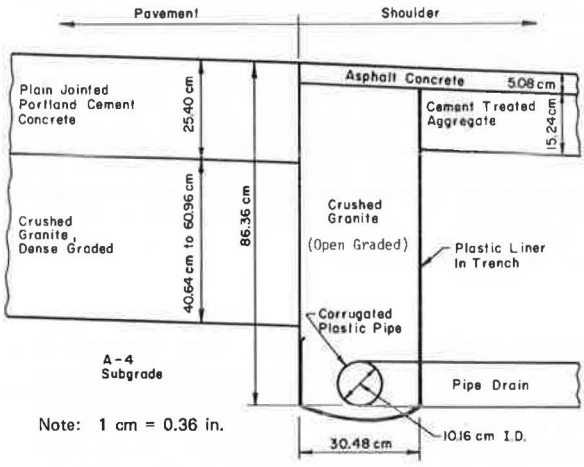

Figure 3. Sawed transverse and longitudinal joints on test section G1.

Figure 4. Transverse and longitudinal sealed joints on test section G2.

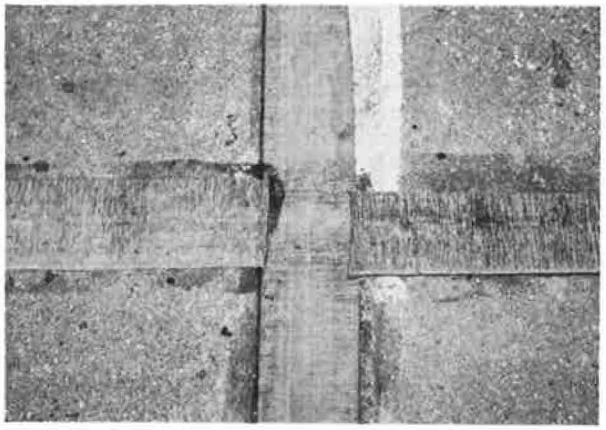

Figure 5. Georgia test site showing cutoff trench, water diversion, and part of section G1.

quantitative field data are needed in order to determine the amount of water entering the pavement system and to analyze the effectiveness of various corrective procedures.

This study was conducted to determine the influence of precipitation, joints, and sealing on pavement drainage. The specific objectives were to

1. Determine relationships between precipitation and drainage outflow,

Figure 6. Drainage flowmeter.

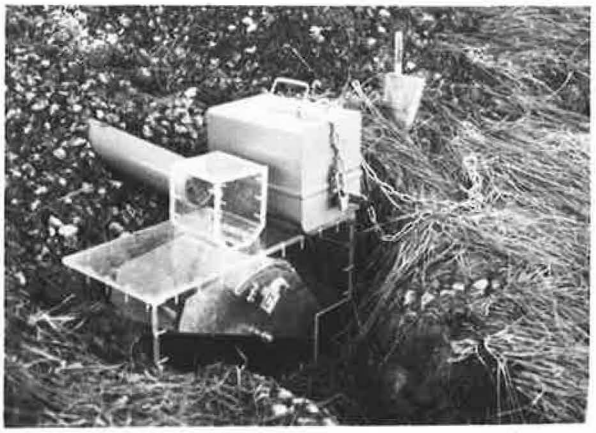

Figure 7. Subdrainage system at test sections I1 and I2.

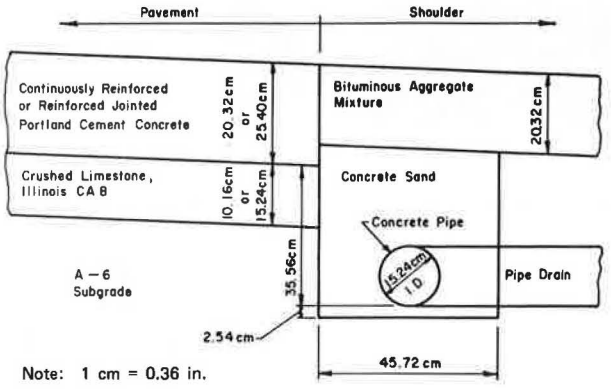

Figure 8. Pavement edge joint on test section I2.

2. Investigate the influence of pavement type on subsurface drainage, and
3. Investigate the effectiveness of joint sealing on water infiltration.

TEST SITES

Location

The drainage studies were conducted on four pavement test sections. Two test sections were located on an abandoned section of I-85 approximately 16 km (10 miles) southwest of Atlanta near the Hartsfield-Atlanta International Airport. The remaining two test sections were located on I-57 about 8 km (5 miles) south of Champaign, Illinois.

Description

A detailed description of the pavement test sections is shown in Table 1. The two test sections in Georgia, designated G1 and G2, were located on the northbound lane of I-85. Each test section was 30.5 m (100 ft) long. The pavement surface thickness was 25.4 cm (10 in) of plain jointed portland cement concrete without reinforcing steel or load-transfer devices. The transverse joint spacing was 9.1 m (30 ft) and the joint faulting was less than 6.35 mm (0.25 in). The base course was a dense-graded crushed granite varying in thickness from 40.6 to 60.9 cm (16 to 24 in). The shoulders were composed of 5.1 cm (2 in) of asphalt concrete placed on 15.2 cm (6 in) of cement-treated aggregate. The subgrade was classified as an A-4 soil with an optimum water content of 20.4 percent and a dry density of 1651 kg/m^3 (103.1 lb/ft^3). The saturated hydraulic conductivities (coefficients of permeability) are shown in Table 1.

Figure 1 shows a detailed layout of test sections G1 and G2. Each test section included three transverse joints. As part of the site preparation, subdrains were placed along the outside edge of the portland cement concrete pavement on each section. The drainage system (Figure 2) was constructed with 10.2-cm (4-in) inside-diameter corrugated and perforated plastic tubing. The outside and bottom of the drainage trench were lined with plastic sheeting before backfilling with open-graded crushed granite in order to keep groundwater seepage from the drain. Asphalt concrete about 5.1 cm (2 in) thick was used to cap the edge-drain trench.

All transverse and longitudinal joints on sections G1 and G2 were sawed with a 5.1-mm-wide (0.20-in) diamond saw to a depth of 7.6 cm (3 in) and thoroughly cleaned (Figure 3). All transverse and longitudinal joints on section G2 were sealed with 30.5-cm-wide (12-in) strips of Bituthene waterproof membrane (Figure 4). All joints on section G1 were initially left unsealed.

As shown in Figures 1 and 5 a deep cutoff trench and water diversion were constructed at the north end of section G1 to keep extraneous surface water from the test sections. The pipe drains from sections G1 and G2 were connected to specially constructed flowmeters that

Figure 9. Sealed pavement edge joint on test section I2.

Table 2. Drainage data for test sections G1 and G2.

Storm No.	Date	Total Precipitation (cm)	G1[a] Precipitation Volume (m^3)	G1[a] Pipe Outflow Volume (m^3)	G1[a] Outflow (%)	Precipitation Volume of G2[b] (m^3)
1	11/6/77	2.51	6.23	0.35	5.6	5.86
2	11/16-17/77	0.25	0.62	0.09	14.5	0.58
3	11/22-23/77	0.48	1.19	0.46	38.6	1.12
4	11/27-28/77	1.98	4.91	0.85	17.3	4.62
5	11/30-12/2/77	0.79	1.96	0.40	20.4	1.84
6	12/14/77	0.79	1.96	0.88	44.9	1.84
7	12/17-18/77	0.68	1.69	0.55	32.5	1.59
8	12/24-25/77	1.19	2.95	0.58	19.7	2.78
9	12/29/77-1/1/78	2.72	6.75	2.35	34.8	6.35
10	1/5-8/78	4.34	10.77	2.70	25.1	10.14
11	1/12-14/78	0.61	1.51	1.32	87.4	1.42
12	1/17-20/78	5.18	12.85	4.40	34.2	12.10
13	1/24-25/78	7.59	18.83	5.09	27.0	17.73
14	2/13/78	0.33	0.82	0.21	25.6	0.77
15	2/18/78 4/6/78	0.30	0.74	0.23	31.1	0.70
16	4/11/78	1.85	4.59	0.08	1.7	4.32
17	4/12-13/78	2.16	5.36	0.11	2.1	5.04
18	4/18/78	2.95	7.32	0.32	4.4	6.89
19	4/24-25/78	1.83	4.54	0.00	0.0	4.27
20	5/1/78	4.09	10.15	0.01	0.1	9.55
21	5/3-4/78	1.02	2.53	0.00	0.0	2.38
22	5/7/78	1.50	3.72	0.00	0.0	3.50
23	5/8/78	3.84	9.53	0.02	0.2	8.97
24	5/13/78	1.60	3.97	0.00	0.0	3.74
25	5/26/78	2.90	7.19	0.00	0.0	6.77
26	5/28/78	3.40	8.44	0.00	0.0	7.94
27	6/6-7/78	4.95	12.28	0.04	0.3	11.56

Note: 1 cm = 0.39 in; 1 m^3 = 264 gal.

[a] All joints initially unsealed until storm 16; then joints sealed.
[b] All joints initially sealed; no measurable pipe outflow volume and thus no percentage outflow.

could continuously monitor outflow (Figure 6). All precipitation data for the Georgia test site were obtained from a weather station located 3.5 km (2.2 miles) away at Hartsfield Airport. Drainage studies at the test site were conducted continuously from November 1, 1977, through June 15, 1978, at which time construction operations in the area forced an end to testing. The pavement edge joint on section G1 was sealed with a waterproof membrane on April 6, 1978, in order to study the influence of the edge joint on water infiltration.

The test sections on Illinois I-57 were of continuously reinforced portland cement concrete pavement and a reinforced jointed portland cement concrete pavement with dowel bars (see Table 1). The pavement test sections were located next to each other on opposite traffic lanes. The continuously reinforced pavement, section I1, con-

Table 3. Drainage data for test sections I1 and I2.

Storm No.	Date	Total Precipitation (cm)	I1 Continuously Reinforced Concrete Pavement			I2 Reinforced Jointed Concrete Pavement		
			Precipitation Volume (m^3)	Pipe Outflow Volume (m^3)	Outflow (%)	Precipitation Volume (m^3)	Pipe Outflow Volume (m^3)	Outflow (%)
1	11/6-9/77	0.98	-	-	-	5.44	3.67	67.5
2	11/20/77	0.28	-	-	-	1.55	0.45	29.0
3	11/23/77	0.16	-	-	-	0.89	0.21	23.6
4	11/30-12/1/77	2.52	14.13	2.53	17.9	13.99	5.08	36.3
5	12/2-3/77	0.58	3.25	1.32	40.6	3.22	1.43	44.4
6	3/20-23/78	2.86	16.04	6.69	41.7	15.88	11.37	71.6
7	4/3-4/78	1.09	6.11	1.15	18.8	6.05	4.85	80.2
8	4/6/78	0.43	2.41	1.56	64.7	2.39	(equipment malfunction)	
9	4/8/78	0.58	3.25	1.33	40.9	3.22	2.14	66.4
10	4/10/78	0.73	4.09	0.45	11.0	4.05	(equipment malfunction)	
11	4/17-19/78	2.63	14.75			14.60	7.33	50.2
12	4/22-23/78	0.63	3.53			3.50	2.25	64.3
13	4/25/78	0.51	2.86	(broken tipping bucket)		2.83	2.37	83.7
14	5/4-5/78	2.78	15.59			15.43	5.01	32.5
15	5/7-8/78	1.21	6.78			6.72	3.60	53.6
16	5/11-15/78	5.16	28.93	3.98	13.8	28.65	(equipment malfunction)	
17	6/1/78	0.28	1.57	0.01	0.6	1.55	0.63	40.6
18	6/7/78 6/8/78[a]	0.43	2.41	0.25	10.4	2.39	0.91	38.1
19	6/18/78	1.50	8.41	2.46	29.3	8.33	1.37	16.4
20	6/20/78	3.15	17.66	1.41	8.0	17.49	1.27	7.3
21	6/30-7/3/78	7.49	42.00	5.74	13.7	41.58	4.54	10.9
22	7/9/78	1.16	6.50	0.46	7.1	6.48	0.59	9.1
23	7/13/78	1.91	10.71	0.21	2.0	10.60	0.97	9.2
24	7/23-24/78	1.00	5.60	1.86	33.2	5.55	0.81	14.6
25	7/26/78	1.02	5.72	1.42	24.8	5.66	0.83	14.7
26	8/2/78	5.47	30.67	4.01	13.1	30.37	3.14	10.3

Note: 1 cm = 0.39 in; 1 m^3 = 264 gal.

[a] Edge joints sealed on this date.

Figure 10. Influence of precipitation on drainage outflow in unsealed test section G1 on 12/14-15/77.

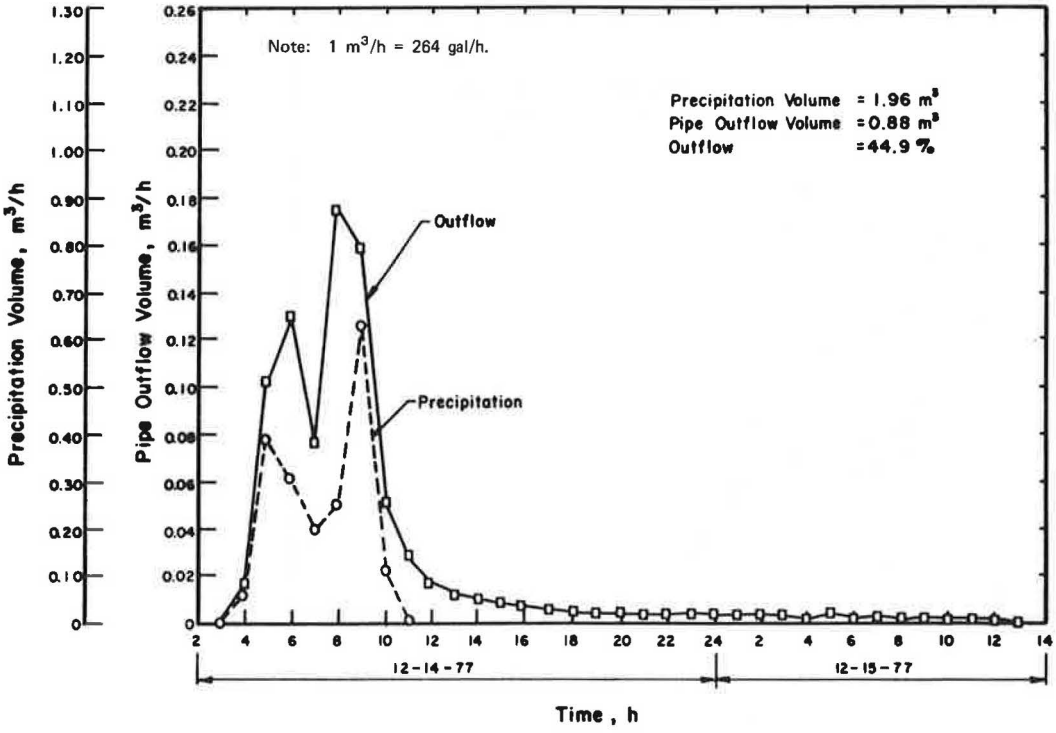

sisted of a 20.3-cm (8-in) concrete surface placed on a 10.2-cm (4-in) crushed-limestone base course. The jointed pavement, section I2, consisted of 25.4 cm (10 in) of concrete surface placed on 15.2 cm (6 in) of crushed-limestone base course. The subgrade for sections I1 and I2 was classified as an A-6 soil. The saturated hydraulic conductivities for the base course and subgrade in the two test sections are shown in Table 1.

Test section I1 was 153.3 m (503 ft) long and test section I2 was 151.8 m (498 ft) long; both had been constructed in 1965.

The bituminous aggregate shoulders were reconstructed in 1976, at which time subsurface drainage (Figure 7) was installed. The shoulder thickness was 20.3 cm (8 in).

The continuously reinforced pavement test section,

Figure 11. Influence of precipitation on drainage outflow in unsealed test section G1 on 11/30-12/1/77.

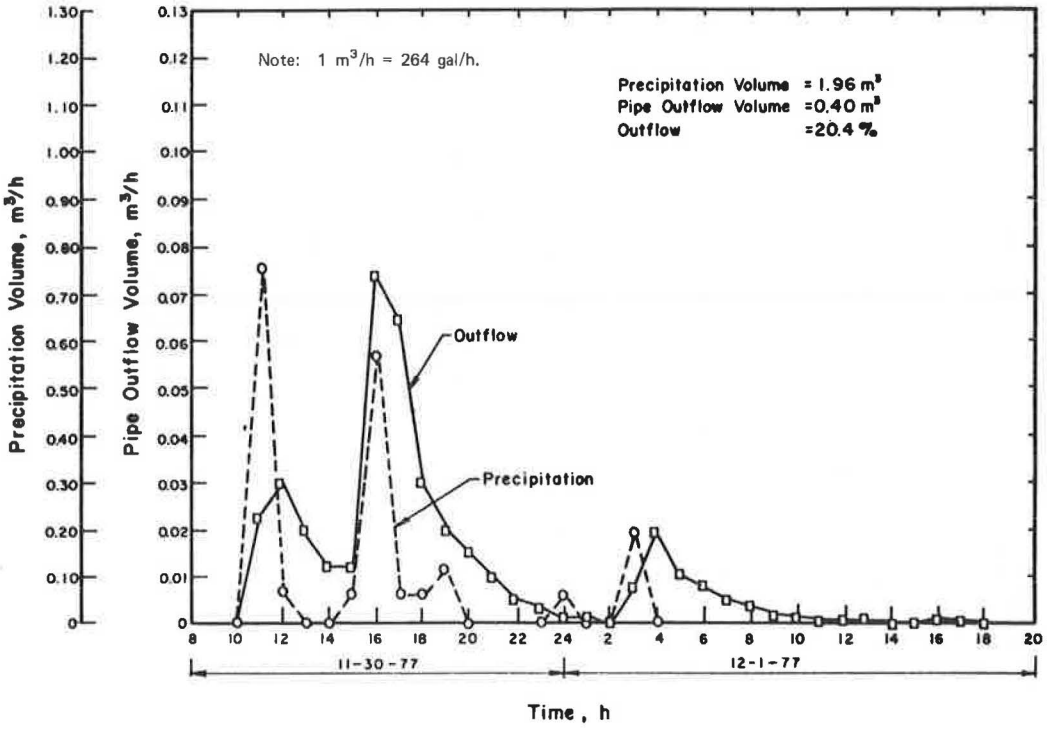

Figure 12. Influence of precipitation on drainage outflow in sealed test section G1 on 4/11-12/78.

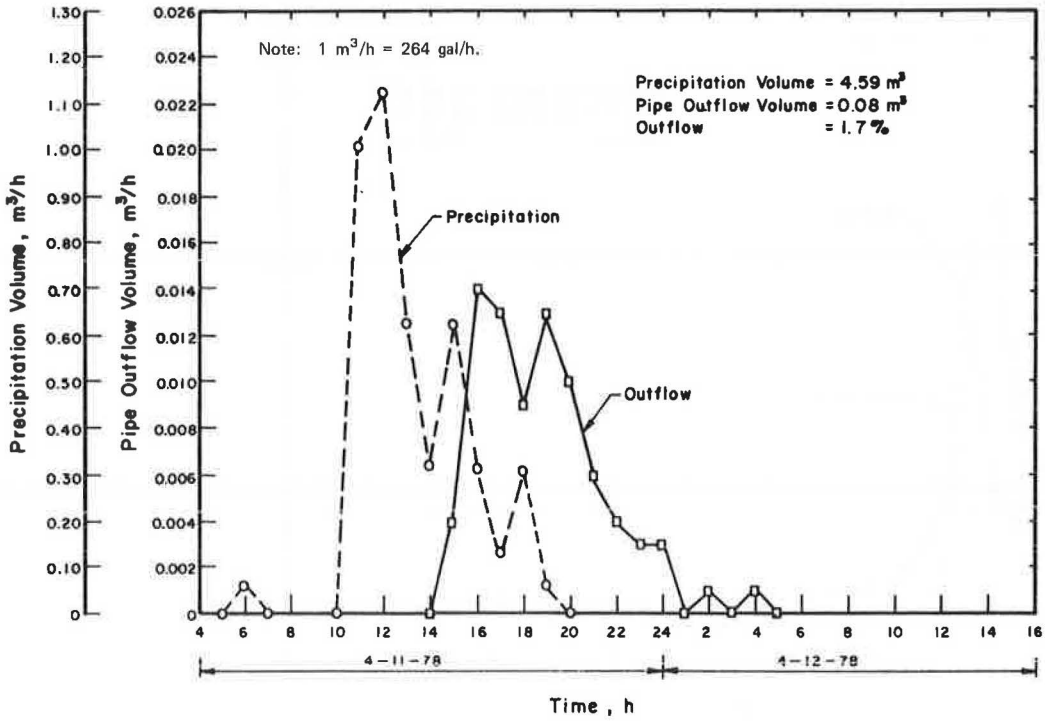

I1, contained approximately 46 transverse cracks of a mean width of 1.6 mm (0.063 in) and a standard deviation of 1.7 mm (0.069 in). Based on 20 random measurements, the mean joint width between the shoulder and the pavement was 7.5 mm (0.294 in) with a standard deviation of 6.3 mm (0.250 in).

The average width of the contraction joints on section I2 was 6.4 mm (0.250 in) and the joint spacing was 30.5 m (100 ft). Only one narrow transverse crack was present on section I2 in addition to the six contraction joints. The mean joint width between the shoulder and pavement on section I2, based on 20 random measurements, was 3.8 mm (0.148 in), with a standard deviation of 3.1 mm (0.122 in); see Figure 8. No attempt was made to clean the pavement transverse or edge joints before the drainage studies were conducted.

The length of each test section was selected to correlate with the distance between subsurface drainage out-

Figure 13. Influence of precipitation on drainage outflow in unsealed continuously reinforced pavement section I1 on 3/20-23/78.

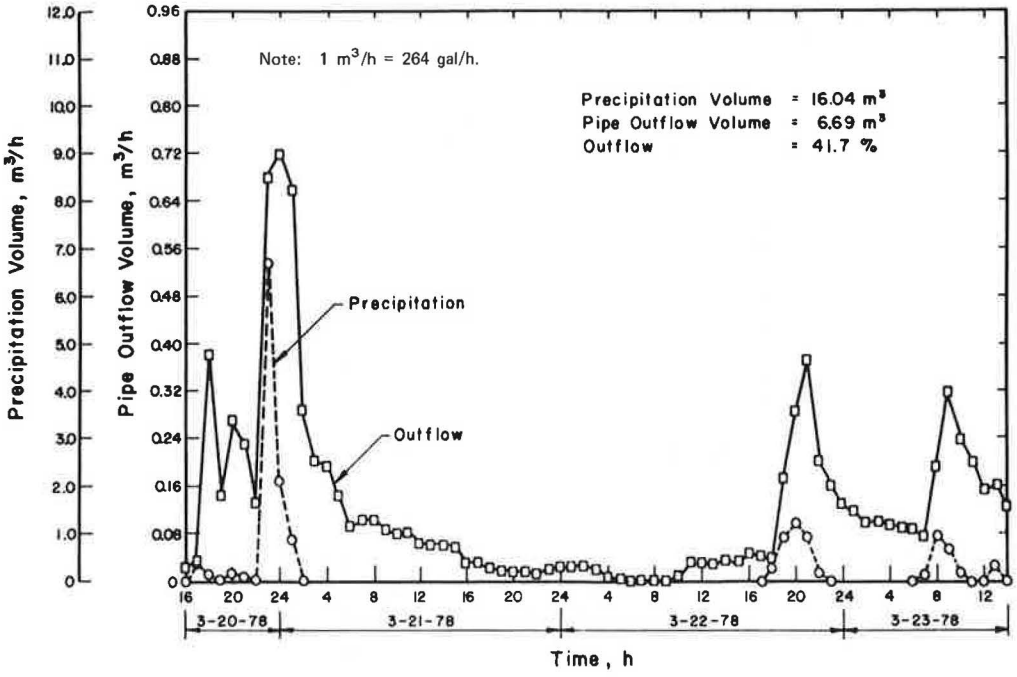

Figure 14. Influence of precipitation on drainage outflow in sealed continuously reinforced pavement section I1 on 6/30-7/3/78.

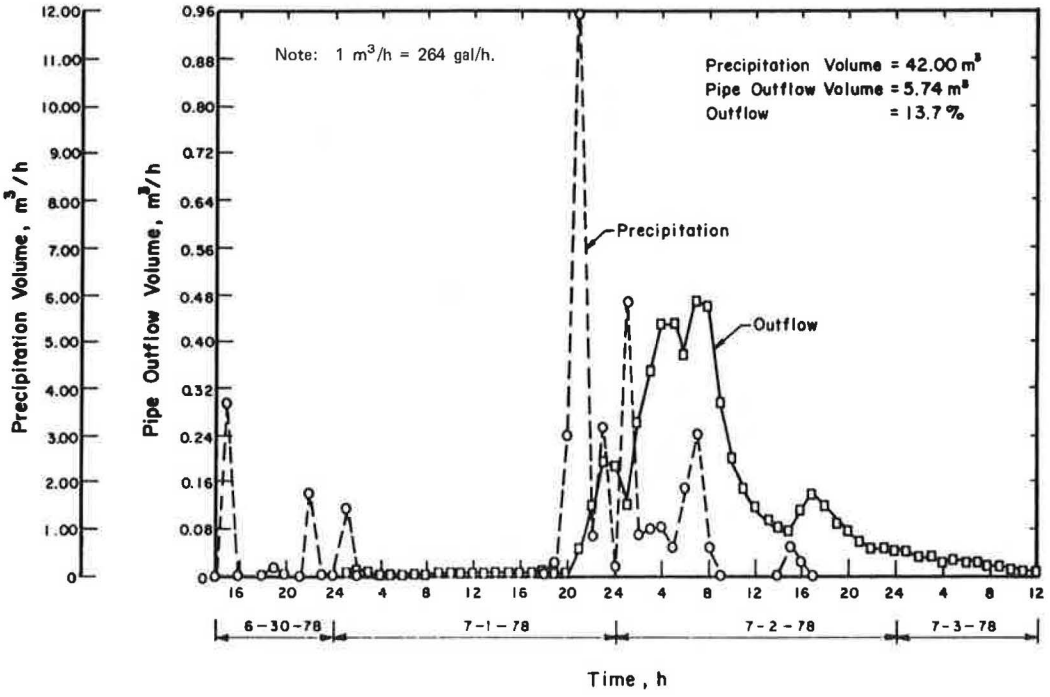

lets. The drain for each test section was connected to a flowmeter (Figure 6) similar to those used at the Georgia test site. Precipitation was measured both at the test site with a nonrecording raingauge and at University of Illinois-Willard Airport 2.4 km (1.5 miles) directly east of the test site, where a recording raingauge was used.

The drainage study on I-57 has been in continuous operation since October 24, 1977. Drainage outflows were monitored continuously and recorded automatically at 15-min intervals; precipitation was recorded at 1-h intervals. On June 8, 1978, the pavement edge joints on both test sections were sealed with a waterproof membrane in order to study the effects of edge-joint sealing on water infiltration. Figure 9 shows the edge joint being sealed on test section I2.

DATA

Table 2 shows the precipitation and outflow data for test sections G1 and G2 on I-85 in Georgia. Similar data are shown in Table 3 for test sections I1 and I2 on I-57 in Illinois.

Figure 15. Influence of precipitation on drainage outflow in unsealed jointed pavement section I2 on 4/17-20/78.

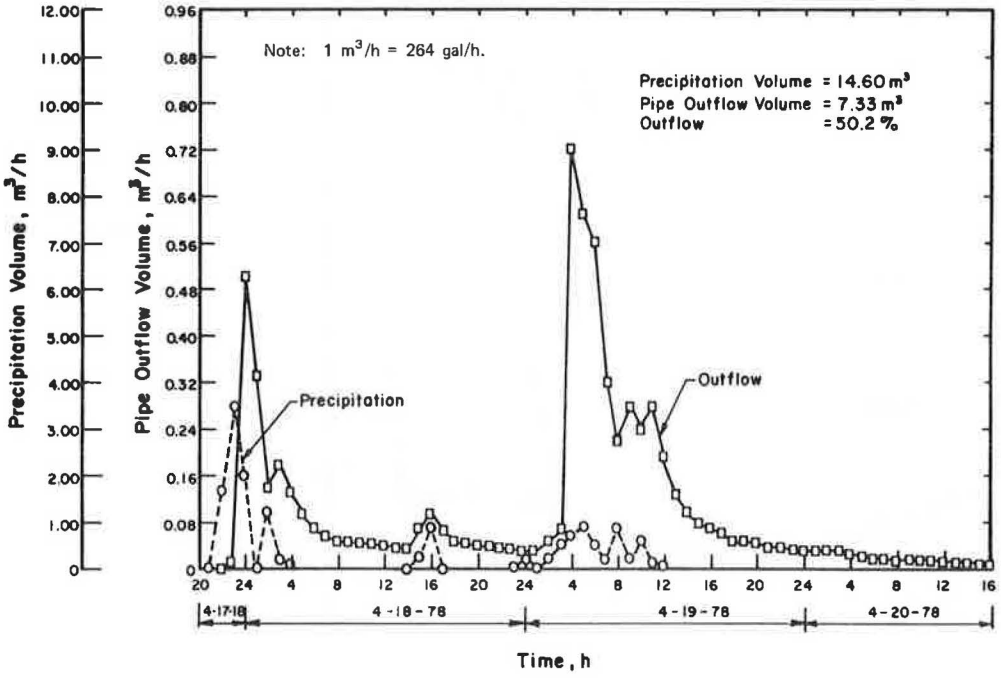

Figure 16. Influence of precipitation on drainage outflow in sealed jointed pavement section I2 on 6/30-7/3/78.

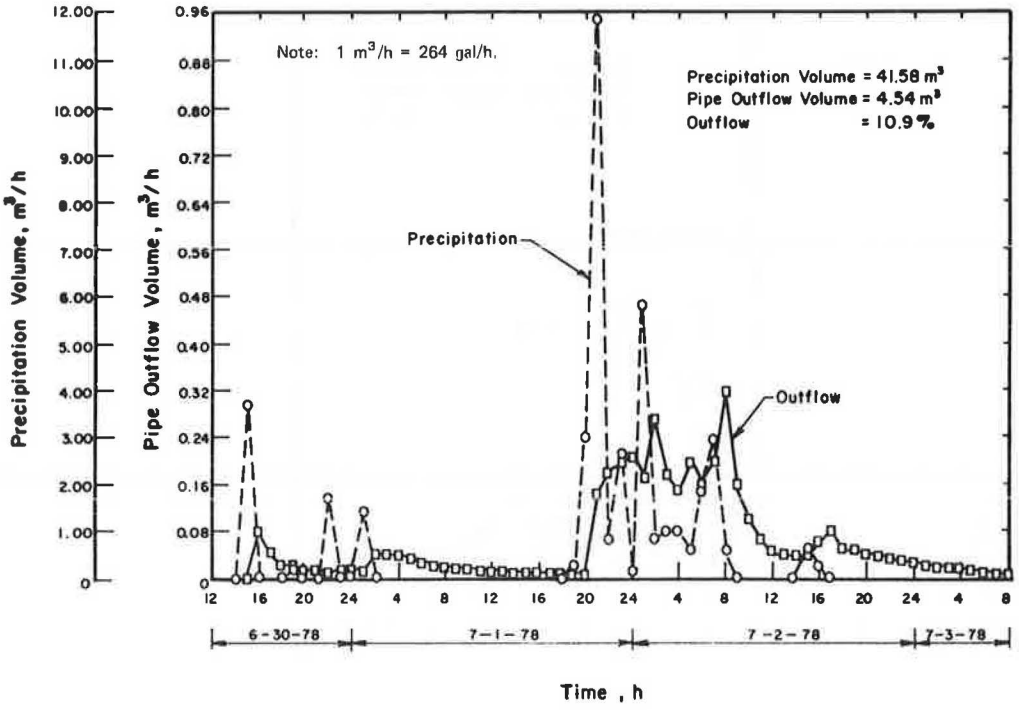

Table 4. Statistical data based on percentage of pipe outflow.

Pavement Test Section	Joint Condition	Mean	Coefficient of Variation	Standard Deviation
Georgia G1	Unsealed	30.6	61.1	18.7
Georgia G1	Sealed	0.7	194.0	1.4
Georgia G2	Sealed	-	-	-
Illinois I1	Unsealed	26.0	76.5	19.9
Illinois I1	Sealed	16.4	69.5	11.4
Illinois I2	Unsealed	52.1	36.7	19.1
Illinois I2	Sealed	11.6	28.4	3.3

The precipitation volumes in Tables 2 and 3 were computed by multiplying the total precipitation at each test site by the test-site drainage area shown in Table 1. The percentage of outflow is determined by the relationship (pipe outflow volume/precipitation volume) × 100.

INSTRUMENTATION

Figure 6 shows the instrumentation used to monitor the drainage outflow. The instrument is a calibrated tipping bucket and a commercially available traffic counter.

Figure 17. Influence of precipitation volume on drainage volume for unsealed test section G1.

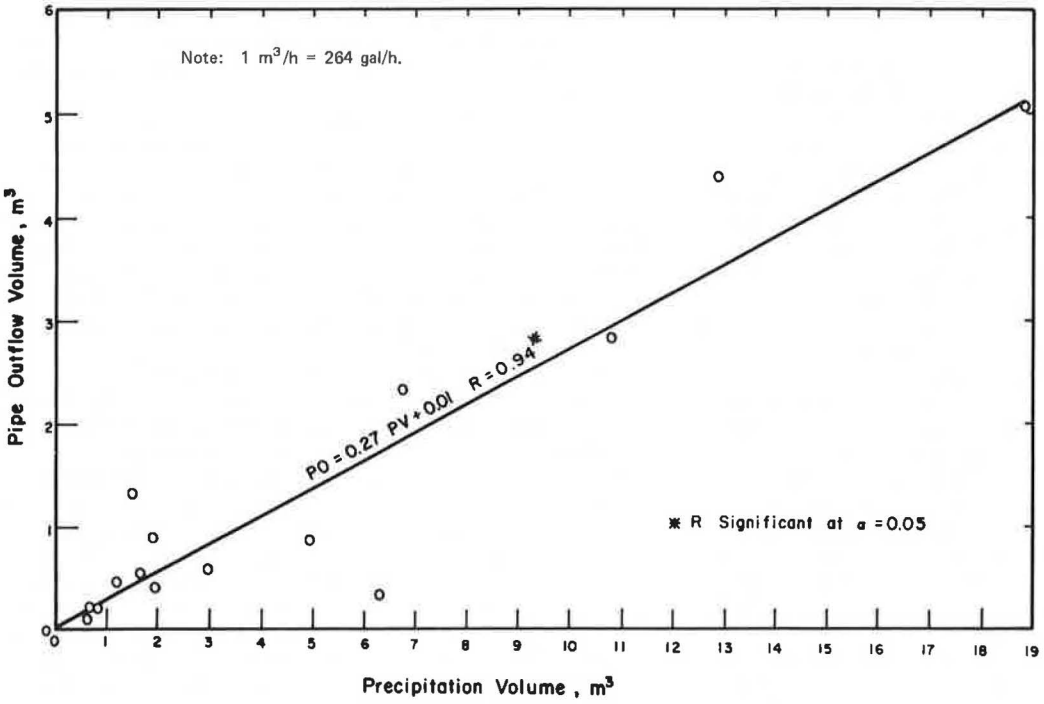

Figure 18. Relationships between precipitation volume and drainage volume for all test sections.

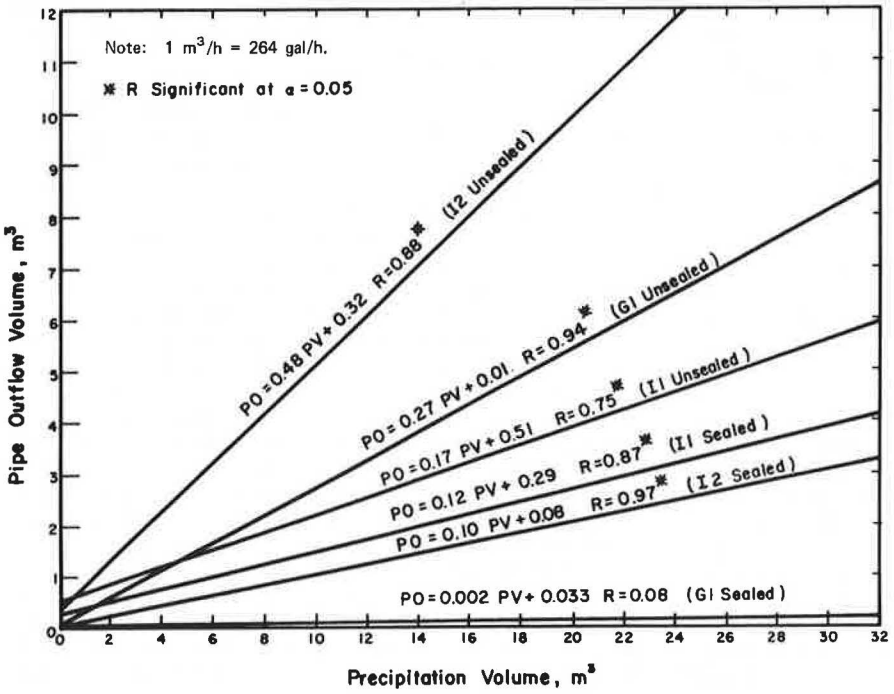

Each bucket tip activates a microswitch that sends a count to the traffic counter, which is battery powered and records the number of bucket tips and time at 15-min intervals on a paper strip chart. The equipment can operate continuously and unattended in the field for about 30 days.

ANALYSIS AND DISCUSSION OF DRAINAGE DATA

A study of the data in Tables 2 and 3 and the statistical data in Table 4 indicates the substantial variability in drainage outflow as influenced by rainfall intensity, pavement type, and joint sealing.

Precipitation-Outflow Volume

Figures 10, 11, and 12 show the precipitation and pipe outflow rates for test section G1. Note in Figures 10 and 11 that the pipe outflow responds almost simultaneously with precipitation and varies with the intensity of precipitation for the unsealed edge-joint condition. For the sealed edge-joint condition, Figure 12 shows that the pipe outflow on section G1 lags behind the start of precipitation by several hours. Figures 10 and 11 also show that pipe outflow continues to diminish over a 16- to 24-h period after rainfall has ceased. Figure 12 shows that the outflow diminished more quickly after rainfall ceased when the pavement edge joint was sealed.

Figures 13 and 14 show precipitation and outflow as a function of time for the continuously reinforced pavement section (I1) with and without edge sealing respectively. Figures 15 and 16 show similar results for the jointed pavement section (I2). Again it is noted that, for pavement sections I1 and I2, the measured outflow responds almost instantaneously to precipitation when the edge joint is unsealed. However, there is some perceived lag in outflow response to precipitation for the sealed edge-joint condition. For the unsealed conditions in both sections I1 and I2 it would appear that more than 24 h are required before outflow essentially ceases after precipitation has stopped. In Figures 14 and 16 it would appear that less time is needed (approximately 16 h) for outflow to diminish when the pavement edge joint is sealed.

In analyzing the data for the test sites it is apparent that the quantity of measured outflow and therefore infiltration was substantially reduced by sealing the edge joint. For the condition of complete sealing of both the edge joint and transverse joints on section G2, there was no measurable drainage outflow. In this case it would have to be assumed that any water that did infiltrate the pavement surface passed through the subgrade to the water table.

Based on the way drainage outflow responds to precipitation, as shown in Figures 10-16, it would appear that rainfall intensity and edge-joint conditions have considerable influence on the amount of water that infiltrates into a pavement.

Pavement Factors Influencing Outflow

It is evident that the size and number of joints and cracks in the pavement will contribute to water infiltration. It is also suggested that the time of year will influence water infiltration because cracks open in concrete in response to temperature and evaporation rates, which vary with temperature. These factors along with the rainfall intensity may be responsible for the outflow differences noted in Figures 10 and 11 (44.9 percent as compared to 20.4 percent) even though the total precipitation volumes are the same [1.96 m^3 (523 gal)]. Analysis of all outflow data for the unsealed pavement sections indicated that the infiltration rates were considerably less than those predicted by the design criteria proposed by Ridgeway (3).

Figures 14 and 16 indicate that both the continuously reinforced pavement, I1, and the jointed pavement, I2, displayed similar outflows for the same storms when the pavement edge joints were sealed. However, a paired t-test shows that the outflow percentages from section I1 are significantly different ($p = 0.05$) from those of section I2 for the unsealed and sealed edge-joint conditions.

Table 4 shows that the average pipe outflow percentage (outflow volume/precipitation volume) in the continuously reinforced pavement was 26.0 percent as compared to 52.1 percent for the jointed pavement for unsealed conditions. By sealing the edge joints the outflow in the continuously reinforced pavement decreased to 16.4 percent and that for the jointed pavement decreased to 11.6 percent.

In order to further study the influence of rainfall and pavement conditions on pipe outflow a linear regression analysis was conducted. Figure 17 shows a significant relationship ($p = 0.05$) between precipitation volume and pipe outflow for section G1 in Georgia. Figure 18 shows that, except for section G1 with the edge joint sealed, there was a significant relationship ($p = 0.05$) between precipitation volume and measured drainage outflow volume for the test sections. In all cases outflow increased with precipitation volume.

In order to determine whether edge-joint sealing significantly influenced drainage outflow, a statistical t-test was conducted to compare the slopes of the regression relationships between pipe outflow and precipitation shown in Figure 18. For the jointed pavement test sections in both Illinois and Georgia (sections G1 and I2) the slopes of the regression relationships for the sealed edge-joint condition were found to be significantly different ($p = 0.05$) from those for the unsealed edge-joint condition. For the continuously reinforced test section (section I1) there was no significant difference ($p = 0.05$) between the slopes of the regression relationships for the sealed and unsealed edge-joint condition. Based on an analysis of the relationships between pipe outflow and precipitation, we might conclude that edge-joint sealing will significantly decrease ($p = 0.05$) the infiltration of water into jointed pavement systems. However, sealing may not have a significant effect on continuously reinforced pavement systems.

In Figure 18 it is noted that, for unsealed edge-joint conditions, the continuously reinforced pavement (section I1) experienced less outflow than the jointed pavement sections in sections G1 and I2, respectively, for similar precipitation volumes. As noted earlier, the outflow for the continuously reinforced pavement is significantly less ($p = 0.05$) than that for the jointed pavements for the same storm event. In the continuously reinforced pavement it is evident that there is a need to further investigate the amount of infiltration caused collectively and individually by the edge joint and transverse cracks. It would seem in this study that the edge joint along the continuously reinforced pavement did not contribute as much to infiltration as the edge joints along the jointed pavement test sections. However, as indicated in Figure 18, the transverse cracks in continuously reinforced pavement systems may contribute more to infiltration than the transverse joints in jointed pavement systems. This is obvious when we compare the continuously reinforced pavement section I1 with the jointed pavement section G2 where both transverse and edge joints were sealed. Further analysis of the completely sealed pavement section G2 indicates that joint sealing can help prevent water accumulation in the struc-

tural pavement section, especially if the subgrade is moderately permeable and the water table deep.

CONCLUSIONS

The conclusions of this study are as follows.

1. Significant relationships ($p = 0.05$) were found between precipitation and drainage outflow.
2. Drainage outflow was influenced by pavement type. The outflow for the continuously reinforced pavement was significantly different ($p = 0.05$) from the outflow of the jointed concrete pavement for both the unsealed and sealed edge-joint conditions in Illinois.
3. Edge-joint sealing significantly reduced ($p = 0.05$) drainage outflow in the jointed pavement test sections in Georgia and Illinois. Although edge sealing reduced outflow on the continuously reinforced pavement section in Illinois, there was not a significant improvement ($p = 0.05$).
4. No measurable drainage outflow occurred on the Georgia test section in which all longitudinal and transverse pavement joints and the pavement edge joints had been sealed.
5. Based on relationships between precipitation volume and pipe outflow volume, as well as on the response of pipe outflow to rainfall, the edge joint may be a major factor contributing to water infiltration in jointed pavement systems.
6. In this study the contribution of the transverse cracks in the continuously reinforced pavement section to infiltration was greater than the contribution of the edge joint. Further drainage studies need to be conducted on continuously reinforced pavement systems.

ACKNOWLEDGMENT

This report was prepared as part of a research study on improving subdrainage and shoulders of existing pavements being conducted at the Department of Civil Engineering of the University of Illinois at Urbana under the sponsorship of the Federal Highway Administration. George Ring III of the Federal Highway Administration is the project monitor.

Thanks are due to the Georgia Department of Transportation for its help in preparing the test site on I-85 and to David Morrill, a research assistant, for collecting and processing the data from the Illinois test site.

The contents of this paper reflect our views and we alone are responsible for the facts and the accuracy of the data presented. The contents do not necessarily reflect the official views or policies of the Federal Highway Administration. This paper does not constitute a standard, specification, or regulation.

REFERENCES

1. H. R. Cedergren and K. O'Brien. Development of Guidelines for the Design of Pavement Subdrainage Systems. Literature Review Abstracts, Federal Highway Administration, 1971.
2. B. J. Dempsey, M. I. Darter, and S. H. Carpenter. Improving Subdrainage and Shoulders of Existing Pavements—State-of-the-Art. Univ. of Illinois, Urbana, Interim Rept., 1977.
3. H. H. Ridgeway. Infiltration of Water Through the Pavement Surface. TRB, Transportation Research Record 616, 1976, pp. 98-100.
4. G. W. Ring. Drainage of Concrete Pavement Structures. Proc., International Conference on Concrete Pavement Design, Purdue Univ., West Lafayette, IN, 1977.
5. J. H. Woodstrom. Improved Base Design for Portland Cement Concrete Pavements. Proc., International Conference on Concrete Pavement Design, Purdue Univ., West Lafayette, IN, 1977.
6. R. D. Barksdale and R. G. Hicks. Drainage Considerations to Minimize Distress at the Pavement-Shoulder Joint. Proc., International Conference on Concrete Pavement Design, Purdue Univ., West Lafayette, IN, 1977.
7. M. I. Darter and E. J. Barenberg. Zero-Maintenance Pavements: Results of Field Studies on Performance Requirements and Capabilities of Conventional Pavement Systems. Federal Highway Administration, Rept. FHWA-RD-76-105, 1976.

Publication of this paper sponsored by Committee on Subsurface Drainage and Committee on Environmental Factors Except Frost.

Installation of Straw and Fabric Filter Barriers for Sediment Control

W. Cullen Sherwood, Virginia Highway and Transportation Research Council and James Madison University, Charlottesville
David C. Wyant, Virginia Highway and Transportation Research Council, Charlottesville

Effective temporary erosion and sedimentation controls are critical during construction in the period between onset of earth-disturbing and final stabilizing by vegetation. Among the most common temporary controls used in Virginia and many other states are straw barriers, burlap filter barriers, and silt fences. Despite the large sums of money spent annually on these controls, high failure rates and low trapping efficiencies, particularly for straw barriers, have been reported. In an effort to improve field performance, experiments conducted in Virginia have led to the installation procedures reported in this paper. Procedures for inspection and maintenance of these controls are also described. Finally, it is concluded that the cost effectiveness of straw barriers has proved questionable in many cases; burlap filter barriers may well be an effective and inexpensive substitute for straw.

The early reestablishment of vegetation in areas denuded by construction is generally agreed to be the most effective method of controlling accelerated erosion and sedimentation. However, regardless of how conscientious the efforts at revegetation may be, there will be a critical period between the onset of land disturbance and the final stabilization by vegetation. It is during this critical period that temporary erosion- and sediment-control structures are required.

Through the years many types of temporary erosion- and sediment-control techniques have been developed by agencies concerned with soil conservation and water quality. These controls may be categorized as

1. Mulching of bare soil surfaces to protect from the impact of raindrops and runoff,
2. Structures designed to divert storm waters into stabilized areas,
3. Structures designed to impede and filter runoff, and
4. Structures designed to impound storm waters.

Straw barriers, burlap filters, and silt fences fall into category 3 and are among the most common temporary sediment-control methods in use today. Briefly, straw barriers refer generally to barriers constructed of straw or hay bales; burlap filters are barriers made by stapling burlap cloth to wooden stakes spaced from 0.9 to 1.2 m (3 to 4 ft) apart, and silt fences are barriers made by attaching woven fence wire and commercial filter fabric to fence posts set approximately 3.1 m (10 ft) apart.

PROBLEMS WITH FILTER BARRIERS

According to observations made in Virginia (1, 2), Pennsylvania (3), and other parts of the nation (4), filter barriers have not been as effective in controlling sediment as expected. For example, Weber and Wilson found that the sediment-trapping efficiency of straw barriers in Pennsylvania ranged from 0 to 5 percent (3). Reed, also working in Pennsylvania, noted a 5 percent reduction of sediment load when straw barriers were used on construction (5).

Improper use of filter barriers has been a widespread problem. For instance, straw barriers and silt fences have been used in streams and drainageways where high water velocities and volumes have destroyed or impaired their effectiveness. Another problem has been improper placement of barriers (Figure 1), which has caused undercutting and end flow that have actually increased rather than removed sediment in runoff waters (2). Finally, inadequate maintenance and cleaning have tended to greatly lower the trapping efficiency of all filter barriers.

Figure 1. Straw barrier placed by a contractor; arrows indicate failure by undercutting and end flow.

Because of these problems, straw barriers placed by contractors in Virginia and elsewhere have shown low trapping efficiencies and high failure rates. On one project in Virginia only 2 of 12 straw barriers installed in side ditches were found to be effective in trapping sediment. The poor performance observed statewide and in other states may not be atypical and raises serious questions concerning the continued use of straw barriers in the present manner. On the other hand, results of recent field experiments in Virginia strongly suggest that with proper installation the effectiveness of straw barriers can be greatly increased.

In addition to improved procedures for straw barriers, this paper includes procedures for installing burlap filters and silt fences. Although the failure rates of these last two types of barriers generally have been lower than that of straw barriers, they have been improperly installed occasionally. Experience has shown that following the installation methods outlined below can improve performance.

RECOMMENDED INSTALLATION PROCEDURES

Straw Barriers

The use of straw barriers must be limited to situations in which only low or moderate flows are to be intercepted. A recent Soil Conservation Service publication (6) states that the use of straw bales in Maryland should be limited to situations in which no other control is feasible and only sheet and rill erosion are expected. Also, a recent communication from Maryland authorities has brought to light plans to increase the depth of entrenchment for straw barriers from 0.10 to 0.15 m (4 to 6 in). Use of these barriers is specifically excluded for situations in which water is to be concentrated in a channel or drainageway. In view of the questionable performance of straw barriers thus far, use of these structures will be continued only if installation and maintenance procedures can be significantly improved. The following guidelines provide recommended step-by-step instructions for the installation of straw barriers exposed to moderate or low flows.

Entrenchment of Straw Barriers for Moderate Expected Flow

The term "moderate flow" encompasses sheet flow through channel flow, where rates are not to exceed 0.03 m^3/s (1 ft^3/s). Using the rational method for flow prediction and assuming average surface conditions and a rainfall rate of 0.03 m/hr (1 in/hr), an area of 8094 m^2 (2 acres) should provide approximately 0.03 m^3/s (1 ft^3/s) of flow. Low to moderate flow conditions will prevail in most drainage ditches of a less than 8 percent slope.

The installation procedure for locations with moderate flow rates is given below and illustrated in Figure 2.

1. Excavate a trench the width of a bale and the length of the proposed barrier to a minimum depth of 0.10-0.15 m (4-6 in).

2. Place bales tightly together in the trench. Drive two sturdy wooden stakes or steel pins through each bale and deep enough into the ground to securely anchor the bales.

3. After staking, wedge loose straw between any cracks or other openings.

4. Backfill and compact the excavated soil against the barrier. Backfilled soil should conform to ground level on the downstream side and should be built up to 0.1 m (4 in) against the upstream side of the barrier.

Soil Sealing of Straw Barriers for Expected Low Flow

The term "low flow" is used here to describe sheet or

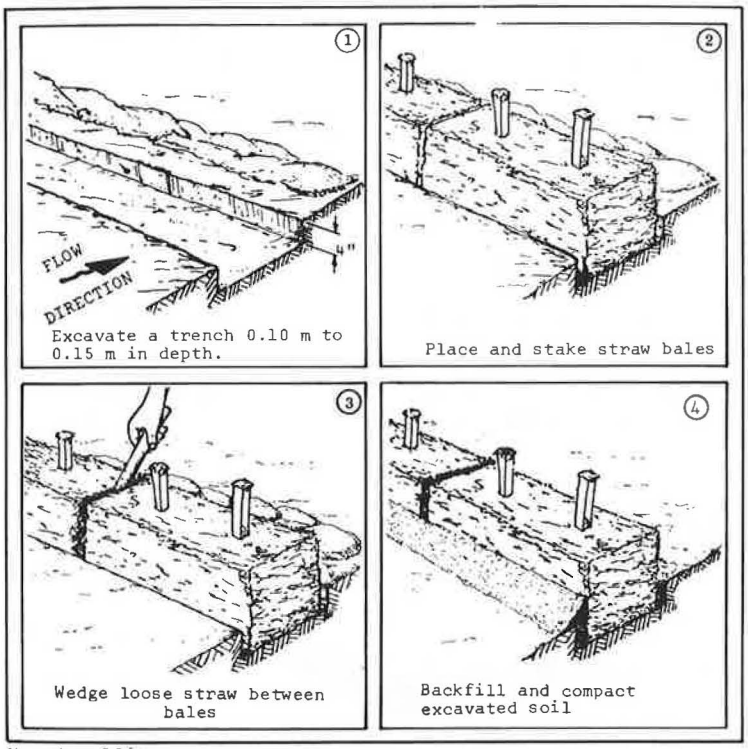

Note: 1 m = 3.3 ft.

Figure 2. Placing a straw barrier at a location of moderate expected flows.

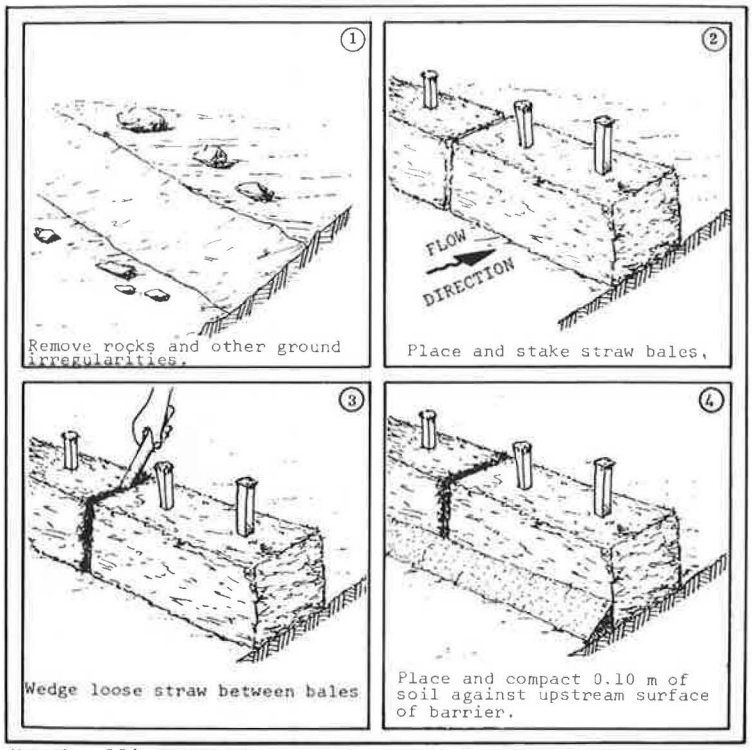

Note: 1 m = 3.3 ft.

Figure 3. Placing a straw barrier at a location of low expected flows.

overland flow. Channel flows are specifically excluded.

The procedure for installing barriers in areas of low flow is described below and illustrated in Figure 3.

1. Prepare a smooth ground surface by removing rocks and leveling soil surface.
2. Place bales tightly together and drive sturdy wooden stakes or steel pins through each bale and into the ground deep enough to securely anchor the bales.
3. Wedge loose straw tightly between bales if required.
4. Place and compact a minimum of 0.1 m (4 in) of soil against the upstream surface of the barrier.

When a barrier is to be placed in a swale or a ditch line, the structure should be extended so that the bottoms of the end bales are higher in elevation than the top of the lowest middle bale (Figure 4).

Burlap Filter Barriers

Burlap filter barriers are inexpensive structures composed of burlap fabric stapled to wooden stakes. This type of barrier can be used interchangeably with straw barriers in many situations. Laboratory flume studies comparing straw bales (2), burlap, and filter fabrics have indicated that flow rates (1 m^3/min = 4.4 gal/min) through burlap are slightly slower and the filtering efficiency somewhat higher than for straw bales (see the table below).

Barrier	Flow Rate (m^3/min)	Filtering Efficiency (%)
Straw	0.021	67
Burlap	0.019	87
Typical filter fabric	0.002	97

Burlap filter barriers are designed for low or moderate flow situations. The height of these barriers should not exceed 0.50 m (20 in) and 0.30-0.38 m (12-15 in) will suffice in most situations. The burlap should be purchased in a continuous roll and cut to the length of the barrier; avoiding seams improves the strength and efficiency of the barrier.

The procedure for installing a burlap filter barrier is given below and illustrated in Figure 5.

1. Excavate a 0.1x0.1-m (4x4-in) trench upstream of where the stakes will be driven.
2. Drive sturdy wooden stakes [at least 25x51 mm (1x2 in) and spaced 0.9 m (3 ft) apart] securely into the ground at the barrier site.
3. Staple the burlap to the wooden stakes. Extend 0.2 m (8 in) of the burlap into the trench. The height of the burlap must not exceed 0.5 m (20 in).
4. Backfill and compact soil in the trench over the burlap.

Silt Fences

The silt fence is a two-component barrier system comprising a support fence and an attached filter fabric. The support fence is made of 14-gage or finer woven

Figure 4. Proper straw barrier placement; points A should be higher than point B.

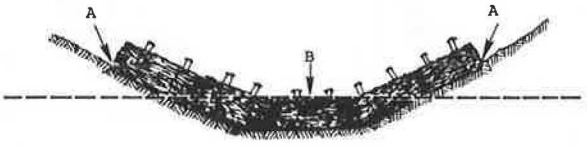

Figure 5. Installation of a burlap filter barrier.

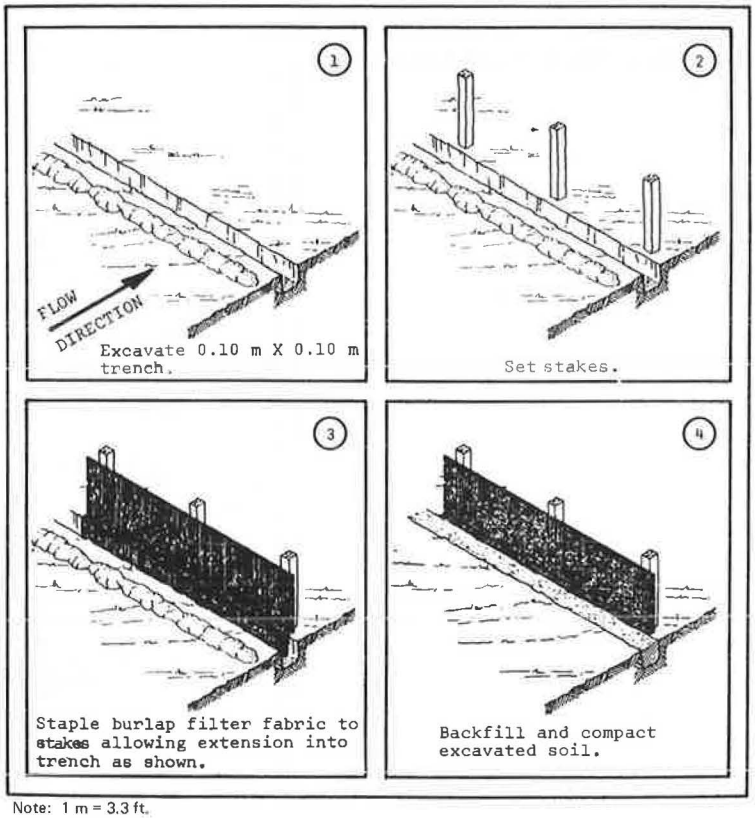

Note: 1 m = 3.3 ft.

wire attached to metal or wooden posts. The filter fabric (several companies manufacture suitable material) is stapled or wired securely to the support fence. Because the filter fabrics have a lower permeability (see the preceding table) than do straw bales and burlap, the use of silt fences should be limited to situations in which only sheet or overland flows are expected; they normally cannot filter the volumes of water generated by channel flows.

In most cases the fabric should not extend higher than 0.9 m (36 in); greater heights may back up enough water to cause the structure to fail. A 0.9-m (36-in) filter fence acts as a dam and traps sediment by the ponding action of inflowing, sediment-laden waters.

Figure 6. Building a silt fence.

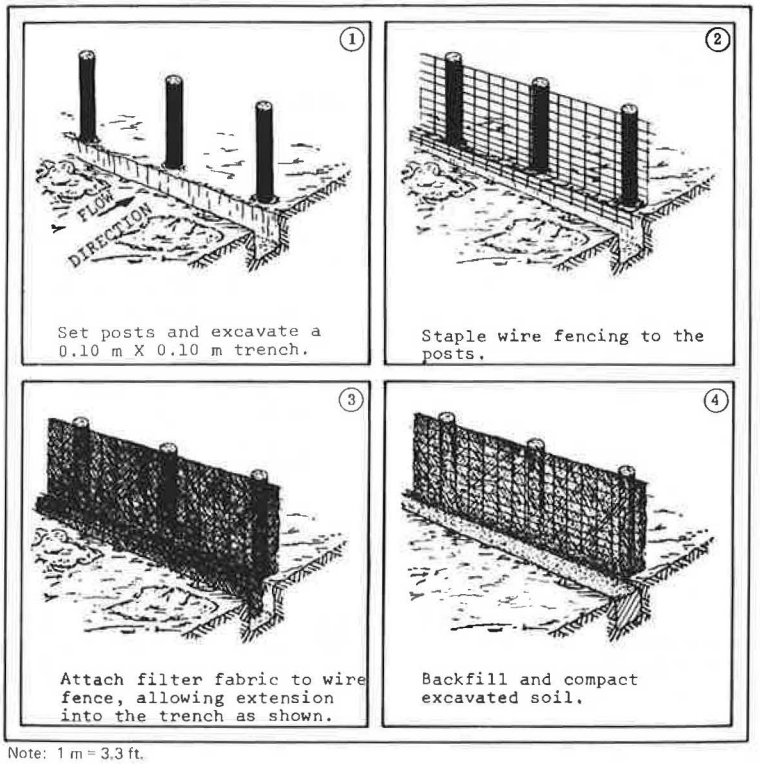

Note: 1 m = 3.3 ft.

Figure 7. Building a silt fence with brush barrier support.

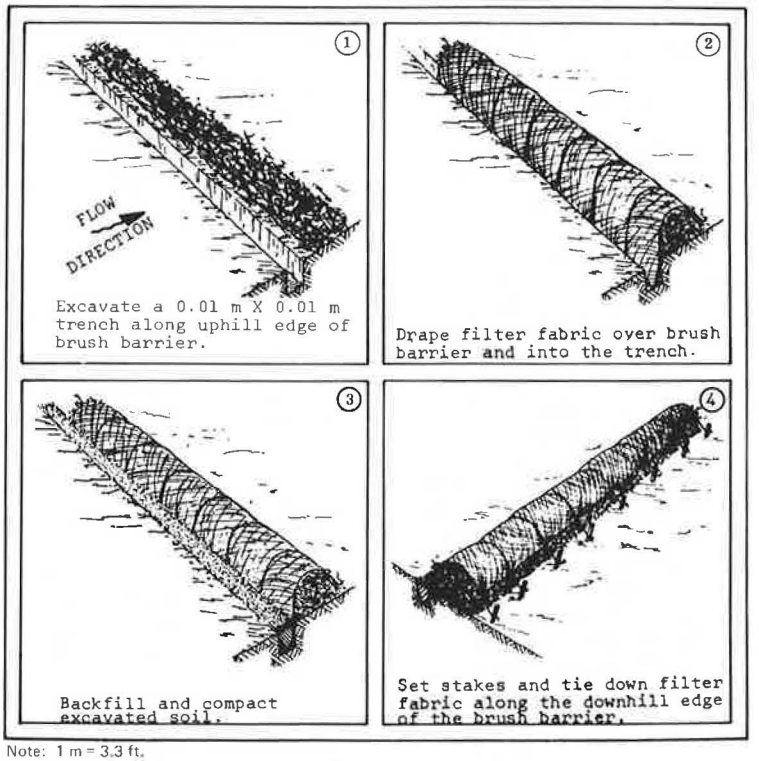

Note: 1 m = 3.3 ft.

The construction of silt fences should conform to the procedures illustrated in Figure 6 and listed below. The method of construction for filter fabric used in conjunction with a filter barrier made from materials such as brush or straw is shown in Figure 7.

1. Set wood or steel posts securely at intervals no greater than 3.1 m (10 ft) apart. Wood posts should be at least 76 mm (3 in) in diameter; with steel, use only the T-shaped posts or a post weighing more than 2.1 kg/m (1.4 lb/ft). Excavate a trench 0.1 m (4 in) wide by 0.1 m (4 in) deep along the upstream base of the fence.
2. Fasten fence wire securely to the upstream side of the posts. Wire should extend into the soil a minimum of 51 mm (2 in) and be at least 0.9 m (36 in) high.
3. Staple or wire the filter fabric to the fence, allowing the fabric to extend into the trench as shown in Figure 6. The fabric should not extend more than 0.9 m (36 in) above the original ground surface on the wire fence.
4. Backfill and compact the soil over the fabric extending into the trench.

If a filter fence is to be constructed across a ditch line or drainageway carrying a low flow, the barrier should be of sufficient length to eliminate end flow. Both the strength and the effectiveness of silt fences can be maximized by constructing the barrier in an arc or horseshoe shape whose ends point up slope.

COST DATA

A check of eight randomly selected construction projects in Virginia yielded a rather wide range in costs for straw barriers and silt fences. Burlap filter barriers are still in the experimental stage in Virginia, so specific field cost data are not yet available; the figures for burlap used here are estimates.

For the eight projects surveyed, costs for straw barriers ranged from a high of $19.80 to a low of $6.60/m ($6.00 to $2.00/ft), and the average cost was about $12.00. These costs are based on contractor prices for materials, installation, and maintenance plus one cleanout. This price is up sharply from an estimated $8.25/m ($2.50/ft) of 1976 (7). Most of the recent increase has resulted from the very high cost of baled straw. Recent market prices for baled straw in Virginia have ranged up to $2.75/bale.

The high cost of straw barriers, together with the relatively low average filter efficiencies of straw bales of 67 percent determined in laboratory flume studies (2), has raised serious questions concerning the future use of straw barriers in Virginia. The likely replacement for straw barriers may be the relatively inexpensive but effective burlap filter barriers. As noted in the table, recent tests in the laboratory flume have shown the average filtering efficiency of burlap to be 87 percent, some 20 percent higher than that of baled straw. While exact cost data are not yet available, it is estimated that the time required to install burlap filter barriers should run roughly the same as that for straw barriers. The burlap material at $0.23/m ($0.07/ft) costs less than the straw bales. Based on these figures, and the eight jobs surveyed, it is estimated that burlap filter barriers should cost approximately $10.49/m ($3.18/ft), which is less per meter than the present cost of straw barriers. This figure may well decrease as burlap barriers become more widely accepted and the users become more proficient in their installation and maintenance procedures.

Cost data for silt fences were also sought on the eight construction projects, and the records on six of the eight contained this information. Based on the same criteria as noted for the straw barriers—that is, materials, installation, maintenance, and one cleanout—silt fence prices ranged from $10.23 to 18.15/m ($3.10-5.50/ft). The average cost was slightly less than that for straw barriers. Considering the vastly greater filter efficiencies and life expectancy of silt fences as compared to straw barriers, it appears that filter fences are a significantly better investment at these prices. Interestingly, the cost for filter fences—$3.77/0.31 m (1 linear ft)—is up only slightly from the $3.50 cost in 1976 (7).

MAINTENANCE

Field experience has shown that, in addition to the proper construction of filter barriers, proper maintenance is absolutely necessary. Poché and Sherwood (2) found that trapping efficiencies of carefully placed straw barriers on one project in Virginia dropped from 57 to 16 percent in one month because of lack of maintenance. It is imperative that all filter barriers be checked after each storm event and that required repairs and alterations be made promptly. Also, frequent cleanouts are necessary if a barrier is to perform properly. Checking barriers during a storm event, although a wet and unpleasant job, can pay great dividends in information on water flow and sediment retention. If observations are not made during storms, information on the effectiveness must be gathered indirectly or after the fact, which can be misleading.

The value of careful and prompt maintenance of all types of filter barriers cannot be overemphasized. Even the most careful installation of these structures does not negate the need for constant and thorough maintenance and regular cleanouts if the sediment control system is to be effective.

CONCLUSIONS

Field and laboratory studies conducted in Virginia have indicated that significant improvements in performance can be attained for three common temporary erosion and sediment controls now in widespread use. The following conclusions have been drawn from investigations of straw barriers, burlap filter barriers, and silt fences.

1. Improper installation and the use of filter barriers in channels carrying high volumes of storm water have led to high rates of barrier failure.
2. The use of all filter barriers should be limited to situations in which either sheet flow or low channel flows of less than 0.03 m^2/s)(1 ft^3/s) are expected.
3. Common failures such as undercutting and end runs can be significantly reduced by following the installation procedures outlined in this paper.
4. All filter barriers should be inspected, cleaned out, and repaired as necessary after each storm event.
5. Inspection of filter barriers during storm events can yield valuable information on both installation and maintenance.
6. Cost and experimental data indicate that burlap filter barriers are less expensive and trap sediment more efficiently than straw barriers.
7. Silt fences, because of very low flow rates and high filtering efficiencies, are recommended for situations where only sheet flow is expected and very high sediment retention is desired.

ACKNOWLEDGMENT

We thank M. O. Harris and G. T. Gilbert, technicians

in the Soils, Geology, and Physical Environment section of the Virginia Highway and Transportation Research Council for their help in the field installation and laboratory evaluations. Special thanks are extended to M. C. Anday and H. T. Craft of the Research Council for their technical guidance and editorial help, respectively. Finally, we express our appreciation to B. Turner of the Research Council for her clerical assistance.

The research on which this paper is based was funded by the Virginia Department of Highways and Transportation. The opinions, findings, and conclusions expressed are ours and not necessarily those of the sponsor.

REFERENCES

1. W. C. Sherwood and D. C. Wyant. An Evaluation of the Erosion-Siltation Control Program of the Virginia Department of Highways—Summer 1973. Virginia Highway Research Council, Charlottesville, VHRC 73-R33, 1974.
2. D. Poché and W. C. Sherwood. Sediment Trapping Efficiency of Straw and Hay Bale Barriers and Gabions. TRB, Transportation Research Record 594, 1975, pp. 10-14.
3. W. G. Weber, Jr., and C. Wilson. Evaluation of Sediment Control Dams. Pennsylvania Department of Transportation, Harrisburg, Research Project No. 73-21, 1976.
4. R. B. Thornton. Erosion Control on Highway Construction. NCHRP, Synthesis of Highway Practice No. 18, 1973.
5. L. A. Reed. Effectiveness of Sediment-Control Techniques Used During Highway Construction in Central Pennsylvania. U.S. Geological Survey, Water-Supply Paper 2054, 1978.
6. Standards and Specifications for Soil Erosion and Sediment Control in Developing Areas. U.S. Department of Agriculture; Water Resources Administration, Maryland Department of Natural Resources, College Park, 1975.
7. W. C. Sherwood and D. C. Wyant. Installation of Straw Barriers and Silt Fences. Virginia Highway and Transportation Research Council, Charlottesville, VHTRC 77-R18, 1976.

Publication of this paper sponsored by Committee on Subsurface Drainage and Committee on Environmental Factors Except Frost.

Part 2
Subgrades, Soil Moisture, and Frost

Subgrade Stability

Marshall R. Thompson, Department of Civil Engineering, University of Illinois, Urbana

Subgrade stability refers to the strength and deformation properties of a soil. Both properties significantly influence (a) the response of a subgrade to the heavy repeated loading of construction traffic and operations, (b) the ability to place and compact overlying material layers, and (c) the long-term performance of the pavement subgrade. Ideally the subgrade should be strong enough to prevent excessive rutting and shoving and sufficiently stiff to minimize resilient deflection. Techniques and procedures currently used for characterizing soil type seem adequate, but those for evaluating field soil moisture regime are inadequate. The procedures described can be used to evaluate this regime. Subgrade stability requirements are primarily dictated by pavement construction considerations. Analyses of equipment sinkage and paving material compaction operations indicate that a minimum in situ California bearing ratio (CBR) of 6-8 is required. Many typical fine-grained soils do not develop CBR in excess of that when compacted at or wet of AASHTO T99 optimum water content. Thus, remedial procedures must be followed frequently to provide adequate subgrades for pavement contraction. Three such procedures—undercut and backfill, moisture-density control, and admixture stabilization—are described and evaluated. Undercut and backfill and admixture stabilization offer the greatest potential for permanently improved performance of the completed pavement.

Subgrade stability refers to a soil's strength and deformation properties, which significantly influence (a) the response of a subgrade to the heavy repeated loading of construction traffic and operations, (b) the future success of placement and compaction of overlying layers, and (c) the long-term performance of the pavement subgrade. Ideally the subgrade should be strong enough to prevent excessive rutting and shoving and sufficiently stiff to minimize resilient deflection.

To ensure adequate stability, certain minimum strength and stiffness levels must be achieved in the subgrade soil to the depth influenced by construction traffic as well as by vehicles using the completed pavement. Because the magnitude of the wheel load, tire pressure, and the relative stiffness of the various layers determine depth of influence, subgrade stability must be defined for a given loading and traffic condition.

CHARACTERIZATION OF FIELD CONDITIONS

Recent studies (1, 2) have demonstrated that for fine-grained soils the major factor that influences strength and stiffness is water content. A recent Indiana study (3) showed that "Water content appears as the dominant variable (with regard to strength) in the field and Standard Proctor regressions."

Inadequate subgrade stability is generally associated with a moisture content that exceeds the optimum as measured in the AASHTO T99 compaction test. In all cases of inadequate subgrade stability evaluated in an Illinois study, field moisture contents were significantly wet of optimum. Knight (4) has indicated that, if the soil moisture content is greater than optimum, the cone index will generally be less than 300, an equivalent California bearing ratio (CBR) of 6 or 7.

A study of placement moisture contents (1) for a variety of soils from two Interstate highway sections (District 5, Paris, Illinois, I-57 and I-70), each approximately 16 km (10 miles) long, revealed that sizable quantities of the subgrades were placed wet of optimum. The compaction moisture content averaged 97.2 percent of optimum and had a standard deviation of 15.1 percent of optimum for the 1213 observations. On these projects 43 percent of the soil embankment was placed wet of optimum, 20 percent above 110 percent of optimum, and 7 percent above 120 percent of optimum. Similar data developed by the Illinois Department of Transportation (DOT) and others also indicate the potential of embankment construction with soils wet of optimum.

In many cases the field moisture contents at the borrow areas in the above studies were probably higher but were reduced by aeration during placement and compaction. Since compaction wet of optimum apparently occurs frequently, subgrade stability problems are bound to be common. The field identification of potential subgrade stability problem areas requires knowledge of the soil type and the moisture content. Density has a very minor influence on soil strength and stiffness when compacted wet of optimum, assuming that densities in the region of 95 percent of maximum (γ_b max) are achieved.

Soil Type Considerations

The current uses of pedologic soils information, previous soil reports, geologic data, drilling, sampling, and testing activities for considering soil type are fairly well defined. The early work of Thornburn and Liu (2) at the University of Illinois and the Illinois DOT Soils Manual (5) serve as excellent sources of information on the properties, characteristics, and distribution of surficial soil deposits in Illinois. Similar data have been developed by other transportation agencies. It should be noted that soil type and distribution do not change with time. If particularly bad soil types are not detected during the soils investigation, they can be easily located and identified during construction.

The adverse effects (loss of strength and reduction of stiffness) of a high moisture content vary according to soil type. Compare, for example, the CBR-water relations in Figures 1 and 2. The high-plasticity Drummer B (Figure 1) is fairly insensitive to moisture content change, while the low-plasticity Fayette C (Figure 2) is extremely sensitive. Illinois data (1) indicate that the resilient moduli of soils with high clay contents and high plasticity are less sensitive to moisture content increases than the soils of higher silt content and lower plasticity index (PI). Permanent deformation data developed for typical Illinois soils [Figure 3 for AASHTO Class A-7-6(28) and Figure 4 for AASHTO Class A-4 (9)] also indicate that soil type has an effect on moisture sensitivity.

It is therefore important to have adequate soil characterization data for consideration of potential subgrade stability problems. Soil texture and plasticity appear to be the two major factors that need to be considered.

Moisture Considerations

The most significant factor influencing the strength and stiffness of any fine-grained soil is moisture content. Unfortunately soil moisture content in the field shows tremendous spatial variability and is constantly changing with time. The intricacies of moisture movement and moisture content changes in soils have been well docu-

mented by Dempsey and Elzeftawy (6).

Although it is not practical to accurately predict field soil moisture content as a function of location, depth, and time, significant advances are being made in that regard, and the available technology certainly is of great value in rendering improved qualitative engineering decisions concerning field moisture conditions. It is very important to acknowledge the fact that soil moisture content will change after placement.

Several procedures are available for characterizing field moisture conditions. The more useful ones are described briefly below.

Natural Soil Drainage Classes

The Soil Conservation Service of the U.S. Department of Agriculture uses seven natural soil drainage classes. The brief descriptions of these classes that follow have been adapted from more complete descriptions in the Soil Survey Manual (7). These soil drainage classes refer to the soil moisture equilibrium in the natural landscape and should not be confused with surface drainage, which is influenced by human activity.

1. Very poorly drained: Water is removed from the soil so slowly that the water table usually remains at the surface. Soils in this drainage class usually occupy level or depressional sites and are frequently

Figure 1. CBR as a function of water content for Drummer B.

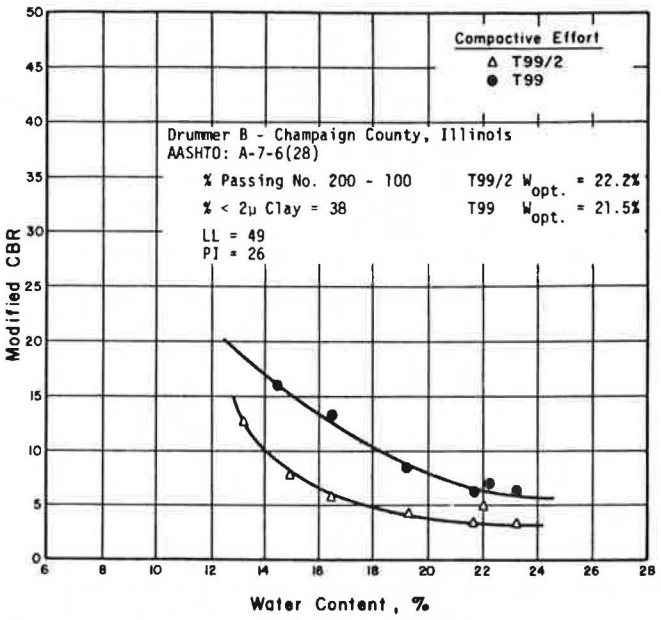

Figure 2. CBR as a function of water content for Fayette C.

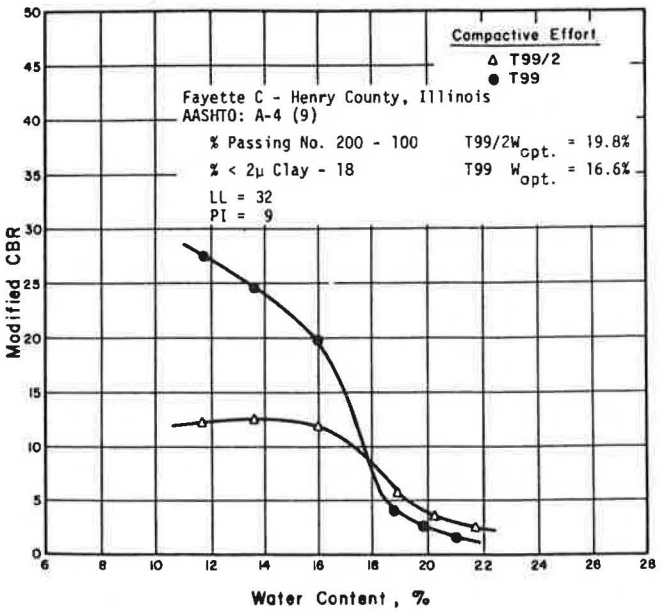

Figure 3. Permanent deformation behavior of Drummer B.

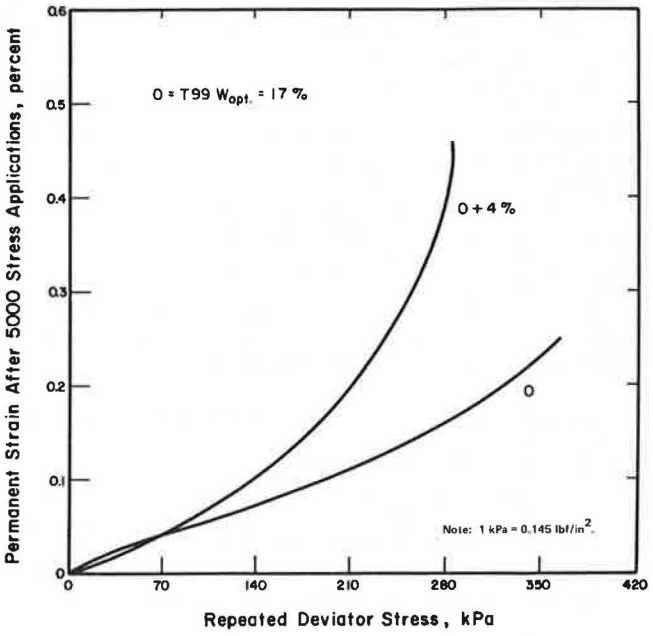

Figure 4. Permanent deformation behavior of Fayette C.

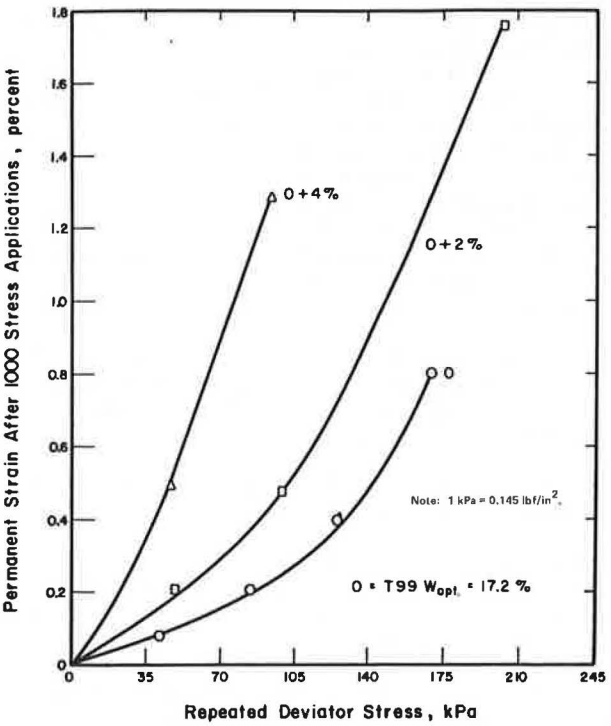

ponded. They are predominantly gray and show distinct evidence of gleying. Some have dark and mucky surfaces.

2. Poorly drained: Water is removed slowly so that the soil remains wet most of the time and the water table is often near the surface. These soils are predominantly gray, often with dark surface horizons and some yellow mottling in the subsoils.

3. Imperfectly drained: Water is removed from the soil slowly enough to keep it wet for significant periods but not continuously. These soils are uniformly gray, brown, or yellow in the upper A horizon and are commonly mottled in the lower A and in the B and C horizons.

4. Moderately well drained: Water is removed from the soil somewhat slowly, causing the profile to be wet for short but significant periods. These soils are uniformly colored in the A and upper B horizons, with some mottling in the lower B and in the C horizons.

5. Well drained: Water is removed from the soil easily, but not rapidly. These soils have little mottling, except occasionally deep in the C horizon or below depths of a few meters.

6. Somewhat excessively drained: Water is removed from the soil rapidly. Many of these soils are sandy and very porous, and most are free of mottling throughout the profile.

7. Excessively drained: Water is removed from these soils very rapidly. These soils often occur on steep slopes or are very porous or both.

Figure 5 shows the general relationship of the depth of the water table to the natural slope of the ground surface for each of these soil drainage classes. In medium-textured, moderately permeable soils the depth to the water table varies directly with slope. In finer-textured materials more poorly drained soils occur on steeper slopes, and in coarser materials well-drained soils occur on gentler slopes.

Illinois Drainage Guide

The Cooperative Extension Service and the Agricultural Experiment Station at the University of Illinois, in conjunction with the Soil Conservation Service, have jointly prepared a drainage guide for Illinois soils (8). The primary characteristics used to group the soils in the guide are soil premeability or hydraulic conductivity and the degree of wetness before any drainage practices have been applied. This classification is established for use in drainage recommendations for Illinois soils.

Drainage groups are indicated in tabular form by a number (1-4) combined with a capital letter (A or B). Soil permeability is denoted by the numbers. Definitions are given on the basis of centimeters of water that will move through the soil in an hour as given below:

1. Rapidly permeable [more than 15 cm/h (6 in/h)], moderately rapidly permeable [5-15 cm/h (2-6 in/h)];
2. Moderately permeable [1.5-5 cm/h (0.6-2 in/h)];
3. Moderately slowly permeable [0.5-1.5 cm/h (0.2-6 in/h)]; and
4. Slowly permeable [1.5-5 mm/h (0.06-0.2 in/h)], very slowly permeable [less than 1.5 mm/h (0.06 in/h)].

The capital letter in the drainage group designates the natural soil drainage or wetness before artificial drainage is applied. The natural drainage classes are combined into the two groups below.

A. Poorly drained: Without manmade drainage, the water table would be at or near the surface during the wetter seasons of the year.

Very poorly drained: Without manmade drainage, the water table would remain at, near, or above the surface much of the time.

B. Somewhat poorly drained: Without manmade drainage, the water table would be near the surface only during the very wettest periods.

The various surficial soils of Illinois are listed in the drainage guide (8) by number and type, both numerically and alphabetically. If one knows the soil type and drainage classification, it is possible to qualitatively predict potential subgrade soil moisture problems. A similar approach could be used for other locations.

Rational Method

Dempsey and Elzeftawy (6) have summarized the various rational procedures for predicting field moisture contents; they also present a computer-based model. The U.K. Transportation and Road Research Laboratory (TRRL) procedure (9, 10, 11, 12) was used in this study to demonstrate the effect of soil type and depth of water table on the field moisture content. The procedure has been described in an Organization for Economic Cooperation and Development (OECD) publication (13) and in a University of Illinois report (6).

OECD has indicated that the rational method is a valuable tool for predicting the water content of soils regardless of the soil type. This method considers only a paved, closed system without water movement to or from the pavement surface or adjacent soil masses and is only valid for subgrade profiles that have a relatively shallow water table. Table 1 shows, for typical Illinois soils, the calculated equilibrium water content at several depths in the profile for water table depths of 60, 120, and 240 cm (2, 4, and 8 ft) below the surface. The soils were assumed to be 100 percent saturated at the water table, and the moisture content variation above the water table appeared to be small. It is apparent that, for shallow water table conditions, subgrades will frequently approach 100 percent saturation.

Langfelder (14) demonstrated that the suction-water content relations for compacted typical Illinois soils are basically independent of molding water content and density. The data shown in Table 1 are thus not dependent on initial placement conditions. Placing a soil dry of optimum, or at optimum does not ensure that the moisture content will not subsequently increase.

SITE REQUIREMENTS

Subgrade Stability-Requirements

Subgrade stability requirements are dictated by construction requirements and pavement performance. The most pertinent of these are rutting and shoving and the need to effectively and efficiently place and compact the various pavement layers. The primary pavement performance considerations related to subgrade stability are the resilient deflection of the pavement and the permanent deformation accumulation in the subgrade.

Pavements can be designed to provide adequate performance for a broad range of subgrade support conditions if soil type and moisture conditions (present and future) are carefully assessed. It is important that the design subgrade support be achieved at construction and maintained throughout the desired design life.

Construction subgrade stability requirements are more restrictive than the pavement performance re-

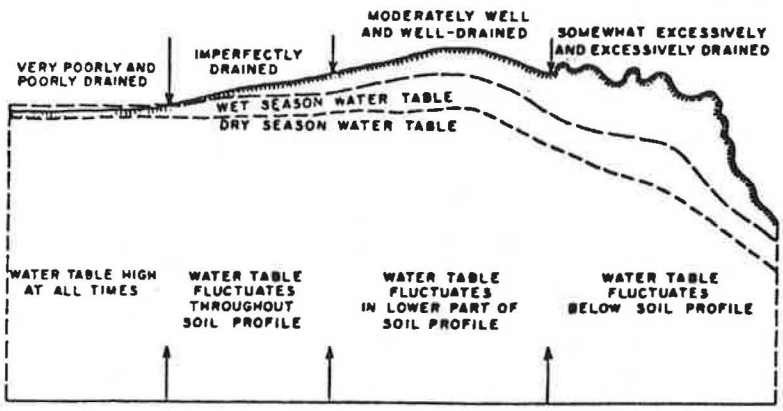

Figure 5. Water-table depth and natural soil drainage relation for medium-textured soils.

Table 1. Influence of water-table depth on soil moisture content.

Water Table Depth[a] (cm)	Calculated Moisture Content (%)			
	Champaign Loam Till	Fayette C Horizon	Muscatine C Horizon	Tama B Horizon
60 cm below pavement surface				
0	19.5	34.0	31.40	32.20
15	19.55	34.1	31.45	32.25
30	19.60	34.3	31.50	32.35
33[b]	19.65	34.3	31.50	32.40
1.2 m below pavement surface				
0	18.8	33.1	31.15	31.40
15	18.90	33.2	31.15	31.50
30	19.05	33.4	31.20	31.55
60	19.25	33.6	31.25	31.70
94[b]	19.35	33.8	31.30	31.80
2.4 m below pavement surface				
0	17.45	31.95	30.55	29.80
6	17.50	32.0	30.60	29.80
12	17.55	32.1	30.60	29.85
24	17.80	32.2	30.65	29.95
48	18.10	32.8	30.70	30.15
72	18.50	33.0	30.80	30.20
85[b]	18.75	33.1	30.80	30.30

Note: 1 cm = 0.39 in; 1 m = 3.3 ft.
[a]Below soil surface. Pavement assumed to be 28 cm thick. [b]Groundwater level.

quirements. Although load-induced stresses, strains, and displacements are greater in the subgrade during construction than at any other time, the subgrade may also be the most important factor influencing ultimate pavement performance.

Construction-Related Requirements

Sinkage

Equipment sinkage (rutting) is an important construction consideration. Rutting creates an uneven grade that makes it difficult to control the thickness of the subsequent pavement layer. Severe subgrade rutting causes a significant loss in equipment efficiency. Current Illinois DOT specifications indicate that ruts deeper than 5 cm (2 in) are unacceptable. In reality, even shallower ruts are often intolerable because of strict controls on layer thicknesses.

Rutting is bearing-capacity failure and permanent deformation caused by repeated loading at stresses near the shear strength of the material. In terms of equipment mobility, the bearing-capacity portion of the rutting is probably the most significant.

The effects of stress level, number of load applications, and moisture content on the permanent deformation behavior of two typical Illinois soils are illustrated in Figure 6 [AASHTO class A-4 (9)] and Figure 7 [AASHTO Class A-7-6 (29)]. Note that a large portion of the permanent deformation is accumulated during the first few load applications.

Traylor and Thompson (15) used two of the most promising procedures for predicting sinkage on subgrades of varying strengths. Figure 8 (15) illustrates the effect of subgrade strength on sinkage. To limit sinkage of a 40-kN (9000-lbf) wheel load with a 550-kPa (80-lbf/in^2) tire pressure to 12 mm (0.5 in) or less, the subgrade strength should be in the CBR range of 5.5-8.5. For a 6-mm (0.25-in) sinkage, the corresponding CBR strength range is 8.0-8.5. Minimizing rutting damage of the finished grade probably requires a subgrade CBR of at least 6.

Compaction of Paving Materials

The shear strength and stiffness of the subgrade significantly influence the process of compacting pavement materials such as crushed stone, gravel, and stabilized bases. Compaction effectiveness and efficiency are influenced by subgrade support. Results of controlled field compaction tests demonstrate that there are practical, achievable density limits for given types of equipment, layer thickness, and subgrade support.

Field studies summarized by Heukelom and Klomp (16) led to the conclusion that "The degree to which layers of unbound materials can be compacted depends to a large extent on the reaction of the subsoil." When successive layers of materials were compacted over the first granular layer, it was possible to achieve higher levels of compaction in the upper layers as indicated by the dynamic modulus of elasticity.

Heukelom and Klomp suggested, then, that the states of compaction, stability, and decompaction of a granular layer over a subgrade can be examined in terms of the tensile stress condition at the bottom of the granular layer. They indicated that, because of intergranular friction, the vertical component of the stress would permit the granular material to withstand certain radial tensile stress without decompacting or expanding. If the subgrade soil at the granular material-subgrade interface has a very low shear strength, it may not be possible to develop the full potential of the frictional stress needed to resist the radial displacement of the granular layer, and decompaction may follow. A low-modulus subgrade results in high tensile stresses developing at the bottom of the granular layer, which also leads to decompaction.

Barenberg's shear layer theory (17) also demonstrates the importance of maintaining a high shear strength in the soil at the granular material-subgrade interface. The theory shows that the loss of shear strength at the granular material-subgrade interface

causes a substantial decrease in load-distribution capability and increases the deflection of the granular layer, thus preventing additional compaction.

Stress-dependent finite-element analyses were conducted to determine the effect of subgrade support on the compaction behavior of granular layers such as crushed stone, gravel, cement aggregate mixture, bituminous aggregate mixture, or pozzolanic aggregate mixture. Realistic loading conditions for a pneumatic roller were used. Figure 9 shows the relations among subgrade compressive strength, roller tire pressure, and thickness of layer for soft and stiff subgrade conditions and can be used to approximate the granular layer and subgrade compaction interaction. If the system cannot withstand sufficiently high tire pressures, field compaction (which involves shear failure in the granular layer during densification) cannot be accomplished. If tire pressures are too high, significant permanent deformation and shoving will develop in the subgrade.

It is apparent that certain minimum levels of subgrade strength and stiffness are needed to ensure adequate compaction. A minimum compaction CBR of approximately 6 seems reasonable and also checks favorably with the minimum stability required for construction sinkage control.

If paving materials are placed in a plastic state, consolidated by using vibratory procedures, and then cured, compaction-related subgrade stability requirements are less stringent. Econocrete is a good example of such a material.

Performance-Related Requirements

Subgrade stability in the completed construction must be at least equal to the value used in establishing the

Figure 6. Stress level and permanent strain relations for Fayette C.

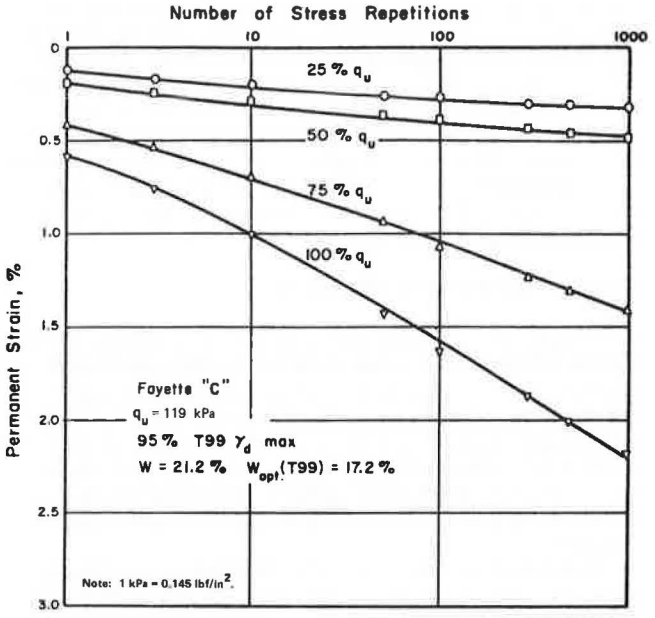

Figure 7. Stress level and permanent strain relations for Muscatine B.

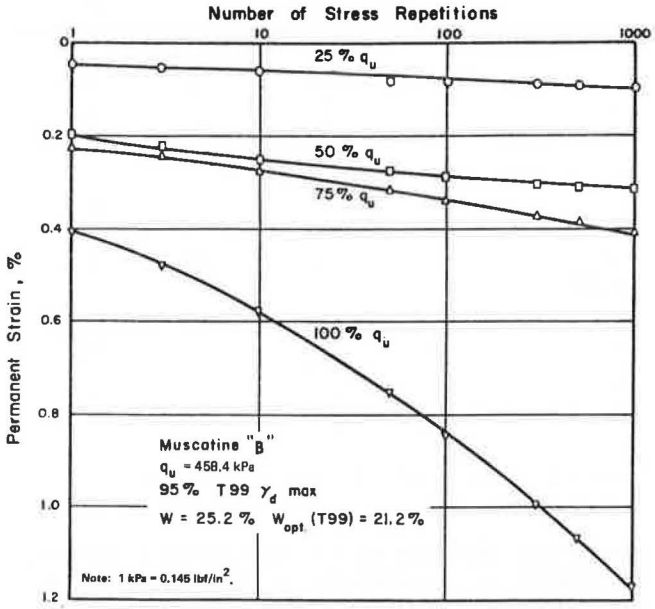

Figure 8. Soil strength-sinkage relations for a 40-kN wheel load.

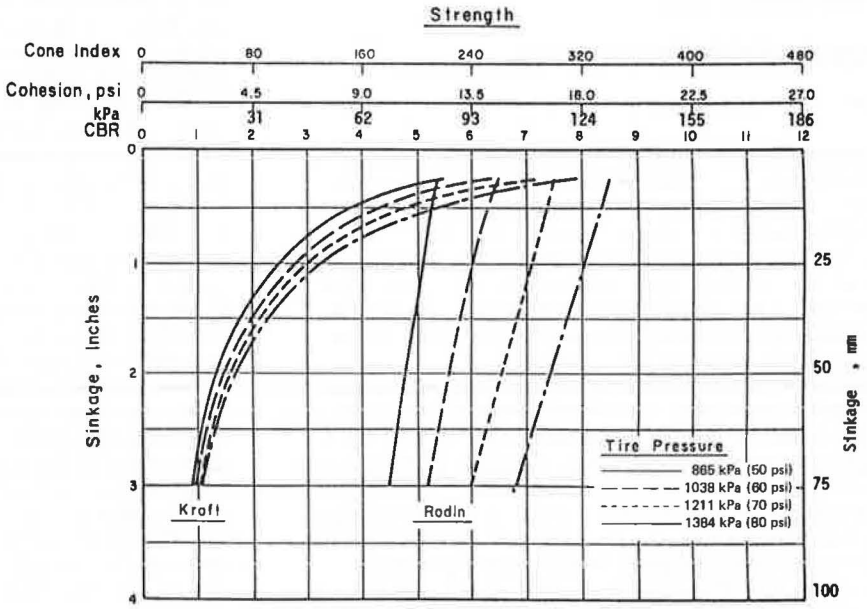

Figure 9. Tire pressure-subgrade strength and layer thickness compaction relations.

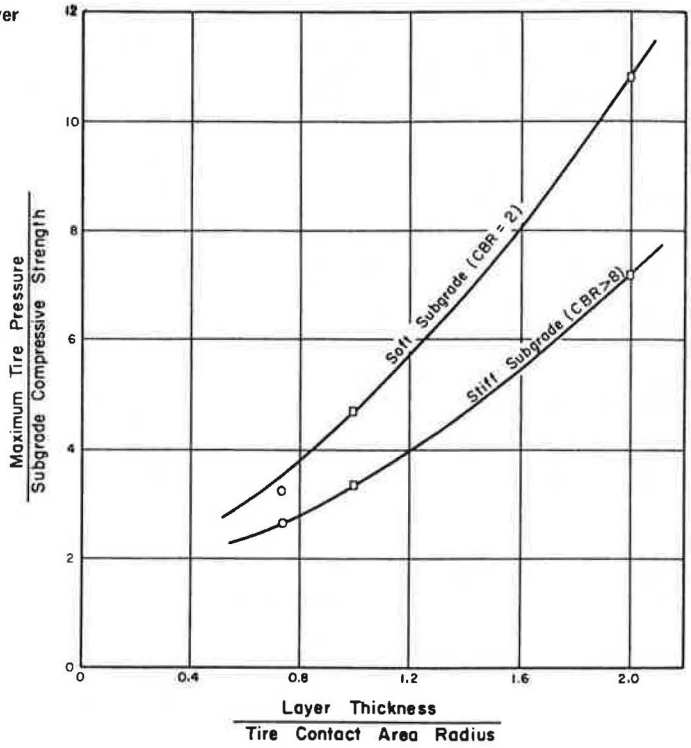

pavement design. The minimum acceptable level of subgrade support (based on design thickness considerations) should be stated in the project plans and documents. To ensure adequate performance over the design life of the pavement, the subgrade support, which will vary with time, should meet those stability levels assumed in design.

The major factors influencing support changes are moisture fluctuation and freeze-thaw action. The effects of moisture on strength and resilient properties have already been discussed. Freeze-thaw softening problems for typical Illinois soils have been considered by Robnett and Thompson (18). Typical detrimental effects (expressed as a reduction in resilient modulus during freezing and thawing) may reduce resilient moduli by a factor of two or three.

The need for careful consideration of the temperature and moisture regime (relative to pavement performance) is obvious. Dempsey and Thompson (19) have developed analysis procedures for considering temperature effects in pavement systems. Frost-action depths can be estimated fairly accurately by using those procedures. The work of Dempsey and Elzeftawy (6) can also be used to determine moisture change with time and space. Moisture movement theory indicates that the projected moisture content as a function of space and time for a given pavement profile is not significantly influenced by the moisture-density condition of the soil at placement.

Summary

Construction operations and pavement performance should be considered whenever one is establishing subgrade stability requirements. In most situations construction-based stability requirements will predominate. It is interesting to note that in an Illinois study (1) the average CBR (immediate penetration) of typical Illinois soils compacted at T99 optimum moisture content to 100 percent of AASHTO T99 maximum density was 8.6 with a standard deviation of 3. Approximately 20 percent of the soils had a CBR of less than 6. Many soils having moisture contents in excess of T99 optimum will have compacted CBR less than 6.

REMEDIAL ACTION

A comparison of subgrade stability requirements with the properties of typical Illinois soils compacted at a range of commonly found water contents indicates that, in many instances, the compacted soil will not possess adequate strength or stiffness or both. Among the appropriate remedial procedures that have been successfully used are undercut and backfill, moisture density control, and admixture stabilization (physical mixing of soil and admixture).

Undercut and Backfill

One popular procedure is to cover the soft subgrade with a thick layer of granular material or to remove a portion of the soft material to a predetermined depth below the gradeline and replace it with granular material. This granular layer distributes the wheel loads over the unstable subgrade and serves as a working platform on which construction equipment can operate.

Two conditions must be satisfied for a firm working platform: First, the granular layer must be thick enough to develop acceptable pressure distribution over the soft subgrade; second, the backfill material must be able to limit rutting under the applied wheel loads to acceptable levels.

Moisture-Density Control

It has been shown above that the stability, or strength and stiffness, of a cohesive soil is influenced primarily by moisture content and, to a lesser extent, by density. Wet of optimum, moisture is the primary factor influencing stability. Given low density or excessively high moisture content (which is generally the problem),

it is difficult to achieve a sufficiently good working platform for efficient use of construction equipment and adequate subgrade support for the finished pavement.

On the subject of compaction Wahls (20, p. 99) has said that

> Compaction specifications may indicate the procedure by which the compaction is to be accomplished, the required quality of the compacted materials, or some combination of procedure and required results. The specified procedure may include moisture control, lift thickness, type and size of compaction equipment, and the number of coverages of the equipment. The quality of the compacted material generally is specified in terms of dry density, which is usually expressed as a percentage of the maximum dry density achieved in a specified laboratory compaction test.

He discussed in detail the embankment and subgrade compaction specifications used in the United States. In 1967 he said,

> A statement regarding moisture requirements is included in the specifications for embankments in all but two states and for subgrade in all but nine. However, in approximately 60 percent of the states the moisture conditions for both embankment and subgrades are specified in a qualitative manner which leaves the interpretation largely to the judgment of the inspector.

A major problem in implementing moisture control is the proper establishment of permissible compaction moisture contents. Figures 10, 11, and 12 illustrate the relations among compaction moisture content, CBR, and compactive effort. Previously a minimum CBR of 6 was suggested for adequate subgrade stability. From Figure 11 it is obvious that the compaction moisture content must be less than 110 percent of optimum to ensure a CBR of 6 in half the soils tested. In many instances the on-site soils or borrow materials are significantly wet of optimum and require extensive drying.

That the use of density control in embankment con-

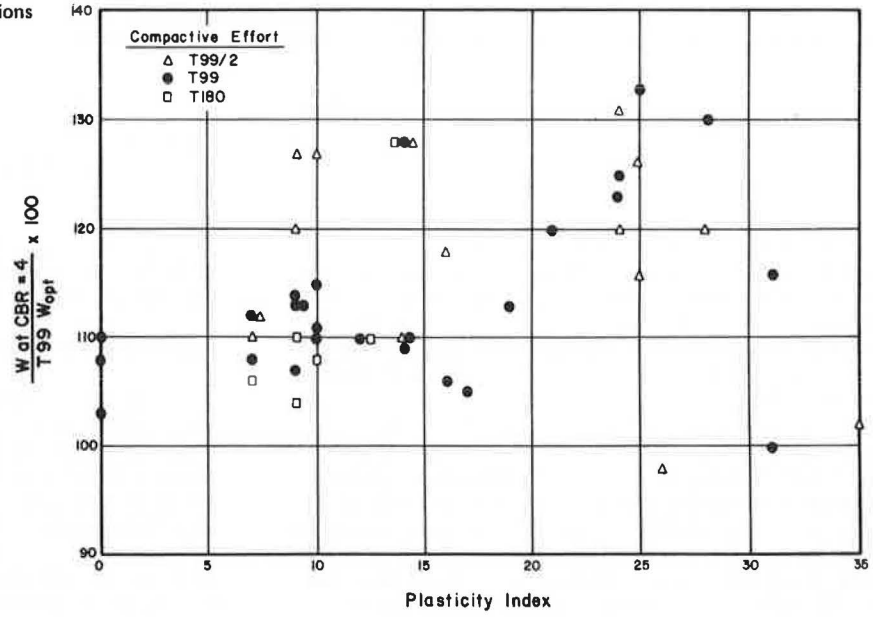

Figure 10. CBR and moisture content-PI relations for typical Illinois soils of CBR 4.

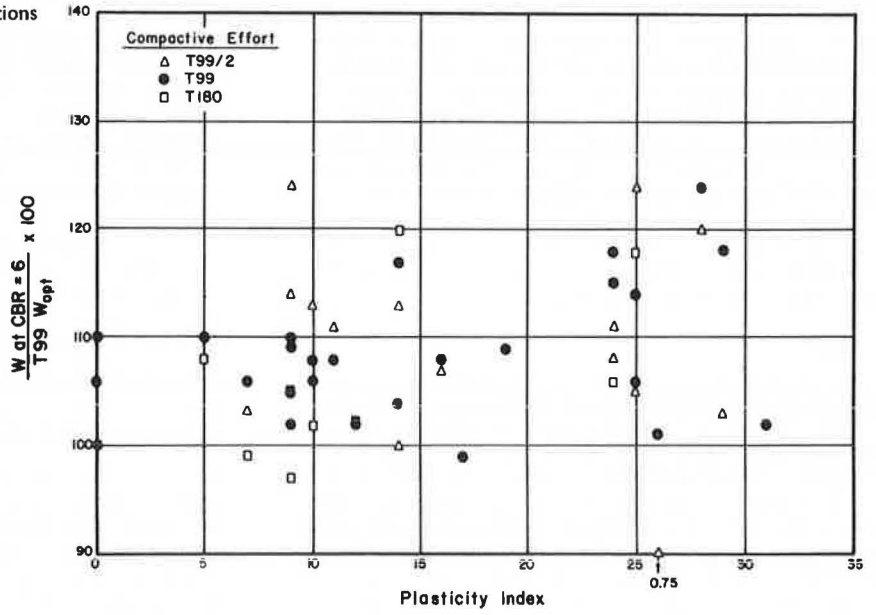

Figure 11. CBR and moisture content-PI relations for typical Illinois soils of CBR 6.

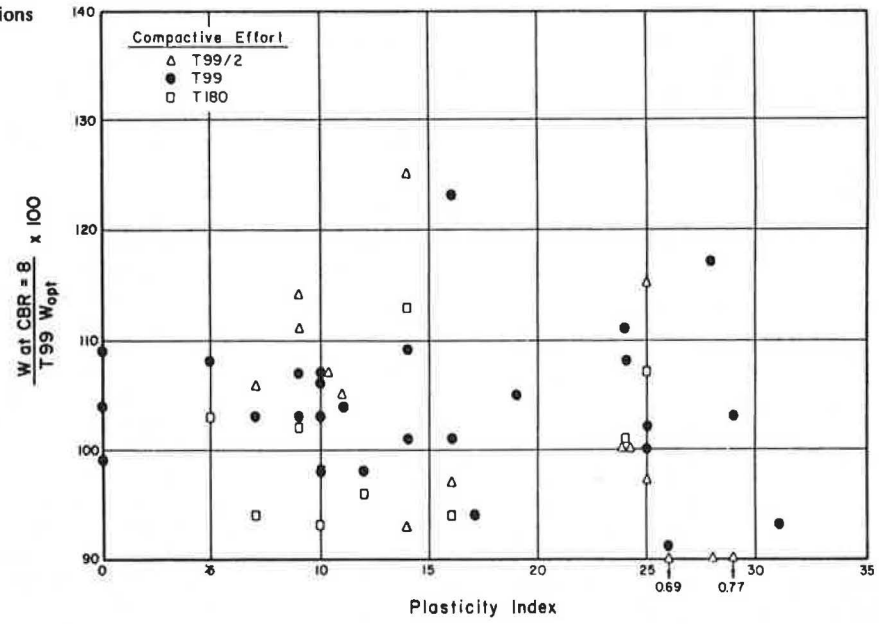

Figure 12. CBR and moisture content-PI relations for typical Illinois soils of CBR 8.

struction as a means of improving subgrade stability is widely accepted is indicated by its overall use in specifications. The use of moisture control is also accepted but generally as a qualitative requirement. The quantification of moisture control would help increase subgrade stability, at least on a temporary basis. Three major problems are involved in the use of moisture-density control as a remedial measure.

1. Specified compaction densities and moisture contents are formulated in the laboratory, so it is necessary to approximate the field compaction method by the laboratory test used. There are data that indicate that the densities and physical properties of samples compacted by laboratory impact methods (most widely used method) may differ significantly from the properties of the same material compacted by construction equipment in the field.
2. It is possible to have an acceptable density but not a stable subgrade because of soil type. No matter how much compactive effort is expended, it is impossible to achieve a stable subgrade with certain soils, particularly if they are wet of optimum.
3. Several major problems are encountered in achieving a specified water content before compaction and then maintaining the water content of the finished subgrade.

Water Content Control

Many present specifications for controlling excess moisture provide for draining the grade and drying the top several centimeters of the subgrade. Drainage of the area will remove surface water, but will not significantly reduce the water content of fine-grained soils. Drying is accomplished through evaporation. Disking and manipulating the soil increase the amount of exposed surface area to increased evaporation that can speed drying. The factors involved in the evaporation process and some models used to predict evaporation are examined below.

Evaporation can be defined as the conversion of soil surface water into vapor in the atmosphere. Three basic conditions are necessary for the evaporation process to occur.

1. There must be a heat supply, because the rate of evaporation increases with the water temperature.
2. There must be a vapor pressure gradient to the atmosphere, which allows removal of the vapor.
3. There must be a continual supply of water from or through the soil profile, because, if there is no water, there is no evaporation.

The first and second conditions are external to the soil and are influenced by climatic factors such as air temperature, solar radiation, humidity, and wind velocity, of which the first two are the most important.

Evaporation reduces the soil water content at the surface, thus increasing soil water suction at the surface. The pressure gradient draws water from the layers below. If the water table is low, the surface materials will be dried; if the water table is high, it is quite possible for the evaporation process to draw a continual flow of water to the surface. A crust can form at the surface, but wet, soft, potentially troublesome soils could remain below.

In order to quantify the potential for drying by evaporation, Thompson and others (21) considered some of the many models for predicting evaporation that have been developed. Most of them use variables that cannot be determined easily, but two models that use commonly available variables have been proposed by Thornthwaite (22) and Hamon (23, 24) to predict evaporation from an open pool of water.

Hamon's (23, 24) simplified expression for potential evapotranspiration is

$$E_p = CD^2P_t \quad (1)$$

where

E_p = potential evapotranspiration in millimeters per day;
D = possible hours of daily sunshine in units of 12 h;
P_t = saturated water-vapor concentration at the mean temperature in grams per cubic meter; and
C = 0.0055, an empirically developed constant.

Values of D^2 and P_t have been tabulated in Hamon's paper (24). For illustration purposes, potential evapotranspiration data (based on Hamon's equation) are presented in Figure 13 (25) for central Illinois. Also shown in the figure is the theoretical percentage of moisture removed from a 0.1-m^2 (1-ft^2) block of soil, 20 cm (8 in) deep.

It should be noted that calculated evapotranspiration is likely to exceed actual evaporation from a subgrade. The methods are for ideal conditions and do not allow for precipitation during the calculated period. Both methods use mean temperature, which does not give as good an indication of potential as radiation, and both include removal of water by transpiration, which will not occur on an earthen surface. Neither method takes soil type into account.

The Hamon predictions are an optimistic appraisal of expected evaporation from the soil. Although some drying can be expected from evaporation, it is improbable that large amounts of water will be removed from the subgrade over a short time span. It is particularly important to note (see Figure 13) that, during periods of low prevailing temperatures, very little drying occurs. The process of tilling may or may not be beneficial, depending on evaporation stage and soil type.

Maintenance of Subgrade Water Content

As previously indicated, many surficial soils are poorly or imperfectly drained. Although one might be able to place a subgrade soil that is in an area of prevailing high water table at or near the optimum water content, it is difficult to maintain that moisture condition. Higher suction in the drier soil will draw the moisture up through the subgrade from the underlying soil until an equilibrium condition is reached. The equilibrium water content with a shallow water table is generally considerably above the optimum water content. In addition, precipitation will cause surface wetting and subsequent moisture increases in the subsurface zone.

Admixture Stabilization

Admixture stabilization (mixing and blending a liquid, slurry, or powder with the soil) is a technique that has been successfully used for improving soil strength and stiffness properties and thus improving subgrade stability.

Those admixtures most widely used for remedial treatment of subgrade soils are lime, lime-fly ash, and cement. Fly ash, cement kiln dust, and lime kiln dust have also been used and frequently are available at a low cost. One particularly attractive characteristic of fly ash and kiln dusts in their low energy value, which makes them very attractive in terms of energy conservation.

Several construction procedures have been used in wet-soil treatment operations. Conventional rotary mixers can readily handle lifts as thick as approximately 30 cm (12 in). Special procedures or deep plowing may be needed to construct thicker layers; the former have been described in detail by Thompson (25). Lime-treated layers as thick as 60 cm (24 in) have been constructed in one lift in Illinois. In some instances, wet borrow soils have been 100 percent treated to form a stable embankment. Admixture stabilization can be accomplished by using borrow pit mixing procedures, or the wet borrow can be spread on the embankment in a normal lift thickness and then stabilized.

Construction specification and procedures for remedial subgrade soil treatment are frequently less stringent than those for stabilization, where the stabilized material may be used as a structural pavement layer. Improved job mobility, fewer working days lost by wet weather, and a general expediting of construction are frequently mentioned benefits of admixture-stabilized subgrades.

Admixture stabilization is in many instances a very cost-effective procedure. Significant energy savings, relative to other remedial procedures, may also be achieved.

The technologies associated with the various forms of admixture stabilization are fairly well established. Careful consideration should be given to admixture treatment levels, construction techniques and operations, and construction control.

SUMMARY

Soil type and moisture content are the major factors influencing and controlling subgrade stability. The current use of pedologic soils information (previous soil reports, geologic data, drilling, sampling, and testing to identify soil type) is fairly well defined and

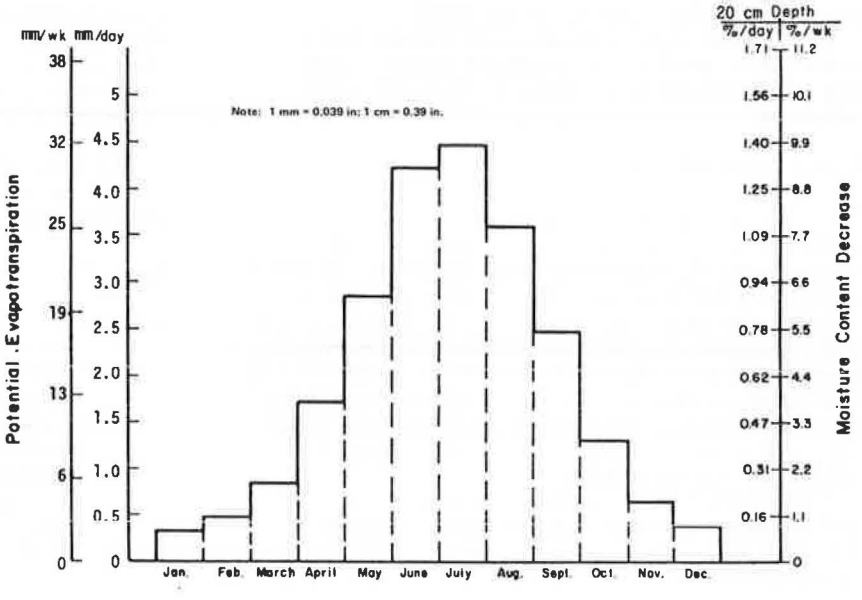

Figure 13. Potential evapotranspiration for central Illinois (Urbana data) based on Hamon's procedure.

seems adequate for subgrade stability evaluation. But techniques and procedures currently used to characterize field soil moisture regime are inadequate. It is essential to acknowledge that field soil moisture content is not static but varies constantly with time. The TRRL procedure described in this report can be used to evaluate the field soil moisture regime.

Subgrade stability requirements are primarily dictated by pavement construction demands. Analyses of equipment sinkage and paving-material compaction operations indicate that a minimum in situ CBR of 6-8 is required. Many typical fine-grained soils do not develop CBRs in excess of this when compacted at or wet of AASHTO T99 optimum water content. Thus, remedial procedures must often be used to provide adequate subgrades for pavement contraction.

Three such procedures—undercut and backfill, moisture-density control, and admixture stabilization—were described and evaluated. Undercut and backfill and admixture stabilization offer the greatest potential and provide a permanent solution that has significant carry-over effects beneficial to the ultimate performance of the completed pavement.

ACKNOWLEDGMENT

This report was prepared as a part of the Illinois Cooperative Highway and Transportation Research Program on subgrade stability at the Department of Civil Engineering in the Engineering Experiment Station, University of Illinois at Urbana, in cooperation with the Illinois DOT. The contents of this paper reflect my views and I alone am responsible for the facts and accuracy of the data presented. The contents do not necessarily reflect the official views or policies of the Illinois DOT.

REFERENCES

1. M.R. Thompson and Q.L. Robnett. Final Report—Resilient Properties of Subgrade Soils. Illinois Cooperative Highway and Transportation Research Program, Dept. of Civil Engineering, Univ. of Illinois, Urbana, Transportation Engineering Series 5, No. 160, June 1976.
2. T.K. Liu and T.H. Thornburn. Investigation of Surficial Soils by Field Vane Test. American Society for Testing and Materials, Philadelphia, Special Tech. Publ. 351, 1964.
3. J.L. Peterson. Improving Embankment Design and Performance: Prediction of As-Compacted Field Strength by Laboratory Simulation. Joint Highway Research Project, Purdue Univ., West Lafayette, IN, Rept. 75-22, 1975.
4. S.J. Knight. Some Factors Affecting Moisture Content-Density-Cone Index Relations. Waterways Experiment Station, U.S. Army Corps of Engineers, Vicksburg, MS, Miscellaneous Paper 4-457, Nov. 1961.
5. Soils Manual. Bureau of Design, Illinois Department of Transportation, Springfield, 1977.
6. B.J. Dempsey and A. Elzeftawy. Interim Report—Moisture Movement and Moisture Equilibria in Pavement Systems. Illinois Cooperative Highway and Transportation Research Program, Dept. of Civil Engineering, Univ. of Illinois, Urbana, Civil Engineering Studies, Transportation Engineering Series 15, No. 161, 1976.
7. Soil Survey Staff. Soil Survey Manual. U.S. Department of Agriculture, Handbook 18, 1951.
8. Drainage Guide for Illinois. Cooperative Extension Service and Agricultural Experiment Station, Univ. of Illinois, Urbana; Soil Conservation Service, U.S. Department of Agriculture.
9. W.P.M. Black, D. Croney, and J.C. Jacobs. Field Studies of the Movement of Soil Moisture. British Road Research Laboratory, Crowthorne, England, BRRL Technical Paper 41, 1958.
10. K. Russam. The Distribution of Moisture in Soils at Overseas Airfields. British Road Research Laboratory, Crowthorne, England, BRRL Technical Paper 58, 1962.
11. J.D. Coleman and K. Russam. The Effect of Climatic Factors on Subgrade Moisture Conditions. Geotechnique, Vol. 11, March 1961.
12. Estimation of Subgrade Moisture Content. British Road Research Laboratory, Crowthorne, England, BRRL Leaflet LF 98, 1967.
13. Water in Roads: Prediction of Moisture Content of Road Subgrades. Organization for Economic Cooperation and Development, Paris, 1973.
14. L.J. Langfelder. An Investigation of Initial Negative Pore Water Pressures in Statically Compacted Cohesive Soils. Dept. of Civil Engineering, Univ. of Illinois, Urbana, Ph.D. thesis, 1964.
15. M.L. Traylor and M.R. Thompson. Sinkage Prediction-Subgrade Stability. Dept. of Civil Engineering, Univ. of Illinois, Urbana, Civil Engineering Studies, Transportation Engineering Series, No. 17; Illinois Cooperative Highway and Transportation Series No. 168, June 1977.
16. W. Heukelom and A.J.G. Klomp. Dynamic Testing as a Means of Controlling Pavements During and After Construction. Proc., 1st International Conference on the Structural Design of Asphalt Pavements, Ann Arbor, MI, 1962.
17. E.J. Barenberg. A Shear Layer Concept for Flexible Pavements. Paper presented at the 47th Annual Meeting, HRB, 1968.
18. Q.L. Robnett and M.R. Thompson. Effect of Lime Treatment on the Resilient Behavior of Fine-Grained Soils. TRB, Transportation Research Record 560, 1976, pp. 11-20.
19. B. J. Dempsey and M. R. Thompson. A Heat-Transfer Model for Evaluating Frost Action and Temperature-Related Effects in Multilayered Pavement Systems. HRB, Highway Research Record 342, 1970, pp. 39-56.
20. H.E. Wahls. Current Specifications. Field Practices and Problems in Compaction for Highway Purposes. HRB, Highway Research Record 177, 1967, pp. 98-111.
21. M.R. Thompson and others. Final Report—Subgrade Stability. Illinois Cooperative Highway and Transportation Research Project, Dept. of Civil Engineering, Univ. of Illinois, Urbana, Civil Engineering Studies, Transportation Series 18, No. 169, June 1977.
22. C.W. Thornthwaite. An Approach Toward a Rational Classification of Climate. Geographical Review, Vol. 38, 1948.
23. W.R. Hamon. Estimating Potential Evapotranspiration. Massachusetts Institute of Technology, Cambridge, B.S. thesis, 1960.
24. W.R. Hamon. Estimating Potential Evapotranspiration. Journal of Hydraulics Division, Proc., ASCE, Vol. 87, No. HY3, May 1961.
25. M.R. Thompson. Deep Plow Lime Stabilization for Pavement Construction. Journal of Transportation Engineering Division, Proc., ASCE, Vol. 98, No. TE2, 1972.

Publication of this paper sponsored by Compaction and Stabilization Section.

Predicting Field Compacted Strength and Variability

J. T. Price, A. G. Altschaeffl, and C. W. Lovell, Department of Civil Engineering, Purdue University, West Lafayette, Indiana

A sheepsfoot and a rubber-tired roller compacted samples in the field that were tested to determine how water content, dry density, and compactive effort affect the magnitude and variability of the unconfined shear strength of a glacial, silty clay soil. The samples taken were tested in both the as-compacted and the soaked conditions. Statistical analyses were used to determine the most useful predictive models for the dry density and shear strength for each roller type and soil condition. In all cases, only the wet-of-optimum water content results could be studied. The regression models for the as-compacted unconfined strength indicated that water content and compactive effort were the most influential variables regardless of the roller type and had the greatest effect on the soaked strength of the soil compacted by the rubber-tired roller. No significant model was found for the soaked soil compacted by the sheepsfoot roller. Variability from field operations appears to be a major cause of differences between field and laboratory compacted soils. Variability in the magnitude of unconfined strength in the field was found to be significant, predictable, and larger than in the laboratory and prevents consistently accurate determination of the true state of the compacted mass by a few samples. This variability can be reduced by controlling variability of the water content at compaction.

The engineer designing an embankment must select or estimate the expected soil strength and devise specifications to ensure its achievement. One method for estimating expected strength is to construct a special fill section by using a range of compaction processes and then to test samples from the soil mass after each process.

Such a test pad and the associated costs of field sampling, laboratory testing, and analysis, however, are not economically feasible for most projects. The problem is compounded if more than one soil type is used within the proposed embankment. Therefore, the design engineer must infer the strength behavior of field compacted soils from laboratory developed compaction curves. Because this inference process may not be the most desirable, our objective in this paper is to develop a rational method of predicting the field post-compaction strength response from laboratory tests.

A special test pad was constructed from which samples were taken and tested for unconfined strength. The water content, dry density, and compactive effort were known for each sample. Relations among the variables were developed to formulate prediction equations for field strength.

Because soil type and condition are not uniform and because compaction processes and sampling and testing programs cannot be precisely duplicated, the resulting dry density and strength characteristics vary within some definitive range. This report investigates variation in the field compacted soil and attempts to develop a method to predict its magnitude. This will allow a design engineer to predict both the expect average unconfined soil strength and the expected variation from it. It will also give him or her a tool with which to better control field variability. Once this has been been accomplished, the engineer will have a method for developing a compaction specification for subgrades and low embankments that ensures a minimum soil strength.

PROJECT PURPOSE

Strength-Density Assumptions

Engineers who design fill sections and embankments are concerned with developing compaction specifications that ensure adequate strength behavior of the compacted soil mass. Three general types of specifications are currently in use.

The first type, which requires a desired end result, usually demands the post-compaction field density to be some predetermined percentage of the maximum density derived from a standard laboratory compaction test. Also, a range in permissible water content is usually stated.

The second specification format requires the use of a particular compaction process. Equipment type and operation, lift thickness, and number of passes are partially or wholly regulated.

The third format is a combination of the first two. Density, water content, lift thickness, equipment type, and equipment use are all specified. This is the most rigid of the specification types and requires a highly competent engineer to achieve an economical design result.

All three compaction-specification formats are similar in that they are either directly based on or are concerned with the resulting field density relative to standard laboratory compaction test density on the same soil. None directly addresses the soil strength property, even though it is often the primary reason for compacting the soil.

One reason for specifying density rather than strength is economics. The cost of an inspector's making a few density control-test determinations is less than that of a field sampling and laboratory testing program for shear strength determinations. Another reason for regulating density rather than strength is that, while little research has been undertaken to relate the field conditions and compaction processes directly to the resulting strength, much research on field compacted soils has been directed toward the determination of the resulting density. Similarly, an enormous quantity of research has been published on the relationship between soil conditions and compaction processes and the density and shear strength results of laboratory compacted soil. As a result, field shear strength derived from any of the specification formats is usually inferred from the measurement of the density.

This inference process may not be the most desirable because it is based on three assumptions whose applicability varies according to soil types, soil conditions, and compaction processes. The first assumption is that strength varies directly with density for a given water content; the second assumption is that the strength curve must be similar, both in shape and in orientation, to the density curve corresponding to the same compaction process; the third assumption is that field strength is related to the laboratory density in a manner nearly identical to that of laboratory strength.

There are two possible approaches to making the transition from field strength to laboratory strength. The first directly relates the field strength obtained from a particular soil condition and compaction process to the laboratory strength derived under similar conditions. The second assumes that field strength is related to field density as laboratory strength is to laboratory density. A correlation must then be shown to exist between the field and laboratory compaction curves.

A review of the literature by Price (1) showed that inferring strength from measurements of water content and density may not ensure that a minimum desired strength has been achieved. A first step in devising a better method of predicting the field strength from laboratory compaction and strength tests was finding relationships for field compaction results.

Variation of Compaction Results

Variation in compaction results occurs regardless of the stringency of methods taken to prevent it. Just as uniformity in soil strength characteristics is one criterion necessary for providing an adequate foundation for highway pavements, so should compaction techniques that reduce the resulting variability as much as is economically feasible be employed.

Williamson and Yoder (2) and Williamson (3) performed tests on a wide variety of soils compacted in the field by sheepsfoot, rubber-tired, and steel-wheeled rollers. Measurements of water content, density, and standard maximum density were taken by using accepted procedures of the following field control-testing equipment: sand cone, water-filled rubber balloon, and three calibrated nuclear gauges. They concluded that there were three major contributors to variance.

1. Compaction process variability: This involved the inability to compact the soil in a precisely replicative manner throughout the fill section or between different fill sections. Variations in equipment type, roller operating speed, soil temperature, air humidity, lift thickness, material handling procedures, and amount of compactive effort all contribute to this.
2. Testing variability: Any conventional field sampling and testing program is difficult if not impossible to duplicate. Equipment accuracy and precision and operator proficiency largely determine this variability. The amount usually increases if more than one operator performs the tests, if different instruments of the same kind are used, or if different equipment types are employed.
3. Material variability: Soil within any fill lift can vary to some degree because of the heterogeneous conditions within the borrow area. Mixing various soil types during the soil-handling process can make the fill soil even less homogeneous. Changing water content within a test lift also causes soil conditions to differ and further contributes to the material variability.

Tables 1 and 2, reprinted from Essigmann (4), indicate the results of attempts to isolate the effects of material variability and equipment. Of importance in these tables are the great density variabilities that have been found and can be expected to be found by using normal construction procedures.

Essigmann also developed a technique for predicting expected dry density and unconfined strength variabilities for a clayey silt tested in the as-compacted condition. Scott (8) used a similar analysis for the same soil tested in the soaked condition. In both studies, the soil was laboratory compacted by the impact method. The results indicate that the variations in dry density and strength depend on the compaction process and soil conditions at the time of compaction. Also disclosed in these works is the first indication that interrelationships between the compaction process and soil conditions can significantly influence density and strength magnitude and variability. This means that discussions of the effects of variables one-on-one with a property could be failing to include a major consideration.

As all the above research studies indicate, the great variations in dry density and unconfined strength that exist can be attributed to varying soil conditions, testing ability, and compaction processes. Only a few of the currently used compaction specifications regulate both the soil conditions and compaction process, and no specification known to us has been devised to account for the expected variability found in compacted soil. Without knowing expected variability in density or strength and without using this information when specifying an end result of the compaction process, the design engineer's ability to predict the strength property of the fill or embankment is severely handicapped.

EXPERIMENTAL PROCEDURE

A special test pad was prepared by the Indiana State Highway Commission (ISHC); the soil, similar to that used by Essigmann (4) and Scott (8), was compacted and then sampled. A sheepsfoot roller compacted half the test-pad soil while a rubber-tired roller compacted the other half. Samples from each roller's work were tested in unconfined compression in the as-compacted and in the laboratory-induced soaked condition, which simulates that of an in-service soil. The data from these tests were statistically analyzed to establish relationships among the water content, dry density, compaction effort, and unconfined strength.

Soil Classification and Testing Schedule

The soil was obtained from a borrow area located within the right-of-way along state road 109 near Anderson, Indiana. The table below summarizes the identification tests performed on this soil.

Test	Value
Liquid limit, %	28
Plastic limit, %	18
Plastic index, %	10
Specific gravity of solids	2.73
Unified classification	CL
AASHTO classification	A-4(7)
Descriptive name	Silty clay

Once the test lift soil had been prepared in a routine manner (in sections, each section at a different water content), the compaction equipment made a designated number of routine passes over the entire test lift. Five samples were taken from each test section. The location of each sample was selected from a random number chart, and each sample was assigned its testing role in this manner.

Compaction and Sampling Program

Specifications for the sheepsfoot and the rubber-tired roller are shown in the lists below. For the sheepsfoot roller they are

Case Model 815,

Operating weight 18.1 t (20 tons),
Wheels, tamping foot,
Drum width 97 cm (38 in),
Chevron foot pattern,
60 feet per wheel,
12 feet per row,
116 cm^2 (18 in^2) per foot, and
Foot length 19 cm (7.5 in).

The specifications for the rubber-tired roller are

Ferguson Model RT-2511,
Operating weight 22.7 t (25 tons),
Tires 9:00 x 20 SWTC,
Tire loading 2066 kg (4545 lb),
Tire pressure 586 kPa (85 lbf/in^2),
Contact area 388 cm^2 (60 in^2),
Ground pressure 515 kPa (74.7 lbf/in^2), and
Tire deflection 2.629 cm (1.035 in).

Thin-walled, stainless steel tubes that were 27.9 cm (9 in) long and of a 5.1-cm (2-in) outside diameter and a 0.17-cm (0.066-in) wall thickness were driven into the test section to obtain samples. Samples were extruded from the tubes and each was placed in a plastic bag and carefully positioned in a styrofoam chest for transportation to the laboratory.

At the Purdue soil mechanics laboratory, each sample was trimmed, measured, weighed, and prepared for the as-compacted compression test or stored for the soaked compression test. End trimmings of the samples prepared for the soaked tests were used to find original water content. The as-compacted compression sample was placed in a plastic bag and stored for five days in a humidifier in a constant-temperature room to cure it and to produce the lowest strength test results (4).

The samples used for the soaked tests were individually wrapped in cellophane and then dipped in a parafin bath until a thick coating of wax formed around each sample. Two plastic bags were placed around the samples, which were then stored in constant humidity (≅ 100 percent) and temperature. Lack of available equipment made it necessary to store these samples for as long as eight months. A small change in the water content (average of 0.5 percent) usually resulted from storage.

It must be noted that the use of relatively routine field operations created nonhomogeneities that caused some attrition in samples.

Table 1. Effect of soil homogeneity on density variability.

Source	Soil Type	N	Dry Density	
			Mean (% $\gamma_{d_{max}}$)	SD(%)
Sherman, Watkins, and Prysock (5)	Clayey, silty sand, medium plasticity, homogeneous	50	92.9	2.4
	Clayey, silty sand, boulders to 15 cm, heterogeneous	50	90.5	3.1
	Heavy clay, sand, stone, shale, very heterogeneous	44	93.6	5.5
Jorgenson (6)	Glaciated soil area	100	88.7	4.5
	End moraine area	98	89.9	8.04
	Nonglaciated area	54	97.8	4.8
Williamson (2)	Silt to silty clays, low plasticity, homogeneous	200	92.4	5.76
	Low plasticity silty to moderately plastic clays, heterogeneous	140	95.5	6.02
	Highly plastic clayey sand, very heterogeneous	138	96.1	6.33
Smith and Prysock (7)	Uniform material, none greater than 1.8 cm	200	92.86	2.44
	Fairly uniform material greater than 1.8 cm to occasional 15 cm	200	90.54	3.09
	Extremely heterogeneous	176	93.64	5.52

Note: 1 cm = 0.39 in.

Table 2. Effect of compaction equipment on density variability.

Compaction Method	No. of Samples	Dry Density[a] (%)		Moisture Content[a] (%)	
		Mean	SD	Mean	SD
Sheepsfoot roller	70	98.4	7.1	-2.0	3.2
Sheepsfoot and pneumatic tire equipment[b]	101	95.1	4.5	-5.2	2.9
Turtle[c]	40	93.1	5.3	-3.1	3.3
Total	211	94.9	5.7	-3.5	3.2

[a] With respect to maximum density and optimum moisture from AASHTO T99-70.
[b] Areas where sheepsfoot and rubber-tired construction equipment were operating.
[c] A hand-operated vibratory compactor used in small confined areas.

Laboratory Testing Program

The as-compacted samples were tested in unconfined compression following the procedure of Essigmann without exception. All tests were run at a small temperature fluctuation of ± 2°C from an average of 22°C (average 70° ± 3.5°F).

All field samples used to simulate the in-service conditions were soaked [in triaxial cells with a cell pressure of about 351 kPa (51 lbf/in^2) and a back pressure of 345 kPa (50 lbf/in^2)] and tested by using the procedure of Scott (5) with minor changes as listed by Price (1).

ANALYSIS OF DATA

A total of 168 field-compacted samples were tested in unconfined compression. Of these, 74 were compacted by the sheepsfoot roller, 62 were tested in the as-compacted condition, and 12 were tested in the soaked condition. The remaining 94 samples were compacted by the rubber-tired roller; 72 of these samples were tested as compacted and 22 were soaked before testing.

Twelve as-compacted samples for each roller type were separated from the remaining samples before the statistical analysis was performed. These samples were used to verify the predictive ability of the regression models derived from the larger group of samples. A random number chart was used to select samples for the verification process. As a result, the statistical analysis for the as-compacted specimens was performed on 50 samples from the sheepsfoot roller and 60 from the rubber-tired roller. Because so few samples were tested in the soaked condition, no soaked samples were excluded from the statistical analysis and no corresponding verification was made of the in-service predictive models.

Dry Density and Unconfined Strength

The initial portion of this analysis isolated the prediction models that best estimated the "true" or population relationships between the dependent and independent variables. Three successive steps were employed to identify these models.

In the first step the dependent variables were plotted against each independent variable—dry density against water content and compactive effort, unconfined strength against water content, compactive effort, and dry density. If the scattergrams showed a linear relationship with first-order variables, higher-order terms were not used in further analyses. However, if a distinctly linear

Table 3. Dry density and strength regression models.

Roller Type	Soil Condition	Model Type	Regression Model
Sheepsfoot	As compacted	Original	$\hat{\gamma}_d = -22.37w + 2134.88$
		Original	$\hat{q}_u = -14.20w + 4.036E + 2.437\gamma_D + 117.23$
		After substitution	$\hat{q}_u = -17.60w + 4.036E + 442.22$
Rubber tired	As compacted	Original	$\hat{\gamma}_d = -0.762w^2 + 2.704E + 1959.36$
		Original	$\hat{q}_u = -15.34w - 1.069E + 0.506\gamma_D + 358.18$
		After substitution	$\hat{q}_u = -0.0241w^2 - 15.34w - 0.987E + 420.21$
Rubber tired	Soaked	Original	$\hat{\gamma}_d = 24.46E - 1.533wE + 1772.0$
		Original	$\hat{q}_u = 8.204w + 1.346E + 6.697\gamma_D - 816.75$
		After substitution	$\hat{q}_u = 8.204w + 11.56E - 0.639wE - 77.00$

Note: γ_D is in kilograms per cubic meter; w is in percentages; and q_u is in kilopascals.

trend was not found, all terms were considered important.

In the second step of the isolation process we used Purdue computer programs developed by Nie and others (9) to select prediction models in a manner identical to that explained by Essigmann (4). As suggested by Scott (8), the residuals were examined to determine if they were normally distributed independent random variables.

The model isolation process was completed by the use of a Purdue computer program developed by Casella and de Branges (10). The prediction models selected by the first two steps of the isolation process were inserted into this program. Essentially, the computer replicated the data manipulation of the first program but added a designated amount of bias to the variable coefficients on each successive run for each model. As more bias was added to the coefficients, each coefficient was eventually driven to zero. If the variable coefficients were extremely sensitive to the data (a small change in the data produces a large change in the coefficients), a small amount of bias added to a regression run would cause the coefficients to quickly approach zero. Models whose coefficients exhibited this trend were not considered for continued analyses.

Once all three isolation processes were completed, the selection of the most appropriate prediction model for each independent variable had been made. The results of the statistical analysis are presented in Table 3.

Variability of Dry Density and Unconfined Strength

Two measures of the dry density and strength variabilities are of interest to this report's objectives. Although each test-pad section was planned to have a nearly constant water content, a large variation in the water contents persisted and prevented determination of an optimum water content for any energy level. The average water content for the sheepsfoot and rubber-tired roller sections were 3.3 and 3.7 percent, respectively. The assumption was made that the variations found within the samples were no greater than the variations found within the test-pad section. Thus the average range of water content found within the test-pad sections was considered the expected range that must be accounted for in predicting the dry density and shear strength variabilities.

The compactive effort was measured in number of passes and, as such, no variation in the measurements is assumed. The magnitude of the dry density variability changes the degree of confidence that is chosen. We arbitrarily use a 95 percent confidence criterion here. Thus, 95 percent of the compacted soil from which the samples were taken should have a dry density within the range bounded by the expected mean value, plus or minus the appropriate factor times the standard deviation.

Once the dry density variability is evaluated, the expected variation in shear strength can be determined. The amount of variation assumed for this evaluation is zero for compactive effort, plus or minus the test-pad sections' half-range variation for water content and plus or minus the 95 percent confidence variability found for dry density $V(\hat{\gamma}_d)_{0.95}$. The table below presents these limits.

Variability Item	Sheepsfoot Roller	Rubber-Tired Roller
Compactive effort, no. of passes	± 0	E ± 0
Water content, %	± 1.65	w ± 1.85
Dry density, kg/m^3	$\gamma_d \pm V(\hat{\gamma}_d)_{0.95}$	$\gamma_d \pm V(\hat{\gamma}_d)_{0.95}$

Typical results of the unconfined strength variability analysis are presented in Figure 1 for the sheepsfoot roller, as-compacted condition.

Verification of Prediction Equations

To verify whether or not the regression equations obtained by the statistical analysis were good prediction models, the data from the 24 samples that were withheld from the analysis were compared to regression results obtained from the sample data. Dry density was calculated for each sample by using the regression equation suitable for the roller type by which the sample had been compacted. Figure 2 shows a plot of the expected values of dry density against the measured values of dry density for the sheepsfoot roller. The points must lie reasonably close to the 45° line for the regression equation to be considered a good prediction equation.

The same method was used for comparing the expected and measured values of the unconfined strength (see Figure 3). Again, the smaller the deviation from the 45° line, the better the model's predictive ability. Some deviation was expected, though, because of the variability associated with the compaction process and the testing program.

The total data show that a large difference may exist between an expected value and the corresponding value observed during testing. This does not mean that the model poorly represents the relationship between the variables; it suggests, rather, that the condition of a compacted soil after construction is very heterogeneous. Therefore any one measurement of either the dry density or the strength parameter can be unrepresentative of the average value of the parameter and as such does not reflect the true quality of the compaction results.

DISCUSSION OF RESULTS

Field Compaction Results

Dry Density and Strength Magnitude

A major benefit of determining prediction models for

Figure 1. Expected dry density and unconfined compressive strength variability versus water content for sheepsfoot roller, as-compacted condition.

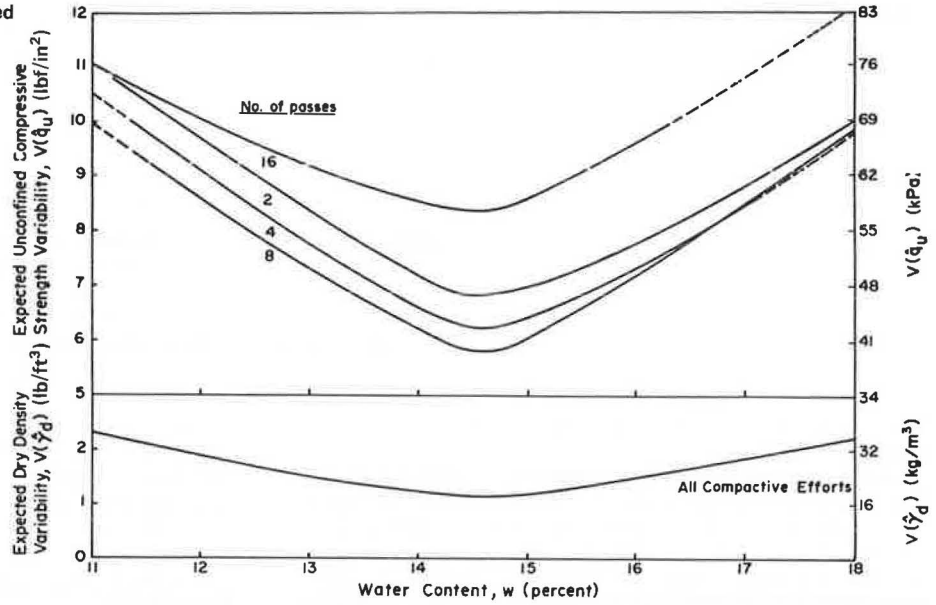

Figure 2. Expected versus measured dry density for sheepsfoot roller, as-compacted condition.

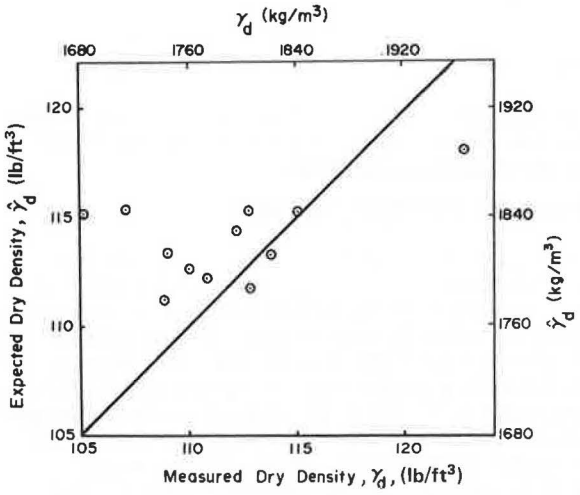

Figure 3. Expected versus measured unconfined strength for sheepsfoot roller, as-compacted condition.

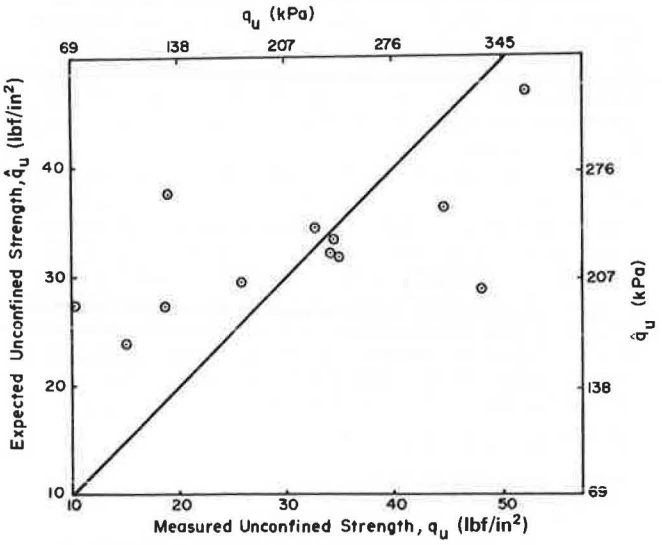

Figure 4. Dry density-strength relationship for rubber-tired roller, as-compacted condition.

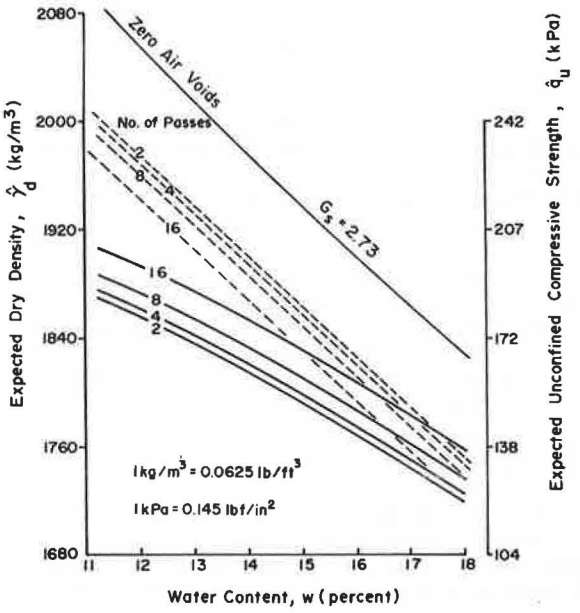

both density and strength is that the density equation can be substituted into the strength equation. This enables the soil strength and its variability to be estimated by knowing only water content, water content variability, and compactive effort. Table 3 shows the statistical models of strength after substitution. Complete discussions of these relationships are found in Price (1). Only those for the rubber-tired roller are discussed here.

Rubber-Tired Roller, As-Compacted Condition

Dry density is dependent on the compactive effort level and increases with compactive effort as shown in Figure 4. The density curves become nearly parallel to the zero air-voids curve for the higher water contents.

Figure 5. Dry density-strength relationship for rubber-tired roller, soaked condition.

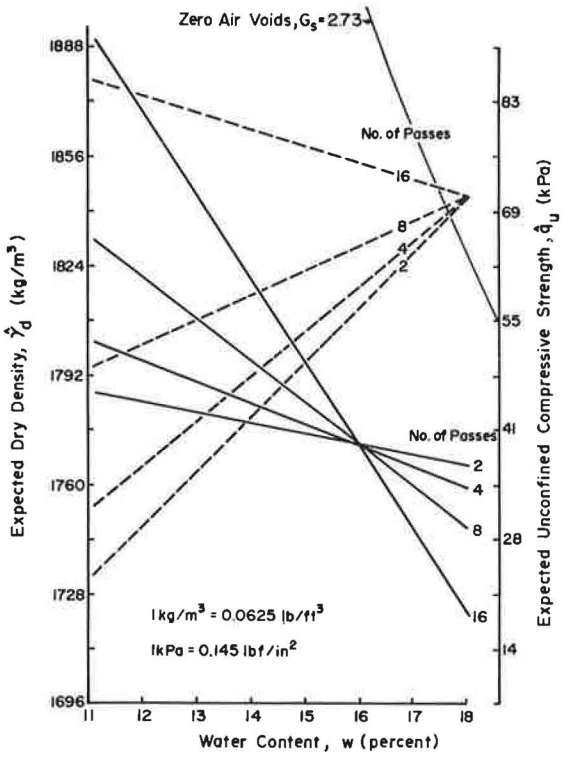

Figure 6. Isometric presentation of the minimum expected unconfined strength for rubber-tired roller, as-compacted condition.

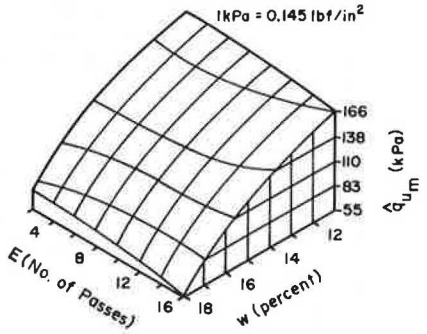

Figure 7. Isometric presentation of the minimum expected unconfined strength for sheepsfoot roller, soaked condition.

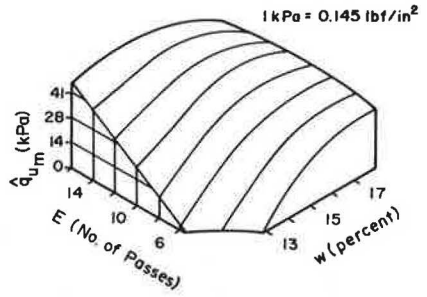

This indicates that extrapolation of the density-energy relationship beyond the 16-pass range could be in error. If the limit of compaction efficiency has been nearly reached with 16 passes, a sizable increase in compactive effort could cause only a small or negligible increase in dry density for the wetter soils.

Figure 4 presents the relationship between the expected dry density and the expected unconfined strength. The slopes of the density curves not only are different from the slopes of the strength curves but also change

Figure 8. Effect of water content variability on unconfined strength variability for sheepsfoot roller, as-compacted condition, 276 kPa expected strength.

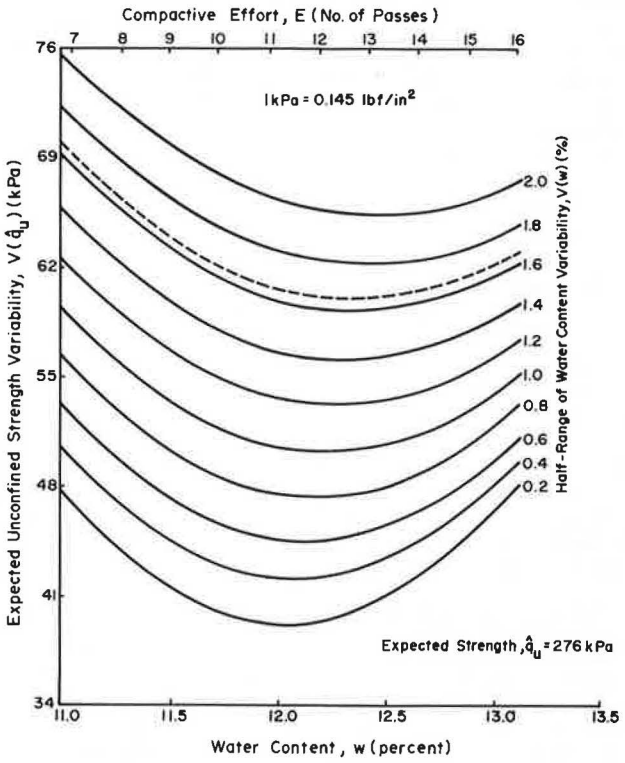

with respect to the strength slopes. This complicates the strength-density prediction process; although, if the same criteria are met as described earlier, strength may be reasonably forecast from knowing the water content, compactive effort, and dry density of the soil mass. Of particular interest is that the density increases and the strength decreases with increasing compaction effort at a constant water content. This indicates that, if an inspector requires additional compaction with intentions of increasing the density to some minimum specification values, compaction may in fact reduce the strength (a form of overcompaction).

Rubber-Tired Roller, Soaked Condition

The density-water content relationship is shown in Figure 5. Of interest in this illustration is the decreasing slope trend for decreasing compactive effort in the lower water contents. This trend suggests that differences in water content are more influential on the density magnitude at high compactive efforts than at lower compactive efforts. Again, this would suggest that swelling influence increases with increasing compaction energy.

Figure 5 shows the association between the expected dry density and the expected unconfined strength. Of importance is the sign difference of the slopes for the two curve types in the lower energy levels. The dry density decreases with additional water content while the strength increases.

Variability in Dry Density and Strength

Figures 6 and 7 show the minimum expected unconfined strength surface in the water content-compactive effort-

strength space system for the as-compacted and soaked soil conditions of the rubber-tired roller. The minimum unconfined strength is defined as the expected strength minus the expected variability in the strength. In each case, the surface is significantly different from the expected strength surface. Similar figures for the dry density surfaces would show comparable differences between the expected and minimum expected surfaces. Illustrated in these graphs is the notion that the variability in compaction results is significant and must be provided for in the project specifications in order to ensure a minimum strength compatible with the project needs.

By reducing the variability in the data, the probability that the regression model will represent the true relationship between the variables would be increased and the expected variability would be reduced.

Figure 8 shows the effect of reducing the water content variability on the expected strength variability. As shown, for any given water content and compactive effort, a higher degree of water content homogeneity results in significantly reduced strength variation. The design engineer is interested in accurately forecasting expected strength, so compaction specifications should include provisions that control the variability in the soil and compaction process.

Laboratory-to-Field Correlation

This report has shown marked differences between the relationships for a field and laboratory compacted soil. Variability appears to be larger in the field operation. More attention needs to be focused on this variability if reliable prediction of field behavior of compacted soils is to be possible.

The need for establishing the laboratory-to-field correlation is imperative for the economical implementation of this research. It is hoped that a number of test pads and similar research programs will allow a suite of density and strength relationships for various soil types and compaction processes to be developed. Without the corresponding research, similar to that of Essigmann (4) and Scott (8), and the proper correlation between the laboratory and field curves, the design engineer must require a test pad for each soil type. If, however, the correlation between the laboratory and field compacted soils can be made, the design engineer can simply take bag samples from the borrow area and perform compaction and strength tests. Then, from the results, he or she can determine where the soil matches the suite of curves. Therefore, with the proper laboratory-to-field correlation relationships, the design engineer can extrapolate the results of a relatively small number of test pads and corresponding laboratory studies for a large number of project soils without having to resort to extensive and expensive field sampling and testing programs.

CONCLUSIONS

Given the constraints established by the project, specifically the wet-of-optimum water-content limitation, the following conclusions (1) may be reached for this silty clay soil.

1. For the soil compacted by a sheepsfoot roller (a) the variable contributing most to the resultant as-compacted dry density magnitude is water content, and (b) the variables contributing most to the resultant as-compacted unconfined strength magnitude are water content and compactive effort.
2. For the soil compacted by a rubber-tired roller (a) the variables contributing most to the resultant as-compacted dry density magnitude are compactive effort and the square of the water content; (b) the variables contributing most to the resultant soaked dry density magnitude are compactive effort and the interaction between compactive effort and water content; (c) the variables contributing most to the resultant as-compacted unconfined strength magnitude are the water content, square of the water content, and compactive effort (an increase in the water content or compactive effort causes a decrease in the shear strength); and (d) the variables contributing most to the resultant soaked unconfined strength magnitude are water content, compactive effort, and the interaction between water content and compactive effort. The influence of either the water content or the compactive effort on strength depends on the magnitude of the other independent variable.
3. The magnitude of the strength variability from both rollers is reduced if water content variability is reduced.
4. The inherent variability in the compacted soil mass prevents consistently accurate measurement of the true construction quality by a one- or two-sample testing program. The average of a number of samples (possibly between five and seven) must be used as a measurement of water content, dry density, or unconfined strength.

ACKNOWLEDGMENT

We appreciate the financial support given by the Joint Highway Research Project of Purdue University, the Indiana State Highway Commission, and the Federal Highway Administration.

REFERENCES

1. J. T. Price. Soil Compaction Specification Procedure for Desired Field Strength Response. Purdue Univ., West Lafayette, IN, master's thesis, May 1978, 151 pp.
2. T. G. Williamson and E. J. Yoder. An Investigation of Compaction Variability for Selected Highway Projects in Indiana. HRB, Highway Research Record 235, 1968, pp. 1-12.
3. T. G. Williamson. Embankment Compaction Variability—Control Techniques and Statistical Implications. HRB, Highway Research Record 290, 1969, pp. 9-22.
4. M. F. Essigmann. An Examination of the Variability Resulting from Soil Compaction. Purdue Univ., West Lafayette, IN, master's thesis, Aug. 1976, 108 pp.
5. G. B. Sherman, R. O. Watkins, and R. H. Prysock. A Statistical Analysis of Embankment Compaction. HRB, Highway Research Record 177, 1967, pp. 157-185.
6. J. L. Jorgensen. Measuring the Variability of Compacted Embankments. HRB, Highway Research Record 290, 1969, pp. 23-34.
7. T. W. Smith and R. H. Prysock. Discussion of paper, Quality Control of Compacted Earthwork, by W. J. Turnbull, J. R. Compton, and R. G. Alvin. Journal of Soil Mechanics and Foundations Division, Proc., ASCE, Vol. 92, No. SM1, Sept. 1966.
8. J. C. Scott. Examination of the Variability of the Soaked Strength of a Laboratory Compacted Clay. Purdue Univ., West Lafayette, IN, master's thesis, June 1977, 97 pp.
9. N. H. Nie. SPSS: Statistical Package for the Social Sciences, 2nd ed. McGraw-Hill, New York, 1975, 675 pp.
10. G. Casella and Branges. Ridge Regression. Computer Program, Purdue Univ., West Lafayett, IN, 1977, p. 1.

Publication of this paper sponsored by Committee on Compaction.

Membrane Technique for Control of Expansive Clays

Douglas Forstie, Harold Walsh, and George Way, Materials Services, Arizona Department of Transportation

Much northeastern Arizona highway is built on expansive clay. Changes in the moisture content of these clay subgrades cause volume changes that in turn cause excessive pavement deterioration and thus affect safety. During initial construction, a variety of experimental sections were built to test such stabilization methods as moisture and compaction control, chemical admixtures, electro-osmosis, overexcavation, ditch widening, underdrains, and membranes, alone or combined. Some methods were relatively successful when compared to the rapid deterioration of the untreated highways. These findings led to choosing impermeable rubber membranes to control moisture in the clay subgrades. The first trial of the technique at full contract scale was an 18-km (11-mile) overlay on I-40 completed in 1975. After the slopes were flattened for safety, the roadway prism under the asphalt concrete overlay and down the shoulder slopes was covered with the asphalt-rubber membrane. The control section was an adjacent overlay of the same design but with no membrane. In 1976, a 5-km (3-mile) overlay on US-89 with asphalt-rubber membranes and shoulder and ditch paving was constructed. This report presents the data on the three full-scale overlays and the success of the membrane.

Expansive clay is a major problem for the state of Arizona. Changes in moisture content in clay subgrades lead to volume changes great enough to cause serious deterioration of the pavement structure. The problem is most severe in the northeastern corner of the state, where 483 km (300 miles) of state highways are on the clays of the Chinle formation. The cost of simply maintaining these highways in safe condition, apart from repairing damage to the structural capacity of the roadway, is excessive.

In the early 1960s a variety of experimental techniques for controlling expansion began to be tried on new construction. Success varied from worse than none to very good. After analyzing all the various treatments, it became apparent that, to successfully control expansive clay subgrades, changes in moisture content must be kept to a minimum. The degree of success of each treatment seemed to depend on the extent to which it accomplished this.

In 1973, two test sections in cuts on a new two-lane highway at the south edge of the Petrified Forest had full-depth asphalt concrete pavement, and a third cut had a catalytically blown asphalt membrane on the clay subgrade under the normal pavement design of select material and asphalt concrete. Also, in all cuts the seal was carried across the ditches, which were paved with thinner asphalt concrete from the regular pavement out to 30 cm (1 ft) up the back slope. The apparent success of these tests led to an early trial of membranes for the newly arisen problem of treating the many deteriorating kilometers of highway on Chinle clay. Asphalt-rubber membrane was selected because of its waterproofing properties and ease of application. The asphalt-rubber membrane serves a threefold purpose: It reduces evapotranspiration of moisture from the subgrade; it prevents infiltration of moisture from surface runoff; and it prevents reflective cracking in the new overlay.

This report presents and discusses data on the first three projects built as trials of asphalt-rubber membranes. Two of these were 18-km (11-mile) overlay contracts on I-40, one built in 1975 with the membrane, the other adjacent and built in 1974 without it. Both were of similar design, including flattened slopes for safety. On the third project, located on US-89 north of Cameron, asphalt-rubber membranes were used in conjunction with shoulder and ditch paving. All three projects were monitored for changes in roughness, moisture content, and surface elevation and tested periodically with the Dynaflect. A short description of Chinle clay is followed by a review of the earlier field trials of the various other treatments used on it.

OCCURRENCE AND PROPERTIES

In northeastern Arizona the majority of the expansive soils are contained in the Chinle formation. Figure 1 illustrates the present exposure of the Chinle formation and 483 km (300 miles) of highways located on it.

The Chinle formation is predominantly clay, although there are some thin layers of sandstone, siltstone, and conglomerate. Where erosion is too rapid for vegetation to develop in a weathered surface layer, the clay erodes to the rounded hummocks and gullied slopes typical of clay deposits, but with massive layers of varying colors, as in the scenic Painted Desert. Beneath any weathered and softened surface layer, the in-place clay is typically strong and hard with a moisture content from 5 to 20 percent, dry densities from 1442 kg/m^3 to 1842 kg/m^3 (90 lb/ft^3 to 115 lb/ft^3), and textures and strengths that may cause it to be identified as sandstone or siltstone as often as shale or clay. Vigorous wet rubbing can reduce a sandy textured chip to resembling a clay-cemented sandstone; after thorough soaking 80 percent or more will pass a 75-μm (no. 200) sieve.

In the laboratory, the properties of various samples varied widely and included nonplastic silts and fine sands, although a rocklike core of deceptive texture may have a liquid limit of 65, a plastic index (PI) of 38, and a T99 maximum density of 1522 kg/m^3 (95 lb/ft^3) at an optimum 32 percent moisture content. These clays are bentonitic, but the bentonite is disseminated. In other layers, a more clayey or shale-like appearance is found in a finely fissured structure with seams and nodules of pure bentonite.

CONTROL OF EXPANSIVE SOILS

Clay formations in the field are usually disturbed when the roadbed embankment and subgrades are constructed. This creates the worst possible case of maximum expansion. Historically, attempts have been made to control this expansion during original construction. Some of the experimental trials were

1. Overexcavation up to 1.5 m (5 ft) and replacement with granular materials and french drains;
2. Lime ponding, which involved spreading lime on Chinle clay subgrade and then ponding with water;
3. Lime post holes drilled to various depths into the clay on a grid pattern and then filled with lime slurry;
4. Lime treating the top 150 mm (6 in) of subgrade;
5. Ponding with potassium chloride solution;
6. Electro-osmosis using potassium chloride solution; and

7. Widening of cut ditches and paving shoulder slopes.

The success of the experimental trials varied enormously, from detrimental to very successful. A detailed account of the original construction features and overlay experiments is found elsewhere (1).

A very large portion of the 483 km (300 miles) of highways over the Chinle formation received little special treatment during original construction. After 10 or 12 years of service, excessive distortions had made it necessary to overlay some sections of these highways. Normally the distorted highway was surveyed to determine the amount of leveling needed to obtain a suitable riding surface with proper geometrics. Arizona uses a Missouri computer program that designs asphalt concrete overlays, in one or two lifts, to a smooth grade line and prints out superelevation, centerline profile grade, accumulated quantity and thickness of the top lift (binder course), accumulated quantity left and right of centerline for the leveling course, and thicknesses of the leveling course at various offset points. The program uses only the submitted existing roadway cross-section data, specified minimum thicknesses, desired superelevation transition data, and unit weight of asphalt concrete to compute grades and quantities. A detailed description is contained in Damgaard (2). The program came from Missouri, but alterations were made by Arizona and the name of the program became AZ-MO Overlay Program or just AZ-MO. By obtaining survey elevations across the highway (an elevation at centerline and each quarter point on the highway, five elevations) and at each even 7.6-m (25-ft) distance (station 0+00, 0+25, 0+50, 0+75, 0+100, etc.) it was possible to compute the amount of leveling needed before overlay.

The necessary overlaying of the distorted highway provided a good opportunity to try some method of treatment to improve overlay performance. Previous experience in Arizona and on US-180 and Colorado (3) showed that paved cut ditches and subgrade membranes have been successful in controlling volume changes of expansive clay subgrades. On I-40 two adjacent overlays were to be built over a highway badly distorted by the action of expansive clay. In order to determine whether the membrane sealing concept would work for an overlay, both projects were to be designed and built in the same manner but one would have a membrane seal across the pavement and down the slopes. The projects were designated as follows.

1. I-40-5 (38) County Line-Pinta: From milepost 307.2 to 318.8 eastbound (EB) and westbound (WB) or from station 0+00 to 613+00 EB and WB. This project was designed for an AZ-MO leveling plus a 31.8-mm (1.25-in) layer of asphalt concrete. In addition the slopes were flattened from 6:1 to 10:1. Likewise the cuts were laid back an additional 3.7 m (12 ft). Figure 2 shows the typical section for both fill and cut.
2. I-40-5 (44) Pinta-McCarroll: From milepost 318.8 to 330.6 EB and WB or station 613+00 to 1237 EB and WB. This project was designed and built like project I-40-5 (38) except the asphalt-rubber waterproofing membrane was placed over the pavement and 3.7 m (12 ft) down the shoulder slopes in both cut-and-fill sections. The membrane on the earth shoulder slopes was protected with 152.4 mm (6 in) of soil. Figure 2 depicts the typical section for a fill and cut on this project.

There were two further overlay projects built with membranes. Project I-40-5 (45), also on I-40, was identical to I-40-5 (44) but lay approximately 40 km (25 miles) east and not adjacent to the control project. Project F 037-2-502 was built on US-89 over a very badly distorted highway. This project differed from the other overlay projects in several ways. First of all, in cut sections the membrane covered the entire roadway as well as the shoulder slopes and cut ditches. Second, 50.8 mm (2 in) of asphalt concrete were paved over the membrane for protection. Figure 3 depicts a cross-sectional view of this project.

The performance of the above four projects forms the basis of this report.

PROJECT CONSTRUCTION

The construction of all four overlay projects was essentially the same. First the leveling course was applied to the old pavement, and then the shoulder slopes were bladed and compacted to a uniform slope. Before the asphalt-rubber membrane was applied, the soil slopes were primed with a light shot of emulsion 0.36 L/m^2 (0.08 gal/yd^2). The asphalt-rubber mixture was applied to the slopes by using a special boot truck with a mast arm off the side of the truck. This allowed the truck to drive on the pavement while applying the membrane to the shoulder slopes. An Arizona Department of Transportation (DOT) report (4) presents details of the field construction of asphalt-rubber membranes.

The asphalt-rubber mixture used on all four projects was identical and consisted of 25 percent ground vulcanized rubber reacted with asphalt at high temperatures [177°C (350°F)]. This mixture is brought together in the boot truck and normally requires an hour for complete reaction to occur. This reaction time, however, depends on the temperature, rubber gradation and type, and the asphalt crude source. After complete reaction has occurred, the composition consists of a thick jellied material with good elastomeric properties.

The high viscosity of the asphalt-rubber composition is reduced with a small quantity of kerosene introduced into the mixture. This temporarily reduces viscosity and facilities application of the asphalt rubber. After not more than 2 h, the composition returns to its original high viscosity (5).

On the I-40 projects the asphalt rubber was applied at a rate of 3.4 L/m^2 (0.75 gal/yd^2) on the earthen shoulder slopes and 2.7 L/m^2 (0.60 gal/yd^2) on the leveled asphalt concrete. The asphalt rubber applied to the asphalt concrete was immediately covered with chips to provide a wearing surface and facilitate load transfer in the completed pavement. The membrane on the shoulders was protected with 15 cm (6 in) of soil. The spread rate on the US-89 project was 3.2 L/m^2 (0.70 gal/yd^2) on the leveled asphalt concrete. On this project chips were spread on the asphalt rubber used on the earth shoulder slopes as well as on the roadway. The application rate of the chips varied between 19.2 and 21.8 kg/m^2 (35 and 40 lb/yd^2). The membrane on the shoulders was protected with 5 cm (2 in) of asphalt concrete.

In Arizona, the asphalt-rubber mixture is paid for under a special item, AR-1000 (rubberized-membrane seal) and includes AR-1000 asphalt, granulated rubber, and kerosene and is calculated at the equivalency of 0.90 kg/hot L (7.5 lb/hot gal). The chips are paid for under a separate item. Both materials are paid for at the contract price for work completed in place. For asphalt-rubber projects undertaken in 1977, the cost per customary ton of asphalt rubber varied from $311 to $430. Using an average of these figures yields an average cost of asphalt rubber and chips in place of $1.81/m^2 ($1.50/yd^2).

PROJECT PERFORMANCE

The objectionable characteristics of the highways before

Figure 1. Map of northeastern Arizona.

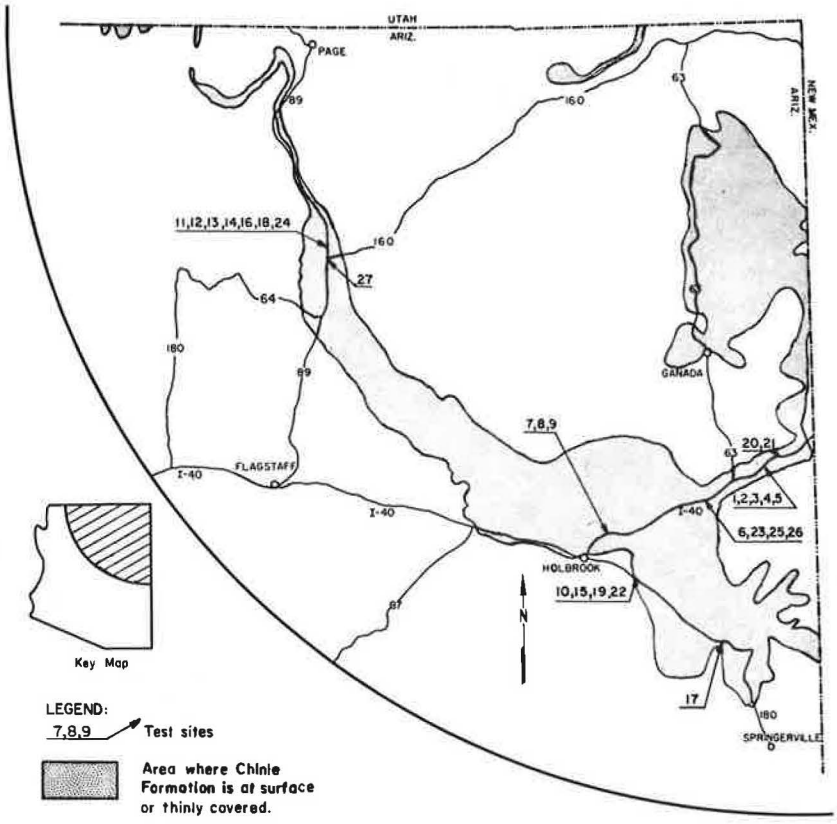

Figure 2. I-40 typical sections.

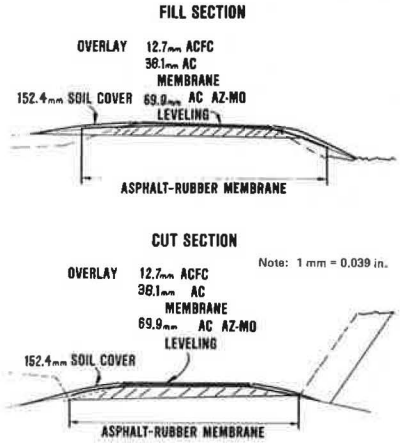

Figure 3. US-89 typical sections.

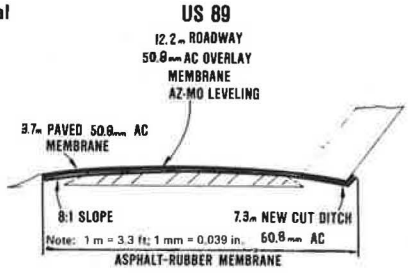

overlay included pavement distortion, cracking, and excessive maintenance. The picture in Figure 4 shows the typical condition of a highway before overlay. Visual observations of the projects were sufficient to indicate the nature and extent of the distress, but the following measurements indicated the severity of the problem:

Figure 4. Highway condition before overlay.

1. Ride, or the roughness as measured by Mays ride meter (6);
2. Percentage of cracking as measured by the Arizona DOT percent cracking index (7);
3. Centerline profile change from plans as determined by comparing the plans elevation to actual elevation and computing the variance; and
4. Change in subgrade moisture as measured by the nuclear depth moisture probe (8).

In addition to this continuous field monitoring, the Arizona DOT collected samples from selected locations. Samples included drive samples for in-place density and moisture determination and auger samples for disturbed percentage of swell and expansive pressure measurements. In addition, the U.S. Army Engineer Waterways Experiment Station took undisturbed Dennison samples from the same location as part of a national project (9). Table 1 contains results of tests by the Arizona DOT.

In general the following observations can be drawn from the test results. Moisture content of the fills was

Table 1. Test results from field samples.

Project	Section	Depth (m)	Moisture (%)	Dry Density (kg/m³)	Swell (%)	PI	Percent Passing 75 μm Sieve
I-40-5(38)	Fill	0.6	11.1	1980	0.20	2	25
		1.2	10.0	1730	1.25	5	31
		1.8	13.4	1759	1.23	5	43
		2.4	17.4	1754	0.07	2	31
		3.0	14.1	1655	-	-	-
	Cut	0.0	11.3	1701	0.03	4	23
		1.2	11.6	1842	1.86	14	37
		1.8	6.2	1855	0.10	3	21
		2.4	10.0	1865	4.25	16	58
		3.0	13.5	1754	-	-	-
I-40-5(44)	Fill	0.6	7.7	1842	0.00	NP	20
		1.2	15.5	1671	0.11	2	31
		1.8	23.0	1544	0.88	8	43
		2.4	22.6	1509	10.19	30	62
		3.0	22.3	1366	-	-	-
	Cut	0.6	7.3	1671	0.20	3	30
		1.2	17.9	1857	2.49	16	57
		1.8	11.1	1663	0.41	10	47
		2.4	12.4	1849	3.57	16	63
		3.0	14.3	1549	-	-	-

Note: 1 m = 3.3 ft; 1 kg/m³ = 0.062 lb/ft³; 75 μm sieve = no. 200 sieve.

Table 2. Mays ride roughness history before overlay.

Project	Rate of Roughness Increase per Year	Years to Objectionable Ride
I-40-5(38)	15	14
I-40-5(44)	16	14
I-40-5(45)	18	12
F 037-2(7)	15	15

Table 3. Predicted ride roughness after overlay.

Project	Annual Rate of Roughness Increase	Predicted Years to Objectionable Ride
No membrane		
I-40-5(38)	14	16
With membrane		
I-40-5(44)	6	36
I-40-5(45)	6	36
F 037-2(7)	6	26

Table 4. Analysis of evaluation differences.

Project	Section	Largest Heave (mm)	Average Heave Plus Settle	Variance of Elevation
I-40-5(38)	Fill	55.9	-0.91	0.001 07
Untreated	Cut to fill	50.8	10.52	0.001 14
	Cut	12.7	1.07	0.000 27
I-40-5(44)	Fill	15.2	0.66	0.000 10
Treated	Cut to fill	10.2	-0.66	0.000 34
	Cut	35.6	-0.51	0.000 45

Note: 1 mm = 0.039 in.

greater than the cuts for the same depth from the surface. Dry densities in the cut were higher than in the fills for the same depth from the surface, and the percentage of swell and expansive pressure were directly related and increased in parallel fashion. Depending on the location, the swelling layer could be as deep as 3.0 m (10 ft) below the surface of the pavement or as shallow as the top of subgrade. However, even deep formations could exert a change in elevation.

With the above in mind the following will detail the analysis of project performance.

ANALYSIS OF PERFORMANCE DATA

Pavement smoothness or ride quality is a very important consideration when examining project performance.

Tables 2 and 3 show the project ride history for the four projects under study. The following observations can be determined.

1. It took 10-12 years for the originally constructed pavement to reach an unacceptable level of roughness and maintenance.
2. Since overlaying, the control project is increasing in roughness at such a rate that it will take approximately 16 years to reach the objectionable level of roughness.
3. Since overlaying, the treated projects are increasing in roughness at a rate such that it will take 33 years to reach the objectionable level of roughness.

At present the rate of increase in objectionable ride characteristics is so small that estimates even longer than 20 years are predicted. However, these values seem a little too optimistic. The treated sections seem to be increasing in roughness at a rate no more than half as fast as the untreated sections. In other words, the treated sections should last twice as long.

CRACKING

Before overlaying, all projects had a level of cracking of 10 percent or more. At present the treated projects show no cracking, whereas the untreated have shrinkage cracks on the order of 1 percent cracking.

CHANGES IN ELEVATION

Three elevation test grids 91.4 m (300 ft) long were established after overlay construction on the adjacent treated and untreated projects, I-40-5 (44) and I-40-5 (38), respectively. Test grids on 91.4 m (301.6 ft) of highway 116 m (382.8 ft) wide represented a 1.5-m (5-ft) fill, a cut-to-fill transition, and a cut section. There were 217 survey points per location. Table 4 shows results of measurements for the overlay new and 2.5 years old. The larger the variance is, the more total distortion will take place. From this information we can say that none of the test sections are showing excessive heaves at this time, although the untreated sections are showing larger heaves, and that the overall variance would indicate that the membrane is working particularly well in the fills and the cut-to-fill transitions.

MOISTURE

Since construction of the overlays, the percentage of moisture has been monitored with nuclear depth mois-

Figure 5. Weight percentage moisture changes with time.

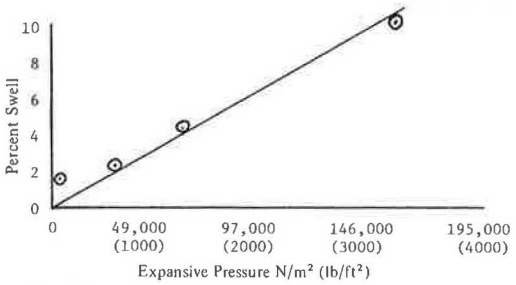

Table 5. Moisture change with depth for locations of travel lane tubes.

Section	Depth Below Asphalt Concrete Surface (m)	No Membrane I-40-5(38) Average Moisture (%)	Variance	With Membrane I-40-5(44) Average Moisture (%)	Variance
Fill	0.6	11.4	0.3	10.6	0.1
	1.2	11.2	0.5	11.2	0.1
	1.8	15.4	1.0	23.9	0.1
	2.4	13.0	0.3	21.8	0.1
	3.0	8.6	0.5	21.5	0.3
Cut	0.6	12.4	0.4	7.3	1.0
	1.2	9.9	0.2	18.6	0.2
	1.8	14.1	1.8	12.5	0.5
	2.4	9.0	3.6	12.2	0.1

Note: 1 m = 3.3 ft.
*This variance is unique because no wetting and drying takes place; rather, the soil has continued to become wetter with time.

ture equipment. Figure 5 shows a typical moisture plot for a cut-and-fill section. Table 5 gives the moisture values and variance for comparable cut-and-fill locations on project I-40-3 (38) and I-40-5 (44). The following observations can be drawn.

The membrane sections in cut and fill show less moisture variance over time than the untreated control sections for all depths except the 0.6-m (2-ft) treated cut. This location is the depth at which the moisture has continued to increase with time, which represents a redistribution of moisture. The cut-and-fill sections with and without treatment do not appear to be becoming consistently wetter or drier, but rather appear to be oscillating about the mean.

CONCLUSIONS

Field observations plus objective measurements now indicate that the membrane treatment over the badly distorted highway has improved the overlay performance. This improvement, obviously, is attributable to the membrane's ability to seal out moisture. Although some moisture redistribution is taking place, the significant observation is that less moisture fluctuation (dry to wet to dry) is taking place under the membrane. In addition and as predicted in an earlier report on reflective cracking (10), the membrane is preventing cracking, which also prevents moisture from entering the expansive soil.

Arizona's experience with asphalt concrete overlays with some form of membrane treatment to prevent cracking, plus shoulder and ditch paving, has led to the following conclusions.

1. Such treatment will prevent reflective cracking, as predicted in an earlier report (10).
2. Shoulder and ditch membrane treatments (asphalt rubber, paved shoulders and ditches, or any other suitable waterproofing membrane layer) can and will improve the long-term ride performance of a highway over an expansive soil.
3. If ride is improved and cracking severity is reduced, maintenance costs will undoubtedly fall.

Such positive conclusions from all the accumulated information have led Arizona to implement the membrane process of control on an operational basis for all expansive soil subgrades.

ACKNOWLEDGMENT

The contents of this report reflect our views, and we only are responsible for the facts and the accuracy of the data presented. The contents do not necessarily reflect the views or policies of the Arizona DOT or of the Federal Highway Administration. This report does not constitute a standard, specification, or regulation. Trade or manufacturers' names that may appear here are cited only because they are considered essential to the objectives of the report. The United States government, the state of Arizona, and the Transportation Research Board do not endorse products or manufacturers.

REFERENCES

1. D. Forstie, H. Walsh, and G. B. Way. Arizona's Attempts to Control Expansive Soil. Arizona Department of Transportation, Phoenix, Aug. 1978.
2. K. K. Damgaard. Arizona-Missouri Overlay Program. Arizona Department of Transportation, Phoenix, Nov. 1970.
3. B. A. Brakey and J. A. Carroll. Experimental Work, Design and Construction of Asphalt Bases and Membranes in Colorado and Wyoming. Proc., Association of Asphalt Paving Technologists, Minneapolis, Vol. 40, 1971, pp. 31-63.
4. H. G. Lansdon. Construction Techniques of Placement of Asphalt-Rubber Membranes. 13th Paving Conference, Univ. of New Mexico, Albuquerque, Jan. 1976.
5. R. E. Olsen. Rubber-Asphalt Binder for Seal Coat Construction. Federal Highway Administration, Implementation Package 73-1, 1973.
6. G. J. Allen, J. B. Burns, C. Cornell, and J. Eisenberg. Pavement Evaluation in Arizona. Arizona Department of Transportation, Phoenix, Jan. 1974.
7. G. B. Way. Asphalt Properties and Their Relationship to Pavement Performance in Arizona. Association of Asphalt Paving Technologists, Minneapolis, Feb. 1978.
8. G. B. Way. Environmental Factor Determination From In-Place Temperature and Moisture Measurements Under Arizona Pavements. Arizona Department of Transportation, Phoenix, June 1975.
9. D. R. Snethen, L. D. Johnson, and D. M. Patrick. An Investigation of the Natural Macroscale Mechanisms That Cause Volume Change in Expansive Clays. Federal Highway Administration, FHWA-RD-77-75, Jan. 1977.
10. G. B. Way. Prevention of Reflective Cracking in Arizona Minnetonka-East. Arizona Department of Transportation, Phoenix, May 1976.

Publication of this paper sponsored by Committee on Environmental Factors Except Frost.

Soil-Water Potential and Resilient Behavior of Subgrade Soils

Tuncer B. Edil, Department of Civil and Environmental Engineering and Department of Engineering Mechanics, and
Sabri E. Motan, Department of Civil and Environmental Engineering, University of Wisconsin, Madison

The special significance water has for pavement systems is that such structures are generally associated with soils close to ground surface, are subject to large moisture content variations, and are strongly influenced by environmental conditions. The object of this study is to establish experimentally the relationship between the strength and deformation characteristics under highway loading conditions and the soil moisture regime in terms of the soil-water potential (or soil suction). To do this, laboratory specimens of a mixture of a typical Wisconsin subgrade soil and 25 percent sand were compacted at optimum and ±2 percent of optimum moisture content. These were subsequently equilibrated to a range of suction values up to 1500 kPa (217.4 lbf/in^2) in a soil moisture extractor. The specimens were subjected to a repetitive uniaxial compression loading of 80 kPa (11.6 lbf/in^2) at a frequency of 0.5 cycle/s up to 10 000 loading repetitions. After the computed values of resilient modulus and residual strain were studied as a function of the moisture parameters, it was concluded that soil suction is the fundamental parameter in characterizing the moisture state and its effects on the mechanical behavior of soils. For the silt loam soils (low-plasticity clays) considered, compaction at dry-of-optimum moisture content results in subgrades more susceptible to moisture changes. There appear to be significant advantages in taking suction-related improvements in the mechanical properties into account if the regional climatic conditions are to ensure a suitable range of moisture index. However, there seems to be a limit to the increases in resilient modulus with increasing soil suction because the resilient moduli decrease for suction values greater than a critical value.

When a pavement is subjected to a wheel load, it undergoes both recoverable (resilient or elastic) and irrecoverable (permanent or plastic) deformations. The most significant factor influencing the design of a flexible pavement for given traffic and environmental conditions is subgrade soil support.

In recent years, the importance of resilient deformation, the major component of the total deformation for adequately designed pavements, has been studied extensively. Numerous field studies have established that pavement performance is controlled by the magnitude of resilient deformation responsible for fatigue failures in asphalt concrete surface courses (1). Several studies have shown that repetitive loading tests can be used to establish appropriate resilient properties for fine-grained subgrade soils (2, 3, 4), and, since then, the deformation characteristics of soils under repetitive action of compression loads have been studied extensively.

One very important parameter for cohesive soils is the moisture state of soil. In order to fully describe and control the mechanical behavior of subgrade soils, methods for predicting (a) moisture movement and equilibria in pavement systems and (b) influence of moisture on pavement behavior are needed (5). The emphasis in this investigation is on the latter aspect, and we expect the findings to be a complement to the research on moisture movement and equilibria by other investigators (6, 7).

Water has special significance in highway pavement systems because such structures are generally associated with the surficial boundaries of the terrain. Therefore, they are subject to large moisture content variations and are strongly influenced by environmental conditions. It is for this reason that the problems of controlling moisture changes and accumulation in soils under covered areas are of prime importance in relation to pavement design, construction, and performance. The recent advances in theoretical soil physics have provided researchers with a better understanding of the energy status of soil water (potential or suction). This has encouraged the application of the principles of soil suction to the mechanical response characterization (8).

The research reported here was further facilitated by the introduction of soil suction measuring devices that are practically applicable for all ranges of soil suction encountered (9).

The energy of a soil-water system can be expressed as a function of its characteristic water retention curve, or the relationship between water content and total soil-water potential or soil suction, where the latter is the difference between the free energy of water in the soil and that of pure water in a free surface condition. Total soil-water potential or soil suction is defined as the work required to remove an infinitesimal quantity of water from the soil and provides a measure of the combined effects of the forces holding the water in the soil. With the exception of cementation bonds, it implicitly includes the effects of the fundamental interaction forces that influence the deformation characteristics of the soil. The total soil-water potential of a soil varies with its water content, mineralogy, solutes present in the pore water, and soil fabric, among other parameters. This potential can be divided into several components.

Two of these components of primary interest are "matric potential", which arises from both capillarity and particle surface adsorption, and "solute potential", which arises from osmotic effects when water of a different solute content than pure water is extracted from the soil (9). In water retention curves, the data are usually presented in terms of equilibrium or steady-state values of water content, as related to some component of the soil-water potential. Expressed in terms of water content, sorption values are lower than desorption values; this is referred to as hysteresis. Soil-water extractors consisting of a pressure chamber containing a porous membrane of an appropriate bubbling pressure (for example, a ceramic plate) are commonly used for measuring or controlling matric suction. Solute suction can be evaluated by using freezing-point depression measurements and vapor-pressure depression measurements by thermocouple psychrometers (9).

The soil suction concept provides a fundamental soil parameter that reflects mechanical behavior (10). Another analytic advantage of soil-water potential over moisture content stems from the fact that a small error in moisture content may lead to a very serious error in the mechanical properties when the moisture content approaches saturation, whereas it takes correspondingly large values of suction to cause the same error. Furthermore, an indication of the effect of location and topography on soil suction values occurring under pavements can be obtained by correlating field suction

values with a climatic moisture index such as Thornthwaite moisture index (11). O'Reilly, Russam, and Williams (12) have shown a broad correlation between the average value of soil suction in the top 0.6 m (2 ft) of the subgrade under the pavement and the Thornthwaite moisture index for a number of soil groupings.

The few existing investigations that relate the mechanical response under repetitive loading conditions to soil suction (13, 14, 15, 16, 17, 18) indicate that soil suction is an important moisture variable for describing resilient behavior and relating it to the soil environment. Consequently, the study of soil suction is of ever-increasing importance to the design of pavements for arid areas, to the selection of placement conditions for base-course materials on expansive subgrades, and to the prediction of pavement performance. However, the resilient behavior of soils as a function of suction and other moisture parameters is not yet well understood, and only a very few investigations into it have been undertaken in this connection.

Therefore, the general objectives of this paper are to present experimental results concerning the resilient properties of selected fine-grained soils and to identify and quantify the effect of soil water in terms of soil suction and other pertinent parameters on the resilient and strength characteristics under typical pavement loading conditions.

PROPERTIES OF SOILS USED

The basic material selected for the testing program is Fayette silt loam from Richland County, Wisconsin. It is typical of the soils adopted for subgrade construction by the Wisconsin Department of Transportation. The Fayette series of soils, which are available in several southwestern counties in Wisconsin, develop over clay residium from dolomite bedrock (19). These are moderately permeable soils with high available water. They have moderate frost heave potential and bearing value and are considered fair to good in compaction but poor as road subgrade.

Fayette silt loam and a mixture of it with Keweenaw sand were used in the testing program. For ease in identification, we shall call them Fayette and sandy mix.

Sandy mix, selected from a number of trial mixtures, was intended to produce a soil with textural characteristics different from those of Fayette silt loam. The sand used in preparing sandy mix was a reddish-brown loamy sand from Douglas County, Wisconsin. The final mixture used in the testing program contained 75 percent Fayette silt loam and 25 percent Keweenaw sand. Pertinent engineering properties of the soils used are listed in the table below (1 mm = 0.039 in; 1 N = 0.22 lbf; 1 KN/m^3 = 5.647 lb/ft^3).

Item	Fayette Silt Loam	Sandy Mix
Liquid limit (%)	39	33
Plasticity index	18	12
Sand (0.074-4.76 mm) (%)	2.4	21.6
Silt (0.002-0.074 mm) (%)	77.6	63.5
Clay (<0.002 mm) (%)	20.0	14.9
AASHO soil classification	A-6(11)	A-6(9)
Unified soil classification	CL	CL
Optimum moisture content (%)	18.2	15.8
Maximum dry unit weight (kN/m^3)	17.3	18.3
Specific gravity	2.69	2.71

The compaction characteristics of the two soils used were determined by using the Harvard miniature compactor following the procedure given by Wilson (20) and using a compressive force of 178 N (40 lbf). Based on the results of the compaction tests, specimens at approximately optimum moisture content and nominally 2 percent dry and wet of it were compacted to be used in the repetitive loading tests, again using the Harvard miniature compactor.

Addition of 25 percent sand to Fayette silt loam resulted in higher maximum dry density and lower optimum moisture content than found in the natural state. Preparation of nominally ±2 percent of optimum moisture content specimens was successful in the natural Fayette; however, the wet-of-optimum specimens turned out to have molding moisture contents very close to the optimum in the case of sandy mix (a situation that could not be ascertained until after the termination of the testing program).

EXPERIMENTAL PROCEDURES

The experimental phase of the investigation involved three stages: (a) preparation of soil samples, (b) equilibration of samples to various suction values, and (c) repetitive load testing and subsequent compression testing of samples.

Sample Preparation

The test specimens were prepared from the two soil samples by compaction with controlled moisture content by using a miniature Harvard compactor in accordance with the procedures described by Wilson (20). Three sets of test specimens were compacted with molding moisture contents in the range of ±2 percent of optimum. Each set contained nine specimens to be equilibrated and load tested at suctions of 6.25, 12.50, 25, 50, 100, 200, 400, 800, and 1500 kPa (0.9, 1.8, 3.6, 7.3, 14.5, 29.0, 58.0, 116.0, 217.5 lbf/in^2).

During compaction the Harvard compactor was equipped with a 178-N (40-lbf) spring. Compacted specimens were allowed to equilibrate in sealed jars for about a week to ensure more uniform internal moisture distribution. The procedure described here results in reasonably homogeneous, reproducible specimens with controlled moisture contents. The compaction and subsequent moisture extraction resulted in moisture contents (weight basis) ranging from 12 to 25 percent. The dry density, once fixed during the compaction process, did not vary significantly during subsequent moisture extraction; therefore, no conclusive relationships between density and the observed behavioral patterns could be discerned.

Another important soil parameter, soil fabric, was not controlled or measured. During compaction of soils fabric is influenced primarily by the method of compaction and the compaction moisture content (21). Johnson and Sallberg (22) report that the kneading compaction method best represents the soil fabric obtained in the field. For this reason, among others, the Harvard method was used to prepare all specimens. The influence of compaction moisture content was included by preparing specimens at optimum as well as dry- and wet-of-optimum moisture contents.

Equilibration of Specimens to Various Soil Suctions

The soil moisture extractors were used to equilibrate the soil samples to various matric (soil) suctions. One of the extractors, which contained a ceramic plate of 100 kPa (14.5 lbf/in^2) air-entry pressure, operated within the range of 6.25-50 kPa (0.91-7.25 lbf/in^2), whereas the other one, which contained a 1500 kPa (217.4 lbf/in^2) air-entry pressure plate, was used in the 100-1500 kPa (14.5-217.4 lbf/in^2) range. By

doing this, it was possible to substantially reduce the total equilibration time for the whole series.

After they were placed in the extractors, the samples were left to equilibrate with water under zero chamber pressure until no noticeable flow of water into the extractors' pressure plates was observed. Then chamber pressures of 6.25 kPa (0.91 lbf/in^2) and 100 kPa (14.5 lbf/in^2), respectively, were applied as the first increment; the pressures were doubled when equilibrium was reached under each incremental pressure. As soon as the air pressure inside the chamber is raised above the atmospheric pressure, the higher pressure inside the chamber forces excess water through microscopic pores in the porous membrane (ceramic plate). The high-pressure air, however, will not flow through the pores because they are filled with water and the surface tension of the menisci formed at the gas-liquid interface at each of the pores supports the pressure in much the same way as a flexible rubber diaphragm would. When the air pressure is increased inside the extractor, the radius of curvature of this interface decreases. However, the menisci will not break and let air pass throughout the whole pressure range of the extractor. At any given air pressure in the chamber, soil water will flow from around each of the soil particles and out through the porous membrane to the space under it, which is kept at atmospheric pressure by a tube connected to the atmosphere.

This process continues until such time as the effective curvature of the water films throughout the soil are the same as those in the pores of the porous membrane. When this occurs, equilibrium is reached and the flow of moisture ceases. At equilibrium the air pressure in the extractor and the soil suction are equal.

Each time the equilibrium between the chamber pressure and pore-water pressure in the samples was reached, three samples (with dry-of-optimum, optimum, and wet-of-optimum compaction moisture contents) were taken out, weighed, measured, trimmed (if necessary to provide parallel top and bottom surfaces for resilience testing), reweighed, and remeasured after trimming.

Repetitive Load Testing

Cylindrical specimens [approximately 70 mm (2.76 in) high and 35 mm (1.38 in) in diameter] equilibrated to desired soil suctions were subjected to repetitive loading tests in an apparatus capable of applying repeated dynamic loads of controlled magnitude and duration with a choice of a number of loading functions. Repetitive loading tests were carried out under uniaxial loading conditions. Factors considered in adopting the unconfined compression procedure included

1. Simplicity and ease of testing,
2. The very small [normally less than 40 kPa (6.0 lbf/in^2)] magnitude of confining pressure that exists in the upper regions of the subgrade of a typical flexible pavement, and
3. Difficulty in assessing change in induced soil suctions as a result of the application of an all-around pressure, which introduces problems in correlating the resilient behavior with soil suction.

During repetitive load testing, an initial axial load of 20 N (4.5 lbf) was applied; this axial load was then varied between 20 and 100 N (4.5 and 22.5 lbf), which resulted in a repetitive axial stress of approximately 80 kPa (11.6 lbf/in^2). The load-time curve form chosen was haversine, and a series of pilot tests was performed with frequency of loading varying from 0.2 to 2 cycles/s and number of cycles running up to 10 000 repetitions.

Based on these tests, and the time constraints, a maximum of 5000 repetitions, a frequency of loading of 0.5 cycle/s, and a loading time of 0.3 s/repetition at a time interval of 2 s between two consecutive loadings were adopted as reasonable values in the main testing effort. Half of the Fayette series was carried to 10 000 repetitions.

Resilient deformation and the applied load were taken directly from a built-in recorder, and the resilient moduli were calculated. After the resilience testing, the unconfined compressive strength of each specimen was determined by a conventional unconfined compression testing apparatus following standard procedures (23).

EXPERIMENTAL RESULTS

Definition of Mechanical Parameters

The term "stress" refers to the average load per unit area, and "strain" is defined as the ratio of the average change in a dimension (deformation) to the original value of that dimension. Resilient or elastic strain is the ratio of that portion of the total deformation that is recovered after the repeated axial load is removed to the original specimen length. Residual or plastic strain is the ratio of that portion of the total deformation that is not recovered after the repeated axial load is removed to the original specimen length. Resilient modulus is the ratio of the repeated axial stress (or the repeated principal stress difference) to the resilient strain. And soil suction is the energy with which water is held in soil and is measured by the work required to move an infinitesimal quantity of water from the soil to a pressure-free and pure state.

Soil suction, when expressed as energy per unit volume, is a negative quantity with dimensions of pressure. However, in engineering use, its absolute value or positive magnitude is normally used for ease of discussion. This usage is also adopted in this study. Thus, a soil suction of -800 kPa (-116 lbf/in^2) is referred to as a suction of 800 kPa (116 lbf/in^2).

The influence of the moisture state variables on the resilient properties and post-repetitive loading strengths is demonstrated and discussed in the following sections.

Water Retention Curves

After they were prepared, the cylindrical specimens were allowed to stand on the moisture extractor plate with access to free water. In response to the suction pressures induced during compaction, the specimens tended to absorb water, which they were allowed to do until there was no noticeable movement of water into the extractor. The specimens were then brought to equilibrium at various soil suctions, always following a fixed pressure schedule, i.e., always doubling the previous pressure. Only variations from the initially nearly saturated state were studied by means of a desorption schedule. Some of the specimens were taken out after equilibrium at various suctions to determine their equilibrium water contents and dry densities. They were tested in uniaxial repeated loading and static compression for resilient deformation and strength characteristics. The ceramic plate extractor primarily controlled the specimens' matric potential; the solute potential was not considered to be a significant component of the total potential for the materials and the conditions of this study.

The characteristic water retention curves associated with the indicated desorption schedule are given in Figure 1 for the two soils tested. The gradual concave shape of the curves for the specimens molded

at the optimum and wet-of-optimum moisture contents (O to W specimens) indicates that, within the range tested, each of these specimens had a wide distribution of pore sizes, because the presence of a dominant pore size would have yielded a rapid decrease in water content at the value of the soil suction associated with the water-holding capacity of a pore of that given size. This was observed in the case of the specimens molded at dry-of-optimum moisture content (D specimens), particularly of Fayette and, to a degree, of sandy mix.

The variety of complex interactions between clay particles and water made it virtually impossible to calculate theoretically the water-retaining characteristics of a given soil. However, the measurement of water retention can be made without regard to the individual forces holding the water in the clay, and a qualitative interpretation of the different possible mechanisms can be advanced.

Two factors affecting the matric potential of a soil at equilibrium to a large degree are the pore size and number and the adsorptive forces associated with the particles' surfaces. Accordingly, soil fabric strongly influences the pore-size distribution and consequently the shape of the characteristic water retention curves, especially in the low suction range.

Figure 1. Water retention curves for Fayette and sandy mix.

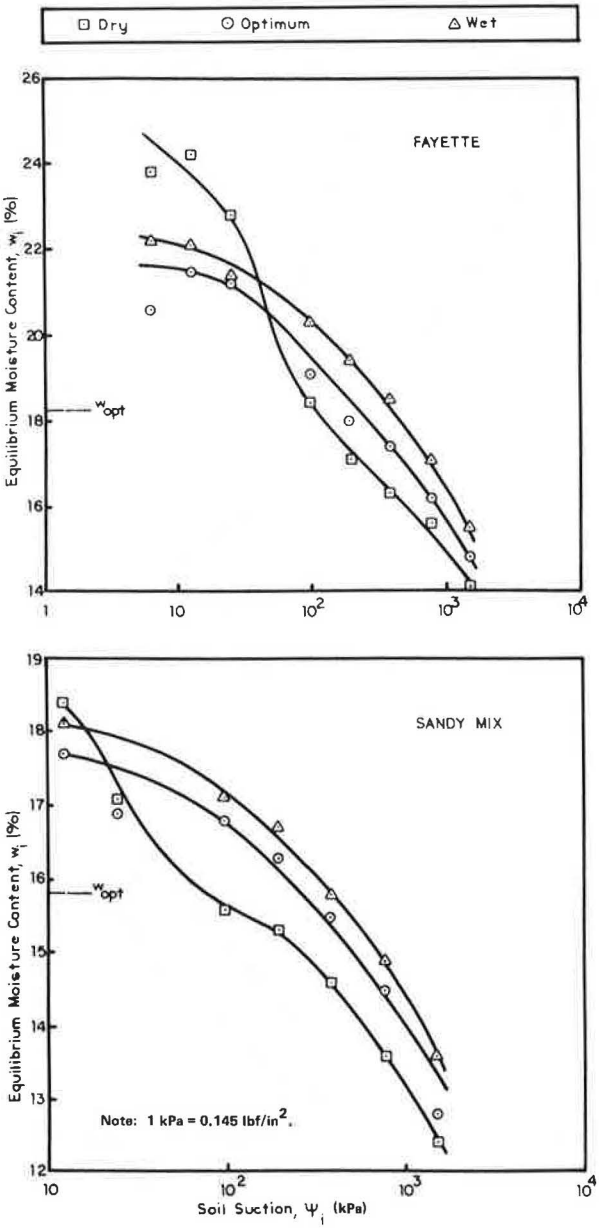

The individual points on a given water retention curve were obtained by testing different specimens with hypothetically the same initial fabric and dry density. Specimens compacted wet and dry of optimum as well as at optimum moisture content follow distinct curves throughout the moisture-extracting process. These water retention curves do not tend to merge at higher suctions, which reflects the dominant influence of the initial fabric characteristics (i. e., pore sizes and shapes) on the water retention rather than the role of the surface adsorptive forces holding water in the soil for the range of soil suctions used.

This rationalization is based on the premise that, as the soil suction increases, the larger pores empty and shrink, and the role of surface adsorptive forces is increased. Therefore, water-retaining characteristics tend to be increasingly governed by the specific surface area of the particles rather than by the fabric. Since specific surface area is expected to be the same for specimens of compositionally the same soil, the retention curves can be expected to merge at sufficiently high suctions.

The D specimens seem to have a fabric distinctly different from that of the O or W specimens. This is reflected in the shape of their respective water retention curves. It appears that the D specimens contain a large portion of relatively large pores of roughly equal size when compared to the O and W specimens at approximately the same void ratio (average molding void ratios were 0.55 and 0.48 for Fayette and sandy mix, respectively).

This observation conforms with the reported open, flocculant fabric of specimens compacted dry of optimum versus the oriented, dispersed fabric of specimens compacted wet of optimum (21). Furthermore, the stress-strain curves obtained in the unconfined compression testing of the compacted specimens indicated a peak for the D specimen, whereas smooth curves were obtained for the O and W specimens. This again reflects the variation in the fabrics of these specimens.

In order to demonstrate these inferences, a more direct approach was adopted, and the fabric of specimens wet, dry, and optimum were observed under a scanning electron microscope (SEM). A difference between the fabric of the D specimen and O or W specimens was discernible on the micrographs, and the preponderance of voids in the micrograms was compared in a qualitative manner. There appeared to be hardly any discernible difference between O and W specimens, and the fabric differences of sandy mix specimens were much more subtle.

The soil suctions corresponding to the as-compacted state of the wet, dry, and optimum specimens can be estimated indirectly by reading the suction values corresponding to the molding moisture contents from the respective retention curves. The average compaction suction values in kilopascals (kPa = 0.145 lbf/in^2) of the specimens prepared are given below.

	Suction (kPa)		
Soil Sample	Dry of Optimum	Optimum	Wet of Optimum
Fayette	530	250	130
Sandy mix	280	200	25

These values could differ from the actual as-compacted suctions; nevertheless, the specimens compacted dry of optimum indicate much higher suction values and a more

open fabric than the wetter specimens. When allowed access to water, as in this study in the extractor before the desorption cycle, they absorb much more water than the wetter specimens (Figure 1).

For instance, the dry Fayette and sandy mix specimens gained 7.8 percent and 2.5 percent in moisture content, respectively, when allowed access to water in the extractor under a small suction pressure [6.25 kPa (0.91 lbf/in^2) and 14 kPa (2.03 lbf/in^2), respectively], whereas the optimum and wet-of-optimum Fayette and sandy mix specimens gained, under the same conditions, on the order of 2.1 and 1.2 percent in moisture content, respectively.

Practical implications are important in that certain soils when compacted to the same density, if the compaction moisture content is dry of optimum, will be more susceptible to moisture changes. In the presence of moisture they may equilibrate to higher moisture contents than the corresponding soils compacted wetter. Since structural properties have a general dependency on moisture content, this would result in inferior performance.

All the observations made above were more distinct for Fayette than for sandy mix. This was probably because sandy mix packed better with its 25 percent sand and less clay.

Repetitive Loading Test Results

Uniaxial repetitive loading tests were performed on more than 60 specimens from the two soil samples. The results were analyzed in terms of the resilient modulus (E_r) and the residual strain (ϵ_p). These two parameters define the behavior of subgrade soils and are useful in the design of highway and airfield pavements.

Figure 2 shows the variation of E_r and ϵ_p as a function of the number of loading cycles (N). Both E_r and ϵ_p steadily increase with increasing N, and the soil be-

Figure 2. Resilient modulus and residual strain versus number of loading cycles.

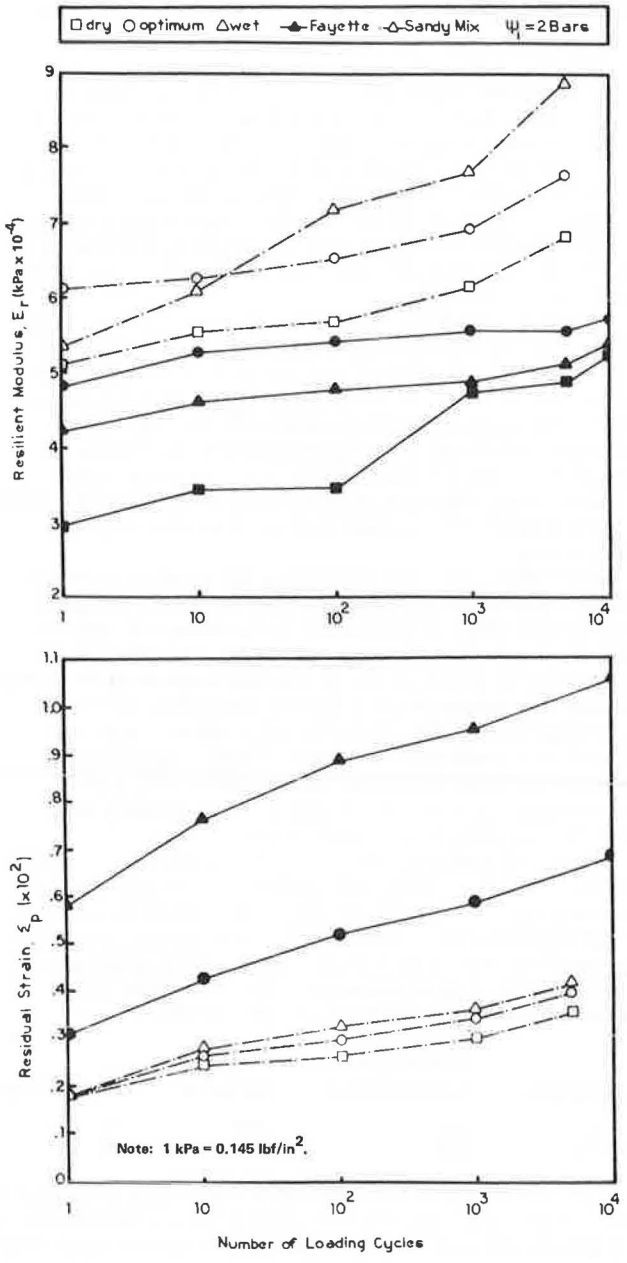

Figure 3. Resilient modulus and residual strain versus compaction moisture content.

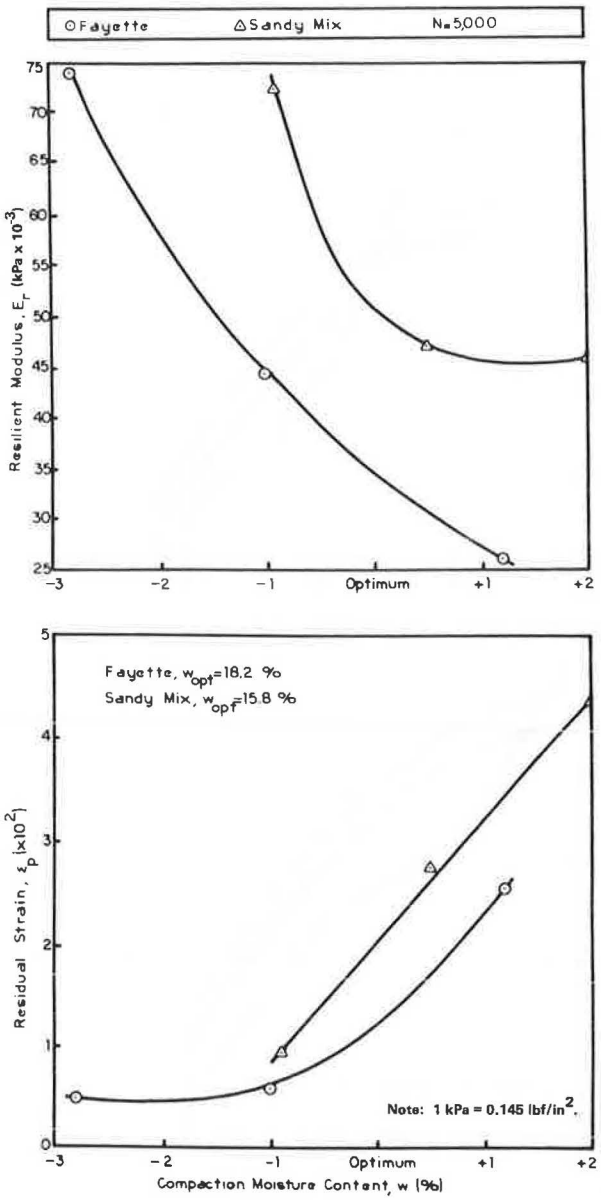

comes less elastic. This behavior was usually observed for all the specimens at all suctions. E_r increases approximately 1.4-fold for both soils over a range of 1000-5000 N (225-1125 lbf), and ϵ_p increases approximately 2- and 3-fold for sandy mix and Fayette, respectively, over the same range.

The general influence of compaction moisture content on E_r and ϵ_p is shown in Figure 3. Variations in compaction moisture content on the dry side of optimum result in more significant changes in E_r than similar variations on the wet side of optimum. In the case of ϵ_p, the opposite of the resilient modulus response is observed.

Permanent strains increase rapidly for the specimens compacted wet of optimum. However, one must remember that moisture content of the soil may change after compaction in response to environmental conditions. In order to investigate this response, compacted specimens were equilibrated to a range of moisture regimes in the laboratory and tested.

Figure 4 gives the resilient modulus and residual strain at 5000 load repetitions as a function of the equilibrium moisture content and the degree of saturation for Fayette silt loam. The data indicate a general tendency for E_r to decrease as w_i increases. Changes in E_r for moisture contents greater than the optimum are relatively small, whereas significant changes occur with moisture content in the dry-of-optimum range. Small variations occur in ϵ_p for moisture contents equal to or less than optimum. However, for states wetter than optimum, residual strains rapidly increase with moisture content. The data points are not scattered much, which indicates a strong dependency on equilibrium moisture content.

The moisture-density relations for soils can also be considered in terms of degree of saturation. In Figure 4 a trend is noted between E_r and ϵ_p and the degree of saturation (S_i). Resilient modulus decreases at saturations less than 75 percent for the range of S_i. The specimens tested at a suction of 1500 kPa (217.4 lbf/in^2) had consistently lower moduli than the ones tested at 800 kPa (116 lbf/in^2).

Figure 4. Resilient modulus and residual strain versus moisture content and degree of saturation.

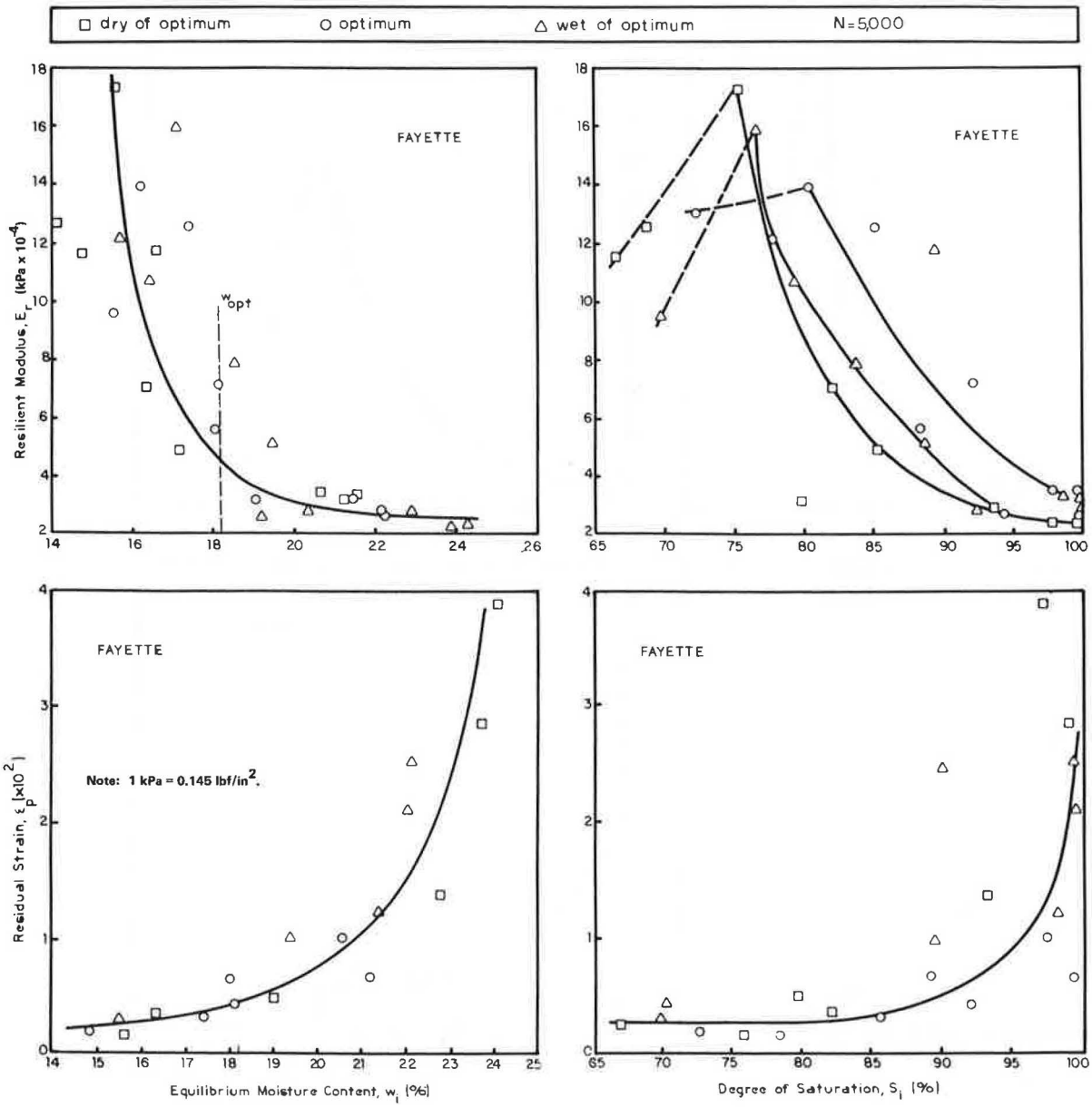

This change in behavior trends at a suction roughly corresponding to 800 kPa is responsible for the lower moduli for degrees of saturation less than the critical value of S_t (75 percent for Fayette silt loam). Residual strains remain relatively constant for S_t equal to or greater than 95 percent. Significant changes in ϵ_p take place when the soil is nearly saturated (S_t is smaller than 95 percent). Residual strains are apparently more strongly dependent on moisture content than on degree of saturation.

A volume measurement is required to determine degree of saturation, and this introduces significant inaccuracies. Consequently, the data points were quite scattered (especially for sandy mix). It is noted from Figure 4 that the use of moisture content or degree of saturation alone to characterize moisture regime of a soil is, in general, inadequate.

Figure 5 shows the range of values for the resilient modulus and residual strain as a function of the initial soil suction (ψ_i) for the two soils. E_r does not change appreciably up to ψ_i = 100 kPa (14.5 lbf/in^2). Thereafter, there is generally a sharp increase in E_r with increasing ψ_i except at ψ_i = 1500 kPa (217.4 lbf/in^2). The drop in E_r at ψ_i = 1500 kPa was observed for both soils and was verified with duplicate specimens prepared and tested in the same manner. It is therefore believed to be an intrinsic behavioral characteristic rather than an experimental error.

The critical suction value at which the change in behavior occurs cannot be precisely determined; however, it probably has a value slightly in excess of 800 kPa. This critical suction corresponds to a moisture content approximately 2 percent dry of optimum. Similar observations with regard to the changes in mechanical behavior at certain critical suctions have been reported. Krizek and Edil (24) reported a change in the static compression behavior of kaolinitic soil samples at a suction of 500-600 kPa (72.5-86.9 lbf/in^2). Edris and Lytton (16) refer to a change in resilient modulus response of certain Texas soil samples from

Figure 5. Resilient modulus and residual strain versus soil suction.

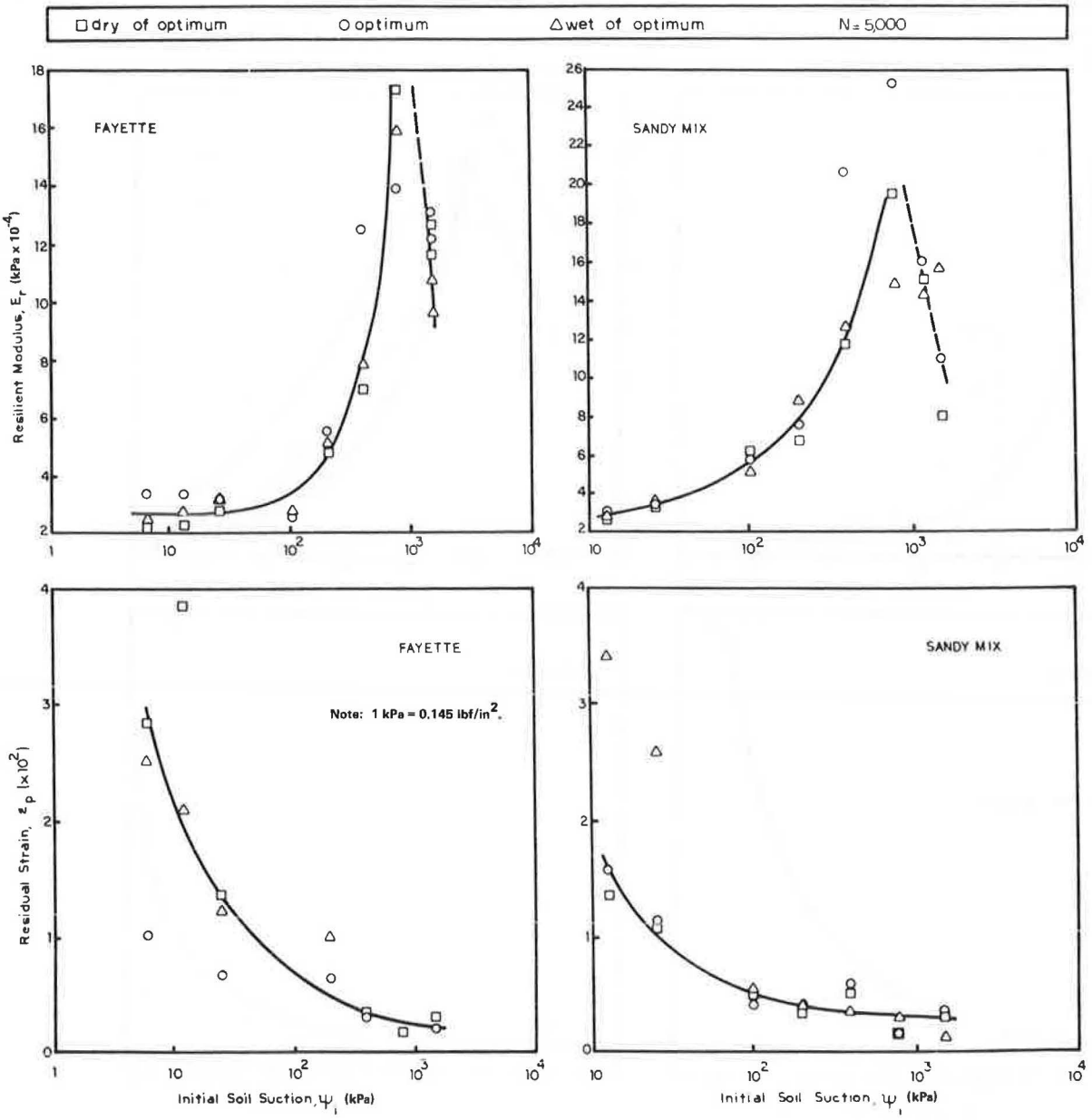

Figure 6. Effect of repetitive loading on unconfined compressive strength.

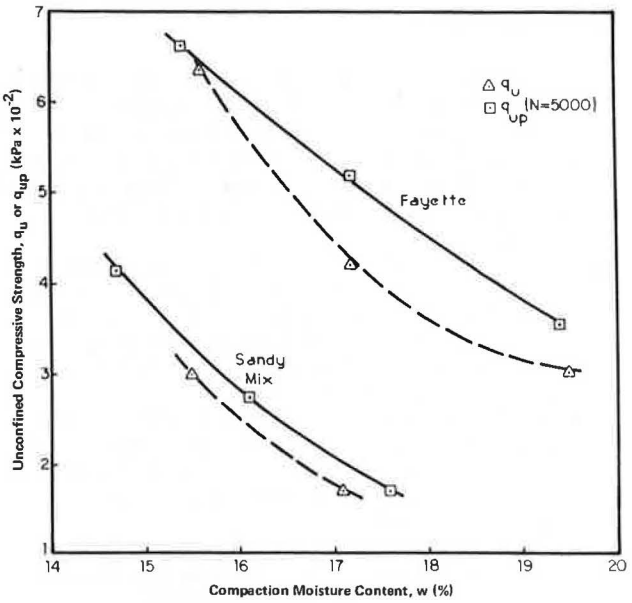

Figure 7. Post-loading unconfined strength versus soil suction.

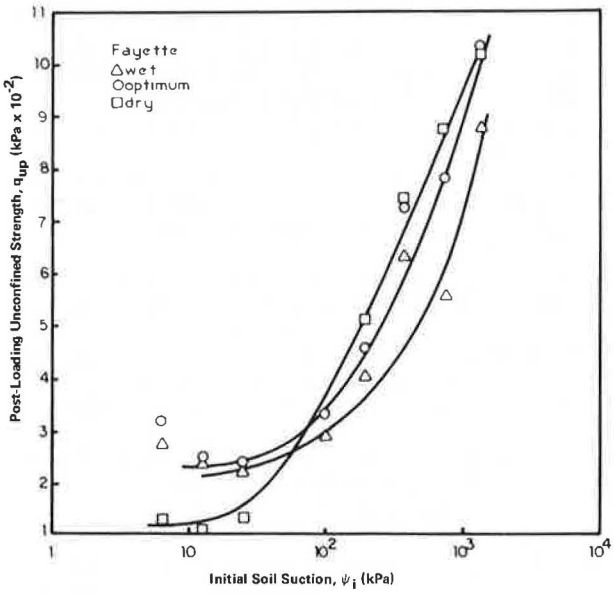

"effectively saturated" to "effectively unsaturated" at a suction corresponding to 2 percent dry-of-optimum moisture content. The reasons for this change in behavior have not yet been identified. The dependency of E_r on ψ_i for dry, wet, and optimum samples appears similar; however, there are no distinguishable trends with respect to the compaction moisture content and the resultant fabric.

Major changes in ϵ_p take place for the suction range less than 100 kPa (14.5 lbf/in^2), beyond which irrecoverable strain stabilizes and remains, in general, equal to or less than 5×10^{-3}. As suction increases from 6.25 to 100 kPa (0.91-14.5 lbf/in^2), ϵ_p decreases 2.5- to 7-fold, depending on the specimen's compaction condition (i.e., wet, dry, or optimum).

Figure 8. Post-loading unconfined strength versus water content.

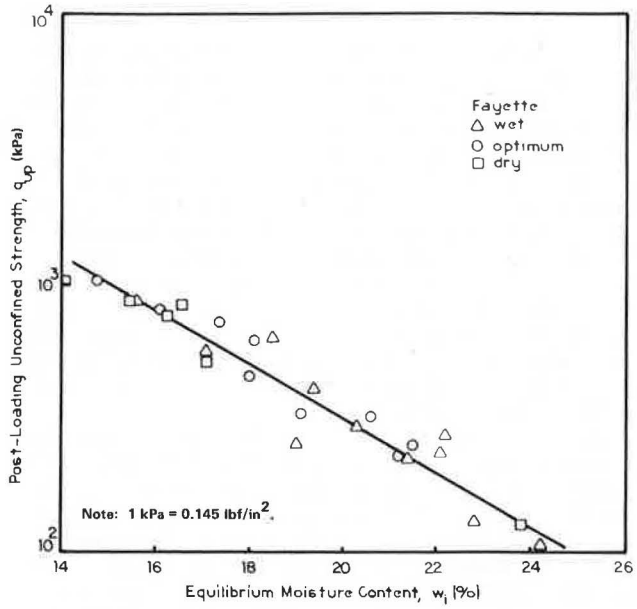

Compressive Strength After Repetitive Loading

The specimens that were used in the repetitive loading tests were subsequently subjected to unconfined compression tests. This strength is referred to as the "post-loading unconfined compressive strength" and is designated q_{up}. The q_{up} value represents the soil's strength after 5000-10 000 cycles of repetitive loading to a stress level only a fraction of its strength.

As a result of the repetitive loading, the initial characteristics of the specimens are expected to change somewhat. The post-loading strength of compacted specimens are compared in Figure 6 with those of the specimens not subjected to repetitive loading. The specific repetitive loading level used causes a slight increase in unconfined strength. No attempt was made to measure the final suction at the end of the repetitive loading. Based on the data presented by Edris and Lytton (16), the ratio of final to initial suction is very nearly one for the soils tested in this program. Consequently, the variation of q_{up} values with the known initial suction (ψ_i) is considered and presented in Figure 7 for Fayette soil. As shown in this figure, q_{up} increases with increasing values of ψ_i.

Similar behavior by kaolinite samples prepared by consolidation from a slurry has been reported by Edil and Krizek (10). At each suction value, there is a range of q_{up} values that results from the difference in water contents of dry, wet, or optimum specimens equilibrated to the same soil suction. In order to demonstrate the effect of water content, log q_{up} is plotted versus w_i in Figure 8; there is a distinct dependency on water content and q_{up} varies with w_i in approximately an exponential manner.

SUMMARY AND CONCLUSIONS

A study of the relationship between the resilient modulus, residual strain, post-repetitive loading strength and the moisture regime of two fine-grained soils has been made. Based on the behavior of the silt loam soils investigated here, the following conclusions can be drawn. The application of these conclusions to similar soils may be possible in a qualitative manner;

however, for quantitative comparisons caution must be exercised.

1. Characteristic water retention curves are useful for reflecting the susceptibility of compacted soils to moisture changes. The silt loam soils compacted dry of optimum are found to be more susceptible to moisture content changes than are the ones compacted at optimum or wet-of-optimum moisture contents at comparable compaction densities. For example, the specimens compacted dry of optimum equilibrated to higher moisture contents than the optimum and the wet-of-optimum specimens at low soil suctions. Since most mechanical properties are adversely affected by increasing moisture content, the necessity of specifying the compaction moisture content in addition to the compaction density becomes apparent in field compaction of fine-grained soils.
2. The resilient modulus and strength strongly depend on compaction moisture content on the dry side of optimum with insignificant dependency on the wet side (within the range of ±2 percent of optimum), whereas the residual strain exhibits the opposite behavior.
3. The moisture regime subsequent to compaction can be expressed most suitably in terms of soil suction. It is an intrinsic parameter of the moisture equilibrium and reflects the effects of soil type and fabric, climate, and position of groundwater table on the mechanical response better than moisture content or degree of saturation alone.
4. Resilient modulus and post-repetitive loading strength are primarily related to soil suction. For silt loam soils investigated, variations in these properties were small for suction values less than 100 kPa (14.5 lbf/in^2). This suction corresponds roughly to 2 percent dry-of-optimum moisture content. For suctions greater than this, however, significant increases in mechanical properties (on the order of three- to six-fold) are obtained.
5. The opposite of this behavior is obtained in the case of residual strain. Major decreases in residual strain take place up to a suction of 100 kPa. However, for suctions greater than this, residual strain remains virtually constant.
6. Resilient modulus increases monotonically for soil suctions from 100 kPa to a critical suction beyond which it decreases. This critical suction appears to be about 800 kPa (116 lbf/in^2) (corresponding moisture content is 2 percent dry of optimum) for the soils tested. This anomaly in behavior was not observed in the case of residual strain or strength.
7. The significant range of soil suctions is from 100-800 kPa for the soils considered. This corresponds to a range of Thornthwaite moisture index of from -15 to +15 for the soils tested. In the regions where the climatic moisture in terms of rainfall and evapotranspiration yields a moisture index in this range, an advantage of improved mechanical properties as a function of soil suction can be taken. In terms of moisture content, this significant range corresponds to ($w_{optimum}$) to ($w_{optimum}$ - 2 percent).
8. Number of loading cycles results in significant increases in resilient modulus and residual strain (the latter is not very desirable) and some increase in compressive strength.

ACKNOWLEDGMENT

This work was supported in part by a grant from the National Science Foundation to investigate soil-moisture equilibrium and behavior of highway pavement systems. Other financial assistance was provided by the Graduate School of the University of Wisconsin, Madison.

REFERENCES

1. A.L. Robnett and M.R. Thompson. Development of Testing Procedure: Phase I—Interim Report, Resilient Properties of Subgrade Soils. Illinois Cooperative Highway Research Program, Department of Civil Engineering, Univ. of Illinois, Urbana, Transportation Engineering Series 5, No. 139, June 1973.
2. H.B. Seed, D.K. Chan, and C.E. Lee. Resilience Characteristics of Subgrade Soils and Their Relation to Fatigue Failures in Asphalt Pavements. Proc., 1st International Conference on the Structural Design of Asphalt Pavements, Ann Arbor, MI, 1962, pp. 611-636.
3. C.L. Monismith and others. Prediction of Pavement Deflections from Laboratory Tests. Proc., 2nd International Conference on the Structural Design of Asphalt Pavements, Ann Arbor, MI, 1967, pp. 109-140.
4. H.B. Seed and others. Prediction of Flexible Pavement Deflections from Laboratory Repeated-Load Tests. NCHRP, Rept. 35, 1967.
5. Water on Roads: Prediction of Moisture Content of Road Subgrades. Organization for Economic Cooperation and Development, Paris, 1973.
6. B.J. Dempsey and A. Elzeftawy. Interim Report—Moisture Movement and Moisture Equilibria in Pavement Systems. Illinois Cooperative Highway Research and Transportation Program, Department of Civil Engineering, Univ. of Illinois, Urbana, Transportation Engineering Series 15, No. 161, 1976.
7. R.L. Lytton. Theory of Moisture Movement in Expansive Clays. Center for Highway Research, University of Texas, Austin, Research Rept. 118-1, Sept. 1969.
8. D. Croney and J.D. Coleman. Soil Structure in Relation to Soil Suction (pF). Journal of Soil Science, Vol. 1, 1954, pp. 75-84.
9. L.A. Richards. Physical Condition of Water in Soil. In Agronomy: No. 9—Methods of Soil Analysis, Madison, WS, P.1, 1965, pp. 128-152.
10. T.B. Edil and R.J. Krizek. Influence of Fabric and Soil-Water Potential on the Mechanical Behavior of a Kaolinitic Clay. Geoderma, Vol. 15, 1976, pp. 831-840.
11. C.W. Thornthwaite. An Approach Toward a Rational Classification of Climate. Geographical Review, Vol. 38, No. 1, 1948, pp. 55-94.
12. M.P. O'Reilly, K. Russam, and F.H.R. Williams. Pavement Design in the Tropics. British Road Research Laboratory, Crowthorne, Berkshire, England, Technical Paper 80, 1968.
13. E.K. Sauer and C.L. Monismith. Influence of Soil Suction on Behavior of a Glacial Till Subjected to Repeated Loading. HRB, Highway Research Record 215, 1968, pp. 18-23.
14. B.G. Richards and R. Gordon. Prediction and Observation of the Performance of a Flexible Pavement on an Expansive Clay Subgrade. Proc., 3rd International Conference on the Structural Design of Asphalt Pavement, Ann Arbor, MI, 1972, pp. 133-143.
15. B. Shackel. Changes in Soil Suction in a Sand-Clay Subjected to Repeated Triaxial Loading. HRB, Highway Research Record 429, 1973, pp. 29-34.

16. E.V. Edriss, Jr., and R.L. Lytton. Dynamic Properties of Fine Grained Soils. Proc., 9th International Conference on Soil Mechanics and Foundation Engineering, Tokyo, Vol. 2, 1977, pp. 217-224.
17. D.G. Fredlund, A.T. Bergan, and E.K. Sauer. Deformation Characterization of Subgrade Soils for Highways and Runways in Northern Environments. Canadian Geotechnical Journal, Vol. 12, No. 2, 1975, pp. 213-223.
18. D.G. Fredlund, A.T. Bergan, and P.K. Wong. Relation between Resilient Modulus and Stress Conditions for Cohesive Soils. TRB, Transportation Research Record 642, 1977, pp. 73-81.
19. Soil Manual. Wisconsin Department of Transportation. 1972.
20. S.D. Wilson. Small Soil Compaction Apparatus Duplicates Field Results Closely. Engineering News-Record, May 1950, pp. 34-36.
21. T.W. Lambe. The Structure of Compacted Clay. Journal of Soil Mechanics and Foundations Division, Proc., ASCE, Vol. 84, No. SM2, 1958, pp. 1-34.
22. A.W. Johnson and J.R. Sallberg. Factors That Influence Field Compaction of Soils. HRB, Bull. 272, 1960, pp. 29-48.
23. T.B. Edil and S.E. Motan. Soil-Moisture Equilibria and Behavior of Highway Pavement Systems. National Science Foundation, Grant ENG75-10558, 1978, 68 pp.
24. R.J. Krizek and T.B. Edil. Experimental Study of Clay Deformability in Terms of Initial Fabric and Soil-Water Potential. Rheologica Acta, No. 13, 1974, pp. 803-813.

Publication of this paper sponsored by Committee on Environmental Factors Except Frost.

Comparison of the Precise Freezing Cell with Other Facilities for Frost-Heave Testing

R.H. Jones and S.J-M. Dudek, Department of Civil Engineering, University of Nottingham, England

Identification of frost-susceptible materials on the basis of their physical properties is too imprecise for many practical purposes, and direct freezing tests need to be employed. Heave is measured by two main types of test: the constant rate of penetration test and the constant boundary temperature test. The latter has the advantage of greater simplicity of operation and is easier to model mathematically. Nevertheless, its reproducibility is relatively poor and improvements are being sought. The development of a self-refrigerated unit (SRU) is outlined and likely future revisions to the constant boundary temperature test specification discussed briefly. A precise freezing cell (PFC) that uses the Peltier effect and permits unidirectional freezing with the boundary temperatures controlled to ±0.1°C has been developed. Specimens heave much less in the PFC than in the SRU because the heat extraction is more rapid and a constant temperature is applied to the moving boundary (top of specimen) rather than to the stationary boundary. Thus the penetration of the zero isotherm is accompanied by high suctions that favor ice penetration over segregation. The role of the PFC lies in research, not in routine testing, particularly in connection with the development and evaluation of mathematical models.

The process of frost heaving, which occurs when the zero isotherm penetrates below the bound materials of a typical road structure (Figure 1), can be explained in terms of the capillary theory (1, 2, 3). This postulates that, to pass through the neck of a pore, the radius of curvature of the ice front (r_{iw}) must be reduced to a critical value (r_o) (Figure 2). The curved interface is associated with both a pressure difference and a freezing-point depression according to the equation

$$p_i - p_w = 2\sigma_{iw}/r_{iw} = L\Delta T/V_w T_o \quad (1)$$

where

p_i, p_w = ice and water pressures respectively (Pa),
r_{iw} = radius of ice-water interface at a particular instant (m),
σ_{iw} = interfacial energy (ice-water) (J/m²),
L = latent heat of fusion (J/kg),
ΔT = freezing point depression (K),
V_w = specific volume of water (m), and
T_o = 273 K.

Because in the absence of restraint p_i will not differ significantly from atmospheric pressure, p_w will be less than atmospheric, which will give rise to a suction that draws water continuously toward the freezing front. In frost-susceptible materials, there is a tendency for the radius of curvature to remain above r_o for long periods, which results in ice segregation and excessive frost heave. For materials with a range of grain (and hence pore) sizes, various suggestions have been made regarding the selection of a characteristic critical pore radius (4).

Identification of frost-susceptible materials continues to be a significant problem for both designers and research workers. Direct tests based on the fundamental work of Taber (5) have been developed by the U.S. Cold Regions Research and Engineering Laboratory (CRREL) (6-8) and by the U.K. Transport and Road Research Laboratory (TRRL) in Great Britain (9). In both, cylindrical specimens from either undisturbed samples or recompacted material are subjected to unidirectional freezing from the top, while their bases are kept in contact with unfrozen water.

In the CRREL procedure, the top temperature is adjusted to give a specified rate of penetration, while in

Figure 1. Typical road structure.

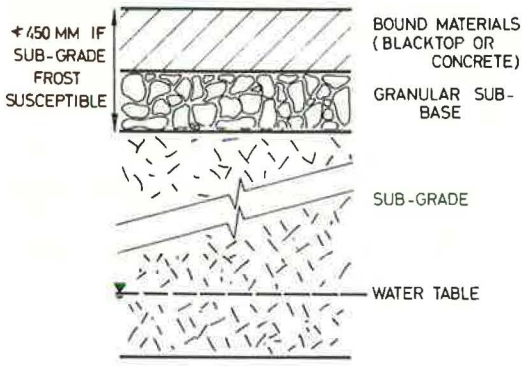

Figure 2. Capillary model of ice penetration.

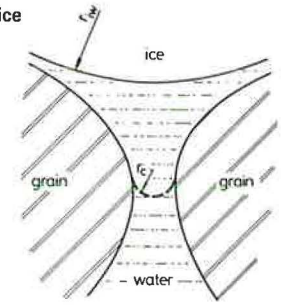

the TRRL test the air temperature above the specimens remains constant. The classification of materials is, however, broadly similar for both tests (10). Several alternative direct tests have been proposed (11), including those in which the development of heaving pressure during restrained heave tests (which mirrors the heave in an unrestrained test) is measured.

In addition, many attempts have been made to assess frost susceptibility indirectly on the basis of material characteristics such as grain- or pore-size distributions (12). For example, an osmotic suction method has shown promise in ranking the frost susceptibility of limestone subbase materials (13). Nevertheless, whatever approach is used, there are considerable reservations about the accuracy of the assessment of frost susceptibility, and investigations, including those described in this paper, are continuing to develop simpler and more reliable methods.

Even so, the assessment of frost susceptibility of the materials subject to ice penetration is only a first step in determining the precautions necessary to prevent frost-heave damage. It is then necessary to assess whether the amount of heave of the road surface will be acceptable. The heave that can be tolerated will depend on the importance of the road, its construction, and economic factors. The actual heave will depend on climatic conditions (which largely control the depth of frost penetration), the depth of the water table, and the capillarity and effective permeability of the materials between the water table and the freezing front.

An additional factor when the freezing front remains in compacted materials (which is typical of British conditions) is that the density or grading of the material as compacted on site may differ from those achieved in the laboratory (14, Chap. 3).

Relationships between the results of laboratory frost-susceptibility tests and the design of actual roads built on or with the materials tested have been developed (9, 15). In Great Britain, where hard winters occur infrequently, the empirical correlation between laboratory and field performance originally made for subgrade soils has also been applied to subbases. The introduction of mathematical models, (16-20) mainly based on the capillary theory heralds a more rigorous approach not only to the interpretation of past and future field observations and pilot scale trials but also to the design process itself.

However, while progress has been made in several aspects of mathematical modeling, current models require further development to deal fully with the central problem of coupling the heat and water flows (21). We are developing an improved model in which we hope to quantify the variations in space and time of suction, suction gradient, and effective permeability in relation to one or more of the physical characteristics of the materials.

For steady-state conditions, the continuity equation requires that the product of suction gradient and effective permeability be constant. However, individually, neither the suction gradient nor the permeability (which is suction dependent) is constant (22, 23). In view of the complexities and uncertainties, any proposed mathematical model of frost heaving requires rigorous experimental verification before it can be adopted with confidence.

Against this background, precisely controlled direct frost-heave tests have a multiple role in providing (a) a measurement of frost susceptibility under standard conditions, (b) an insight into the frost-heaving process, and (c) a means of verifying proposed mathematical models. Although constant boundary temperature tests are simpler to perform than constant rate of penetration tests and have the advantage of subjecting all the specimens to the same conditions, the poor reproducibility of the original TRRL test (24) was of considerable concern.

This paper describes two developments of this type of test. The first deals with routine commercial testing and the move toward recognizing the self-refrigerated unit (SRU) rather than the cold room (CR) as the principal testing facility. The second development is of a precise freezing cell (PFC) incorporating Peltier cooling, in which a single specimen is subjected to closely controlled conditions. Results obtained in the various units are presented and the implications discussed.

DEVELOPMENT OF THE TRRL TEST

In the TRRL test (9), nine cylindrical specimens 102 mm in diameter and 152 mm high are placed in an insulated trolley that is wheeled into a cold room operating at -17°C. The specimens rest on porous ceramic disks inside copper carriers. The disks are in contact with water maintained at +4°C. The sides of the specimens are wrapped with waxed paper and the intervening space filled with loose, dry sand (5-2.36 mm fraction). Push rods bearing on caps placed on top of the specimens enable the heave to be measured.

From the start of the test, heave measurements and topping up of the water level are undertaken every 24 h. Materials are judged frost susceptible if, during 250 h, they heave more than 13 mm (in England and Wales) or 18 mm (in Scotland).

At Nottingham, improved repeatability resulted from modifications introduced to give a closer control of the water-bath temperature (25). More recently, a revised interim specification for the test has been introduced by TRRL in which the cold-room facility and procedure, including specimen preparation, is defined more closely (26). Granular specimens continue to be compacted in two stages (tamping in layers followed by static compac-

Figure 3. Self-refrigerated unit.

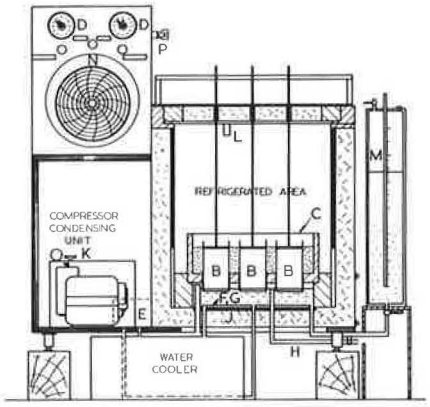

ting), but there have been significant changes in detail. A further revision is expected in which compaction by vibrating hammer and testing in an SRU will be included (27).

These changes have been anticipated in our laboratory where granular specimens have been prepared by precompaction in layers with a vibrating hammer followed by a final static compaction since 1973 (25). The static loads required are much reduced, less than 100 kN even for subbase aggregates, compared with the maximum of 400 kN needed by the TRRL procedure (26). The specimens are extruded from their molds by a hydraulic jack.

The TRRL interim specification stipulates that the air temperature shall be maintained at -17 ±1°C. However, during defrosting periods, which occur every 8 or 12 h in the cold rooms in current use, it is recognized that greater variations will occur. At Nottingham, evidence that the defrosting periods could significantly affect results was obtained from heaving pressure tests (22), and attention was switched to the development of an SRU in which defrosting during the test was unnecessary.

Development of SRUs in the United Kingdom commenced in the mid-1960s, when the TRRL test was adopted as a compliance test for subbase materials (28). Several workers developed chilled tank units (29, 30) or forced-air units (31). The former are similar to domestic deep freezes, but the latter have fan-assisted units that blow cold air over the specimens and are thus in effect miniature cold rooms. Only the forced-air units require defrosting during the test.

For this reason the chilled-tank principle was chosen for further development. A prototype (Figure 3) that incorporated satisfactory features of existing designs was developed in our laboratory in conjunction with P.S. Snow and Company of Leicester. Like most other British units, it was designed to operate under normal laboratory temperatures. The chilled tank is cooled by refrigerant circulating from a 0.4-kW compressor through tubes embedded within the walls. The internal dimensions of the tank and water bath, the configuration of specimens, and the specimen support system match those of the cold-room trolley.

Facilities additional to those then (1976) featured on commercially available units include a chart recorder that gives a continuous trace of air and water temperatures, independent cooling systems for air and water, an air-circulating fan, and a Mariotte tube (29) to maintain a constant water level throughout the 250-h test. In addition, an alternative inner box was made to permit testing of specimens 152 mm in diameter.

Previous SRUs had relied on the low temperature of the tank walls and the enclosed air space to promote sufficient cooling of the water bath. This had not always been successful, particularly in very hot summers (32), and a more positive system was thought necessary. Originally, a heat exchanger consisting of a coil wound around the copper pipe taking the refrigerant from the compresser to the tank cooling coils was fitted. This system gave unacceptable temperature fluctuations and was abandoned.

Two further systems were tried. First, cooling coils beneath the water bath, in series with the tank coils, were brought into use. Second, with these coils by-passed, using valve K (Figure 3), a separate water cooler was connected into the circuit. Although the independent cooler is preferred for research tests, the series coil system has been adopted for the subsequent units that are now available commercially. Fine control of the water temperature is obtained from heaters activated by a mercury contact thermometer. In the prototype unit, the standard deviation of the water temperature beneath the specimens is 0.35°C and that of the top of the specimen is 1°C when all nine specimens are considered.

THE PRECISE FREEZING CELL

Previous Work

Greater control of the temperature at the top of the specimen can be better achieved by direct refrigeration of an individual top cap than by controlling the temperature of the air space above a number of specimens. Direct refrigeration is conveniently provided by a thermoelectric device in which electric current passing through a series of dissimilar semiconductors exhibits the Peltier effect (33). This may be thought of as a reverse thermocouple so that cold and hot faces are produced. The cold plate is in contact with the specimen, and the hot plate is cooled by circulating cooling water. The heat extracted by the cold plate Q_c (watts) is given by

$$Q_c = a_m T_c I - \tfrac{1}{2} I^2 R_M - K_m \Delta T \qquad (2)$$

where

a_m = mean value of the Seebeck coefficient (V/K),
R_M = mean value of the resistance (ohms),
K_m = mean value of the thermal conductance (W/K),
T_c = temperature of the cold plate (K),
I = current (A), and
ΔT = difference between hot- and cold-plate temperatures (K).

Peltier cells of 16- to 88-W capacity have been used by many other investigators, particularly in connection with heaving pressure measurements (11, 34, 35), although proposals for using a Peltier device for heave measurements have been made (36). In the early days, Peltier devices were criticized for being costly and unreliable and for giving nonuniform temperature distributions (37), but their use in conjunction with servo-controls maintained temperatures within close limits (±0.02°C) (35). With improved semiconductor technology and quality control, the Peltier system appeared to be both feasible and economical for the maximum of four units envisaged in this research.

Description of the Cell

A cutaway isometric view of the cell is shown in Figure 4. The principal dimensions are 300 mm outside diameter, 200 mm inside diameter, and 400 mm overall height. The body is formed of thin PVC tubes closed at

Figure 4. Precise freezing cell.

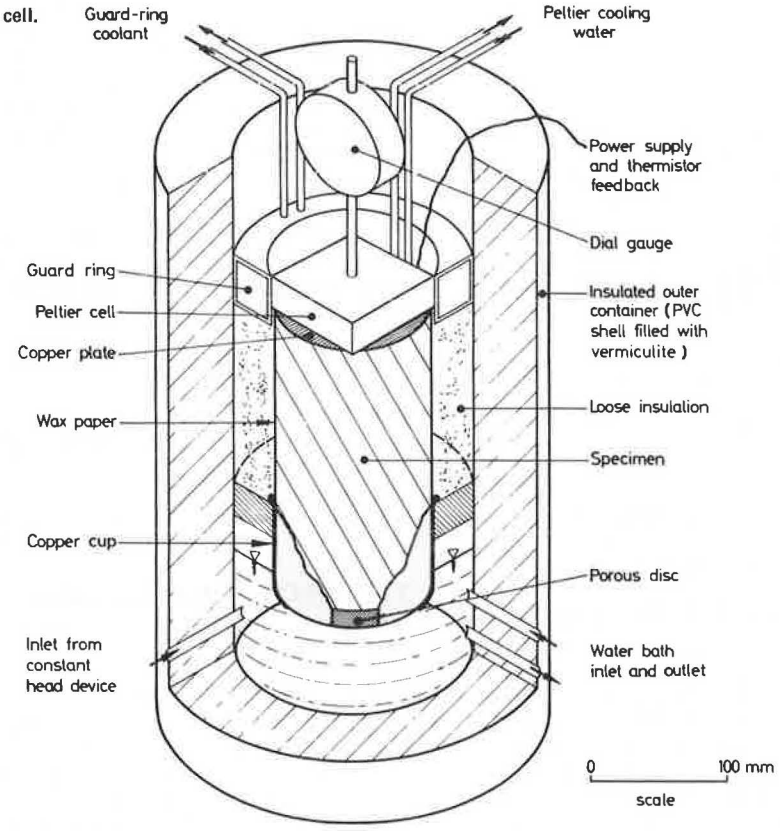

their lower ends and separated by approximately 50 mm of vermiculite insulation. The lower part of the inside of the cell, being watertight, forms a water bath of 2.4-L capacity, which is serviced by three ports that pass through the cell wall. Two of these ports connect to a pumped circulatory system incorporating an external cooler operating at +4 ±0.1°C. The third port connects to a Mariotte vessel that provides a constant head supply similar to that used in the SRU (Figure 3). A scale on this vessel permits measurement of the rate at which water is taken up.

A wooden staging with a central hole enables the specimen to be supported on a porous disk within a copper cup in exactly the same way as in the TRRL test. Likewise, the annular space was filled with loose, dry sand.

The specimen is surmounted by a copper plate of the same diameter on which the Peltier unit (Cambion 806-7242-01, 19-W capacity) rests. A coating of zinc-oxide-loaded silicon grease between the plate and the unit ensured good thermal contact. A thermistor, embedded in the lower face of the copper plate, is coupled to the feedback control capable of maintaining a constant temperature to within ±0.1°C. The Peltier unit was cooled by water that was run to waste. On top of the sand insulation is a guard ring through which methyl alcohol is circulated. The alcohol is cooled by being circulated through a coil in the adjacent cold room and maintains the guard-ring temperature at ±0.5°C. The heave was measured by a dial gauge fixed above the Peltier unit.

The cells are housed in a commercial refrigerator that has two chambers 0.5x0.5x1.2 m giving a +4 ±1°C environment. Cooling is from refrigerated coils and temperature uniformity is improved by using a small supplementary fan. Defrosting during testing is not necessary. With some difficulty, the refrigerator could accommodate four cells and their ancillary equipment, but to date the system has operated with two cells.

The capital cost per specimen of the PFC facility (including controller) is perhaps three times that of an SRU.

Control and Monitoring System

To ensure electronic stability, all the control and monitoring equipment is situated in a constant-temperature (21 ±1°C) enclosure.

Since the coefficients of Equation 2 are temperature dependent, a controller is needed to ensure either a constant rate of heat extraction or, as in this case, maintenance of constant temperature. The system adopted obviates the need for precise control of the cooling-water temperature and protects the Peltier unit from electrical overload.

Three power-pack and control units have been constructed, each of which provides a current of up to 6 A at not more than 5 V. The power supplied to the Peltier battery is regulated by the feedback signal from the thermistor embedded in the top cap. In controller 1 the feedback device operates as an on-off control to the power supply so that the temperature is maintained within the tolerance. The operating voltage can be set manually to give some control of the rate of cooling. A proportional system is used in controllers 2 and 3 so that the rate of cooling slows down as equilibrium is approached. In principle, the second method should give more precise control. However, the damping effect of the thermal mass of the Peltier battery and the top cap masks this effect, and the control achieved by the two types of unit is not significantly different.

Controllers 1 and 3 are fitted with a cycling facility. Essentially, each has two channels that could be set at

Figure 5. Thermocouple positions and vertical temperature gradient.

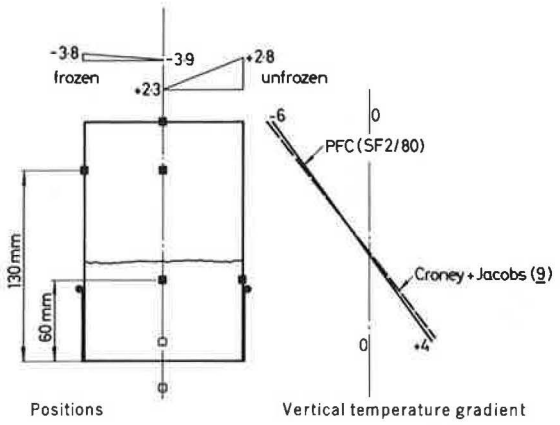

Table 1. Temperature gradients and radial heat flow.

Facility	No. of Tests	Radial Temperature Gradient (°C/m)		Ratio of Radial Heat Flow to Vertical Heat Flow (x 100%)	
		Frozen Zone	Unfrozen Zone	Frozen Zone	Unfrozen Zone
CR	3	10	15	15	22
SRU	2	12	16	18	24
PFC	6	2	10	3	15

Note: The vertical temperature gradient is 67°C/m in all units.

Figure 6. Temperature fluctuations.

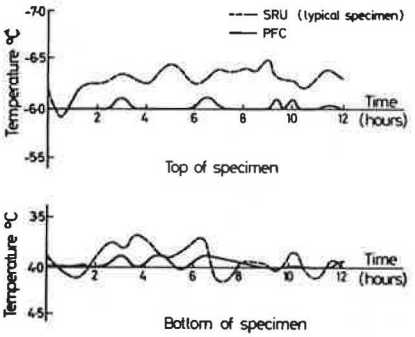

different subzero temperatures. After completing a period of between 2 and 32 h at the lower temperature, the specimen is allowed to warm naturally to the higher temperature, at which it is maintained by the controller for the remainder of the time interval before the cycle is repeated. Controller 3 can be used in conjunction with a guard ring that contains two 19-W Peltier units so that the guard-ring temperature can also be cycled.

Temperature measurements are made using copper constantan thermocouples in conjunction with a reference oven that gives a system accurate to ±0.1°C. The thermocouples are connected to a 70-channel data logger with a punched tape output that permits continual scanning at intervals as long as 2 h.

Test Procedure

The specimen is compacted first by vibrating hammer (3 s on each of three layers), then by static compaction. Thermocouples are positioned as required, and the apparatus set up as described previously. The specimen is left to equilibriate in the refrigerator at +4°C for 24 h.

The controller is then switched on to initiate freezing. In the standard test, both the controller and the guard-ring system are adjusted to give -6°C. This value was chosen as typical of the top-of-specimen temperatures achieved in the cold room and SRU. The full current of 6 A is available for cooling as necessary. In the retarded test, on the other hand, the maximum available current is stepped manually, 0.5 A every 4 h, eventually reaching 6 A. This gives a much slower rate of penetration. Daily readings of temperature and water level are taken.

In both types of test, it was frequently found that all heave had ceased before 250 h had elapsed. Tests were terminated when the heaving rate became negligible (<0.1 mm/day), i.e., after five days in the series of tests described below.

RESULTS AND DISCUSSION

Temperature Control

Concrete dummy specimens, 102 mm in diameter and 152 mm high, in which thermocouples had been inserted in predrilled holes at the positions indicated in Figure 5, were used to investigate fluctuations in temperature. The thermocouples were bedded in plasticine to ensure good thermal contact and stable positioning. Concrete specimens were used because (a) they do not change significantly between tests, (b) they are not subject to heave that would change the elevation of the thermocouples, and (c) freezing has relatively little influence on the thermal properties of concrete.

Typical temperature gradients achieved in the various facilities are shown in Figure 5 and Table 1. The values in Table 1 are the results of readings taken every hour throughout the test. Spurious readings obtained during the passage of the zero isotherm through the thermocouple position have been ignored. The readings for radial heat flow as a percentage of the vertical flow indicate how nearly the condition of unidirectional flow is approached. The PFC is better than the other units, and within the frozen zone the radial heat flow is very small.

Individual temperature gradients in the frozen zone in the PFC were within ±0.1°C/m of the mean and the other individual radial gradients were within ±1°C/m of the mean. The improved performance of the PFC compared to the other units is presumably due to its being operated in a +4°C environment. Conversely, the very cold air circulating in the gap between the inner box and the tank walls is the most likely cause of the relatively high radial flow noted in the SRU. Filling this gap with insulating material may give some improvement.

In all the units the radial heat flow in the unfrozen zone is much higher than in the frozen zone, which probably reflects the influence of the copper specimen carriers. Substituting plastic carriers and lowering the staging to reduce the air gap might be advisable in the PFC, particularly when it is used to verify mathematical models. Although such changes would reduce the similarity of conditions in the PFC to those currently specified in the TRRL test, the benefits would appear to outweigh this disadvantage.

Typical temperature fluctuations are shown in Figure 6. Although the SRU top and bottom temperatures for the single specimen are both within the ±0.5°C specified for the water bath (26), the much better performance of the PFC is obvious. Furthermore, the bottom-of-specimen temperature in the SRU averages slightly below +4°C because of temperature gradients through

Figure 7. Penetration of zero isotherm.

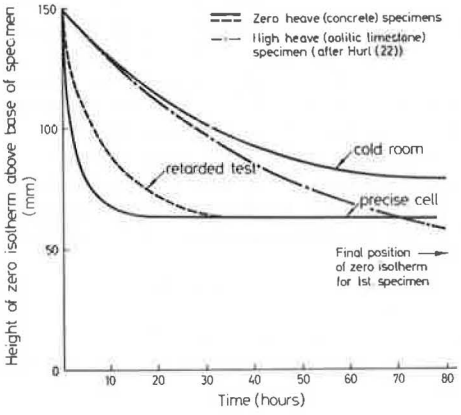

Figure 8. Grading curves.

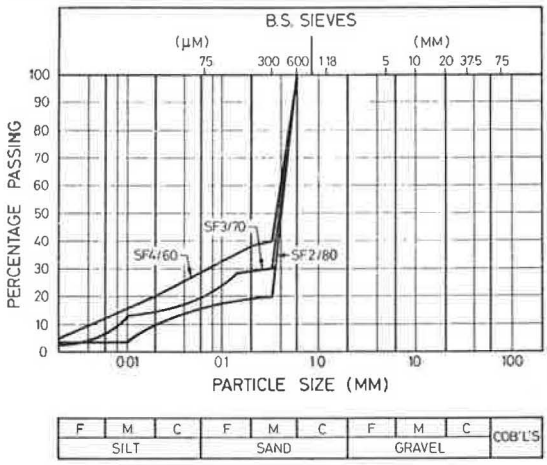

Table 2. Heave of sand and limestone filler mixtures.

		Cold Room and SRU Tests			PFC Tests				
Material	Facility	No. of Tests	Mean Heave, H_T (mm)	SD (mm)	Rate of Penetration	No. of Tests	Mean Heave, H_p (mm)	SD (mm)	H_p/H_T (x100%)
SF 2/80	Both	39	20.1	2.4	S	10	6.7	1.1	33.3
					R	7	9.3	0.8	
SF 3/70	CR	3	44.2	6.4	S	8	13.9	1.0	31.4
SF 3/60	CR	9	76.7	6.7					(24.5)
SF 4/60					S	8	18.8	2.4	

Note: SF is sand and limestone filler mixture; S is standard; R is retarded rate of penetration. SF 3/60 and SF 4/60 have the same proportions and nominal grading but are derived from different batches of filler. Their frost susceptibilities may be slightly different.

Figure 9. Curves for heave versus time.

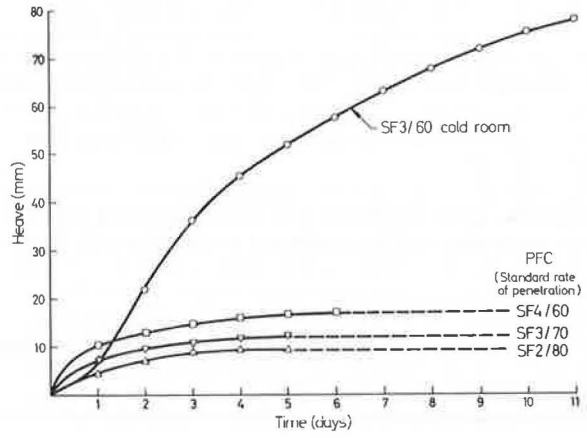

the porous disk. The PFC system is adjusted to give +4°C at the base of the specimen. Figure 7 shows that rate of penetration of the zero isotherm even in the retarded test is much faster in the PFC than in the cold-room test. The implications of this will be discussed in the next section.

Heave Tests

A series of tests was performed on sand-limestone filler mixtures. Standard Leighton Buzzard sand in the size range of 600-300 μm was mixed with limestone filler in various proportions to give the gradings shown in Figure 8. Specimens of the sand and limestone filler mixtures (SF) were compacted to the maximum dry density at the optimum moisture content (38) are given below.

Material	Optimum Moisture Content (%)	Maximum Dry Density (Mg/m^3)
SF 2/80	9.0	2.00
SF 3/70	9.5	2.01
SF 4/60	9.9	2.03

As previous investigators have found (28, 30), the heaves obtained in the cold room and SRU were not significantly different (39); either can be used as a reference against which the PFC results can be judged. The results obtained are summarized in the table below. Details of individual PFC results are given in Table 2, and typical curves for heave versus time are shown in Figure 9.

Heave (mm)			
SF 2/80		SF 3/70	SF 4/60
Standard	Retarded	Standard	Standard
8.0	9.5	14.5	16.5
8.0	9.1	14.8	16.9
6.7	10.7	14.1	18.3
4.8	9.0	11.8	21.9
7.0	9.7	13.9	17.0
5.0	8.7	14.4	17.1
6.5	8.0	14.2	20.8
7.2		13.7	22.3
6.8			
7.1			

The striking feature of these results is the much lower heaves obtained in the PFC than in the other units. Furthermore, the ratio of PFC heave to CR-

Figure 10. Boundary conditions in tests.

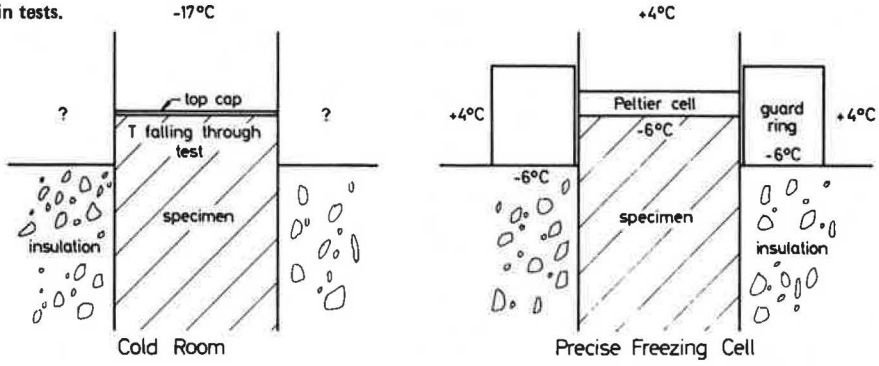

SRU heave decreases with increasing heave. Since the sidewall conditions are similar, friction and adfreezing can be discounted as possible explanations. The surcharge from the pressure of the Peltier unit (1 kPa) is also much too small to account for the effect.

More probable explanations are to be found in differences in (a) the rate of penetration of the zero isotherm and (b) the application of the boundary conditions. It was postulated earlier that ice segregation occurs when the suction is too low and the temperature is correspondingly too high to permit ice penetration. Thus, during the penetration isotherm (PI) stage, a slow rate of heat extraction favors the growth of intermediate ice lenses. A fast penetration of the zero isotherm, on the other hand, yields high heaving rates (40) associated with maximum suction (22). The high rates, however, occur for a limited time, so that the total heave observed is less than with a lower heaving rate extending over a longer period.

Intermediate ice lenses (rhythmic ice banding) are associated with the PI stage. As equilibrium approaches, the isotherms cease to penetrate and may even recede slightly. In this nonpenetrating isotherm (NPI) stage, the terminal lens will continue to grow until the heat input and output are balanced. In general, a terminal lens will commence under PI conditions and end with NPI conditions. With rapid heat extraction, the PI stage will be short, which will lead to low overall heave. The greater heave experienced in the retarded penetration test (Table 2) affirms this explanation.

Closer examination of the temperature boundary conditions applied in the PFC compared with those in the cold room (Figure 10) indicates a significant difference. Essentially, in the PFC the constant temperature is applied to a moving boundary, while in the cold room the constant temperature is specified and maintained at the level of the top of the trolleys. Immediately above the specimens, the temperature tends to be raised somewhat higher by heat conducted from below.

The temperatures in the SRU are intended to be similar to those in the cold room. Thus, in both units a high-heaving specimen experiences considerable additional cooling from its sides as it protrudes above the sand insulation. Consequently, the final position of the zero isotherm becomes lower as the heave (after 250 h) increases (Figure 7). In practice, the TRRL test condition appears to approximate a constant boundary temperature at the level of the original top surface of the specimens. It is arguable that the PFC more nearly reflects field conditions.

While the very wide range of heave values experienced in CR and SRU tests should make for easier classification, this advantage is offset by the greater scatter obtained with high-heave specimens. The above interpretation suggests that particular attention should be given to obtaining uniform air temperatures in the CR and SRU within the zone into which specimens heave.

Further Work

The comparison between the performance of the PFC and those of the other facilities needs to be extended to other materials, including subbase aggregates. Also, we intend to test specimens of rock cores that have been split horizontally. The feedback thermistor will be placed in the split so that an ice lens can be formed at that level. The results will be compared with those from compacted aggregate specimens on identical rock. Thus we hope to gain further insight into the relative contributions that within-particle and between-particle pore systems (13) make to frost heaving of aggregates. Pilot studies in the cold room have indicated that this technique is feasible.

The PFC, with its close control of temperature and water level, offers considerable benefit in the study of many variables such as suction, suction gradient, heat, and water flow required in the development of mathematical models. The apparatus can be adapted to measure thermal conductivity in the vertical direction; this is an alternative to the radial measurement obtained in the line source method (41). However, its major value is likely to be in verifying the predictions made with mathematical models. We hope that the cycling facility, yet to be evaluated, will enable the effects of diurnal temperature variations to be modeled.

For most of these applications, which are essentially of a research nature, the temperature stability of the present cold room and SRU are inadequate. We anticipate, however, that the continued development of techniques will enable routine testing in the foreseeable future to be undertaken in the SRU.

CONCLUSIONS

1. A precise freezing cell (PFC) has been constructed in which freezing is achieved in an open system by the application of constant boundary temperatures controlled to ±0.1°C. The temperature stability of the PFC is much better than that of the cold rooms and self-refrigerated units currently being used for routine testing in the U.K.
2. The radial heat flow in the frozen zone (3 percent of the vertical flow) is small, so a close approximation of unidirectional flow is achieved. Conditions are less satisfactory in the unfrozen zone, and modifications to improve this situation are proposed.
3. In two years' operation, the PFCs have proved quite reliable and less prone to minor faults than the other facilities.
4. For identical specimens, the heave achieved in

the PFC is much less than that in a cold room or SRU. The ratio of PFC to SRU heave decreases as heave increases.

5. The reduction in heave is due partly to the greater heat extraction rate and partly to constant boundary temperatures being applied to a moving level rather than to a fixed level.

6. For the present, routine testing in Great Britain is likely to continue in cold rooms and SRUs because the capital cost per specimen is only about a third of that for the PFC. Nevertheless, the PFC has a useful role in highlighting areas where modifications might be made to the standard test to give improved reproducibility.

7. Some form of precise cell is considered essential for research purposes, particularly for the development and verification of mathematical models. The apparatus described appears well suited for this purpose.

ACKNOWLEDGMENT

We wish to thank the Science Research Council for providing a research studentship for S. Dudek, the British Quarrying and Slag Federation for financial support in the development and evaluation of the SRU, the staff of the TRRL research team for their continuing cooperation, R.C. Coates of the Department of Civil Engineering, University of Nottingham, for his constant encouragement and support, A. Onalp of the University of Trabzon, Turkey, for his efforts during a sabbatical year at Nottingham, J.T. Holden of the Department of Theoretical Mechanics, past and present members of the research team, and David Snow of P.S. Snow and Company for their many helpful contributions.

REFERENCES

1. E. Penner. Frost Heaving in Soils. Proc., 1st International Conference on Permafrost. Purdue Univ., West Lafayette, IN, 1963, pp. 197-202.
2. D.H. Everett and J.M. Haynes. Capillary Properties of Some Model Pore Systems with Special Reference to Frost Damage. International Union of Testing and Research Laboratories Materials and Structures, Paris, Bull. New Series 27, 1965, pp. 31-38.
3. P.J. Williams. Properties and Behaviour of Freezing Soils. Norwegian Geotechnical Institute, Oslo, Publication 72, 1967.
4. H.B. Sutherland and P.N. Gaskin. Pore Pressure and Heaving Pressures Developed in Partially Frozen Soils. Proc., 2nd International Conference on Permafrost, Yakutsk, Yakutsk Autonomous Soviet Socialist Republic, National Academy of Sciences, Washington, DC, 1973, pp. 409-419.
5. S. Taber. Freezing and Thawing of Soils as Factors in the Destruction of Road Pavements. Public Roads, Vol. 11, No. 6, 1930, pp. 113-132.
6. J.F. Haley and C.W. Kaplar. Cold Room Studies of Frost Action in Soils. HRB, Special Rept. 2, 1952, pp. 246-247.
7. K.A. Linell and C.W. Kaplar. The Factor of Soil and Material Type in Frost Action. HRB, Bull. 225, 1959, pp. 81-126.
8. C.W. Kaplar. A Laboratory Freezing Test to Determine the Relative Frost Susceptibility of Soils. Cold Regions Research and Engineering Laboratory, Hanover, NH, CRREL Technical Note, 1965.
9. D. Croney and J.C. Jacobs. The Frost Susceptibility of Soils and Road Materials. British Road Research Laboratory, Crowthorne, England, LR Rept. 90, 1967.
10. H.B. Sutherland and P.N. Gaskin. A Comparison of the TRRL and CRREL Tests for Frost Susceptibility of Soils. Canadian Geotechnical Journal, Vol. 10, No. 3, 1973, pp. 553-555.
11. S.F. Obermeier. Frost Heave Susceptibility Research. Proc., Symposium on Frost Action in Roads, Organization for Economic Cooperation and Development, Paris, 1973, Vol. 1, pp. 251-266.
12. D.L. Townsend and T.I. Csathy. A Complication of Frost Susceptibility Criteria Up to 1961. Queens Univ., Kingston, Ontario, Rept. 14, 1961.
13. R.H. Jones and K.G. Hurt. An Osmotic Method for Determining Rock and Aggregate Suction Characteristics with Applications to Frost Heave Studies. Quarterly Journal of Engineering Geology, Vol. 11, No. 3, 1978, pp. 245-252.
14. R.H. Jones. Frost Damage and Its Prevention. In Developments in Highway Pavement Engineering (P.S. Pell, ed.), Applied Science Publishers, Barking Essex, 1978.
15. K.A. Linell, F.B. Hennion, and E.F. Lobacz. Corps of Engineers' Pavement Design in Areas of Seasonal Frost. HRB, Highway Research Record 33, 1963, pp. 76-128.
16. R.L. Harlan. Analysis of Coupled Heat-Fluid Transport in Partially Frozen Soils. Water Resources Research, Vol. 9, No. 5, 1973, pp. 1314-1323.
17. S. Outcalt. A Numerical Model of Ice Lensing in Freezing Soils. Proc., 2nd Conference on Soil-Water Problems in Cold Regions, Edmonton, Alberta, 1976, pp. 63-74.
18. G.S. Taylor and J.N. Luthin. Numerical Results of Coupled Heat-Mass Flow During Freezing and Thawing. Proc., 2nd Conference on Soil-Water Problems in Cold Regions, Edmonton, Alberta, 1976, pp. 155-172.
19. J. Aguirre-Puente, M. Fremond, and J.M. Menot. Gel dans les Milieux Poreux Permeabilite Variable et Mouvements d'Eau dans la Partie a Temperature Negative. Proc., International Symposium on Frost Action in Soils, Lulea, Sweden, 1977, Vol. 1, pp. 5-28.
20. R.L. Berg, K.E. Gartner, and G.L. Guymon. A Mathematical Model to Predict Frost Heave. Proc., International Symposium on Frost Action in Soils, Lulea, Sweden, 1977, Vol. 2, pp. 92-109.
21. E. Penner. Discussion. Proc., International Symposium on Frost Action in Soils. Lulea, Sweden, 1977, Vol. 2, p. 46.
22. K.G. Hurt. The Prediction of the Frost Susceptibility of Limestone Aggregates with Reference to Road Construction. Univ. of Nottingham, Ph.D. thesis, 1976.
23. A. Onalp. Calculation of Water Transport in the LR 90 Test. Proc., Colloquium on Frost Heave Testing and Research (R.H. Jones, ed.), Univ. of Nottingham, 1977, pp. 115-126.
24. Annual Report. U.K. Transport and Road Research Laboratory, Crowthorne, England, 1971, p. 83.
25. R.H. Jones and K.G. Hurt. Improving the Repeatability of Frost Heave Tests. Highways and Road Construction, Vol. 43, No. 1787-8, 1975, pp. 8-13.
26. The LR 90 Frost Heave Test—Interim Specification for Use with Granular Materials. U.K. Transport and Road Research Laboratory, Crowthorne, England, Supplementary Rept. 318, 1977.
27. Research on the Frost Susceptibility of Road Making Materials. U.K. Transport and Road Research

Laboratory, Crowthorne, England, Leaflet 611, April 1976.
28. G.R. Nellist. An Apparatus for Testing the Resistance of Road Making Materials to Frost Damage. Journal of Scientific Instruments, Vol. 44, 1967, pp. 553-555.
29. A. Onalp. The Mechanisms of Frost Heave in Soils with Particular Reference to Chemical Stabilization. Univ. of Newcastle upon Tyne, Ph.D. thesis, 1970.
30. R.J. Kettle and R.I.T. Williams. The Development of Frost Testing Equipment. International Union of Testing and Research Laboratories Materials and Structures, Paris, Vol. 6, No. 34, 1973, pp. 299-305.
31. Frost and Susceptibility of Materials. Highway and Traffic Engineering, June 1971, pp. 23-24.
32. J. Hill. Self Refrigerating Units: Frost Cabinet Temperature Distribution. Proc., Colloquium on Frost Heave Testing and Research (R.H. Jones, ed.), Univ. of Nottingham, 1977, pp. 23-27.
33. W. Lechner. Peltier Cooling. Philips Technical Review, Vol. 27, No. 5, 1966, pp. 113-130.
34. P. Hoekstra, E. Chamberlain, and T. Frate. Frost Heaving Pressures. HRB, Highway Research Record 101, 1965, pp. 28-38.
35. P.J. Williams. Thermoelectric Cooling for Precise Temperature Control of Frozen and Unfrozen Soils. Canadian Geotechnical Journal, Vol. 5, No. 4, 1968, pp. 265-267.
36. R.J. Kettle and R.I.T. Williams. Frost Heave and Heaving Pressure Measurements in Colliery Shales. Canadian Geotechnical Journal, Vol. 13, No. 2, 1976, pp. 128-138.
37. C.W. Kaplar. New Experiments to Simplify Frost Susceptibility Testing of Soils. HRB, Highway Research Record 215, 1968, pp. 48-58.
38. Methods of Tests for Soils for Civil Engineering Purposes. British Standards Institution, London, BS:1377, 1975.
39. S.J-M. Dudek. A Preliminary Assessment of the Design and Performance of Frost Susceptibility Testing Facilities. Proc., Colloquium on Frost Heave Testing and Research (R.H. Jones, ed.), Univ. of Nottingham, 1977, pp. 13-21.
40. C.W. Kaplar. Phenomenon and Mechanism of Frost Heaving. HRB, Highway Research Record 304, 1970, pp. 1-13.
41. R. McGaw. Thermal Conductivity of Compacted Sand/Ice Mixtures. HRB, Highway Research Record 215, 1968, pp. 35-47.

Publication of this paper sponsored by Committee on Frost Action.

Subdrainage with a Sand Backfill as a Positive Influence on Pavement Performance

Malcolm L. Steinberg, Texas State Department of Highways and Public Transportation, San Antonio

Expansive soils are an estimated $4 billion-a-year problem in the United States. They cause severe distortion in many human works, including highways. Subdrainage has been used extensively in attempts to intercept or remove excess moisture from expansive clays. Minimizing moisture change is seen as a way of reducing surface distortion and improving pavement performance. Underdrains have been used on many highways to remove excess subsurface water, and one Texas study revealed that their use in expansive soils results in a mixed pattern. The effectiveness of deep underdrains with sand backfill is now being examined. The sand is used to provide a moisture reservoir and stabilizer for the expansive clay and the underdrain will remove the moisture the sand cannot hold. A field test of an Israeli experiment is being conducted on a roadway section, which has resisted considerable previous attention, on US-90 west of D'Hanis and Hondo, Texas. This section cuts through a limestone crust into a clay and has had repeated level-up courses of asphalt. Lime had been placed in holes 45 cm (18 in) in diameter, 1.5 m (5 ft) deep, and on centers. In this test 381 m (1250 ft) of 15.24-cm (6-in) slotted underdrain pipe was placed 2.4 m (8 ft) deep; the sand backfill was placed along the south roadway crown line. Observations indicate that maximum movements are taking place on the nonunderdrained side in 9 of the 12 sections and are averaging three times the movement on the underdrained side. Expansive soil movement under existing pavements probably can be reduced by sand-backfilled underdrains.

Swelling soils cause an estimated $4 billion a year in damages in the United States. More than half of this occurs in our transportation facilities: highways, railroads, airport runways, sidewalks, bikeways, and canals. Even this estimate is probably conservative.

The original $2 billion a year (1) estimated in 1973 reflected the lower side of industry estimates. Pavements damaged by these soils are usually repaired with asphalt products or other equally energy-intensive materials. As long as the price of a barrel of oil rises and other energy sources rise sympathetically, even extending cost increases makes the latest estimate lower than it actually should be.

What can be done about damaged transportation facilities? The roadways that represent half of the damages offer several possibilities. First, we can build them differently in the future and avoid expansive clay areas or remove a significant amount of it, treat it deeply with lime, pond it, or seal off the zones of activity with asphalt, lime, or fabric. All are worthy suggestions. However, some of these concepts do not adapt well to the existing roadway, runway, sidewalk, bikeway, or canal. Their remedy is the asphalt patch, asphalt level-ups, or total replacement.

Figure 1. The US-90 site and test holes.

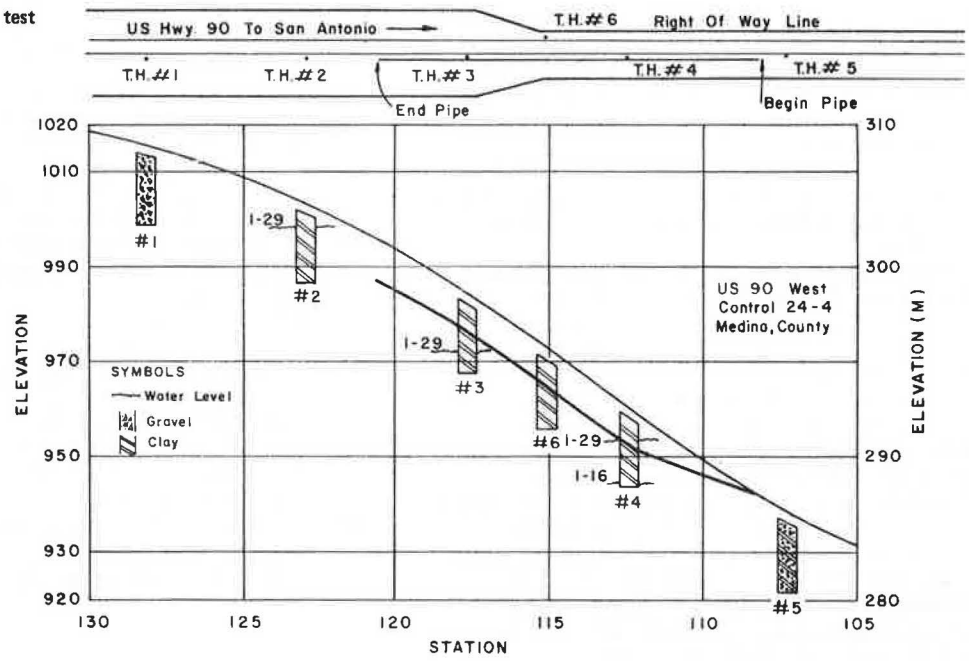

Figure 2. Typical section showing underdrain and backfill.

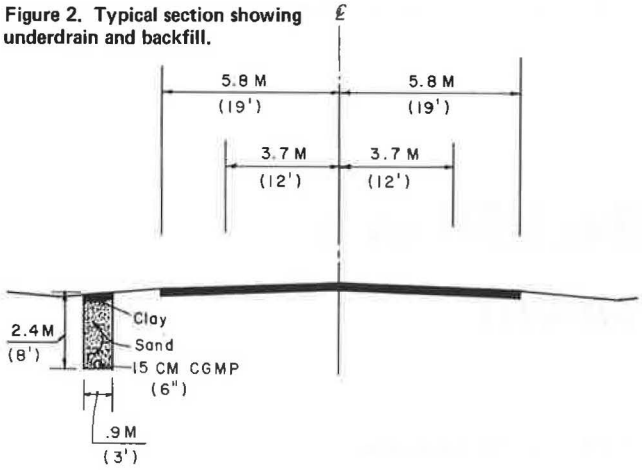

Figure 3. Sand-backfill gradation curve.

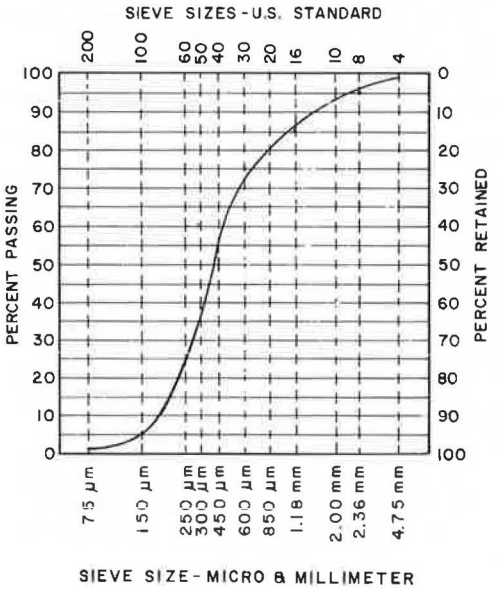

Engineers around the world have made studies of the swelling-soils and expansive-clay problem; a small sampling offers a broad bibliography (2, 3, 4, 5). The Texas State Department of Highways and Public Transportation is among this group that has been involved in searching for solutions to the swelling-soils problems for decades. The need to stabilize moisture variations has been a key element of this search for a solution to swelling-soils movements.

Underdrains have played a significant role in this effort to reduce the wide variations in moisture content. Their depth of placement and backfill material have also received international attention (6, 7, 8, 9, 10, 11, 12). This began with Terzaghi's analysis in the 1920s. Underdrains have been used extensively in many Texas projects. In the San Antonio area, an earlier study revealed an inconsistent record of results of varying success (13).

A previous project emphasized the importance of placing the underdrains at a maximum feasible depth. The ponding study on US-90 West in San Antonio noted the importance of a zone of activity (14). From the finished surface to a depth of 3 m (10 ft) moisture contents ranged from 5-35 percent. Below 3 m the changes were generally from 25 to 30 percent moisture, a fifth or sixth of those occurring in the zone of activity. Elevation rods founded in the zone of activity did the most moving too. This confirmed other studies' conclusions that underdrains must be placed close to the zone's lower level.

Israeli engineers have offered a possible solution for minimizing pavement movements over expansive clays. They examined an airfield runway where one pavement edge moved four times as much as the other, which was relatively stable. The earlier builders of the runway installed a sand-backfilled underdrain along the side that remained stable but not along the other. Expansive clays were moving the pavement, but the underdrained side was substantially stable.

Their laboratory tests suggested that the reservoir created in the sand backfill could stabilize the clay's moisture content. It would allow moisture to move from the sand in time of need and return to it in surplus situations. The underdrain removes the excess moisture the sand cannot handle.

The plan for this study was developed to duplicate in Texas the success of the Israelis' observations. Seco Hill is in Medina County, west of D'Hanis, Hondo, and San Antonio. San Antonio, in the south central part of the state is 80 km (50 miles) east of the site. As US-90 climbs Seco Hill, its gradient breaks through a strata of limestone and enters a clay formation. The clay is very expansive, as evidenced by the waves in the road surface. Over the years this section has claimed many tons of asphalt concrete level-up. It was so troublesome that, after many years of level-ups, holes were drilled 1.5 m (5 ft) deep, 45 cm (18 in) in diameter and on 1.5-m (5-ft) centers, each filled with a sack of lime, water, and backfill base. This did not stop the movement.

Table 1. Crown point movements.

Station	Movement (cm)				
	At 5.8 m	At 3.7 m	At Centerline	At 3.7 m	At 5.8 m
108+40 (end drain)	+3.0	+2.7	+2.1	-0.3	+0.3
109+00	+0.6	+0.9	+2.1	+1.8	+2.7
110+00	+3.9	+4.6	+7.0	+7.6	+6.7
111+00	+1.5	+1.5	+1.8	+1.8	+2.1
112+00	0	+0.3	+0.6	0	-0.3
113+00	-0.6	-0.9	0	+0.9	+0.6
114+00	+0.6	+0.9	+3.6	+3.3	+2.7
115+00	+1.5	-0.6	-0.3	-0.3	-0.3
116+00	+1.2	+0.6	-2.2	+0.9	+0.9
117+00	-0.3	0	-0.6	+1.8	+1.8
118+00	-1.5	-0.9	+2.4	+4.3	+0.6
119+00	-0.9	-0.3	+0.3	+1.2	+2.1
120+00	-0.6	-0.6	0	+0.3	+0.9
121+00 (end drain)	-0.3	0	+0.3	+0.6	+0.9
122+00	-3.4	-3.4	-3.4	-1.5	-3.0
123+00	-2.7	-3.4	-3.0	-3.4	-3.0
124+00	-2.1	+2.4	-0.3	-2.7	-2.4
125+00	-2.7	-2.7	-2.7	-3.0	-3.0
Average movement 108+40 121+00	+0.57	+0.58	+1.22	+1.71	+1.55

Note: 1 cm = 0.39 in; 1 m = 3.3 ft.

The surrounding land has flat valleys and gently rolling hills. Medina County's major enterprises are farming and ranching. Vegetation is varied; crops are usually feedgrains. Much land is in pasture and the livestock industry is important, but there is much brush land with mesquite, huisache, oak, pecan, and some cottonwood. The climate is subtropical. Temperature averages for 30 years indicate a daily mean in the 30-35°C range (90°s F) between June and September. Wintertime averages are in the 15-20°C range (60°s F). The average annual rainfall is 71.2 cm (28.5 in). Usually heavier rainfalls occur between April and June, and during September and October. Summers tend to be hot and dry.

Soil types in the Seco Hill area are generally clays in valleys and gravelly to rocky mixtures on the hills. The Knippa Mercedes and Monteola clay series have light to very high shrink-swell potentials. The Monteola has CH and A 7-6 unified and AASHTO classifications, respectively, with plasticity indices in the 35-45 range. The Olmos Yologo series are generally gravelly loams with moderate to low activity (15). Beneath these surface soils are cretaceous formations generally in the Gulf series.

PROCEDURE

It was decided to evaluate the effectiveness of the sand-backfilled deep underdrain in minimizing pavement movement over a swelling clay. The underdrain would be placed along the south edge of the pavement edge in the clay subgrade area. No underdrain would be placed along the north edge.

A portable rig drilled six test holes on the east slope of Seco Hill on January 16, 1974. Five were in the highway's south ditch line, one in the north line. The holes were 20 cm (8 in) in diameter and 6 m (20 ft) deep. Test hole 1 near the crest of the hill (station 128) showed only gravel. Test holes 2, 3, and 4 in the south ditch line indicated only clay, as did hole 6 in the north ditch line. The hole near the bottom of the hill, hole 5, had a clayey gravel. All but test hole 4, which showed a trace of water, were dry when drilled. By January

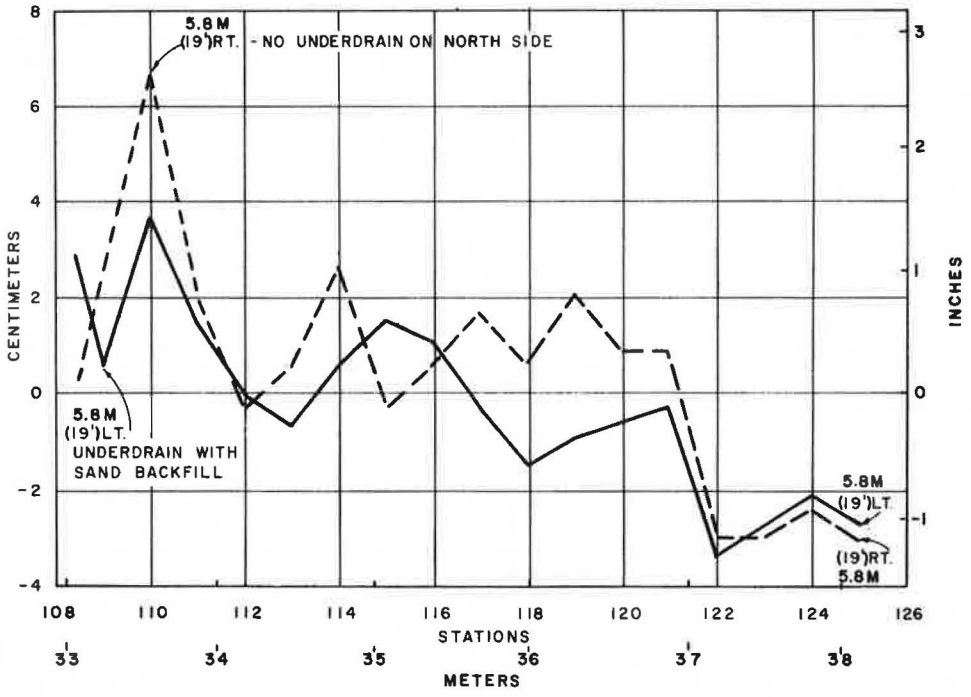

Figure 4. Crown movements at site.

Figure 5. Typical cross-sectional movements.

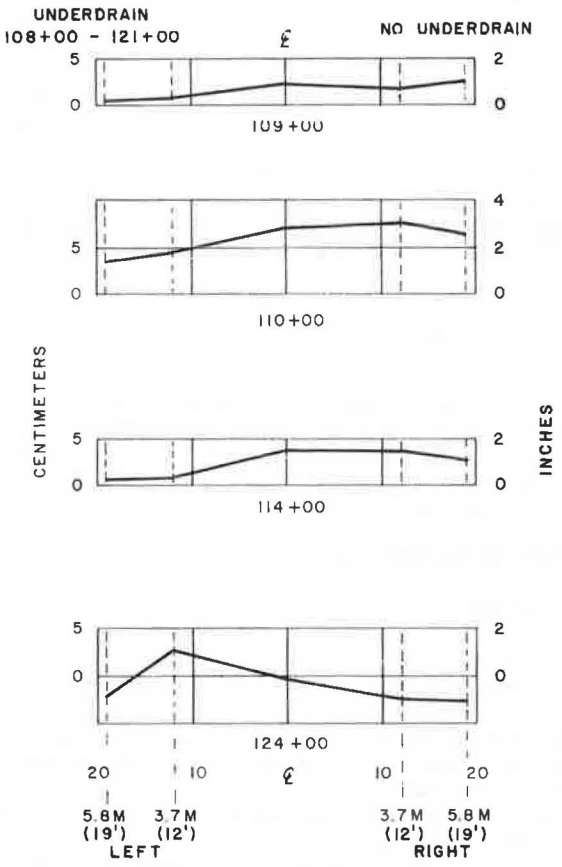

24, 1974, three holes in the south ditch line showed significant amounts of water. Two were filled almost to the top of the hole, while the third was half full (Figure 1).

Atterburg limit tests at two sample sites showed the liquid limits to be from 65 to 67 and plasticity indices from 40 to 42. This would confirm these clays as potentially high-swelling soils according to the Waterways Experiment Station's studies (16, p. 38).

A trench about 2.4 m (8 ft) deep, 0.9 m (3 ft) wide, and 381 m (1250 ft) long was excavated by state maintenance forces along the south ditch line. The water-bearing stratum was uncovered. The 15-cm (6-in) corrugated metal pipe underdrain was placed in the trench (Figure 2). It was backfilled with a fine sand (Figure 3).

Elevations were taken with a level and rod at the centerline and on either side at 3.7 m (12 ft) and 5.8 m (19 ft), the crown points of the roadway. These elevations were taken on the pavement opposite the pipe outfall at station 108+42, and at the pavement stations from 109+00 to 125+00. Readings were taken on September 26, 1975, October 14, 1976, and July 20, 1977.

OBSERVATIONS

The changes in elevation between 1975 and 1977, three years of measurement, indicate least movement closest to the sand-backfilled underdrain. Movements at the stations have been generally uniform. The average changes, calculated between the readings in 1975 and 1977, are shown in Table 1. These average movements were three times greater on the non-underdrained side than on the underdrained side. Average movement at the centerline was twice that of the underdrained side. Changes between stations have been less regular. Larger upward movement generally took place farther away from the underdrain (Figure 4).

Elevations were taken farther up the hill beyond the underdrain at the same distances from the roadway centerline. There the average changes from left to right were 2.72 cm (1.07 in), 1.77 cm (0.7 in), 2.35 cm (0.93 in), 1.90 cm (0.75 in), and 2.85 cm (1.2 in), respectively. They ranged from three to five times greater than those on the underdrained crown. All were downward movements as compared to the upward clay section changes. Possibly the water's being removed resulted in this difference. It is also noted that the underdrains may have affected movement all across the road (Figure 5). Its crown movements were usually less than those beyond the drains.

CONCLUSION

Of the $4 billion dollars' damage a year that expansive clays have caused and continue to cause, more than half was to transportation facilities. This has been the subject of a considerable number of studies over the years.

The result of this study indicates that movements caused by expansive clays can be substantially reduced after structure placement. The sand-backfilled underdrain placed deeply in the zone of activity has resulted in pavement movements that are only a third of those along the unprotected pavement edge. Even the unprotected edge had less than half the movement of the adjacent pavement section without the underdrain.

These results confirm prior Israeli investigations, where a deep sand-backfilled underdrain along one runway crown resulted in one-quarter of the movement that the unprotected crown experienced. Subsequent laboratory tests indicated that the sand acted as a moisture reservoir for the clay. Excess moisture passed from the clay to the sand, and, when the clay needed the moisture, it was drawn from the sand. The change in the clay's moisture content was thus minimized, which significantly reduced movement of the clays.

These field tests substantiate the earlier studies. They put together vital data from previous observations. Expansive clays can be partially controlled by an underdrain set deeply in the zone of activity with a sand backfill that can significantly reduce the expansive clay's movements.

The zone of activity should be carefully considered in locating the underdrain deep enough to help minimize movement. The sand backfill may offer additional assistance in stabilizing moisture variations in the expansive clays.

Although some may feel that swelling clays cannot be controlled, others recognize that identification before construction can minimize destructive results from these soils. Replacement, chemical admixtures (most frequently with lime), horizontal and vertical moisture barriers, and ponding all afford opportunities to reduce the movement before construction. This study provides additional indications that these movements can also be minimized after the structure has been placed.

Reducing movements of expansive soils, which frequently requires energy-intensive remedies that use deep underdrains with sand backfill, may significantly help conserve energy.

ACKNOWLEDGMENT

I express my thanks to the State Department of Highways and Public Transportation, R.E. Stotzer, W.B.

Collier, C.E. Hackebeil, Herman Brucks, Rick Norwood, and Fred White, for their assistance, and to Blyth Lowery and Ruth Thompson for the editing and typing.

REFERENCES

1. D.E. Jones and W.G. Holtz. Expansive Soils—The Hidden Disaster. Journal of Civil Engineering Division, Proc., ASCE, Vol. 43, No. CE 8, Aug. 1973, pp. 49-51.
2. F.H. Chen. Foundations on Expansive Soils. Elsevier, Amsterdam, 1975.
3. G. Kassiff, M. Livneh, and G. Wiseman. Pavements on Expansive Clays. Jerusalem Academic Press, 1969.
4. R. Lytton and others. Study of Expansive Clays in Roadway Structural Systems. Center for Highway Research, Univ. of Texas, Austin, Repts. 118-1-8, 1969-1976.
5. D.R. Snethen and others; U.S. Army Engineer Waterways Experiment Station. A Review of Engineering Experiences with Expansive Soils in Highway Subgrades. Federal Highway Administration, Rept. FHWA-RD-75-48, 1978.
6. Investigation of Filter Requirements for Underdrains. U.S. Waterways Experiment Station, Vicksburg, MS, Technical Memorandum 183-1, Nov. 1941.
7. E.S. Barker and C.L. Sawyer. Highway Subdrainage. Public Roads, Vol. 26, No. 12, Feb. 1952, p. 266.
8. H. Cedergren, J. Arman, and K.H. O'Brien. Development of Guidelines for the Design of Subsurface Drainage Systems for Highway Pavement Structural System. Federal Highway Administration, Rept. FHWA-RD-73-14, Feb. 1973.
9. Slotted Underdrain Systems. Federal Highway Administration, Implementation Package 76-9, June 1976.
10. G.M. Slaughter. Evaluation of Design Methods of Subsurface Drainage Facilities for Highways. Georgia Department of Transportation, Feb. 1973.
11. R. Spaulding. Selection of Materials for Subsurface Drains. U.K. Transport and Road Research Laboratory, Crowthorne, England, TRRL Rept. LR 346, 1970, pp. 2-10.
12. Subsurface Drainage. HRB, Bull. 45, Dec. 1951.
13. M.L. Steinberg. Interceptor Drains in Heavy Clay Soils. Journal of Transportation Engineering Division, Proc., ASCE, Vol. 96, No. TE1, Feb. 1970, pp. 1-10.
14. M.L. Steinberg. Ponding an Expansive Clay Cut: Evaluations and Zones of Activity. TRB, Transportation Research Record 641, 1978, pp. 61-66.
15. G. Dittmar, M.L. Deike, and D.L. Richmond. Soil Survey of Medina County, Texas. Soil Conservation Service, U.S. Department of Agriculture, Aug. 1977.
16. D.R. Snethen, L.D. Johnson, and D.M. Patrick. An Evaluation of Expedient Methodology for Identification of Potentially Expansive Soils. Federal Highway Administration, Rept. FHWA-RD-77-94, June 1977.

Publication of this paper sponsored by Committee on Subsurface Drainage.

Addendum

Richard E. Landau, Malverne, New York

[This is the author's closure to the discussion of the paper Sand Drain Theory and Practice, which was published in Transportation Research Record 678. The reference and equation numbers that follow refer to those in the paper. The paper and discussion can be found on pages 22-36 of Transportation Research Record 678.]

The discussion prepared by R. D. Holtz is appreciated and reflects a degree of effort commensurate with the importance of the subject. It is difficult to justify any controversy relating to the use of the term nondisplacement as a descriptive word for sand drains installed where the cavity is formed by excavation techniques. The nondisplacement characteristic is certainly as approachable as the undisturbed characteristic is approachable in the taking of undisturbed samples, yet I am certain that there is no need to think twice about the practical validity of obtaining undisturbed samples. As a matter of record, Olson has shown that sand drain installations can outperform predictions made from data obtained from the best undisturbed samples (10, p. 101), which suggests that such terms should be considered as adjectives to differentiate between available techniques and not as absolutes.

The omission in the paper of Japanese and European improvements in the type of wick available for use with the Kjellman type of installation does not in any way denigrate the importance of such materials; however, the paper relates to the description of methods of installation. The installations fall into the categories presented: either displacement or nondisplacement techniques.

The paper attempts to broaden the method of sand drain design to the extent that previous publications may not have included all factors involved in the evaluation of installation techniques. To this end, an attempt was made to extend the available theory by providing additional equations that may be useful to the designer, particularly to avoid trial and error procedures, which are normally necessary. Equation 9 is an example, and its derivation is presented:

$$t_p = (T_h D_e^2)/c_h \quad (4)$$

by transposing and substituting $D_e/E_w^{1/2}$ (5, p. 94) for D_e, Equation 4a results, where D_e = the diameter of sand drain influence as constructed:

$$(D_e/E_w^{1/2})^2 T_h = t_p c_h \quad (4a)$$

Substituting from Equation 6 for T_h, and transposing the

term $0.8u_h^{2.5}$, it is found that:

$$(D_o/E_w^{1/2})^2 \log_{10}(n/2) = t_p c_h/0.8u_h^{2.5} \quad (9a)$$

and

$$n = D_c/E_w^{1/2} d_w$$

Equation 9 results from Equation 9a by taking the square root of both sides of the equation, where $M = (t_p c_h/0.8u_h^{2.5})^{1/2}$. Inasmuch as t_p, c_h, and u_h are fixed for any specific design problem, M is a constant that can be used to establish equivalent designs where D_c, E_w, and n can be variables.

I will gladly provide derivations of other equations to those who request the information. Derivations were not provided in the text due to the length of the paper and space limitations imposed.

The vibroflotation Dutch jet-bailer method has been practiced in a manner that is inconsistent with nondisplacement procedures, just as much as the auger method has been similarly misused. There is no tool that can be indiscriminately and uncontrollably raised and lowered, be it a jet or an auger, that will not result in undue subsoil displacement. On the other hand, both tools can be carefully controlled so as to avoid displacement. Holtz suggests that to impose controls on the vibroflotation Dutch jet-bailer method would make its use more costly. I have observed the vibroflotation system in operation on projects where the equipment was used without any plunging of the apparatus allowed. The designer must answer for himself whether or not the risks associated with uncontrolled use of cavity forming apparatus is desirable and consistent with design assumptions, and if it is then perhaps it should be allowed. A number of failures or sharp deviations from design performance have occurred on projects where jetting methods have been used, and this could be related to such lack of controls. Unfortunately, Holtz may not be aware of these since, to the best of my knowledge, they have not as yet been reported in the literature. To avoid the unexpected failure of otherwise sound sand drain designs, close field controls are required for all methods.

We can appreciate the effort presented by Holtz in his discussion. It now remains for the geotechnical practitioner to fully document designs and field performance that, we hope, will provide the profession with the practical results necessary to the making of future judgments as to the performance of various sand drain installation techniques.

16. E.V. Edriss, Jr., and R.L. Lytton. Dynamic Properties of Fine Grained Soils. Proc., 9th International Conference on Soil Mechanics and Foundation Engineering, Tokyo, Vol. 2, 1977, pp. 217-224.
17. D.G. Fredlund, A.T. Bergan, and E.K. Sauer. Deformation Characterization of Subgrade Soils for Highways and Runways in Northern Environments. Canadian Geotechnical Journal, Vol. 12, No. 2, 1975, pp. 213-223.
18. D.G. Fredlund, A.T. Bergan, and P.K. Wong. Relation between Resilient Modulus and Stress Conditions for Cohesive Soils. TRB, Transportation Research Record 642, 1977, pp. 73-81.
19. Soil Manual. Wisconsin Department of Transportation. 1972.
20. S.D. Wilson. Small Soil Compaction Apparatus Duplicates Field Results Closely. Engineering News-Record, May 1950, pp. 34-36.
21. T.W. Lambe. The Structure of Compacted Clay. Journal of Soil Mechanics and Foundations Division, Proc., ASCE, Vol. 84, No. SM2, 1958, pp. 1-34.
22. A.W. Johnson and J.R. Sallberg. Factors That Influence Field Compaction of Soils. HRB, Bull. 272, 1960, pp. 29-48.
23. T.B. Edil and S.E. Motan. Soil-Moisture Equilibria and Behavior of Highway Pavement Systems. National Science Foundation, Grant ENG75-10558, 1978, 68 pp.
24. R.J. Krizek and T.B. Edil. Experimental Study of Clay Deformability in Terms of Initial Fabric and Soil-Water Potential. Rheologica Acta, No. 13, 1974, pp. 803-813.

Publication of this paper sponsored by Committee on Environmental Factors Except Frost.

Comparison of the Precise Freezing Cell with Other Facilities for Frost-Heave Testing

R.H. Jones and S.J-M. Dudek, Department of Civil Engineering, University of Nottingham, England

Identification of frost-susceptible materials on the basis of their physical properties is too imprecise for many practical purposes, and direct freezing tests need to be employed. Heave is measured by two main types of test: the constant rate of penetration test and the constant boundary temperature test. The latter has the advantage of greater simplicity of operation and is easier to model mathematically. Nevertheless, its reproducibility is relatively poor and improvements are being sought. The development of a self-refrigerated unit (SRU) is outlined and likely future revisions to the constant boundary temperature test specification discussed briefly. A precise freezing cell (PFC) that uses the Peltier effect and permits unidirectional freezing with the boundary temperatures controlled to ±0.1° C has been developed. Specimens heave much less in the PFC than in the SRU because the heat extraction is more rapid and a constant temperature is applied to the moving boundary (top of specimen) rather than to the stationary boundary. Thus the penetration of the zero isotherm is accompanied by high suctions that favor ice penetration over segregation. The role of the PFC lies in research, not in routine testing, particularly in connection with the development and evaluation of mathematical models.

The process of frost heaving, which occurs when the zero isotherm penetrates below the bound materials of a typical road structure (Figure 1), can be explained in terms of the capillary theory (1, 2, 3). This postulates that, to pass through the neck of a pore, the radius of curvature of the ice front (r_{iw}) must be reduced to a critical value (r_o) (Figure 2). The curved interface is associated with both a pressure difference and a freezing-point depression according to the equation

$$p_i - p_w = 2\sigma_{iw}/r_{iw} = L\Delta T/V_w T_o \quad (1)$$

where

p_i, p_w = ice and water pressures respectively (Pa),
r_{iw} = radius of ice-water interface at a particular instant (m),
σ_{iw} = interfacial energy (ice-water) (J/m^2),
L = latent heat of fusion (J/kg),
ΔT = freezing point depression (K),
V_w = specific volume of water (m), and
T_o = 273 K.

Because in the absence of restraint p_i will not differ significantly from atmospheric pressure, p_w will be less than atmospheric, which will give rise to a suction that draws water continuously toward the freezing front. In frost-susceptible materials, there is a tendency for the radius of curvature to remain above r_o for long periods, which results in ice segregation and excessive frost heave. For materials with a range of grain (and hence pore) sizes, various suggestions have been made regarding the selection of a characteristic critical pore radius (4).

Identification of frost-susceptible materials continues to be a significant problem for both designers and research workers. Direct tests based on the fundamental work of Taber (5) have been developed by the U.S. Cold Regions Research and Engineering Laboratory (CRREL) (6-8) and by the U.K. Transport and Road Research Laboratory (TRRL) in Great Britain (9). In both, cylindrical specimens from either undisturbed samples or recompacted material are subjected to unidirectional freezing from the top, while their bases are kept in contact with unfrozen water.

In the CRREL procedure, the top temperature is adjusted to give a specified rate of penetration, while in

Figure 1. Typical road structure.

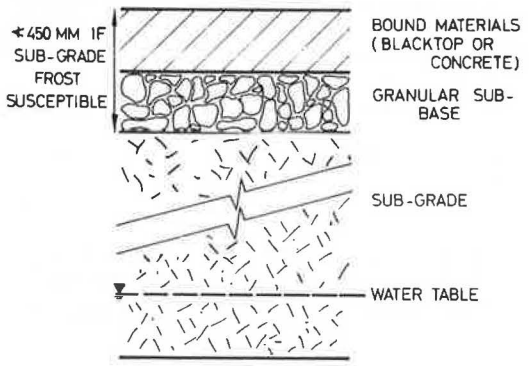

Figure 2. Capillary model of ice penetration.

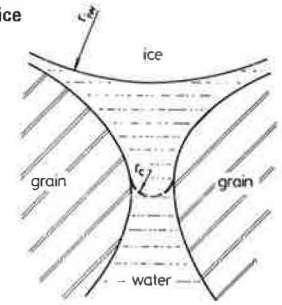

the TRRL test the air temperature above the specimens remains constant. The classification of materials is, however, broadly similar for both tests (10). Several alternative direct tests have been proposed (11), including those in which the development of heaving pressure during restrained heave tests (which mirrors the heave in an unrestrained test) is measured.

In addition, many attempts have been made to assess frost susceptibility indirectly on the basis of material characteristics such as grain- or pore-size distributions (12). For example, an osmotic suction method has shown promise in ranking the frost susceptibility of limestone subbase materials (13). Nevertheless, whatever approach is used, there are considerable reservations about the accuracy of the assessment of frost susceptibility, and investigations, including those described in this paper, are continuing to develop simpler and more reliable methods.

Even so, the assessment of frost susceptibility of the materials subject to ice penetration is only a first step in determining the precautions necessary to prevent frost-heave damage. It is then necessary to assess whether the amount of heave of the road surface will be acceptable. The heave that can be tolerated will depend on the importance of the road, its construction, and economic factors. The actual heave will depend on climatic conditions (which largely control the depth of frost penetration), the depth of the water table, and the capillarity and effective permeability of the materials between the water table and the freezing front.

An additional factor when the freezing front remains in compacted materials (which is typical of British conditions) is that the density or grading of the material as compacted on site may differ from those achieved in the laboratory (14, Chap. 3).

Relationships between the results of laboratory frost-susceptibility tests and the design of actual roads built on or with the materials tested have been developed (9, 15). In Great Britain, where hard winters occur infrequently, the empirical correlation between laboratory and field performance originally made for subgrade soils has also been applied to subbases. The introduction of mathematical models, (16-20) mainly based on the capillary theory heralds a more rigorous approach not only to the interpretation of past and future field observations and pilot scale trials but also to the design process itself.

However, while progress has been made in several aspects of mathematical modeling, current models require further development to deal fully with the central problem of coupling the heat and water flows (21). We are developing an improved model in which we hope to quantify the variations in space and time of suction, suction gradient, and effective permeability in relation to one or more of the physical characteristics of the materials.

For steady-state conditions, the continuity equation requires that the product of suction gradient and effective permeability be constant. However, individually, neither the suction gradient nor the permeability (which is suction dependent) is constant (22, 23). In view of the complexities and uncertainties, any proposed mathematical model of frost heaving requires rigorous experimental verification before it can be adopted with confidence.

Against this background, precisely controlled direct frost-heave tests have a multiple role in providing (a) a measurement of frost susceptibility under standard conditions, (b) an insight into the frost-heaving process, and (c) a means of verifying proposed mathematical models. Although constant boundary temperature tests are simpler to perform than constant rate of penetration tests and have the advantage of subjecting all the specimens to the same conditions, the poor reproducibility of the original TRRL test (24) was of considerable concern.

This paper describes two developments of this type of test. The first deals with routine commercial testing and the move toward recognizing the self-refrigerated unit (SRU) rather than the cold room (CR) as the principal testing facility. The second development is of a precise freezing cell (PFC) incorporating Peltier cooling, in which a single specimen is subjected to closely controlled conditions. Results obtained in the various units are presented and the implications discussed.

DEVELOPMENT OF THE TRRL TEST

In the TRRL test (9), nine cylindrical specimens 102 mm in diameter and 152 mm high are placed in an insulated trolley that is wheeled into a cold room operating at -17°C. The specimens rest on porous ceramic disks inside copper carriers. The disks are in contact with water maintained at +4°C. The sides of the specimens are wrapped with waxed paper and the intervening space filled with loose, dry sand (5-2.36 mm fraction). Push rods bearing on caps placed on top of the specimens enable the heave to be measured.

From the start of the test, heave measurements and topping up of the water level are undertaken every 24 h. Materials are judged frost susceptible if, during 250 h, they heave more than 13 mm (in England and Wales) or 18 mm (in Scotland).

At Nottingham, improved repeatability resulted from modifications introduced to give a closer control of the water-bath temperature (25). More recently, a revised interim specification for the test has been introduced by TRRL in which the cold-room facility and procedure, including specimen preparation, is defined more closely (26). Granular specimens continue to be compacted in two stages (tamping in layers followed by static compac-

Figure 3. Self-refrigerated unit.

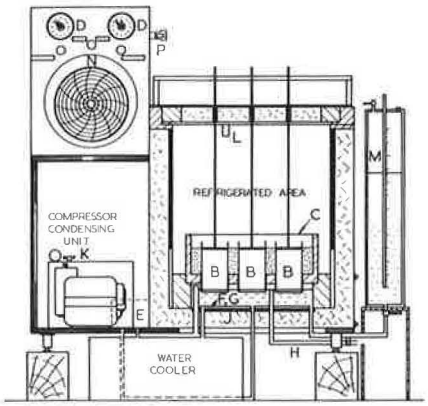

B Specimen
C Removable box
D Temperature indicator/control
E Water pump
F Sparge pipe
G Heater
H Overflow
J Refrigerating coils
K By-pass valves
L Fan
M Mariotte vessel
N Chart recorder
P Lid catch

ting), but there have been significant changes in detail. A further revision is expected in which compaction by vibrating hammer and testing in an SRU will be included (27).

These changes have been anticipated in our laboratory where granular specimens have been prepared by precompaction in layers with a vibrating hammer followed by a final static compaction since 1973 (25). The static loads required are much reduced, less than 100 kN even for subbase aggregates, compared with the maximum of 400 kN needed by the TRRL procedure (26). The specimens are extruded from their molds by a hydraulic jack.

The TRRL interim specification stipulates that the air temperature shall be maintained at -17 ±1°C. However, during defrosting periods, which occur every 8 or 12 h in the cold rooms in current use, it is recognized that greater variations will occur. At Nottingham, evidence that the defrosting periods could significantly affect results was obtained from heaving pressure tests (22), and attention was switched to the development of an SRU in which defrosting during the test was unnecessary.

Development of SRUs in the United Kingdom commenced in the mid-1960s, when the TRRL test was adopted as a compliance test for subbase materials (28). Several workers developed chilled tank units (29,30) or forced-air units (31). The former are similar to domestic deep freezes, but the latter have fan-assisted units that blow cold air over the specimens and are thus in effect miniature cold rooms. Only the forced-air units require defrosting during the test.

For this reason the chilled-tank principle was chosen for further development. A prototype (Figure 3) that incorporated satisfactory features of existing designs was developed in our laboratory in conjunction with P.S. Snow and Company of Leicester. Like most other British units, it was designed to operate under normal laboratory temperatures. The chilled tank is cooled by refrigerant circulating from a 0.4-kW compressor through tubes embedded within the walls. The internal dimensions of the tank and water bath, the configuration of specimens, and the specimen support system match those of the cold-room trolley.

Facilities additional to those then (1976) featured on commercially available units include a chart recorder that gives a continuous trace of air and water temperatures, independent cooling systems for air and water, an air-circulating fan, and a Mariotte tube (29) to maintain a constant water level throughout the 250-h test. In addition, an alternative inner box was made to permit testing of specimens 152 mm in diameter.

Previous SRUs had relied on the low temperature of the tank walls and the enclosed air space to promote sufficient cooling of the water bath. This had not always been successful, particularly in very hot summers (32), and a more positive system was thought necessary. Originally, a heat exchanger consisting of a coil wound around the copper pipe taking the refrigerant from the compresser to the tank cooling coils was fitted. This system gave unacceptable temperature fluctuations and was abandoned.

Two further systems were tried. First, cooling coils beneath the water bath, in series with the tank coils, were brought into use. Second, with these coils bypassed, using valve K (Figure 3), a separate water cooler was connected into the circuit. Although the independent cooler is preferred for research tests, the series coil system has been adopted for the subsequent units that are now available commercially. Fine control of the water temperature is obtained from heaters activated by a mercury contact thermometer. In the prototype unit, the standard deviation of the water temperature beneath the specimens is 0.35°C and that of the top of the specimen is 1°C when all nine specimens are considered.

THE PRECISE FREEZING CELL

Previous Work

Greater control of the temperature at the top of the specimen can be better achieved by direct refrigeration of an individual top cap than by controlling the temperature of the air space above a number of specimens. Direct refrigeration is conveniently provided by a thermoelectric device in which electric current passing through a series of dissimilar semiconductors exhibits the Peltier effect (33). This may be thought of as a reverse thermocouple so that cold and hot faces are produced. The cold plate is in contact with the specimen, and the hot plate is cooled by circulating cooling water. The heat extracted by the cold plate Q_c (watts) is given by

$$Q_c = a_m T_c I - \tfrac{1}{2} I^2 R_M - K_m \Delta T \qquad (2)$$

where

a_m = mean value of the Seebeck coefficient (V/K),
R_M = mean value of the resistance (ohms),
K_m = mean value of the thermal conductance (W/K),
T_c = temperature of the cold plate (K),
I = current (A), and
ΔT = difference between hot- and cold-plate temperatures (K).

Peltier cells of 16- to 88-W capacity have been used by many other investigators, particularly in connection with heaving pressure measurements (11, 34, 35), although proposals for using a Peltier device for heave measurements have been made (36). In the early days, Peltier devices were criticized for being costly and unreliable and for giving nonuniform temperature distributions (37), but their use in conjunction with servocontrols maintained temperatures within close limits (±0.02°C) (35). With improved semiconductor technology and quality control, the Peltier system appeared to be both feasible and economical for the maximum of four units envisaged in this research.

Description of the Cell

A cutaway isometric view of the cell is shown in Figure 4. The principal dimensions are 300 mm outside diameter, 200 mm inside diameter, and 400 mm overall height. The body is formed of thin PVC tubes closed at

Figure 4. Precise freezing cell.

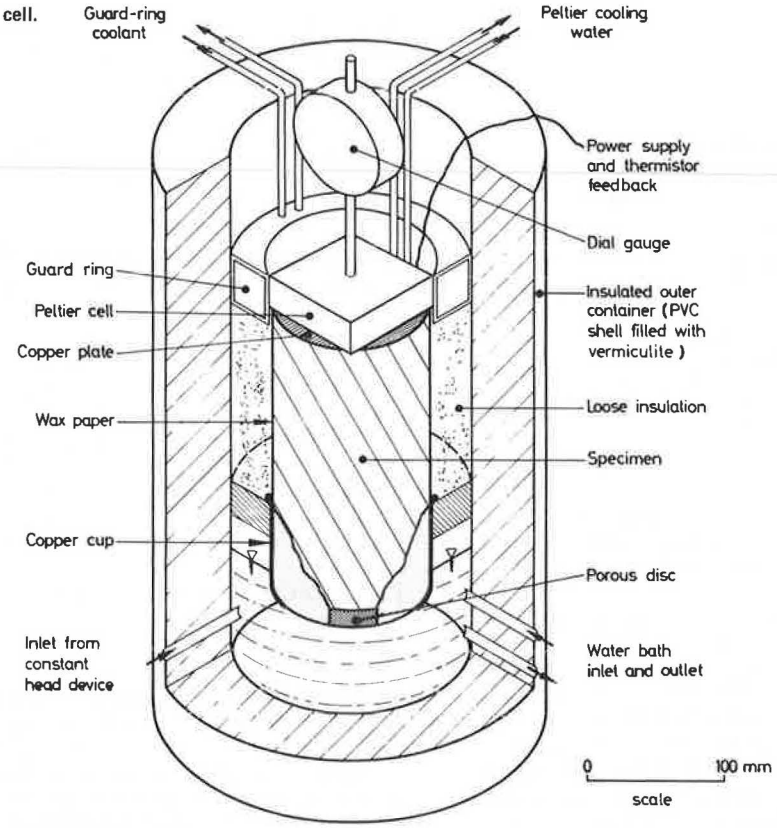

their lower ends and separated by approximately 50 mm of vermiculite insulation. The lower part of the inside of the cell, being watertight, forms a water bath of 2.4-L capacity, which is serviced by three ports that pass through the cell wall. Two of these ports connect to a pumped circulatory system incorporating an external cooler operating at +4 ±0.1°C. The third port connects to a Mariotte vessel that provides a constant head supply similar to that used in the SRU (Figure 3). A scale on this vessel permits measurement of the rate at which water is taken up.

A wooden staging with a central hole enables the specimen to be supported on a porous disk within a copper cup in exactly the same way as in the TRRL test. Likewise, the annular space was filled with loose, dry sand.

The specimen is surmounted by a copper plate of the same diameter on which the Peltier unit (Cambion 806-7242-01, 19-W capacity) rests. A coating of zinc-oxide-loaded silicon grease between the plate and the unit ensured good thermal contact. A thermistor, embedded in the lower face of the copper plate, is coupled to the feedback control capable of maintaining a constant temperature to within ±0.1°C. The Peltier unit was cooled by water that was run to waste. On top of the sand insulation is a guard ring through which methyl alcohol is circulated. The alcohol is cooled by being circulated through a coil in the adjacent cold room and maintains the guard-ring temperature at ±0.5°C. The heave was measured by a dial gauge fixed above the Peltier unit.

The cells are housed in a commercial refrigerator that has two chambers 0.5x0.5x1.2 m giving a +4 ±1°C environment. Cooling is from refrigerated coils and temperature uniformity is improved by using a small supplementary fan. Defrosting during testing is not necessary. With some difficulty, the refrigerator could accommodate four cells and their ancillary equipment, but to date the system has operated with two cells.

The capital cost per specimen of the PFC facility (including controller) is perhaps three times that of an SRU.

Control and Monitoring System

To ensure electronic stability, all the control and monitoring equipment is situated in a constant-temperature (21 ±1°C) enclosure.

Since the coefficients of Equation 2 are temperature dependent, a controller is needed to ensure either a constant rate of heat extraction or, as in this case, maintenance of constant temperature. The system adopted obviates the need for precise control of the cooling-water temperature and protects the Peltier unit from electrical overload.

Three power-pack and control units have been constructed, each of which provides a current of up to 6 A at not more than 5 V. The power supplied to the Peltier battery is regulated by the feedback signal from the thermistor embedded in the top cap. In controller 1 the feedback device operates as an on-off control to the power supply so that the temperature is maintained within the tolerance. The operating voltage can be set manually to give some control of the rate of cooling. A proportional system is used in controllers 2 and 3 so that the rate of cooling slows down as equilibrium is approached. In principle, the second method should give more precise control. However, the damping effect of the thermal mass of the Peltier battery and the top cap masks this effect, and the control achieved by the two types of unit is not significantly different.

Controllers 1 and 3 are fitted with a cycling facility. Essentially, each has two channels that could be set at

Figure 5. Thermocouple positions and vertical temperature gradient.

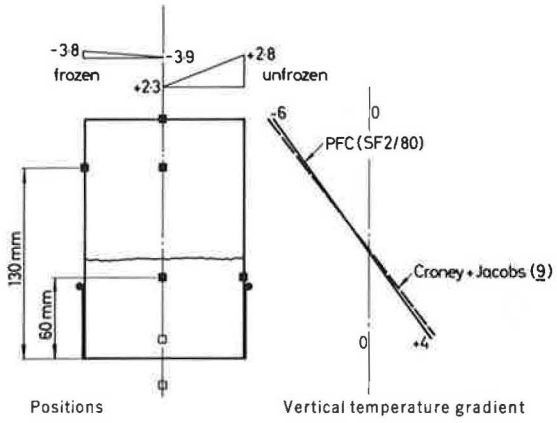

Table 1. Temperature gradients and radial heat flow.

Facility	No. of Tests	Radial Temperature Gradient (°C/m) Frozen Zone	Radial Temperature Gradient (°C/m) Unfrozen Zone	Ratio of Radial Heat Flow to Vertical Heat Flow (x 100%) Frozen Zone	Ratio of Radial Heat Flow to Vertical Heat Flow (x 100%) Unfrozen Zone
CR	3	10	15	15	22
SRU	2	12	16	18	24
PFC	6	2	10	3	15

Note: The vertical temperature gradient is 67°C/m in all units.

Figure 6. Temperature fluctuations.

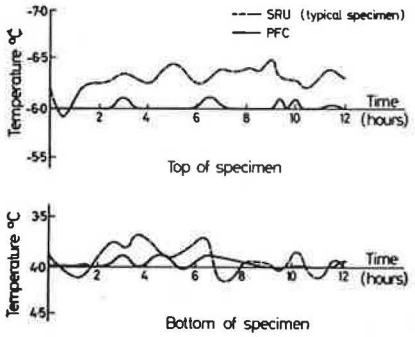

different subzero temperatures. After completing a period of between 2 and 32 h at the lower temperature, the specimen is allowed to warm naturally to the higher temperature, at which it is maintained by the controller for the remainder of the time interval before the cycle is repeated. Controller 3 can be used in conjunction with a guard ring that contains two 19-W Peltier units so that the guard-ring temperature can also be cycled.

Temperature measurements are made using copper constantan thermocouples in conjunction with a reference oven that gives a system accurate to ±0.1°C. The thermocouples are connected to a 70-channel data logger with a punched tape output that permits continual scanning at intervals as long as 2 h.

Test Procedure

The specimen is compacted first by vibrating hammer (3 s on each of three layers), then by static compaction. Thermocouples are positioned as required, and the apparatus set up as described previously. The specimen is left to equilibriate in the refrigerator at +4°C for 24 h.

The controller is then switched on to initiate freezing. In the standard test, both the controller and the guard-ring system are adjusted to give -6°C. This value was chosen as typical of the top-of-specimen temperatures achieved in the cold room and SRU. The full current of 6 A is available for cooling as necessary. In the retarded test, on the other hand, the maximum available current is stepped manually, 0.5 A every 4 h, eventually reaching 6 A. This gives a much slower rate of penetration. Daily readings of temperature and water level are taken.

In both types of test, it was frequently found that all heave had ceased before 250 h had elapsed. Tests were terminated when the heaving rate became negligible (<0.1 mm/day), i.e., after five days in the series of tests described below.

RESULTS AND DISCUSSION

Temperature Control

Concrete dummy specimens, 102 mm in diameter and 152 mm high, in which thermocouples had been inserted in predrilled holes at the positions indicated in Figure 5, were used to investigate fluctuations in temperature. The thermocouples were bedded in plasticine to ensure good thermal contact and stable positioning. Concrete specimens were used because (a) they do not change significantly between tests, (b) they are not subject to heave that would change the elevation of the thermocouples, and (c) freezing has relatively little influence on the thermal properties of concrete.

Typical temperature gradients achieved in the various facilities are shown in Figure 5 and Table 1. The values in Table 1 are the results of readings taken every hour throughout the test. Spurious readings obtained during the passage of the zero isotherm through the thermocouple position have been ignored. The readings for radial heat flow as a percentage of the vertical flow indicate how nearly the condition of unidirectional flow is approached. The PFC is better than the other units, and within the frozen zone the radial heat flow is very small.

Individual temperature gradients in the frozen zone in the PFC were within ±0.1°C/m of the mean and the other individual radial gradients were within ±1°C/m of the mean. The improved performance of the PFC compared to the other units is presumably due to its being operated in a +4°C environment. Conversely, the very cold air circulating in the gap between the inner box and the tank walls is the most likely cause of the relatively high radial flow noted in the SRU. Filling this gap with insulating material may give some improvement.

In all the units the radial heat flow in the unfrozen zone is much higher than in the frozen zone, which probably reflects the influence of the copper specimen carriers. Substituting plastic carriers and lowering the staging to reduce the air gap might be advisable in the PFC, particularly when it is used to verify mathematical models. Although such changes would reduce the similarity of conditions in the PFC to those currently specified in the TRRL test, the benefits would appear to outweigh this disadvantage.

Typical temperature fluctuations are shown in Figure 6. Although the SRU top and bottom temperatures for the single specimen are both within the ±0.5°C specified for the water bath (26), the much better performance of the PFC is obvious. Furthermore, the bottom-of-specimen temperature in the SRU averages slightly below +4°C because of temperature gradients through

Figure 7. Penetration of zero isotherm.

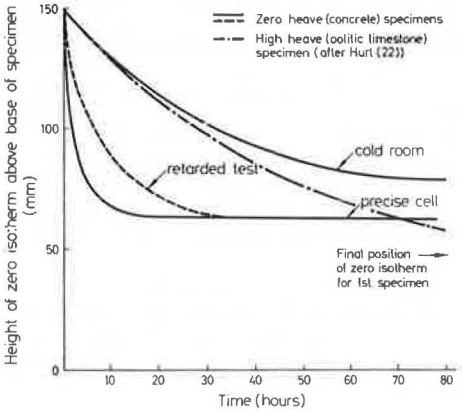

Figure 8. Grading curves.

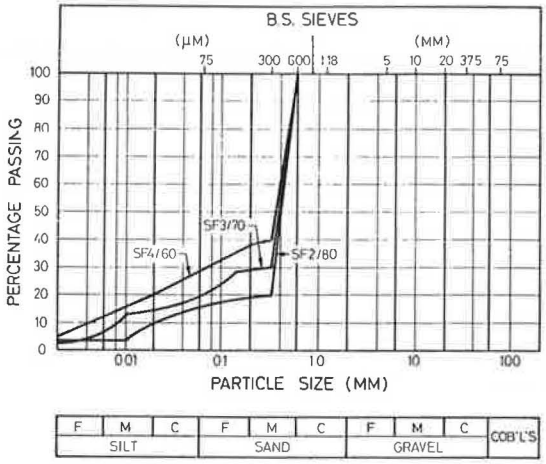

Table 2. Heave of sand and limestone filler mixtures.

		Cold Room and SRU Tests			PFC Tests				
Material	Facility	No. of Tests	Mean Heave, H_T (mm)	SD (mm)	Rate of Penetration	No. of Tests	Mean Heave, H_p (mm)	SD (mm)	H_p/H_T (×100%)
SF 2/80	Both	39	20.1	2.4	S	10	6.7	1.1	33.3
					R	7	9.3	0.8	
SF 3/70	CR	3	44.2	6.4	S	8	13.9	1.0	31.4
SF 3/60	CR	9	76.7	6.7					(24.5)
SF 4/60					S	8	18.8	2.4	

Note: SF is sand and limestone filler mixture; S is standard; R is retarded rate of penetration. SF 3/60 and SF 4/60 have the same proportions and nominal grading but are derived from different batches of filler. Their frost susceptibilities may be slightly different.

Figure 9. Curves for heave versus time.

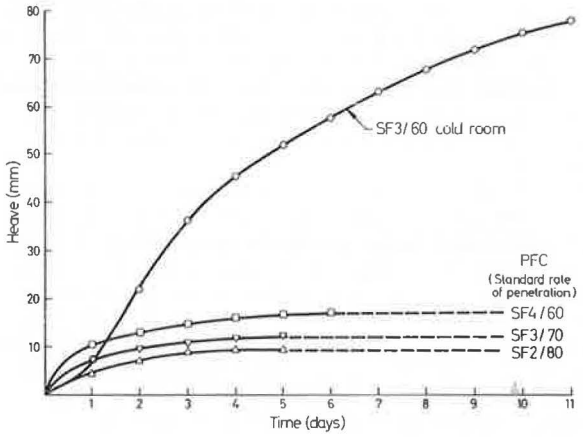

the porous disk. The PFC system is adjusted to give +4°C at the base of the specimen. Figure 7 shows that rate of penetration of the zero isotherm even in the retarded test is much faster in the PFC than in the cold-room test. The implications of this will be discussed in the next section.

Heave Tests

A series of tests was performed on sand-limestone filler mixtures. Standard Leighton Buzzard sand in the size range of 600-300 μm was mixed with limestone filler in various proportions to give the gradings shown in Figure 8. Specimens of the sand and limestone filler mixtures (SF) were compacted to the maximum dry density at the optimum moisture content (38) are given below.

Material	Optimum Moisture Content (%)	Maximum Dry Density (Mg/m^3)
SF 2/80	9.0	2.00
SF 3/70	9.5	2.01
SF 4/60	9.9	2.03

As previous investigators have found (28, 30), the heaves obtained in the cold room and SRU were not significantly different (39); either can be used as a reference against which the PFC results can be judged. The results obtained are summarized in the table below. Details of individual PFC results are given in Table 2, and typical curves for heave versus time are shown in Figure 9.

Heave (mm)			
SF 2/80		SF 3/70	SF 4/60
Standard	Retarded	Standard	Standard
8.0	9.5	14.5	16.5
8.0	9.1	14.8	16.9
6.7	10.7	14.1	18.3
4.8	9.0	11.8	21.9
7.0	9.7	13.9	17.0
5.0	8.7	14.4	17.1
6.5	8.0	14.2	20.8
7.2		13.7	22.3
6.8			
7.1			

The striking feature of these results is the much lower heaves obtained in the PFC than in the other units. Furthermore, the ratio of PFC heave to CR-

Figure 10. Boundary conditions in tests.

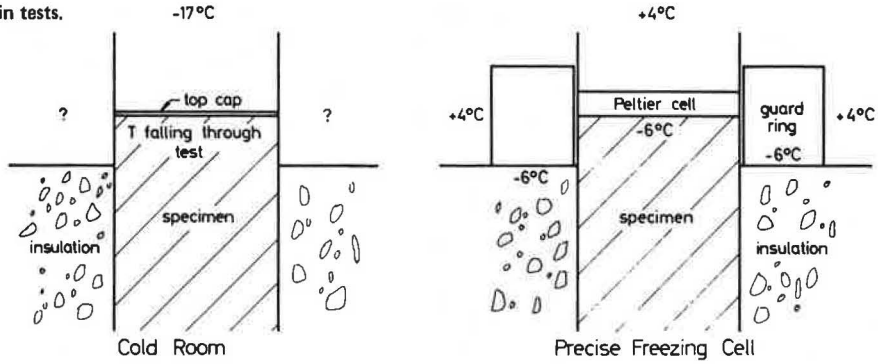

SRU heave decreases with increasing heave. Since the sidewall conditions are similar, friction and adfreezing can be discounted as possible explanations. The surcharge from the pressure of the Peltier unit (1 kPa) is also much too small to account for the effect.

More probable explanations are to be found in differences in (a) the rate of penetration of the zero isotherm and (b) the application of the boundary conditions. It was postulated earlier that ice segregation occurs when the suction is too low and the temperature is correspondingly too high to permit ice penetration. Thus, during the penetration isotherm (PI) stage, a slow rate of heat extraction favors the growth of intermediate ice lenses. A fast penetration of the zero isotherm, on the other hand, yields high heaving rates (40) associated with maximum suction (22). The high rates, however, occur for a limited time, so that the total heave observed is less than with a lower heaving rate extending over a longer period.

Intermediate ice lenses (rhythmic ice banding) are associated with the PI stage. As equilibrium approaches, the isotherms cease to penetrate and may even recede slightly. In this nonpenetrating isotherm (NPI) stage, the terminal lens will continue to grow until the heat input and output are balanced. In general, a terminal lens will commence under PI conditions and end with NPI conditions. With rapid heat extraction, the PI stage will be short, which will lead to low overall heave. The greater heave experienced in the retarded penetration test (Table 2) affirms this explanation.

Closer examination of the temperature boundary conditions applied in the PFC compared with those in the cold room (Figure 10) indicates a significant difference. Essentially, in the PFC the constant temperature is applied to a moving boundary, while in the cold room the constant temperature is specified and maintained at the level of the top of the trolleys. Immediately above the specimens, the temperature tends to be raised somewhat higher by heat conducted from below.

The temperatures in the SRU are intended to be similar to those in the cold room. Thus, in both units a high-heaving specimen experiences considerable additional cooling from its sides as it protrudes above the sand insulation. Consequently, the final position of the zero isotherm becomes lower as the heave (after 250 h) increases (Figure 7). In practice, the TRRL test condition appears to approximate a constant boundary temperature at the level of the original top surface of the specimens. It is arguable that the PFC more nearly reflects field conditions.

While the very wide range of heave values experienced in CR and SRU tests should make for easier classification, this advantage is offset by the greater scatter obtained with high-heave specimens. The above interpretation suggests that particular attention should be given to obtaining uniform air temperatures in the CR and SRU within the zone into which specimens heave.

Further Work

The comparison between the performance of the PFC and those of the other facilities needs to be extended to other materials, including subbase aggregates. Also, we intend to test specimens of rock cores that have been split horizontally. The feedback thermistor will be placed in the split so that an ice lens can be formed at that level. The results will be compared with those from compacted aggregate specimens on identical rock. Thus we hope to gain further insight into the relative contributions that within-particle and between-particle pore systems (13) make to frost heaving of aggregates. Pilot studies in the cold room have indicated that this technique is feasible.

The PFC, with its close control of temperature and water level, offers considerable benefit in the study of many variables such as suction, suction gradient, heat, and water flow required in the development of mathematical models. The apparatus can be adapted to measure thermal conductivity in the vertical direction; this is an alternative to the radial measurement obtained in the line source method (41). However, its major value is likely to be in verifying the predictions made with mathematical models. We hope that the cycling facility, yet to be evaluated, will enable the effects of diurnal temperature variations to be modeled.

For most of these applications, which are essentially of a research nature, the temperature stability of the present cold room and SRU are inadequate. We anticipate, however, that the continued development of techniques will enable routine testing in the foreseeable future to be undertaken in the SRU.

CONCLUSIONS

1. A precise freezing cell (PFC) has been constructed in which freezing is achieved in an open system by the application of constant boundary temperatures controlled to ±0.1°C. The temperature stability of the PFC is much better than that of the cold rooms and self-refrigerated units currently being used for routine testing in the U.K.
2. The radial heat flow in the frozen zone (3 percent of the vertical flow) is small, so a close approximation of unidirectional flow is achieved. Conditions are less satisfactory in the unfrozen zone, and modifications to improve this situation are proposed.
3. In two years' operation, the PFCs have proved quite reliable and less prone to minor faults than the other facilities.
4. For identical specimens, the heave achieved in

the PFC is much less than that in a cold room or SRU. The ratio of PFC to SRU heave decreases as heave increases.

5. The reduction in heave is due partly to the greater heat extraction rate and partly to constant boundary temperatures being applied to a moving level rather than to a fixed level.

6. For the present, routine testing in Great Britain is likely to continue in cold rooms and SRUs because the capital cost per specimen is only about a third of that for the PFC. Nevertheless, the PFC has a useful role in highlighting areas where modifications might be made to the standard test to give improved reproducibility.

7. Some form of precise cell is considered essential for research purposes, particularly for the development and verification of mathematical models. The apparatus described appears well suited for this purpose.

ACKNOWLEDGMENT

We wish to thank the Science Research Council for providing a research studentship for S. Dudek, the British Quarrying and Slag Federation for financial support in the development and evaluation of the SRU, the staff of the TRRL research team for their continuing cooperation, R.C. Coates of the Department of Civil Engineering, University of Nottingham, for his constant encouragement and support, A. Onalp of the University of Trabzon, Turkey, for his efforts during a sabbatical year at Nottingham, J.T. Holden of the Department of Theoretical Mechanics, past and present members of the research team, and David Snow of P.S. Snow and Company for their many helpful contributions.

REFERENCES

1. E. Penner. Frost Heaving in Soils. Proc., 1st International Conference on Permafrost. Purdue Univ., West Lafayette, IN, 1963, pp. 197-202.
2. D.H. Everett and J.M. Haynes. Capillary Properties of Some Model Pore Systems with Special Reference to Frost Damage. International Union of Testing and Research Laboratories Materials and Structures, Paris, Bull. New Series 27, 1965, pp. 31-38.
3. P.J. Williams. Properties and Behaviour of Freezing Soils. Norwegian Geotechnical Institute, Oslo, Publication 72, 1967.
4. H.B. Sutherland and P.N. Gaskin. Pore Pressure and Heaving Pressures Developed in Partially Frozen Soils. Proc., 2nd International Conference on Permafrost, Yakutsk, Yakutsk Autonomous Soviet Socialist Republic, National Academy of Sciences, Washington, DC, 1973, pp. 409-419.
5. S. Taber. Freezing and Thawing of Soils as Factors in the Destruction of Road Pavements. Public Roads, Vol. 11, No. 6, 1930, pp. 113-132.
6. J.F. Haley and C.W. Kaplar. Cold Room Studies of Frost Action in Soils. HRB, Special Rept. 2, 1952, pp. 246-247.
7. K.A. Linell and C.W. Kaplar. The Factor of Soil and Material Type in Frost Action. HRB, Bull. 225, 1959, pp. 81-126.
8. C.W. Kaplar. A Laboratory Freezing Test to Determine the Relative Frost Susceptibility of Soils. Cold Regions Research and Engineering Laboratory, Hanover, NH, CRREL Technical Note, 1965.
9. D. Croney and J.C. Jacobs. The Frost Susceptibility of Soils and Road Materials. British Road Research Laboratory, Crowthorne, England, LR Rept. 90, 1967.
10. H.B. Sutherland and P.N. Gaskin. A Comparison of the TRRL and CRREL Tests for Frost Susceptibility of Soils. Canadian Geotechnical Journal, Vol. 10, No. 3, 1973, pp. 553-555.
11. S.F. Obermeier. Frost Heave Susceptibility Research. Proc., Symposium on Frost Action in Roads, Organization for Economic Cooperation and Development, Paris, 1973, Vol. 1, pp. 251-266.
12. D.L. Townsend and T.I. Csathy. A Complication of Frost Susceptibility Criteria Up to 1961. Queens Univ., Kingston, Ontario, Rept. 14, 1961.
13. R.H. Jones and K.G. Hurt. An Osmotic Method for Determining Rock and Aggregate Suction Characteristics with Applications to Frost Heave Studies. Quarterly Journal of Engineering Geology, Vol. 11, No. 3, 1978, pp. 245-252.
14. R.H. Jones. Frost Damage and Its Prevention. In Developments in Highway Pavement Engineering (P.S. Pell, ed.), Applied Science Publishers, Barking Essex, 1978.
15. K.A. Linell, F.B. Hennion, and E.F. Lobacz. Corps of Engineers' Pavement Design in Areas of Seasonal Frost. HRB, Highway Research Record 33, 1963, pp. 76-128.
16. R.L. Harlan. Analysis of Coupled Heat-Fluid Transport in Partially Frozen Soils. Water Resources Research, Vol. 9, No. 5, 1973, pp. 1314-1323.
17. S. Outcalt. A Numerical Model of Ice Lensing in Freezing Soils. Proc., 2nd Conference on Soil-Water Problems in Cold Regions, Edmonton, Alberta, 1976, pp. 63-74.
18. G.S. Taylor and J.N. Luthin. Numerical Results of Coupled Heat-Mass Flow During Freezing and Thawing. Proc., 2nd Conference on Soil-Water Problems in Cold Regions, Edmonton, Alberta, 1976, pp. 155-172.
19. J. Aguirre-Puente, M. Fremond, and J.M. Menot. Gel dans les Milieux Poreux Permeabilite Variable et Mouvements d'Eau dans la Partie a Temperature Negative. Proc., International Symposium on Frost Action in Soils, Lulea, Sweden, 1977, Vol. 1, pp. 5-28.
20. R.L. Berg, K.E. Gartner, and G.L. Guymon. A Mathematical Model to Predict Frost Heave. Proc., International Symposium on Frost Action in Soils, Lulea, Sweden, 1977, Vol. 2, pp. 92-109.
21. E. Penner. Discussion. Proc., International Symposium on Frost Action in Soils. Lulea, Sweden, 1977, Vol. 2, p. 46.
22. K.G. Hurt. The Prediction of the Frost Susceptibility of Limestone Aggregates with Reference to Road Construction. Univ. of Nottingham, Ph.D. thesis, 1976.
23. A. Onalp. Calculation of Water Transport in the LR 90 Test. Proc., Colloquium on Frost Heave Testing and Research (R.H. Jones, ed.), Univ. of Nottingham, 1977, pp. 115-126.
24. Annual Report. U.K. Transport and Road Research Laboratory, Crowthorne, England, 1971, p. 83.
25. R.H. Jones and K.G. Hurt. Improving the Repeatability of Frost Heave Tests. Highways and Road Construction, Vol. 43, No. 1787-8, 1975, pp. 8-13.
26. The LR 90 Frost Heave Test—Interim Specification for Use with Granular Materials. U.K. Transport and Road Research Laboratory, Crowthorne, England, Supplementary Rept. 318, 1977.
27. Research on the Frost Susceptibility of Road Making Materials. U.K. Transport and Road Research

Laboratory, Crowthorne, England, Leaflet 611, April 1976.
28. G.R. Nellist. An Apparatus for Testing the Resistance of Road Making Materials to Frost Damage. Journal of Scientific Instruments, Vol. 44, 1967, pp. 553-555.
29. A. Onalp. The Mechanisms of Frost Heave in Soils with Particular Reference to Chemical Stabilization. Univ. of Newcastle upon Tyne, Ph.D. thesis, 1970.
30. R.J. Kettle and R.I.T. Williams. The Development of Frost Testing Equipment. International Union of Testing and Research Laboratories Materials and Structures, Paris, Vol. 6, No. 34, 1973, pp. 299-305.
31. Frost and Susceptibility of Materials. Highway and Traffic Engineering, June 1971, pp. 23-24.
32. J. Hill. Self Refrigerating Units: Frost Cabinet Temperature Distribution. Proc., Colloquium on Frost Heave Testing and Research (R.H. Jones, ed.), Univ. of Nottingham, 1977, pp. 23-27.
33. W. Lechner. Peltier Cooling. Philips Technical Review, Vol. 27, No. 5, 1966, pp. 113-130.
34. P. Hoekstra, E. Chamberlain, and T. Frate. Frost Heaving Pressures. HRB, Highway Research Record 101, 1965, pp. 28-38.
35. P.J. Williams. Thermoelectric Cooling for Precise Temperature Control of Frozen and Unfrozen Soils. Canadian Geotechnical Journal, Vol. 5, No. 4, 1968, pp. 265-267.
36. R.J. Kettle and R.I.T. Williams. Frost Heave and Heaving Pressure Measurements in Colliery Shales. Canadian Geotechnical Journal, Vol. 13, No. 2, 1976, pp. 128-138.
37. C.W. Kaplar. New Experiments to Simplify Frost Susceptibility Testing of Soils. HRB, Highway Research Record 215, 1968, pp. 48-58.
38. Methods of Tests for Soils for Civil Engineering Purposes. British Standards Institution, London, BS:1377, 1975.
39. S.J-M. Dudek. A Preliminary Assessment of the Design and Performance of Frost Susceptibility Testing Facilities. Proc., Colloquium on Frost Heave Testing and Research (R.H. Jones, ed.), Univ. of Nottingham, 1977, pp. 13-21.
40. C.W. Kaplar. Phenomenon and Mechanism of Frost Heaving. HRB, Highway Research Record 304, 1970, pp. 1-13.
41. R. McGaw. Thermal Conductivity of Compacted Sand/Ice Mixtures. HRB, Highway Research Record 215, 1968, pp. 35-47.

Publication of this paper sponsored by Committee on Frost Action.

Subdrainage with a Sand Backfill as a Positive Influence on Pavement Performance

Malcolm L. Steinberg, Texas State Department of Highways and Public Transportation, San Antonio

Expansive soils are an estimated $4 billion-a-year problem in the United States. They cause severe distortion in many human works, including highways. Subdrainage has been used extensively in attempts to intercept or remove excess moisture from expansive clays. Minimizing moisture change is seen as a way of reducing surface distortion and improving pavement performance. Underdrains have been used on many highways to remove excess subsurface water, and one Texas study revealed that their use in expansive soils results in a mixed pattern. The effectiveness of deep underdrains with sand backfill is now being examined. The sand is used to provide a moisture reservoir and stabilizer for the expansive clay and the underdrain will remove the moisture the sand cannot hold. A field test of an Israeli experiment is being conducted on a roadway section, which has resisted considerable previous attention, on US-90 west of D'Hanis and Hondo, Texas. This section cuts through a limestone crust into a clay and has had repeated level-up courses of asphalt. Lime had been placed in holes 45 cm (18 in) in diameter, 1.5 m (5 ft) deep, and on centers. In this test 381 m (1250 ft) of 15.24-cm (6-in) slotted underdrain pipe was placed 2.4 m (8 ft) deep; the sand backfill was placed along the south roadway crown line. Observations indicate that maximum movements are taking place on the nonunderdrained side in 9 of the 12 sections and are averaging three times the movement on the underdrained side. Expansive soil movement under existing pavements probably can be reduced by sand-backfilled underdrains.

Swelling soils cause an estimated $4 billion a year in damages in the United States. More than half of this occurs in our transportation facilities: highways, railroads, airport runways, sidewalks, bikeways, and canals. Even this estimate is probably conservative.

The original $2 billion a year (1) estimated in 1973 reflected the lower side of industry estimates. Pavements damaged by these soils are usually repaired with asphalt products or other equally energy-intensive materials. As long as the price of a barrel of oil rises and other energy sources rise sympathetically, even extending cost increases makes the latest estimate lower than it actually should be.

What can be done about damaged transportation facilities? The roadways that represent half of the damages offer several possibilities. First, we can build them differently in the future and avoid expansive clay areas or remove a significant amount of it, treat it deeply with lime, pond it, or seal off the zones of activity with asphalt, lime, or fabric. All are worthy suggestions. However, some of these concepts do not adapt well to the existing roadway, runway, sidewalk, bikeway, or canal. Their remedy is the asphalt patch, asphalt level-ups, or total replacement.